EOS MLS ‘forward model’ meeting

Room 183-718, Jet Propulsion Laboratory

(University of Edinburgh colleagues participating by telecon)

11-12 December 2002

MLS CLEAR-SKY PRODUCTION FORWARD MODEL:

Summary of Issues/Status/Actions in Regards to Spectroscopic and Instrument Calibration Data.

Bill Read

December 12, 2002

ISSUES

- Tentative dates for definitive calibration data.
- Processing for THz filter shapes. Need to include the radiometer sideband frequency gradient in the filter data so as to be consistent with the definition below.

$$\Phi_{\mathrm{B,ch}}(\nu) \qquad r(\nu)\frac{\Phi_{\mathrm{FB,ch}}(\nu-\nu_{\mathrm{lo}})}{\int \Phi_{\mathrm{FB,ch}}(\Delta\nu)\,\mathrm{d}\Delta\nu}, \nu >$$

$$\Phi_{\mathrm{B,ch}}(\nu) \qquad r(\nu)\frac{\Phi_{\mathrm{FB,ch}}(\nu_{\mathrm{lo}}-\nu)}{\int \Phi_{\mathrm{FB,ch}}(\Delta\nu)\,\mathrm{d}\Delta\nu}, \nu <$$

$$r_{\mathrm{u,B,ch}} - \frac{\int_{\nu_{\mathrm{lo}}}^{\infty}\Phi_{\mathrm{B,ch}}(\nu)\,\mathrm{d}\nu}{\int_{-\infty}^{\infty}\Phi_{\mathrm{B,ch}}(\nu)\,\mathrm{d}\nu}$$

$$r_{\mathrm{l,B,ch}} = \frac{\int_{-\infty}^{\nu_{\mathrm{lo}}}\Phi_{\mathrm{B,ch}}(\nu)\,\mathrm{d}\nu}{\int_{-\infty}^{\infty}\Phi_{\mathrm{B,ch}}(\nu)\,\mathrm{d}\nu}$$

- Interface for adding insertion loss radiance baseline calculation in L2.
- Retrieving lo shift for THz?
- scan dependent ξ.
- Replace ν_j with ν in Boltzmann distribution function for computing absorption coefficients.

Goal is to have all these fixes and features in the version 1.2 software. They will be added toward the end of its development cycle.

CALIBRATION DATA

Table 1: Calibration Parameters

Parameter	Priority	Symbol	Responsible Person	Current Status	Launch ready
SPECTROSCOPY					
Catalogue List	1	$\mathcal{C}$	WGR	In progress	01-May-03
Molecule data					
Isotope fraction	1	$[f]$	WGR	L & S, WHF	Ready
Partition Function	1	$Q(T)$	WGR	JPL Catalogue	Ready
Mass	1	$\mathcal{M}$	WGR	WHF	Ready
Continuum	1	CONT_X	FCD	JRP	01-Apr-03
Line $\times$ line data					
Frequency	1	ν_0	WGR	JPL Catalogue	Ready
Lower state energy	1	E_ℓ	WGR	JPL Catalogue	Ready
Strength	1	$\mathcal{I}$	WGR	JPL Catalogue	Ready

Continued on next page

CALIBRATION DATA

Parameter	Priority	Symbol	Responsible Person	Current Status	Launch ready
^{81}BrO(625 GHz)	1				
Width		w_c, n_c	BJD	Measured	Ready
Shift		$\Delta\nu_0$, $n_{\Delta\nu_0}$	BJD	Measured	Ready
^{81}BrO(650 GHz)	1				
Width		w_c, n_c	BJD	Measured	Ready
Shift		$\Delta\nu_0$, $n_{\Delta\nu_0}$	BJD	Measured	Ready
CH_3CN(184 GHz)	2				
Width		w_c, n_c	BJD	Guess	01-Oct-03
Shift		$\Delta\nu_0$, $n_{\Delta\nu_0}$	BJD	Ignored	01-Oct-03
CH_3CN(202 GHz)	2				
Width		w_c, n_c	BJD	Guess	01-Oct-03
Shift		$\Delta\nu_0$, $n_{\Delta\nu_0}$	BJD	Ignored	01-Oct-03
CH_3CN(625 GHz)	2				
Width		w_c, n_c	BJD	Guess	01-Oct-03
Shift		$\Delta\nu_0$, $n_{\Delta\nu_0}$	BJD	Ignored	01-Oct-03

Continued on next page

CALIBRATION DATA

Parameter	Priority	Symbol	Responsible Person	Current Status	Launch ready
CH_3CN(660 GHz)	2				
Width		w_c, n_c	BJD	Guess	01-Oct-03
Shift		$\Delta\nu_0$, $n_{\Delta\nu_0}$	BJD	Ignored	01-Oct-03
CO(231 GHz)	2				
Width		w_c, n_c	BJD	Guess	01-Feb-03
Shift		$\Delta\nu_0$, $n_{\Delta\nu_0}$	BJD	Ignored	01-Feb-03
^{35}ClO(204 GHz)	1				
Width		w_c, n_c		JJO	Ready
Shift		$\Delta\nu_0$, $n_{\Delta\nu_0}$		NA	Ready
^{35}ClO(650 GHz)	1				
Width		w_c, n_c		JJO	Ready
Shift		$\Delta\nu_0$, $n_{\Delta\nu_0}$		NA	Ready
$H^{35}Cl$(626 GHz)	1				
Width		w_c, n_c	BJD	Measured	Ready
Shift		$\Delta\nu_0$, $n_{\Delta\nu_0}$	BJD	Measured	Ready

Continued on next page

CALIBRATION DATA

Parameter	Priority	Symbol	Responsible Person	Current Status	Launch ready
$H^{37}Cl$(625 GHz)	1				
Width		w_c, n_c	BJD	Measured	Ready
Shift		$\Delta\nu_0$, $n_{\Delta\nu_0}$	BJD	Measured	Ready
HCN(177 GHz)	2				
Width		w_c, n_c	BJD	Guess	01-Oct-03
Shift		$\Delta\nu_0$, $n_{\Delta\nu_0}$	BJD	Ignored	01-Oct-03
H_2O(183 GHz)	1				
Width		w_c, n_c		AB & TMG	Ready
Shift		$\Delta\nu_0$, $n_{\Delta\nu_0}$		HCP	Ready
H_2O(2.532 THz)	1				
Width		w_c, n_c	BJD	HITRAN	01-Aug-03
Shift		$\Delta\nu_0$, $n_{\Delta\nu_0}$	BJD	Ignored	01-Aug-03
HNO_3(181 GHz)	1				
Width		w_c, n_c	BJD	Guess	15-Mar-03
Shift		$\Delta\nu_0$, $n_{\Delta\nu_0}$	BJD	Ignored	15-Mar-03

Continued on next page

CALIBRATION DATA

Parameter	Priority	Symbol	Responsible Person	Current Status	Launch ready
HNO_3(206 GHz)	1				
Width		w_c, n_c		TMG	Ready
Shift		$\Delta\nu_0$, $n_{\Delta\nu_0}$		NA	Ready
HNO_3(626 GHz)	2				
Width		w_c, n_c	BJD	Guess	15-Mar-03
Shift		$\Delta\nu_0$, $n_{\Delta\nu_0}$	BJD	Ignored	15-Mar-03
HNO_3(633 GHz)	2				
Width		w_c, n_c	BJD	Guess	15-Mar-03
Shift		$\Delta\nu_0$, $n_{\Delta\nu_0}$	BJD	Ignored	15-Mar-03
HNO_3(651 GHz)	2				
Width		w_c, n_c	BJD	Guess	15-Mar-03
Shift		$\Delta\nu_0$, $n_{\Delta\nu_0}$	BJD	Ignored	15-Mar-03
HNO_3(660 GHz)	2				
Width		w_c, n_c	BJD	Guess	15-Mar-03
Shift		$\Delta\nu_0$, $n_{\Delta\nu_0}$	BJD	Ignored	15-Mar-03

Continued on next page

CALIBRATION DATA

Parameter	Priority	Symbol	Responsible Person	Current Status	Launch ready
$HO^{35}Cl$(636 GHz)	2				
Width		w_c, n_c	BJD	Guess	15-Mar-03
Shift		$\Delta\nu_0$, $n_{\Delta\nu_0}$	BJD	Ignored	15-Mar-03
$HO^{37}Cl$(2.515 THz)	2				
Width		w_c, n_c	BJD	Guess	01-Aug-03
Shift		$\Delta\nu_0$, $n_{\Delta\nu_0}$	BJD	Ignored	01-Aug-03
HO_2(625 GHz)	1				
Width		w_c, n_c	BJD	Measured, in progress	01-May-03
Shift		$\Delta\nu_0$, $n_{\Delta\nu_0}$	BJD	?	01-May-03
HO_2(650 GHz)	1				
Width		w_c, n_c	BJD	Measured, in progress	01-May-03
Shift		$\Delta\nu_0$, $n_{\Delta\nu_0}$	BJD	?	01-May-03
HO_2(660 GHz)	1				
Width		w_c, n_c	BJD	Measured, in progress	01-May-03
Shift		$\Delta\nu_0$, $n_{\Delta\nu_0}$	BJD	?	01-May-03

Continued on next page

CALIBRATION DATA

Parameter	Priority	Symbol	Responsible Person	Current Status	Launch ready
N_2O(201 GHz)	1				
Width		w_c, n_c	WGR	AH, but needs updating	15-Jan-03
Shift		$\Delta\nu_0$, $n_{\Delta\nu_0}$		NA	Ready
N_2O(653 GHz)	1				
Width		w_c, n_c	WGR	AH, but needs updating	15-Jan-03
Shift		$\Delta\nu_0$, $n_{\Delta\nu_0}$		NA	Ready
OH(2.510 THz)	1				
Width		w_c, n_c	BJD	KP	01-Apr-03
Shift		$\Delta\nu_0$, $n_{\Delta\nu_0}$	BJD	Ignored	01-Apr-03
OH(2.514 THz)	1				
Width		w_c, n_c	BJD	KP	01-Apr-03
Shift		$\Delta\nu_0$, $n_{\Delta\nu_0}$	BJD	Ignored	01-Apr-03

Continued on next page

CALIBRATION DATA

Parameter	Priority	Symbol	Responsible Person	Current Status	Launch ready
O_2(118 GHz)	1				
Width		w_c, n_c		HMP	Ready
Shift		$\Delta\nu_0$, $n_{\Delta\nu_0}$		AFK	Ready
O_2(2.502 THz)	1				
Width		w_c, n_c	BJD	KP	01-Jun-03
Shift		$\Delta\nu_0$, $n_{\Delta\nu_0}$	BJD	Ignored	01-Jun-03
$O^{18}O$(234 GHz)	1				
Width		w_c, n_c	BJD	Guess	15-Jan-03
Shift		$\Delta\nu_0$, $n_{\Delta\nu_0}$	BJD	Ignored	15-Jan-03
O_3(184 GHz)	2				
Width		w_c, n_c		JJO	Ready
Shift		$\Delta\nu_0$, $n_{\Delta\nu_0}$		NA	Ready
O_3(206 GHz)	1				
Width		w_c, n_c		JJO	Ready
Shift		$\Delta\nu_0$, $n_{\Delta\nu_0}$		NA	Ready

Continued on next page

CALIBRATION DATA

Parameter	Priority	Symbol	Responsible Person	Current Status	Launch ready
O_3(240 GHz)	1				
Width		w_c, n_c	BJD	Measured	Ready
Shift		$\Delta\nu_0$, $n_{\Delta\nu_0}$	BJD	Measured	Ready
O_3(625 GHz)	1				
Width		w_c, n_c	BJD	Measured	Ready
Shift		$\Delta\nu_0$, $n_{\Delta\nu_0}$	BJD	Measured	Ready
O_3(2.509 THz)	1				
Width		w_c, n_c	BJD	HITRAN	01-May-03
Shift		$\Delta\nu_0$, $n_{\Delta\nu_0}$	BJD	ignored	01-May-03
O_3(2.543 THz)	1				
Width		w_c, n_c	BJD	HITRAN	01-May-03
Shift		$\Delta\nu_0$, $n_{\Delta\nu_0}$	BJD	ignored	01-May-03
SO_2(200 GHz)	3				
Width		w_c, n_c	BJD	Guess	01-Oct-03
Shift		$\Delta\nu_0$, $n_{\Delta\nu_0}$	BJD	ignored	01-Oct-03

Continued on next page

CALIBRATION DATA

Parameter	Priority	Symbol	Responsible Person	Current Status	Launch ready
SO_2(204 GHz)	3				
Width		w_c, n_c		CB	Ready
Shift		$\Delta\nu_0$, $n_{\Delta\nu_0}$		NA	Ready
SO_2(660 GHz)	3				
Width		w_c, n_c	BJD	Guess	01-Oct-03
Shift		$\Delta\nu_0$, $n_{\Delta\nu_0}$	BJD	ignored	01-Oct-03

Continued on next page

CALIBRATION DATA

Parameter	Priority	Symbol	Responsible Person	Current Status	Launch ready
INSTRUMENT					
Filters GHz & THz (FB, MB, WB)					
Frequency	1	$\nu_{\mathrm{sb,B,ch}}$	RFJ		Ready
Shapes	1	$\Phi_{\mathrm{sb,B,ch}}(\nu)$	RFJ	Replicated FB 25	
R1A, R1B	1	$\Phi_{\mathrm{l,1,21,32,34},ch}(\nu)$	RFJ		01-Mar-03
R2	1	$\Phi_{\mathrm{sb,2--6,27},ch}(\nu)$	RFJ		15-Mar-03
R3	1	$\Phi_{\mathrm{sb,7--9},ch}(\nu)$	RFJ		01-Apr-03
R4	1	$\Phi_{\mathrm{sb,10--14,28--31},ch}(\nu)$	RFJ		15-Apr-03
R5	1	$\Phi_{\mathrm{sb,15--20},ch}(\nu)$	RFJ		01-May-03
(DACS)					
Frequency	1	$\nu_{\mathrm{sb,ch}}$	MJS		Ready
Pre-filter Shapes	1	$\Phi_{\mathrm{sb,B}}(\nu)$	MJS	ignored	01-Feb-03
Normalization	1	$\hat{\Phi}_{\mathrm{sb,B,ch}}$	MJS	NA	01-Feb-03

Continued on next page

CALIBRATION DATA

Parameter	Priority	Symbol	Responsible Person	Current Status	Launch ready
SB fraction					
GHz	1	$r''_{\mathrm{sb,B,ch}}$	RFJ	pre-environment	01-May-03
THz	1	$r_{\mathrm{sb,B,ch}}$	HMP	pre-environment	01-Mar-03
Filter quadrature					
Non Magnetic	1	$H_R(\zeta_t, \mathbf{x})$	WGR	Preliminary	01-May-03
Magnetic	1	$H_{\mathrm{R1}}(\zeta_t, \mathbf{x})$	MJS	Non-Magnetic	01-May-03
Antenna Patterns					
GHz	1	$G_{\mathrm{l,1,21,32,34}}(\chi, \chi_o)$	REC	pre-environment	01-Apr-03
GHz	1	$G_{\mathrm{sb,2--6}}(\chi, \chi_o)$	REC	pre-environment	15-Apr-03
GHz	1	$G_{\mathrm{sb,7--9,33}}(\chi, \chi_o)$	REC	pre-environment	15-Apr-03
GHz	1	$G_{\mathrm{sb,10--14}}(\chi, \chi_o)$	REC	pre-environment	01-May-03
Note		$G_{\mathrm{sb,B,ch}}(\chi, \chi_o) = G_{\parallel,\mathrm{sb,B,ch}}(\chi, \chi_o) + G_{\perp,\mathrm{sb,B,ch}}(\chi, \chi_o)$			
R1A, R1B	1	$G_{\parallel,\mathrm{l,B,ch}}(\chi, \chi_o)$	REC	ignored	01-Apr-03
R1A, R1B	1	$G_{\perp,\mathrm{l,B,ch}}(\chi, \chi_o)$	REC	ignored	01-Apr-03

Continued on next page

CALIBRATION DATA

Parameter	Priority	Symbol	Responsible Person	Current Status	Launch ready
R1A, R1B	2	$G_{\vert,\mathrm{l,B,ch}}(\chi,\chi_o)$	REC	ignored	01-Aug-03
R1A, R1B	2	$G_{\circ,\mathrm{l,B,ch}}(\chi,\chi_o)$	REC	ignored	01-Aug-03
THz	1	$G_{\mathrm{B,ch}}(\chi,\chi_o)$	HMP	pre-environment	15-Jan-03
FOV-direction					
GHz	1	$\alpha_{\mathrm{sb,B}}, \epsilon_{\mathrm{sb,B}}$	REC	Pre-environment	01-Feb-03
THz(→GHz)	1	$\alpha_{\mathrm{sb,B}}, \epsilon_{\mathrm{sb,B}}$	REC	Pre-environment	01-May-03
THz(R5V→R5H)	1	$\alpha_{\mathrm{sb,B}}, \epsilon_{\mathrm{sb,B}}$	HMP	$\alpha_{\mathrm{sb,B}}=0, \epsilon_{\mathrm{sb,B}}=0$	Ready
Antenna losses and efficiencies					
GHz	1	$\eta^{\mathrm{AA}}_{\mathrm{sb,B}}, \eta^{k=1,2,3}_{\mathrm{sb,B}}$	REC	ignored	01-Mar-03
GHz	1	$\rho^{k=1,2,3}_{\mathrm{R}}$	REC	ignored	Ready
Notes		$\eta^{\mathrm{A}}_{\mathrm{sb,B}} = \eta^{\mathrm{AA}}_{\mathrm{sb,B}} \prod_{k=1}^{3} \eta^{k}_{\mathrm{sb,B}}$ $\rho^{\mathrm{A}}_{\mathrm{R}} = \prod_{k=1}^{3} \rho^{k}_{\mathrm{R}}$			
Polarization	1	$\xi_{\mathrm{B}=22,26}$	REC	ignored	01-May-03

Introductory Material

Joe Waters

Meeting Objectives

Primary objective

- **Review status of 'flight-ready' spectroscopic and calibration data for the MLS forward model**
  - and determine appropriate milestone dates for incorporating these into our data processing software

Additional objectives

- **Review, briefly, status of cal data for MLS Level 1 data software**
- **Compare some numerical results from different MLS forward models**
- **Review status/plans for:**
  - Cloudy-sky forward models
  - Polarized (magnetic) forward model for O_2 emission

MLS flight instrument

Some Major Milestones

- **Dec 2002**
  - MLS instrument delivery to Aura spacecraft
- **~ May 2003**
  - Complete (including testing) data processing software that could be used for analyzing incoming MLS data after launch
- **~ Sep 2003**
  - Complete (including testing) MLS data processing software that includes ‘everything we can before launch’
- **~ Jan 2004**
  - Aura launch, activate MLS, start data processing

11-12 Dec 2002 EOS MLS Forward Model Meeting

Agenda for Wednesday 11 December

(times, other than start time, are approximate)

➢ 8:30 am	Joe Waters	Introductory material, meeting objectives

1. Mainly clear-sky production-processing forward model and input data for it

➢ 8:40 am	Bill Read	(1) Overview and status of forward model (2) Review required input data items
➢ 9:30 am	Brian Drouin	Spectral linewidth parameters
➢ *10:15 am*	*break, group photo*	
➢ 10:45 am	Frank De Lucia, Andrey Meshkov	Atmospheric 'continuum' parameterization and parameters (including description of laboratory experiments/results)
➢ 11:30 am	Bob Stachnik	Balloon measurements of continuum near 600 GHz
➢ *noon*	*lunch*	
➢ 1:00 pm	Robert Jarnot	Overall status of EOS MLS instrument, and calibration data for production processing software
➢ 1:15 pm	Robert Jarnot	Instrument data for Level 1 software
➢ 1:30 pm	Robert Jarnot	GHz radiometric and spectral data for forward model
➢ *2:30 pm*	*break*	
➢ 2:45 pm	Rick Cofield, Paul Stek	GHz FOV data for forward model
➢ 3:45 pm	Herb Pickett	THz data for forward model

11-12 Dec 2002 EOS MLS Forward Model Meeting

Agenda for Thursday 12 December

(times, other than start time, are approximate)

1. (continued) Mainly clear-sky production-processing forward model and input data for it

- 8:30 am — Bill Read — Summary of status of spectroscopic and calibration data for MLS forward model (MOVED TO BEGINNING OF PRESENTATION)
- 8:45 am — all — Discussion of issues, priorities, and actions related to spectroscopic and calibration data for forward model

2. Comparisons of results from 'other' forward models and MLS production forward model

- 9:15 am — Hugh Pumphrey, Mark Filipiak — Comparisons among results from U of E clear-sky forward model(s) and MLS production-processing forward model
- 10:00 am — Jonathan Jiang — Comparisons between results from Jonathan/Dong's clear-sky forward model and MLS production-processing model
- *10:30 am — break*

3. 'Cloudy-sky' and 'polarized' (magnetic) forward models

- 10:45 am — Jonathan Jiang — JPL 'cloudy-sky' model: overview of model/status/results/plans
- 11:15 am — Cory Davis — U of E 'cloudy-sky' model: overview of plans/status ...
- 11:45 am — Michael Schwartz — Polarized (magnetic) forward model: overview of plans/status
- 12:15 pm — adjourn formal meeting

Afternoon for additional topics that arise and/or informal discussions

Topic 1

Clear-Sky production-processing forward model and input data review

THE EOS MLS GAS-PHASE UNPOLARIZED FORWARD MODEL

Bill Read

December 10, 2002

MEASURED LIMB RADIANCE AT THE SWITCHING MIRROR

$$
\begin{aligned}
\dot{I}_{\mathrm{B,ch}} = & \\
& r_{\mathrm{u,B,ch}} \frac{\int_{\Omega_A}\int_{\nu_{\mathrm{lo}}}^{\infty} I\left(\nu,\Omega,\mathbf{x}\right)\Phi_{\mathrm{u,B,ch}}\left(\nu\right)G_{\mathrm{u,B,ch}}\left(\Omega,\Omega_o\right)\mathrm{d}\nu\mathrm{d}\Omega}{\int_{\Omega_A}\int_{\nu_{\mathrm{lo}}}^{\infty} \Phi_{\mathrm{u,B,ch}}\left(\nu\right)G_{\mathrm{u,B,ch}}\left(\Omega,\Omega_o\right)\mathrm{d}\nu\mathrm{d}\Omega} \\
& + r_{\mathrm{l,B,ch}} \frac{\int_{\Omega_A}\int_{-\infty}^{\nu_{\mathrm{lo}}} I\left(\nu,\Omega,\mathbf{x}\right)\Phi_{\mathrm{l,B,ch}}\left(\nu\right)G_{\mathrm{l,B,ch}}\left(\Omega,\Omega_o\right)\mathrm{d}\nu\mathrm{d}\Omega}{\int_{\Omega_A}\int_{-\infty}^{\nu_{\mathrm{lo}}} \Phi_{\mathrm{l,B,ch}}\left(\nu\right)G_{\mathrm{l,B,ch}}\left(\Omega,\Omega_o\right)\mathrm{d}\nu\mathrm{d}\Omega} \\
& + \sum_{\mathrm{sb=l}}^{\mathrm{u}} r''_{\mathrm{sb,B,ch}} \left\{ \left(\prod_{k=1}^{3} \rho_{\mathrm{R}}^{k} \right) \eta_{\mathrm{sb,B}}^{1} \left(1 - \eta_{\mathrm{sb,B}}^{\mathrm{AA}}\right) P_{\mathrm{sb,B}}^{\mathrm{SA}} \right. \\
& + \sum_{k=1}^{3} \left(\prod_{j=k+1}^{3} \rho_{\mathrm{R}}^{j} \right) \left[\left(1 - \rho_{\mathrm{R}}^{k}\right) \eta_{\mathrm{sb,B}}^{k} P_{\mathrm{sb,B}}^{\mathrm{O}k} \right. \\
& \left. \left. + \left(\eta_{\mathrm{sb,B}}^{k+1} - \eta_{\mathrm{sb,B}}^{k}\right) P_{\mathrm{sb,B}}^{\mathrm{S}k} \right] \right\}
\end{aligned}
$$

FORWARD MODEL DEFINITION

FORWARD MODEL DEFINITION

$$r_{\mathrm{u,B,ch}} = \eta^{\mathrm{A}}_{\mathrm{u,B}}\, \rho^{A}_{\mathrm{R}}\, r'_{\mathrm{u,B,ch}},$$

$$r'_{\mathrm{u,B,ch}} = \frac{\eta^{A}_{\mathrm{u,B}}\, r''_{\mathrm{u,B,ch}}}{\eta^{A}_{\mathrm{u,B}}\, r''_{\mathrm{u,B,ch}} + \eta^{A}_{\mathrm{l,B}}\, r''_{\mathrm{l,B,ch}}},$$

$$r''_{\mathrm{u,B,ch}} = \frac{\int_{\nu_{\mathrm{lo}}}^{\infty} \Phi_{\mathrm{B,ch}}(\nu)\, \mathrm{d}\nu}{\int_{-\infty}^{\infty} \Phi_{\mathrm{B,ch}}(\nu)\, \mathrm{d}\nu}$$

$$r_{\mathrm{l,B,ch}} = \eta^{A}_{\mathrm{l,B}}\, \rho^{A}_{\mathrm{R}}\, r'_{\mathrm{l,B,ch}},$$

$$r'_{\mathrm{l,B,ch}} = \frac{\eta^{A}_{\mathrm{l,B}}\, r''_{\mathrm{l,B,ch}}}{\eta^{A}_{\mathrm{u,B}}\, r''_{\mathrm{u,B,ch}} + \eta^{A}_{\mathrm{l,B}}\, r''_{\mathrm{l,B,ch}}},$$

$$r''_{\mathrm{l,B,ch}} = \frac{\int_{-\infty}^{\nu_{\mathrm{lo}}} \Phi_{\mathrm{B,ch}}(\nu)\ \mathrm{d}\nu}{\int_{-\infty}^{\infty} \Phi_{\mathrm{B,ch}}(\nu)\ \mathrm{d}\nu}$$

$$\eta^{\mathrm{A}}_{\mathrm{sb,B}} = \eta^{\mathrm{AA}}_{\mathrm{sb,B}} \prod_{k=1}^{3} \eta^{k}_{\mathrm{sb,B}}$$

$$\eta^{A}_{\mathrm{sb,B}} = \frac{1}{4\pi} \int_{\Omega_A} G_{\mathrm{sb,B,ch}}(\Omega, \Omega_o)\ \mathrm{d}\Omega$$

APPROXIMATIONS

- Neglect scan motion. A representative "worst case" scenario: channel 1, band 2, tropics, where UTH has a high vertical gradient indicates a maximum error less than 0.06 K.
- Neglect frequency dependence of the antenna pattern within a band. *We can extend this to channel which will be done for the wide band filters.*
- Neglect scan dependence of antenna pattern.
- Neglect azimuthal (cross-track) radiance variability. The cross-track resolution is $\leq$ 6 km so this should be a good approximation.

FORWARD MODEL HIERARCHY

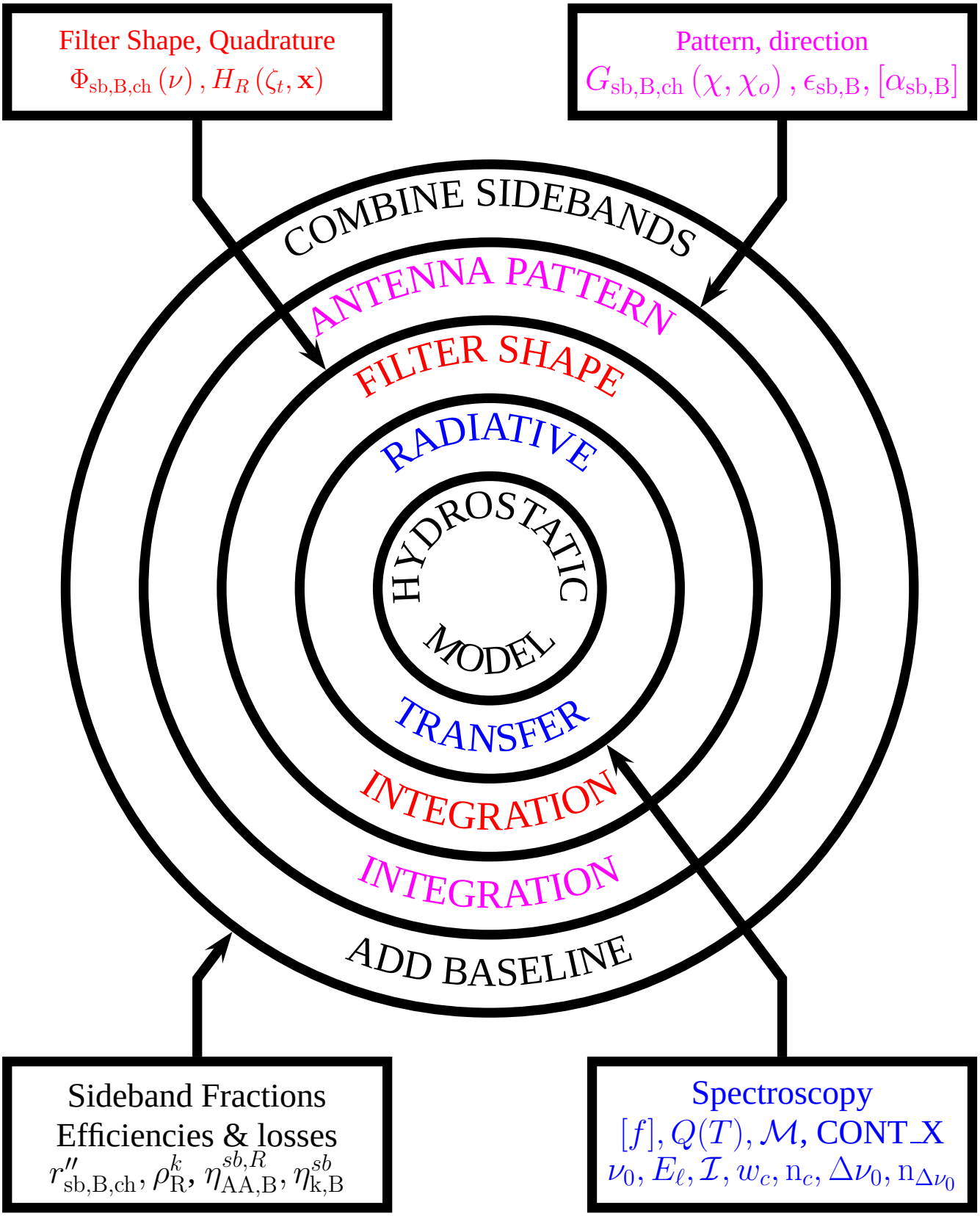

FORWARD MODEL DESCRIPTION

SCAN SMOOTHING

- Assumes pointing is center-of-scan position.
- This treatment is exact if $\frac{\mathrm{d}^2 I}{\mathrm{d}\chi^2} = 0$
- Error caused by using center-of-scan versus a fully smeared treatment for a representative "worst case" scenario should be less than 0.06 K.
- May add a $\Delta\chi$ boxcar ($\frac{\sin x}{x}$) convolution at a later date.

FORWARD MODEL DESCRIPTION

ANTENNA PATTERN INTEGRATION

- Same algorithm as that used for UARS.

$$I_{\mathrm{sb,B,ch}}\left(\chi_o - \epsilon_{\mathrm{sb,B}}, \mathbf{x}\right) = \frac{\int_{-0.1}^{0.1} I_{\mathrm{sb,B,ch}}\left(\chi, \mathbf{x}\right) G_{\mathrm{sbB,ch}}\left(\chi, \chi_o\right) \mathrm{d}\chi}{\int_{-0.1}^{0.1} G_{\mathrm{sbB,ch}}\left(\chi, \chi_o\right) \mathrm{d}\chi},$$

  is evaluated using,

$$\mathcal{F}t\left(I_{\mathrm{sb,B,ch}}\left(\chi_o, \mathbf{x}\right)\right) = \mathcal{F}t\left(I_{\mathrm{sb,B,ch}}\left(\chi, \mathbf{x}\right)\right) \times \mathcal{F}t\left(\mathcal{MI}\left[G_{\mathrm{sbB,ch}}\left(\chi, \chi_o\right)\right]\right)$$

  Where $\mathcal{MI}\left[\,\right]$ means use the mirror image of the measured pattern.

- The Fourier transform produces radiances by χ_o. The radiometer offset is included by interpolation to $\chi_o - \epsilon_{\mathrm{sb,B}}$.

- See Eqn. (4.57) in *Forward Model Algorithm Theoretical Basis Document* for a modified $\epsilon_{\mathrm{sb,B}}$ which includes both $\epsilon_{\mathrm{sb,B}}$ and $\alpha_{\mathrm{sb,B}}$ and other attitude misalignments. This added complexity was not considered useful for UARS processing.

- Special analytical derivative algorithm developed (see Eqn. (6.4) in *Forward Model Algorithm Theoretical Basis Document*)
  - Needed for temperature. Allows for temperature dependence of the HPBW with respect to tangent pressure. Although more complicated the analytical form is faster than finite difference method.
  - Other radiance derivatives can substitute I with $\frac{\mathrm{d}I}{\mathrm{d}x}$ above.

FILTER SHAPE INTEGRATION

- Algorithm for 25, 11 channel filter banks and wide band filters.
  - Integral

$$I_{\mathrm{u,B,ch}}\left(\chi,\mathbf{x}\right)=\frac{\int_{\nu_{\mathrm{lo}}}^{\infty}I\left(\nu,\chi,\mathbf{x}\right)\Phi_{\mathrm{u,B,ch}}\left(\nu\right)\mathrm{d}\nu}{\int_{\nu_{\mathrm{lo}}}^{\infty}\Phi_{\mathrm{u,B,ch}}\left(\nu\right)\mathrm{d}\nu}$$

$$I_{\mathrm{l,B,ch}}\left(\chi,\mathbf{x}\right)=\frac{\int_{-\infty}^{\nu_{\mathrm{lo}}}I\left(\nu,\chi,\mathbf{x}\right)\Phi_{\mathrm{l,B,ch}}\left(\nu\right)\mathrm{d}\nu}{\int_{-\infty}^{\nu_{\mathrm{lo}}}\Phi_{\mathrm{l,B,ch}}\left(\nu\right)\mathrm{d}\nu}$$

  - Radiances for each $\chi(\zeta_t)$ are computed at frequencies specified by the quadrature grid $H_R\left(\zeta_t,\mathbf{x}\right)$.
    - The grid ensures accurate interpolation to within 0.2 K for any frequency.
    - Weak species are substantially inflated (10$\times$ or more) when establishing the quadrature grid.
    - Using the quadrature grid, radiances are interpolated to 161 equally spaced frequency points spanning a channel.
  - Filter shape data is also interpolated to the same 161 points.
  - Integration is executed with Simpson's rule.
  - Currently, the same algorithm is used for DACS but we want to replace with ...

FORWARD MODEL DESCRIPTION

- Algorithm for DACS (courtesy of M. Schwartz).
  - Frequency grid is $k = -2N, 4N, \Delta\nu = 12.5/256$ MHz, where $k = 0$ is the DACS local oscillator frequency and we are oversampling the channel frequency separations by 2.
  - Weight by pre-filter,

$$\hat{I}_{\mathrm{sb,B}}\left(\nu_k, \chi, \mathbf{x}\right) = \Phi_{\mathrm{sb,B}}\left(\nu_k\right) I\left(\nu_k \chi, \mathbf{x}\right).$$

  - Alias correction,

$$\begin{aligned}
\hat{I}'_{\mathrm{sb,B}}\left(\nu_k, \chi, \mathbf{x}\right) &= \hat{I}_{\mathrm{sb,B}}\left(\nu_k, \chi, \mathbf{x}\right) + \hat{I}_{\mathrm{sb,B}}\left(\nu_{-k}, \chi, \mathbf{x}\right), \\
&+ \hat{I}_{\mathrm{sb,B}}\left(\nu_{4N-k}, \chi, \mathbf{x}\right), k = 1, 2N-1, \\
\hat{I}'_{\mathrm{sb,B}}\left(\nu_0, \chi, \mathbf{x}\right) &= \hat{I}_{\mathrm{sb,B}}\left(\nu_0, \chi, \mathbf{x}\right) + \frac{1}{2}\hat{I}_{\mathrm{sb,B}}\left(\nu_{4N}, \chi, \mathbf{x}\right), \\
\hat{I}'_{\mathrm{sb,B}}\left(\nu_{2N}, \chi, \mathbf{x}\right) &= \hat{I}_{\mathrm{sb,B}}\left(\nu_{2N}, \chi, \mathbf{x}\right) + \frac{1}{2}\hat{I}_{\mathrm{sb,B}}\left(\nu_{-2N}, \chi, \mathbf{x}\right).
\end{aligned}$$

  - Convolve with DACS filter shape, $\frac{\sin x}{x}$,

$$\hat{\mathrm{I}}'_{\mathrm{sb,B},j} = \frac{1}{2N}\sum_{k=0}^{2N} \hat{I}'_{\mathrm{sb,B}}\left(\nu_k, \chi, \mathbf{x}\right) \cos\frac{\pi k j}{2N}, j = 0, N,$$

$$\begin{aligned}
I_{\mathrm{sb,B,ch}}\left(\chi, \mathbf{x}\right) = &\left(\hat{\mathrm{I}}'_{\mathrm{sb,B},0} + (-1)^{\mathrm{ch}}\,\hat{\mathrm{I}}'_{\mathrm{sb,B},N}\right. \\
&\left. + \; 2\sum_{j=1}^{N-1} \hat{\mathrm{I}}'_{\mathrm{sb,B},j} \cos\frac{\pi j \mathrm{ch}}{N}\right) / \hat{\Phi}_{\mathrm{sb,B,ch}}, \mathrm{ch} = 0, 128.
\end{aligned}$$

- $\hat{\Phi}_{\mathrm{sb,B,ch}}$ is a normalization of the pre-filter for each DACS channel and is evaluated using the algorithm above but setting $I\left(\nu_k\chi, \mathbf{x}\right) = 1$. This will be precomputed.
- Algorithm needs to be added to existing code.

• Radiance derivatives can substitute I with $\frac{\mathrm{d}I}{\mathrm{d}x}$ above.

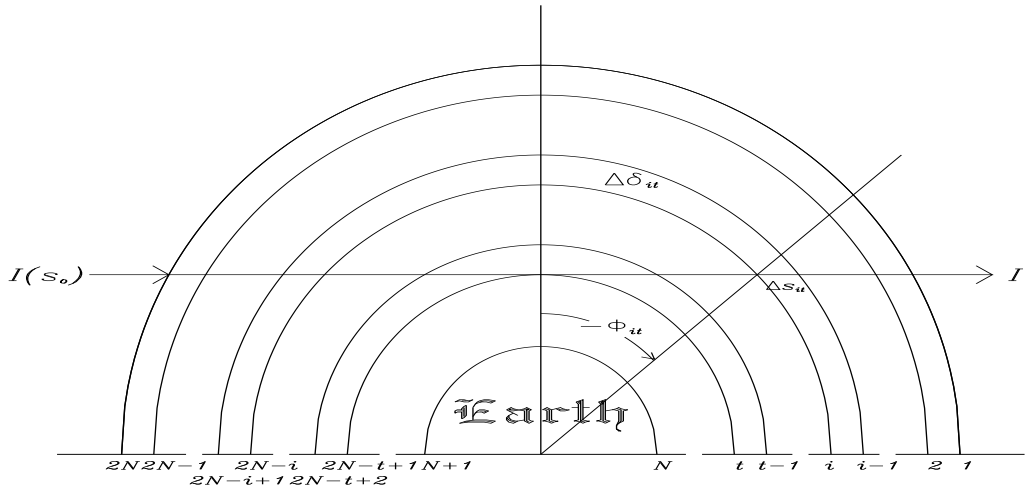

Figure 1: Layering notation for discrete radiative transfer calculations. Note that each line of sight path is associated with a tangent pressure, t, and a pressure/angle index, i. The atmospheric state can be different along an isobar curve (e.g. $i \rightarrow 2N - i$).

RADIATIVE TRANSFER

- Discrete radiative transfer equation,

$$I\left(\nu, \chi\left(\zeta_t\right), \mathbf{x}\right) = \sum_{i=1}^{t} \Delta B_i \mathcal{T}_i + \sum_{i=2N-t+1}^{2N} \Delta B_i \mathcal{T}_i.$$

- Path differential temperature,

$$\begin{aligned} \Delta B_i &= \frac{B_{i+1} - B_{i-1}}{2}, \\ \Delta B_1 &= \frac{B_1 + B_2}{2}, \text{and} \\ \Delta B_{2N} &= I_o - \frac{B_{2N-1} + B_{2N}}{2}. \end{aligned}$$

FORWARD MODEL DESCRIPTION

- Path transmission function,

$$
\begin{aligned}
\text{for } i &\leq t, \\
\mathcal{T}_1 &= 1, \\
\mathcal{T}_i &= \exp\left\{-\sum_{j=2}^{i}\Delta\delta_{j\to j-1}\right\}, \\
\text{for } i &= 2N-t+1, \\
\mathcal{T}_{2N-t+1} &= \Upsilon\mathcal{T}_t, \text{and} \\
\text{for } i &> 2N-t+1, \\
\mathcal{T}_i &= \mathcal{T}_{2N-t+1}\exp\left\{-\sum_{j=2N-t+2}^{i}\Delta\delta_{j-1\to j}\right\}.
\end{aligned}
$$

- Path incremental opacity,

$$\Delta\delta_{i\to i-1} = \sum_{k=1}^{NS}\Delta\delta^k_{i\to i-1}, \text{and}$$

$$
\begin{aligned}
\Delta\delta^k_{i\to i-1} &= \frac{\Delta s^{\text{refr}}_{i\to i-1}}{\Delta s_{i\to i-1}} \\
&\times \int_{\zeta_i}^{\zeta_{i-1}}\sum_{l}^{\text{NH}^k}\sum_{m}^{\text{NP}^k}\sum_{n}^{\text{NF}^k} f^k_{lmn}\eta^k_l(\zeta)\,\eta^k_m(\phi)\,\eta^k_n(\nu) \\
&\times \beta^k(P(\zeta), T(\zeta), \nu).\frac{\mathrm{d}s}{\mathrm{d}h}\frac{\mathrm{d}h}{\mathrm{d}\zeta}\mathrm{d}\zeta
\end{aligned}
$$

- Layering is automatically determined by the vertical representation bases of the constituents, $\eta^k_l(\zeta)$.

- Tangents are computed for each layer.
- Integration is done semi-adaptively, either 3-point Gauss-Legendre with singularity removal or simple rectangle. The derivative of the opacity with respect to path with a user supplied accuracy target determines the integration method used for each layer.
- Features exist for oversampling the representation basis and changing the number of Gauss-Legendre points. Currently we oversample the troposphere/lower stratosphere by 2.

• Cross section function for molecule k,

$$\beta^k\left(P\left(\zeta\right),T\left(\zeta\right),\nu\right)=\left[f\right]\sqrt{\frac{\ln 2}{\pi}}\frac{10^{-6}}{k}\frac{P}{Tw_d}$$
$$\times\left(\sum_j^{\text{lines}}10^{\mathcal{S}_j}\text{LineShape}\left(x_j,y_j,z_j\right)\right),$$

where

$$\mathcal{S}_j = \mathcal{I}_j\left(300\right)-\text{Q_LOG}\left(Q,T\right)+\frac{E\ell_j}{1.600386}\left(\frac{1}{300}-\frac{1}{T}\right)$$
$$+\log\left[\frac{1-\exp\left\{-\nu_j/\left(20836.74T\right)\right\}}{1-\exp\left\{-\nu_j/6251022.0\right\}}\right],$$

FORWARD MODEL DESCRIPTION

$$\mathrm{LineShape}\left(x_j, y_j, z_j\right) =$$

$$\left(\frac{\nu}{\nu_j}\right)^2 \left(\frac{1}{\pi}\int_{-\infty}^{\infty} \frac{\left(y_j - Y_j\left(x_j - t\right)\right)\exp\left\{-t^2\right\}}{y_j^2 + \left(x_j - t\right)^2}\mathrm{d}t\right.$$

$$\left. + \frac{1}{\sqrt{\pi}}\frac{y_j - Y_j z_j}{z_j^2 + y_j^2}\right),$$

$$\begin{aligned}
x_j &= \frac{\sqrt{\ln 2}\left(\nu_j - \nu\right)}{w_d}, \\
y_j &= \frac{\sqrt{\ln 2} w_{cj} P}{w_d}\left(\frac{300}{T}\right)^{n_{cj}}, \\
z_j &= \frac{\sqrt{\ln 2}\left(\nu_j + \nu\right)}{w_d}, \\
\nu_j &= \nu_{0j} + \Delta\nu_{0j} P\left(\frac{300}{T}\right)^{n_{\Delta\nu_{0j}}}, \text{and} \\
Y_j &= P\left(\delta_j\left(\frac{300}{T}\right)^{n_{\delta j}} + \gamma_j\left(\frac{300}{T}\right)^{n_{\gamma j}}\right)
\end{aligned}$$

- Spectroscopic derivatives of $\beta^k\left(P\left(\zeta\right), T\left(\zeta\right), \nu\right)$ can be evaluated.
- Radiance derivatives are computed analytically with

$$\frac{\mathrm{d}I\left(\nu, \chi\left(\zeta_t\right), \mathbf{x}\right)}{\mathrm{d}x_k} = \sum_{i=1}^{t} \mathcal{Q}_i \mathcal{T}_i + \sum_{i=2N-t+1}^{2N} \mathcal{Q}_i \mathcal{T}_i,$$

where

$$\mathcal{Q}_i = \frac{\partial \Delta B_i}{\partial x_k} - \Delta B_i \mathcal{W}_i,$$

and, $\mathcal{W}_i$ is the transmittance derivative given by

$$\begin{aligned}
\mathcal{W}_1 &= 0, \\
\text{for } i &\leq t, \\
\mathcal{W}_i &= \mathcal{W}_{i-1} + \frac{\partial \Delta\delta_{i\to i-1}}{\partial x_k}, \\
\mathcal{W}_{2N-t+1} &= \mathcal{W}_t, \text{and} \\
\text{for } i &> 2N - t + 1, \\
\mathcal{W}_i &= \mathcal{W}_{i-1} + \frac{\partial \Delta\delta_{i-1\to i}}{\partial x_k}.
\end{aligned}$$

- Analytical derivatives are much faster than finite-difference because most $\frac{\partial \Delta\delta_{i-1\to i}}{\partial x_k}$ are zero and can avoid calculating them.

FORWARD MODEL DESCRIPTION

HYDROSTATIC MODEL

- This is the heart of the 2-D radiative transfer model.
- Hydrostatic function,

$$h(\zeta,\phi) = \frac{g_o \overset{\star}{R}{}_o^2}{g_o \overset{\star}{R}_o - k \ln 10 \sum_l^{\mathrm{NH^T}} \sum_m^{\mathrm{NP}^T} \left(f_{lm}^T \eta_m^T(\phi) P_l \right) - \overset{\star}{R}_o + R_o - R^{\oplus}},$$

where,

$$P_l = \int_{\zeta_o}^{\zeta} \frac{\eta_l^T(\zeta)}{\mathcal{M}(\zeta)} \mathrm{d}\zeta,$$
$$g_o = -\mid \vec{\nabla} U_r(R_o,\phi_o) \mid, \text{and}$$
$$\overset{\star}{R}_o = \frac{2 g_o}{-(\partial g/\partial R)_{R=R_o}}.$$

- A vertical profile of $h(\zeta,\phi)$ is computed for each temperature ϕ basis point.
- $\frac{\mathrm{d}h}{\mathrm{d}\zeta}$, $\frac{\mathrm{d}h}{\mathrm{d}T_{lm}}$ computed also.
- Using the matrix of $h(\zeta,\phi)$, path quantities, h, ϕ, $\frac{\mathrm{d}h}{\mathrm{d}\zeta}$, and temperature derivatives are determined for each ray traced through the atmosphere having a tangent ζ_t and ϕ_t.
  - I assume an equivalent Earth sphere representation where the local radius matches the ellipsoid curva-

ture. The center of this sphere is slightly displaced from the ellipsoid center.

- Getting the path quantities is an iterative process. Fortunately it is not a time consuming process at present.
- Large temperature gradients will cause larger errors because the maximum tangent pressure will be displaced from the tangent while the integration assumes pressure monotonically increases with decreasing height. This is a limitation of having pressure be the independent coordinate on a uniform grid.
- Rays are traced straight and neglect curvature due to refraction. The inputted ϕ_t should be corrected for refraction therefore the consequence of this approximation is that path ϕ will accumulate some error as one moves farther from the limb tangent.

• Now that we have ϕ for the traced limb ray we can evaluate the state along that ray and compute radiances fully incorporating horizontal and vertical gradients.

FORWARD MODEL DESCRIPTION

EFFICIENCY ENHANCEMENTS

- Semi-adaptive integration, already implemented and speeds the calculation by a factor of 2–3.
- Prefrequency averaging approximation for weak species.
  - Used for processing some UARS bands.
  - Filter-average the species cross-section and store in look-up table as function of ζ and T.
  - Do a full filter-averaged radiative transfer calculation on the strong signal species.
  - After filter-averaging, add weak species contributions by channel.
  - Error in this approach should behave as the goodness of an approximation where the radiative transfer calculation is a first order expansion in the weak species linearized at $f_{lmn}^{k} = 0$.
  - This approximation can greatly simplify and reduce the number of points in the $H_R(\zeta_t, \mathbf{x})$ quadrature grid, especially for those bands that have a mixture of weak and strong lines. The speed enhancement will be proportional to the ratio of points in the quadrature grids with and without the PFA approximation.
  - Not yet implemented in the code.
- Dynamic basis selection.

FORWARD MODEL DESCRIPTION

- Using derivatives from an L2PC file and an atmospheric state, compute the absolute first-order contribution to the radiances.
- Ignore basis breakpoints whose absolute first-order contributions are less than a user supplied threshold value.
- Run the modified basis through the automatic integration grid selector.
- Efficiency gains would be similar to semi-adaptive approach except it would make the calculation behave fully adaptive.
- Accuracy depends on the quality of L2PC derivatives for the state in question.
- My guess is that this would speed things up by a factor of 2.
- Not yet implemented in the code.

WHAT IS CALIBRATION DATA?

- Inputs needed by the forward model that are not part of the statevector.
- Instrument, measurement, and computational properties that characterize the measurement system, not expected not to change over the course of the mission and is determined before launch.
  - signal strengths,
  - spectral resolution, and
  - spatial resolution.
- Actively measured (and changing) quantities, such as channel noise are not part of the calibration data set.

CALIBRATION DATA

Table 1: Calibration Parameters

Parameter	Priority	Symbol	Responsible Person	Current Status	Launch ready
SPECTROSCOPY					
Catalogue List	1	$\mathcal{C}$	WGR	In progress	01-May-03
Molecule data					
isotope fraction	1	$[f]$	WGR	L & S, WHF	Ready
Partition Function	1	$Q(T)$	WGR	JPL Catalogue	Ready
Mass	1	$\mathcal{M}$	WGR	WHF	Ready
continuum	1	CONT_X	FCD	JRP	TBD
Line $\times$ line data					
frequency	1	ν_0	WGR	JPL Catalogue	Ready
Lower state energy	1	E_ℓ	WGR	JPL Catalogue	Ready
strength	1	$\mathcal{I}$	WGR	JPL Catalogue	Ready

Continued on next page

CALIBRATION DATA

Parameter	Priority	Symbol	Responsible Person	Current Status	Launch ready
^{81}BrO(625 GHz)	1				
Width		w_c, n_c	BJD	Measured	Ready
Shift		$\Delta\nu_0$, $n_{\Delta\nu_0}$	BJD	Measured	Ready
^{81}BrO(650 GHz)	1				
Width		w_c, n_c	BJD	Measured	Ready
Shift		$\Delta\nu_0$, $n_{\Delta\nu_0}$	BJD	Measured	Ready
CH_3CN(184 GHz)	2				
Width		w_c, n_c	BJD	Guess	15-Mar-03
Shift		$\Delta\nu_0$, $n_{\Delta\nu_0}$	BJD	Ignored	15-Mar-03
CH_3CN(202 GHz)	2				
Width		w_c, n_c	BJD	Guess	15-Mar-03
Shift		$\Delta\nu_0$, $n_{\Delta\nu_0}$	BJD	Ignored	15-Mar-03
CH_3CN(625 GHz)	2				
Width		w_c, n_c	BJD	Guess	15-Mar-03
Shift		$\Delta\nu_0$, $n_{\Delta\nu_0}$	BJD	Ignored	15-Mar-03

Continued on next page

CALIBRATION DATA

Parameter	Priority	Symbol	Responsible Person	Current Status	Launch ready
CH_3CN(660 GHz)	2				
Width		w_c, n_c	BJD	Guess	15-Mar-03
Shift		$\Delta\nu_0$, $n_{\Delta\nu_0}$	BJD	Ignored	15-Mar-03
CO(231 GHz)	2				
Width		w_c, n_c	BJD	Guess	01-Feb-03
Shift		$\Delta\nu_0$, $n_{\Delta\nu_0}$	BJD	Ignored	01-Feb-03
^{35}ClO(204 GHz)	1				
Width		w_c, n_c		JJO	Ready
Shift		$\Delta\nu_0$, $n_{\Delta\nu_0}$		NA	Ready
^{35}ClO(650 GHz)	1				
Width		w_c, n_c		JJO	Ready
Shift		$\Delta\nu_0$, $n_{\Delta\nu_0}$		NA	Ready
H^{35}Cl(626 GHz)	1				
Width		w_c, n_c	BJD	Measured	Ready
Shift		$\Delta\nu_0$, $n_{\Delta\nu_0}$	BJD	Measured	Ready

Continued on next page

CALIBRATION DATA

Parameter	Priority	Symbol	Responsible Person	Current Status	Launch ready
$H^{37}Cl$(625 GHz)	1				
Width		w_c, n_c	BJD	Measured	Ready
Shift		$\Delta\nu_0$, $n_{\Delta\nu_0}$	BJD	Measured	Ready
HCN(177 GHz)	2				
Width		w_c, n_c	BJD	Guess	01-Oct-03
Shift		$\Delta\nu_0$, $n_{\Delta\nu_0}$	BJD	Ignored	01-Oct-03
H_2O(183 GHz)	1				
Width		w_c, n_c		AB & TMG	Ready
Shift		$\Delta\nu_0$, $n_{\Delta\nu_0}$		HCP	Ready
H_2O(2.532 THz)	1				
Width		w_c, n_c	BJD	HITRAN	01-Aug-03
Shift		$\Delta\nu_0$, $n_{\Delta\nu_0}$	BJD	Ignored	01-Aug-03
HNO_3(181 GHz)	1				
Width		w_c, n_c	BJD?	Guess	?
Shift		$\Delta\nu_0$, $n_{\Delta\nu_0}$	BJD?	Ignored	?

Continued on next page

CALIBRATION DATA

Parameter	Priority	Symbol	Responsible Person	Current Status	Launch ready
HNO_3(206 GHz)	1				
Width		w_c, n_c		TMG	Ready
Shift		$\Delta\nu_0$, $n_{\Delta\nu_0}$		NA	Ready
HNO_3(626 GHz)	2				
Width		w_c, n_c	BJD	Guess	01-Oct-03
Shift		$\Delta\nu_0$, $n_{\Delta\nu_0}$	BJD	Ignored	01-Oct-03
HNO_3(633 GHz)	2				
Width		w_c, n_c	BJD	Guess	01-Oct-03
Shift		$\Delta\nu_0$, $n_{\Delta\nu_0}$	BJD	Ignored	01-Oct-03
HNO_3(651 GHz)	2				
Width		w_c, n_c	BJD	Guess	01-Oct-03
Shift		$\Delta\nu_0$, $n_{\Delta\nu_0}$	BJD	Ignored	01-Oct-03
HNO_3(660 GHz)	2				
Width		w_c, n_c	BJD	Guess	01-Oct-03
Shift		$\Delta\nu_0$, $n_{\Delta\nu_0}$	BJD	Ignored	01-Oct-03

Continued on next page

CALIBRATION DATA

Parameter	Priority	Symbol	Responsible Person	Current Status	Launch ready
$HO^{35}Cl$(636 GHz)	2				
Width		w_c, n_c	BJD	Guess	15-Mar-03
Shift		$\Delta\nu_0$, $n_{\Delta\nu_0}$	BJD	Ignored	15-Mar-03
$HO^{37}Cl$(2.515 THz)	2				
Width		w_c, n_c	BJD	Guess	01-Aug-03
Shift		$\Delta\nu_0$, $n_{\Delta\nu_0}$	BJD	Ignored	01-Aug-03
HO_2(625 GHz)	1				
Width		w_c, n_c	BJD	Measured, in progress	TBD
Shift		$\Delta\nu_0$, $n_{\Delta\nu_0}$	BJD	?	TBD
HO_2(650 GHz)	1				
Width		w_c, n_c	BJD	Measured, in progress	TBD
Shift		$\Delta\nu_0$, $n_{\Delta\nu_0}$	BJD	?	TBD
HO_2(660 GHz)	1				
Width		w_c, n_c	BJD	Measured, in progress	TBD
Shift		$\Delta\nu_0$, $n_{\Delta\nu_0}$	BJD	?	TBD

Continued on next page

CALIBRATION DATA

Parameter	Priority	Symbol	Responsible Person	Current Status	Launch ready
N_2O(201 GHz)	1				
Width		w_c, n_c	WGR	AH, but needs updating	15-Jan-03
Shift		$\Delta\nu_0$, $n_{\Delta\nu_0}$		NA	Ready
N_2O(653 GHz)	1				
Width		w_c, n_c	WGR	AH, but needs updating	15-Jan-03
Shift		$\Delta\nu_0$, $n_{\Delta\nu_0}$		NA	Ready
OH(2.510 THz)	1				
Width		w_c, n_c	BJD	KP	01-Aug-03
Shift		$\Delta\nu_0$, $n_{\Delta\nu_0}$	BJD	Ignored	01-Aug-03
OH(2.514 THz)	1				
Width		w_c, n_c	BJD	KP	01-Aug-03
Shift		$\Delta\nu_0$, $n_{\Delta\nu_0}$	BJD	Ignored	01-Aug-03

Continued on next page

CALIBRATION DATA

Parameter	Priority	Symbol	Responsible Person	Current Status	Launch ready
O_2(118 GHz)	1				
Width		w_c, n_c		HMP	Ready
Shift		$\Delta\nu_0$, $n_{\Delta\nu_0}$		AFK	Ready
O_2(2.502 THz)	1				
Width		w_c, n_c	BJD	KP	01-Aug-03
Shift		$\Delta\nu_0$, $n_{\Delta\nu_0}$	BJD	Ignored	01-Aug-03
$O^{18}O$(234 GHz)	1				
Width		w_c, n_c	BJD	Guess	15-Jan-03
Shift		$\Delta\nu_0$, $n_{\Delta\nu_0}$	BJD	Ignored	15-Jan-03
O_3(184 GHz)	2				
Width		w_c, n_c		JJO	Ready
Shift		$\Delta\nu_0$, $n_{\Delta\nu_0}$		NA	Ready
O_3(206 GHz)	1				
Width		w_c, n_c		JJO	Ready
Shift		$\Delta\nu_0$, $n_{\Delta\nu_0}$		NA	Ready

Continued on next page

CALIBRATION DATA

Parameter	Priority	Symbol	Responsible Person	Current Status	Launch ready
O_3(240 GHz)	1				
Width		w_c, n_c	BJD	Measured	Ready
Shift		$\Delta\nu_0$, $n_{\Delta\nu_0}$	BJD	Measured	Ready
O_3(625 GHz)	1				
Width		w_c, n_c	BJD	Measured	Ready
Shift		$\Delta\nu_0$, $n_{\Delta\nu_0}$	BJD	Measured	Ready
O_3(2.509 THz)	1				
Width		w_c, n_c	BJD	HITRAN	01-Aug-03
Shift		$\Delta\nu_0$, $n_{\Delta\nu_0}$	BJD	ignored	01-Aug-03
O_3(2.543 THz)	1				
Width		w_c, n_c	BJD	HITRAN	01-Aug-03
Shift		$\Delta\nu_0$, $n_{\Delta\nu_0}$	BJD	ignored	01-Aug-03
SO_2(200 GHz)	3				
Width		w_c, n_c	BJD	Guess	TBD
Shift		$\Delta\nu_0$, $n_{\Delta\nu_0}$	BJD	ignored	15-Mar-03

Continued on next page

CALIBRATION DATA

Parameter	Priority	Symbol	Responsible Person	Current Status	Launch ready
SO_2(204 GHz)	3				
Width		w_c, n_c		CB	Ready
Shift		$\Delta\nu_0$, $n_{\Delta\nu_0}$		NA	Ready
SO_2(660 GHz)	3				
Width		w_c, n_c	BJD	Guess	15-Mar-03
Shift		$\Delta\nu_0$, $n_{\Delta\nu_0}$	BJD	ignored	15-Mar-03

Continued on next page

CALIBRATION DATA

Parameter	Priority	Symbol	Responsible Person	Current Status	Launch ready
INSTRUMENT					
Filters GHz & THz (FB, MB, WB)					
Frequency	1	$\nu_{\mathrm{sb,B,ch}}$	RFJ		Ready
Shapes	1	$\Phi_{\mathrm{sb,B,ch}}(\nu)$	RFJ	Replicated FB 25	01-May-03
(DACS)					
Frequency	1	$\nu_{\mathrm{sb,ch}}$	MJS		Ready
Pre-filter Shapes	1	$\Phi_{\mathrm{sb,B}}(\nu)$	MJS	ignored	01-Feb-03
Normalization	1	$\hat{\Phi}_{\mathrm{sb,B,ch}}$	MJS	NA	01-Feb-03
SB fraction					
GHz	1	$r''_{\mathrm{sb,B,ch}}$	RFJ	pre-environment	01-May-03
THz	1	$r_{\mathrm{sb,B,ch}}$	HMP	pre-environment	01-May-03

Continued on next page

CALIBRATION DATA

Parameter	Priority	Symbol	Responsible Person	Current Status	Launch ready
Filter quadrature					
Non Magnetic	1	$H_R(\zeta_t, \mathbf{x})$	WGR	Preliminary	01-May-03
Magnetic	1	$H_{\mathrm{R1}}(\zeta_t, \mathbf{x})$	MJS	Non-Magnetic	TBD
Antenna Patterns					
GHz	1	$G_{\mathrm{sb,B,ch}}(\chi, \chi_o)$	REC	pre-environment	01-May-03
Note		$G_{\mathrm{sb,B,ch}}(\chi, \chi_o) = G_{\parallel,\mathrm{sb,B,ch}}(\chi, \chi_o) + G_{\perp,\mathrm{sb,B,ch}}(\chi, \chi_o)$			
R1A, R1B	1	$G_{\parallel,\mathrm{l,B,ch}}(\chi, \chi_o)$	REC	ignored	01-May-03
R1A, R1B	1	$G_{\perp,\mathrm{l,B,ch}}(\chi, \chi_o)$	REC	ignored	01-May-03
R1A, R1B	2	$G_{\vert,\mathrm{l,B,ch}}(\chi, \chi_o)$	REC	ignored	TBD
R1A, R1B	2	$G_{\circ,\mathrm{l,B,ch}}(\chi, \chi_o)$	REC	ignored	TBD
THz	1	$G_{\mathrm{B,ch}}(\chi, \chi_o)$	HMP	pre-environment	15-Jan-03
FOV-direction					
GHz	1	$\alpha_{\mathrm{sb,B}}, \epsilon_{\mathrm{sb,B}}$	REC	Pre-environment	01-Feb-03
THz(→GHz)	1	$\alpha_{\mathrm{sb,B}}, \epsilon_{\mathrm{sb,B}}$	REC	Pre-environment	01-Feb-03
THz(R5V→R5H)	1	$\alpha_{\mathrm{sb,B}}, \epsilon_{\mathrm{sb,B}}$	HMP	$\alpha_{\mathrm{sb,B}} = 0, \epsilon_{\mathrm{sb,B}} = 0$	Ready

Continued on next page

CALIBRATION DATA

Parameter	Priority	Symbol	Responsible Person	Current Status	Launch ready
Antenna losses and efficiencies					
GHz	1	$\eta^{\mathrm{AA}}_{\mathrm{sb,B}}, \eta^{k=1,2,3}_{\mathrm{sb,B}}$	REC	ignored	01-Mar-03
GHz	1	$\rho^{k=1,2,3}_{\mathrm{R}}$	REC	ignored	Ready
Notes		$\eta^{\mathrm{A}}_{\mathrm{sb,B}} = \eta^{\mathrm{AA}}_{\mathrm{sb,B}} \prod_{k=1}^{3} \eta^{k}_{\mathrm{sb,B}}$ $\rho^{\mathrm{A}}_{\mathrm{R}} = \prod_{k=1}^{3} \rho^{k}_{\mathrm{R}}$			
Polarization	1	$\xi_{\mathrm{B}=22,26}$	REC	ignored	TBD

Spectral Linewidth Parameters

EOS-MLS Forward Model Meeting
Dec 11-12th 2002

Brian J. Drouin

Overview

- Laboratory
  - New Equipment
  - Apparatus
  - Data Processing
- 640 GHz Band
  - HCl
  - BrO
  - HO_2
  - CH_3CN, HOCl, SO_2
  - HNO_3
  - Summary
- 240 GHz Band
  - O_3
  - CO
  - $O^{18}O$
  - HCN
  - HNO_3
  - Summary
- 2.5 THz Band
  - instrument design
- Timeline
- Acknowledgements

Recent Laboratory Improvements

Thanks to Herschel

WR-40 amplifier
WR-10 detector
WR-10 source module
WR-10 amplifier

Thanks to EOS-Spectroscopy

Radical flow cell, 0.5 meter length
Heating/circulating bath
Static gas cell, 1 meter length inside jacket

Thanks to MLS

Standard flow cell, 0.7 meter length
640 GHz Russian BWO
500+ GHz Planar multiplier

Linewidth Measurement Apparatus

Pressure Gauges 0 - 10 Torr

InSb Bolometer
↓
Modulation Filter
↓
LIA

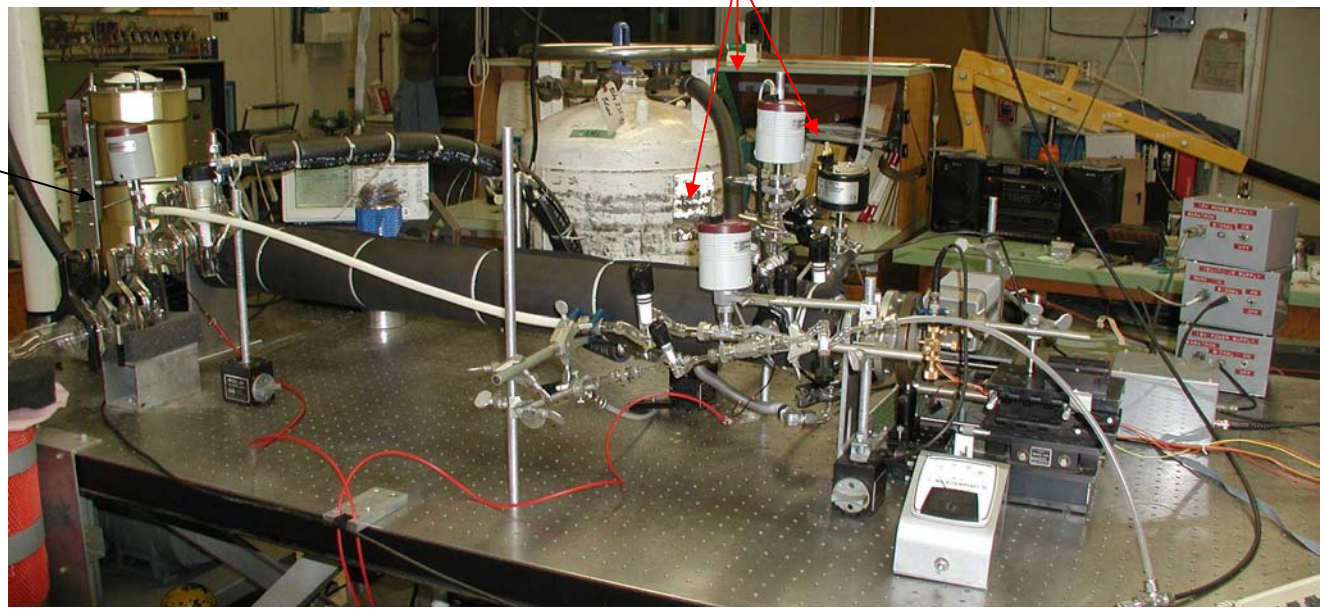

Sweep
12 - 20 GHz
↓
Sextupler
72 - 122 GHz
↓
Harmonic multiplier
x2, x3, x6, x7

Vacuum Pump
24 L/s

Cooling jacket 200 - 350 K
Zeeman coil

Data Processing

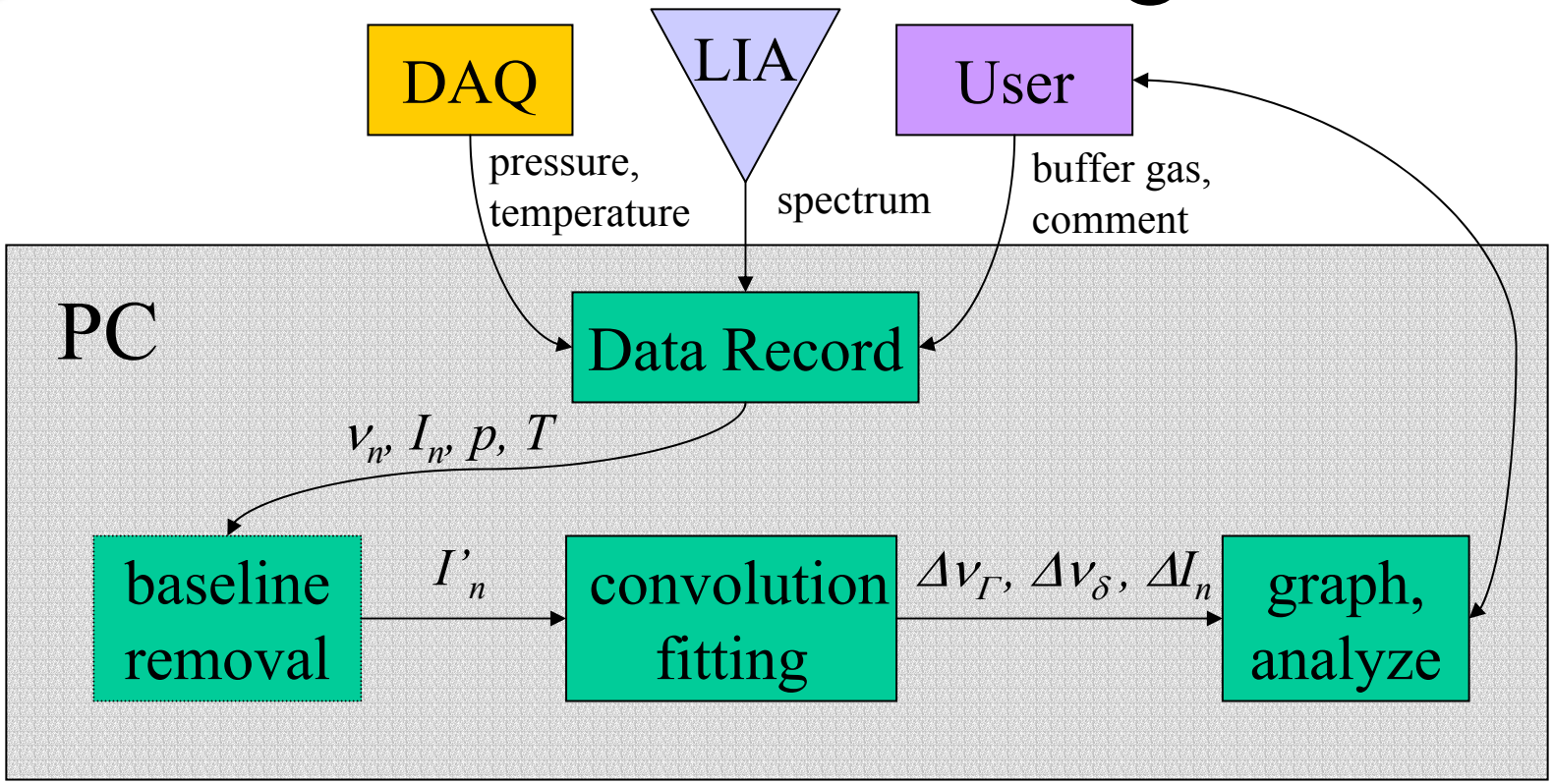

Software has been written for:

Spectrometer control and data recording

Baseline removal and convolution fitting

Graphics and analysis use Excel and SigmaPlot

Lineshape Measurement

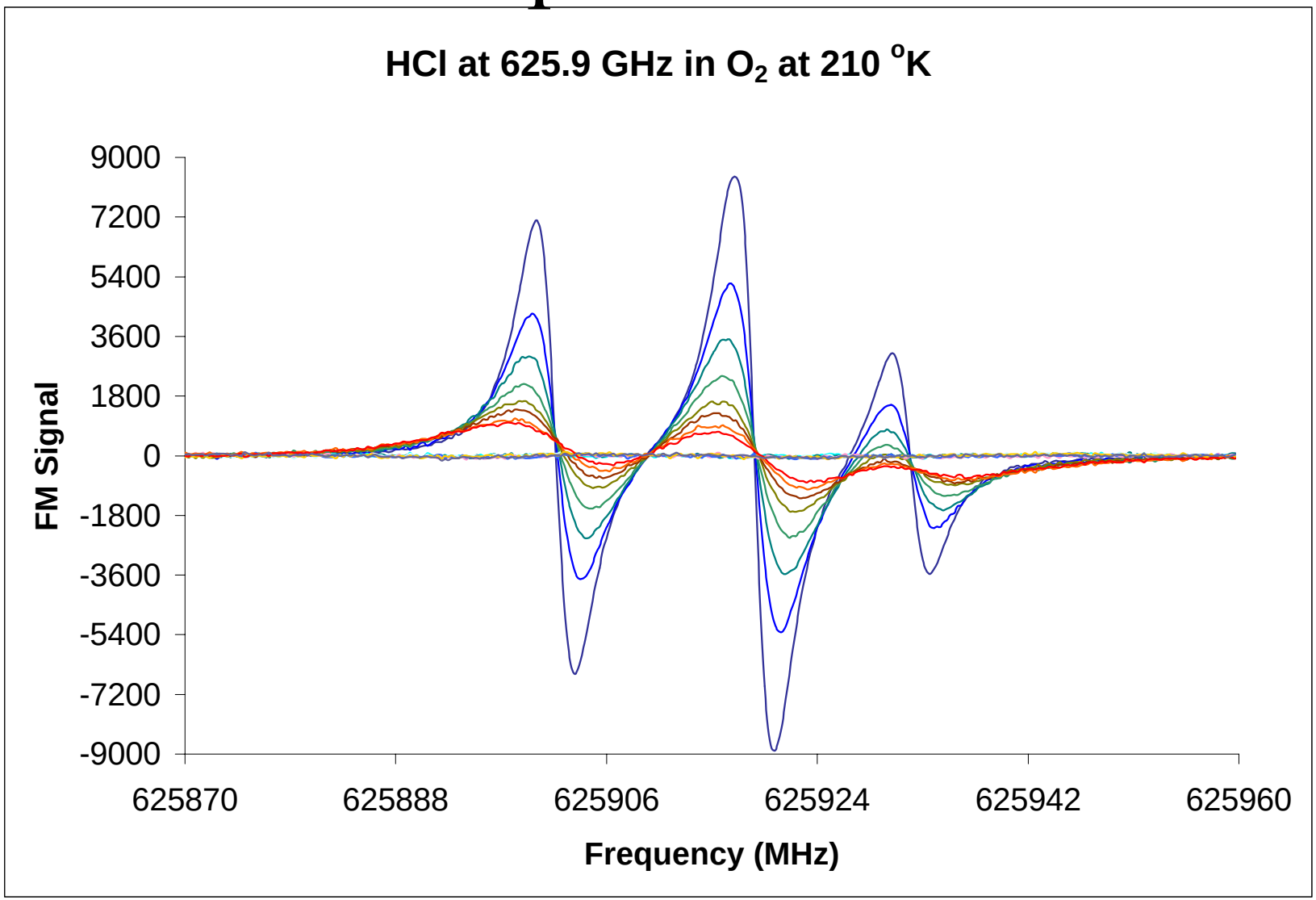

Parametric Fitting of Lineshape Parameters

Fit all measured half-widths
to determine γ_o and n
as well as errors in γ_o, n

Bonus:
Obtain $\chi_{\gamma o,n}$ and
assume $\chi_{\gamma o,p} = \chi_{T,n} = 1$
for calculation of random error in Γ

$$\Gamma(\gamma_o, n, p, T) = \gamma_o p \left[\frac{296}{T}\right]^n$$

$$\Delta T = 1K \quad for$$
$$T = 200 - 350K$$

$$\Delta p = 0.0025\, p$$
$$for\ \ p > 100\, mTorr$$

HCl Half-widths Parametric Fit

	Parametric	Two-step	Units/Correlation
γ_o (N_2)	3.639(7)	3.654(26)	MHz/Torr
n (N_2)	0.71(3)	0.69(4)	$\chi_{\gamma o,n} = 0.401$
γ_o (O_2)	2.595(5)	2.602(14)	MHz/Torr
n (O_2)	0.79(1)	0.77(3)	$\chi_{\gamma o,n} = 0.443$

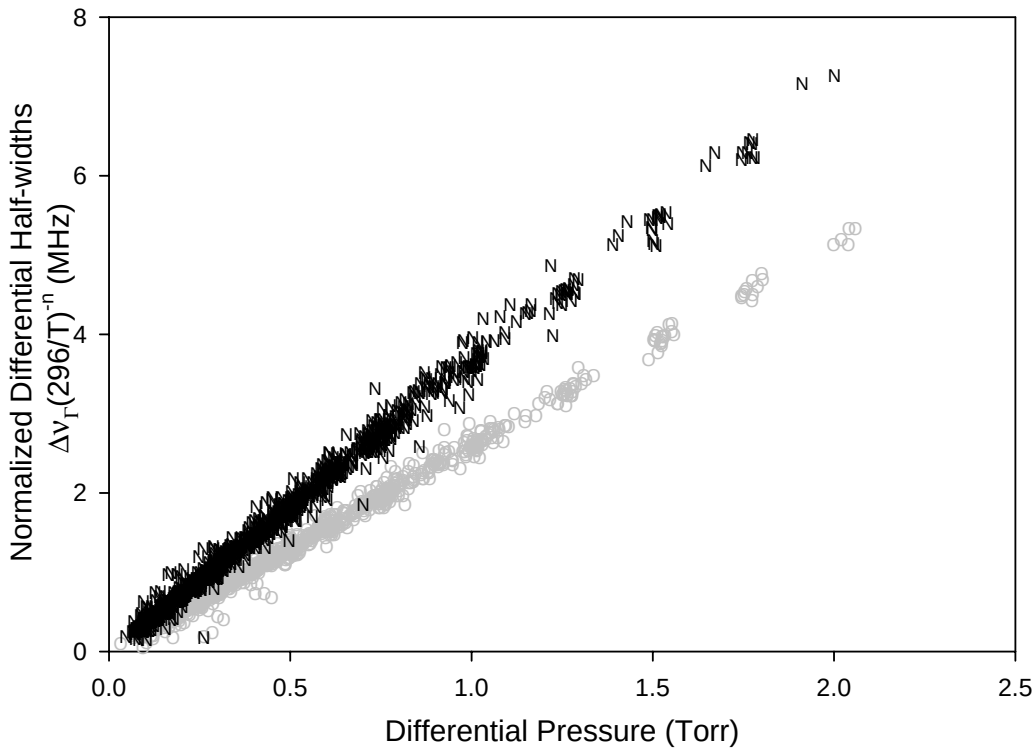

1σ error in parameters

650 data points N_2 (N)

530 data points O_2 (O)

HCl Shift Parametric Fit

	Parametric	Two-step	Units/Correlation
γ_o (N_2)	0.111(3)	0.097(12)	MHz/Torr
n (N_2)	0.36(19)	0.49(66)	$\chi_{\gamma o,n} = 0.369$
γ_o (O_2)	0.280(1)	0.266(7)	MHz/Torr
n (O_2)	0.50(3)	0.60(14)	$\chi_{\gamma o,n} = 0.405$

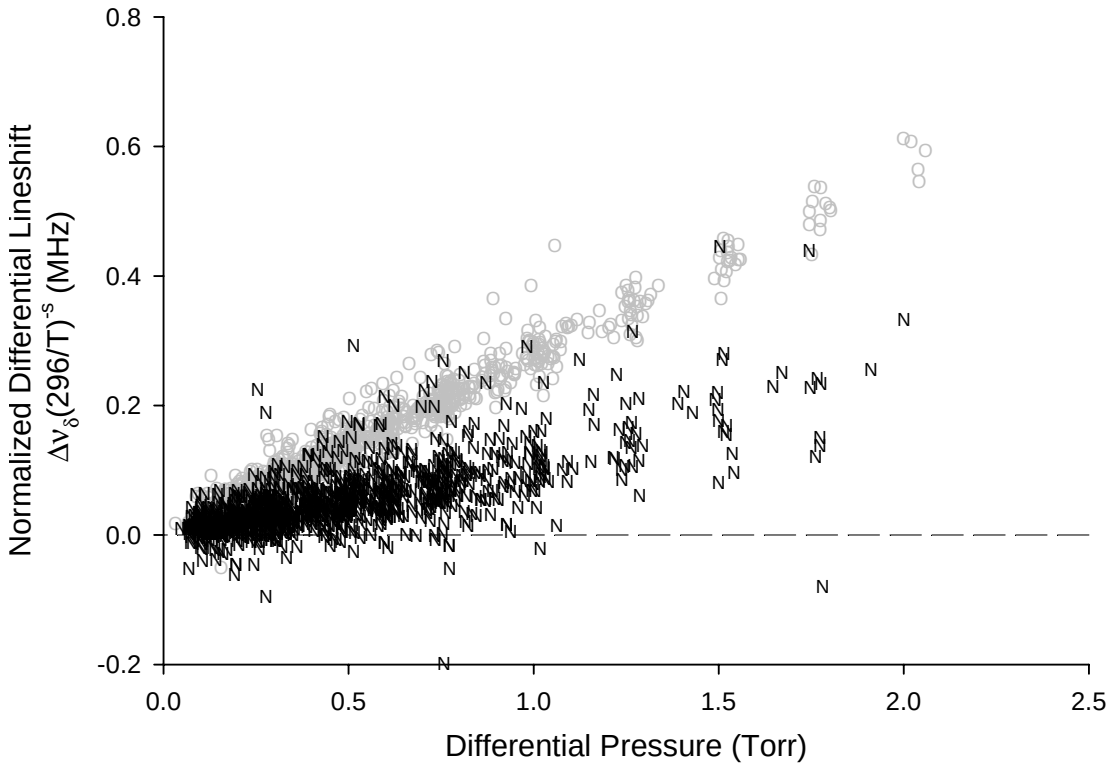

1σ error in parameters

650 data points N_2 (N)

530 data points O_2 (O)

Single points vs. Parametric Curve

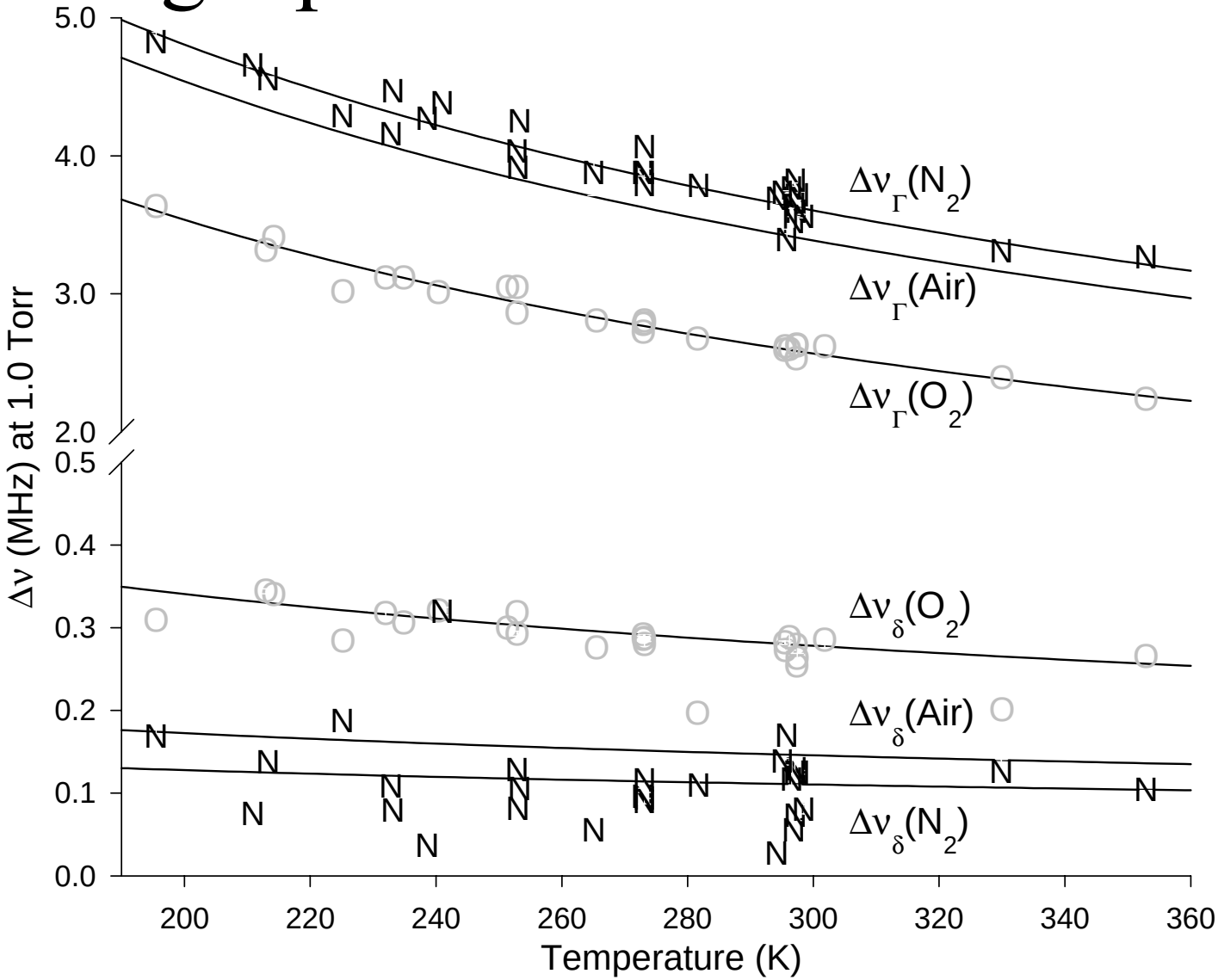

BrO experiments

$Br_2 + O_2 + \lightning$ => flow cell
624.7 and 650.2 GHz
convolution method

- RF Discharge in sidearm
- Multiplier source
- 1 m glass cell
- cooled MeOH in direct contact with glass
- 208 - 296 K
- 50 - 1600 mTorr
- 1f detection

- DC discharge in sidearm
- BWO source
- 1.7 m glass cell
- cooled MeOH in copper sleeve
- 224 - 293 K
- 50 - 400 mTorr
- 2f detection

BrO

Collaboration with Ibaraki University

some divergence at low temperature- recommendation from global analysis

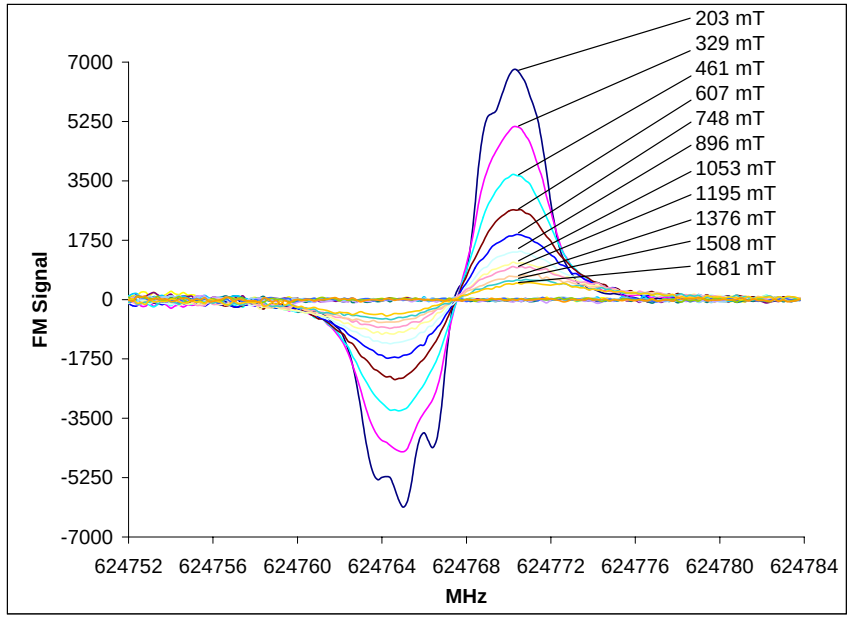

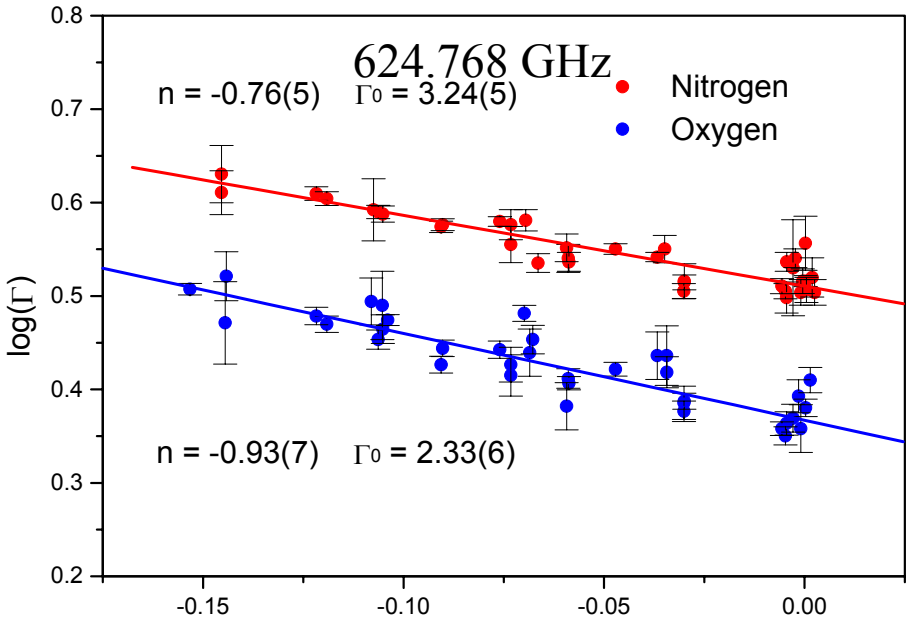

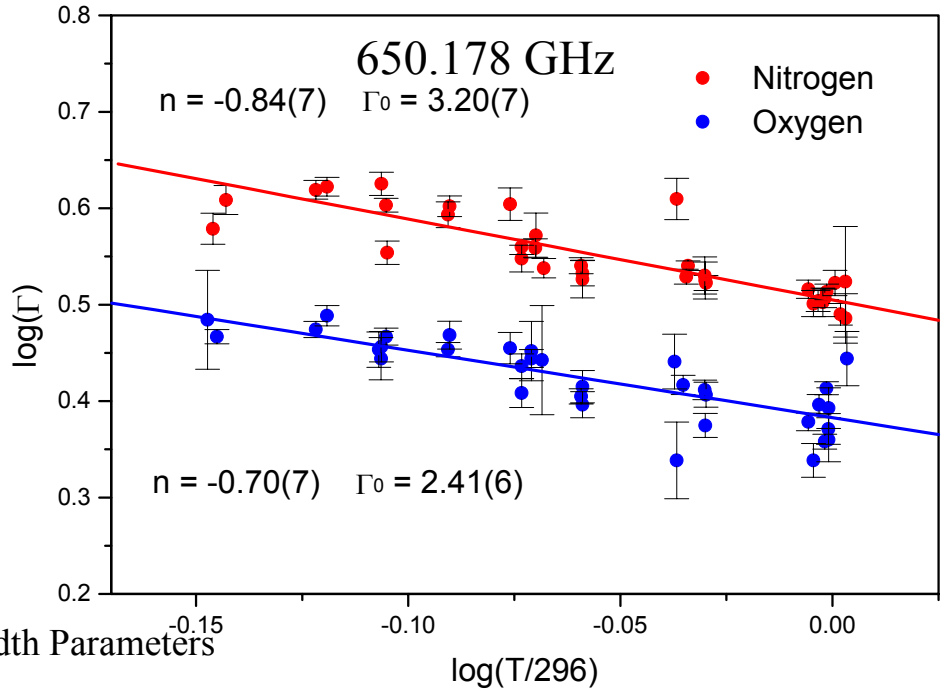

$Cl + CH_3OH + O_2$

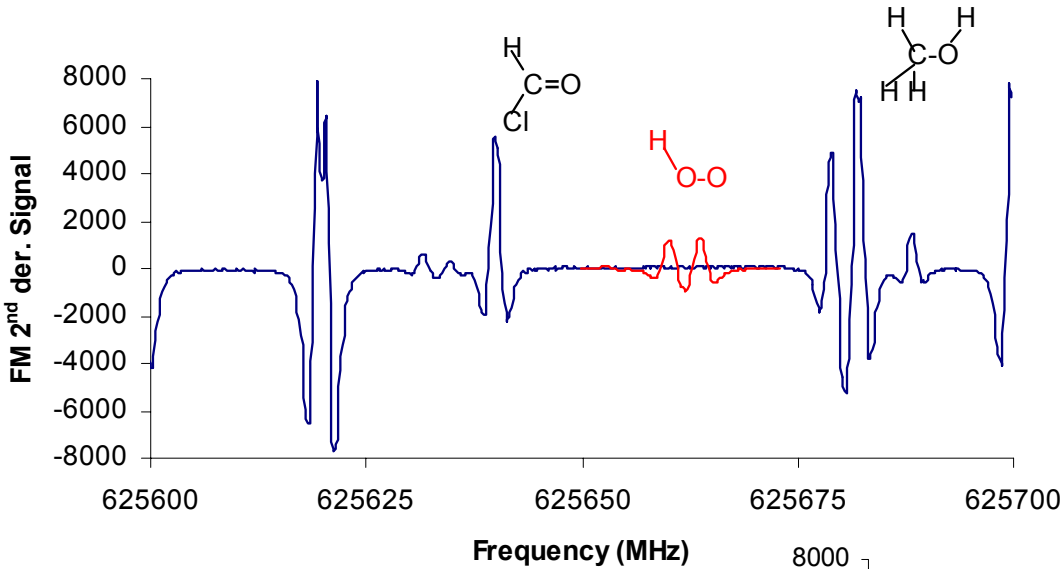

HO_2 Chemistry is complex, Signal is weak

$O + CH_2CHCH_2OH$

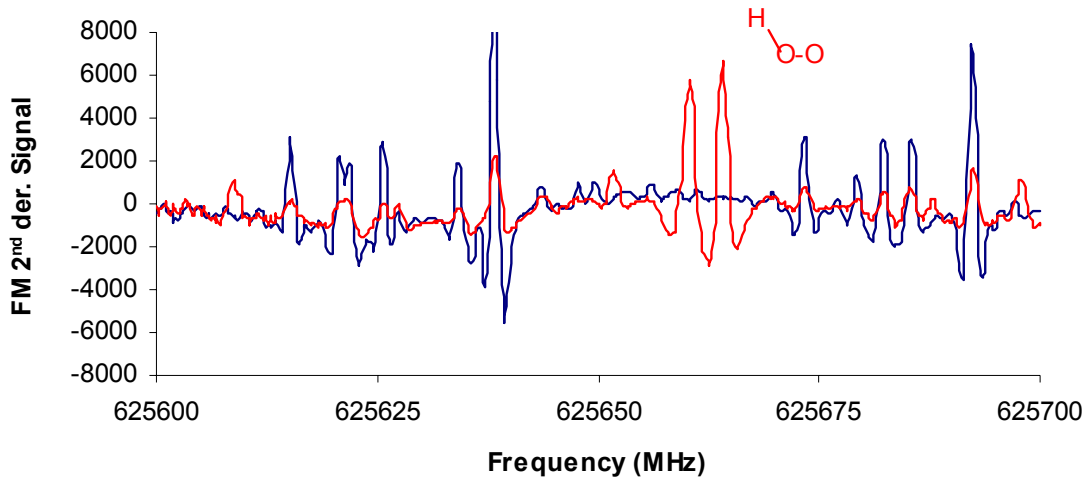

HO_2 Halfwidths

Freq(GHz)	Γ_{air}(MHz/Torr)	n	$J'_{Ka'Kc'} \leftarrow J_{KaKc}$
625.6	3.0		$10_{1,9} \leftarrow 10_{0,10}$
642.2	2.6		$10_{1,10} \leftarrow 10\ 9_{1,9}$
649.7	2.74	-0.2(3)	$10_{2,9} \leftarrow 9_{2,8}$
660.5	2.81	0.63	$10_{1,9} \leftarrow 9_{1,8}$

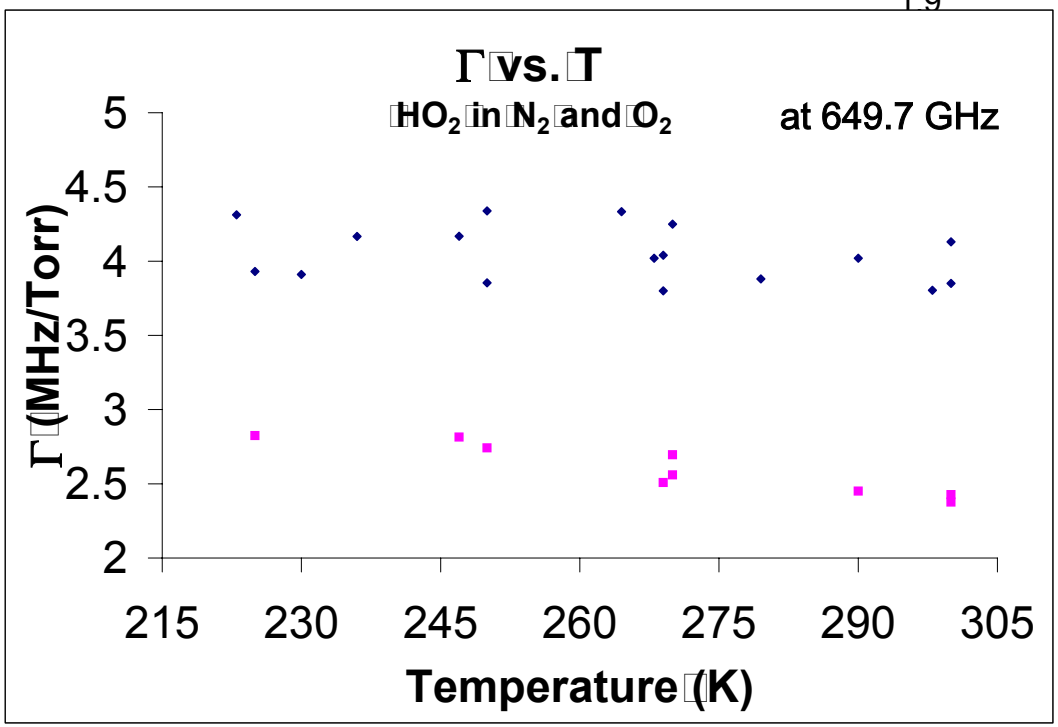

Methyl Cyanide

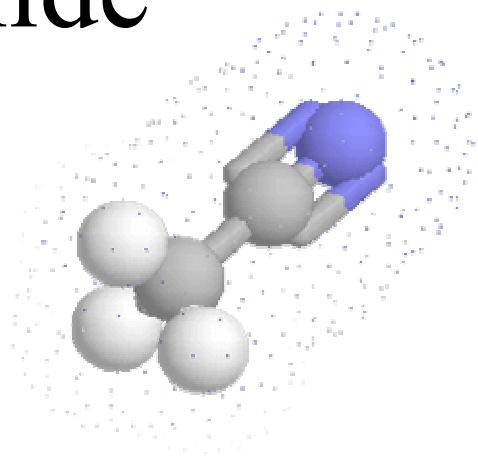

- Commercially available
- Volatile liquid
  - easy to prepare for study
  - possible condensation at extreme low temps
- large dipole moment, multiple vibrational states
  - good for S/N
  - may contaminate other measurements

Methyl Cyanide

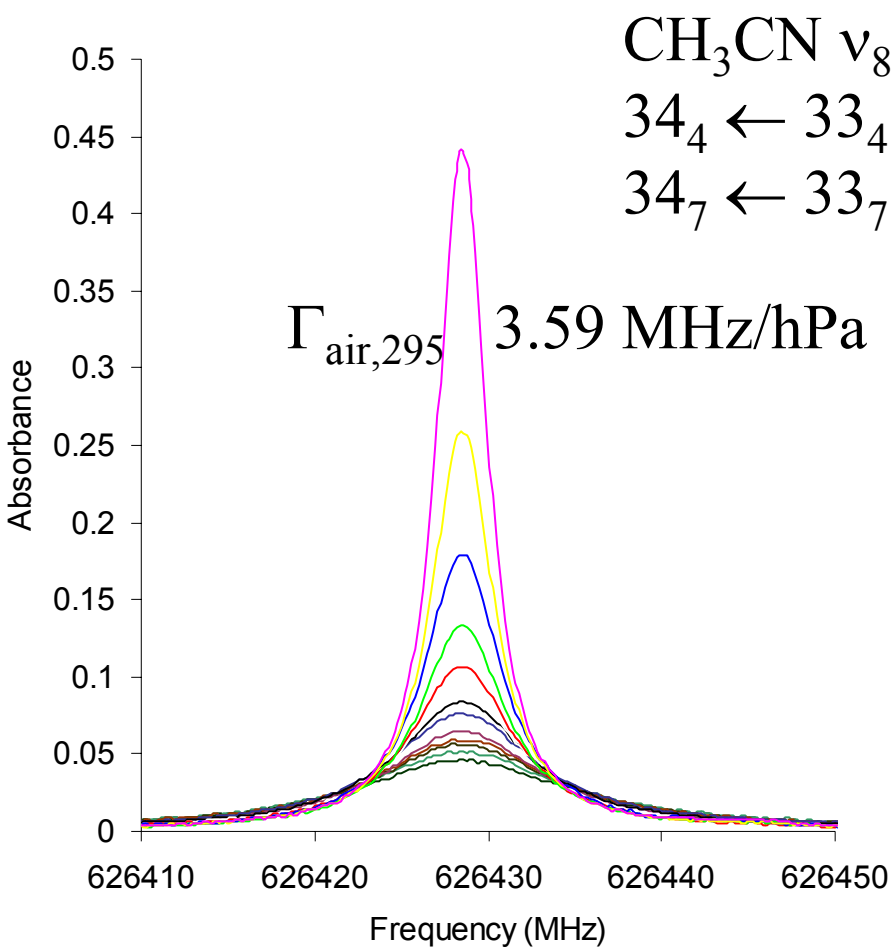

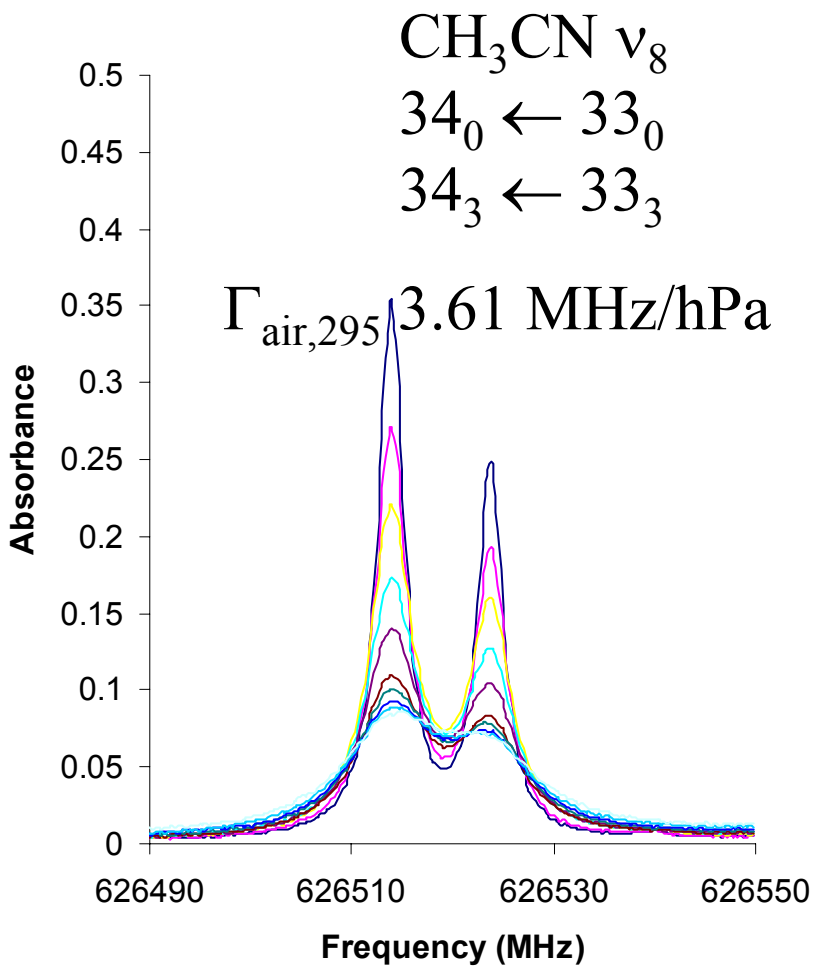

Pressures span 0.1 to 1.5 Torr air, no obvious K dependence

SO_2 Studies

- Pure gas in cylinder
- Medium - strong lines
- Mildy reactive/toxic
- Widespread spectra
- Contamination problems

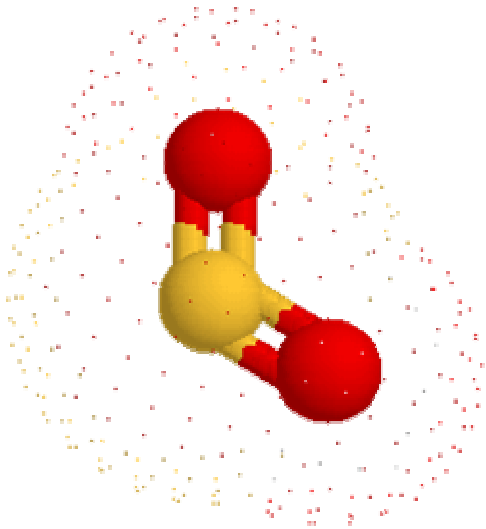

SO_2 ^rQ branch

660472.6960 $23_{7,17} \leftarrow 23_{6,18}$

660918.3140 $22_{7,15} \leftarrow 22_{6,16}$

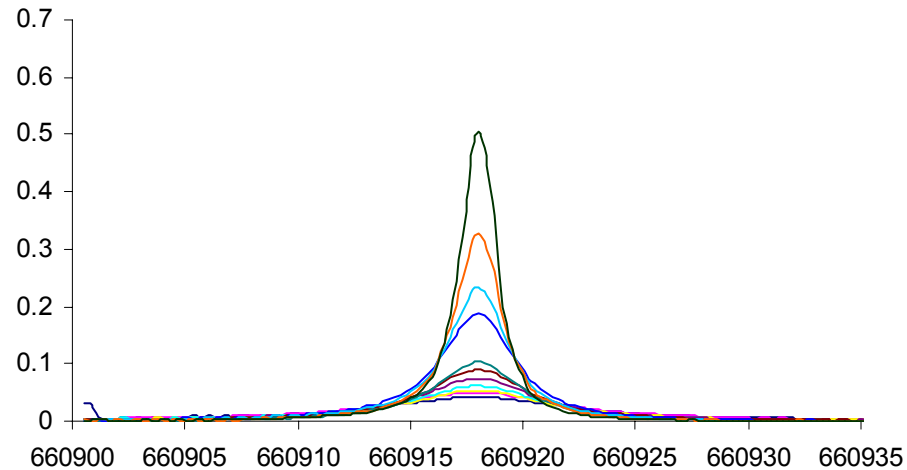

$\Gamma_{air,295}$ 2.87 MHz/hPa

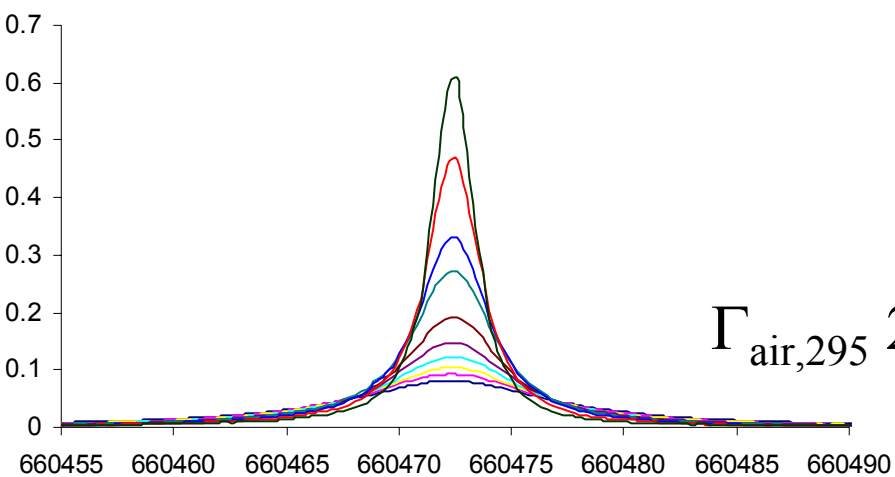

$\Gamma_{air,295}$ 2.80 MHz/hPa

Nitric Acid

No linewidth data from JPL yet
200 GHz OSU data

$H^{15}NO_3$
is a good example of
the frequency scanning
possible with this
spectrometer

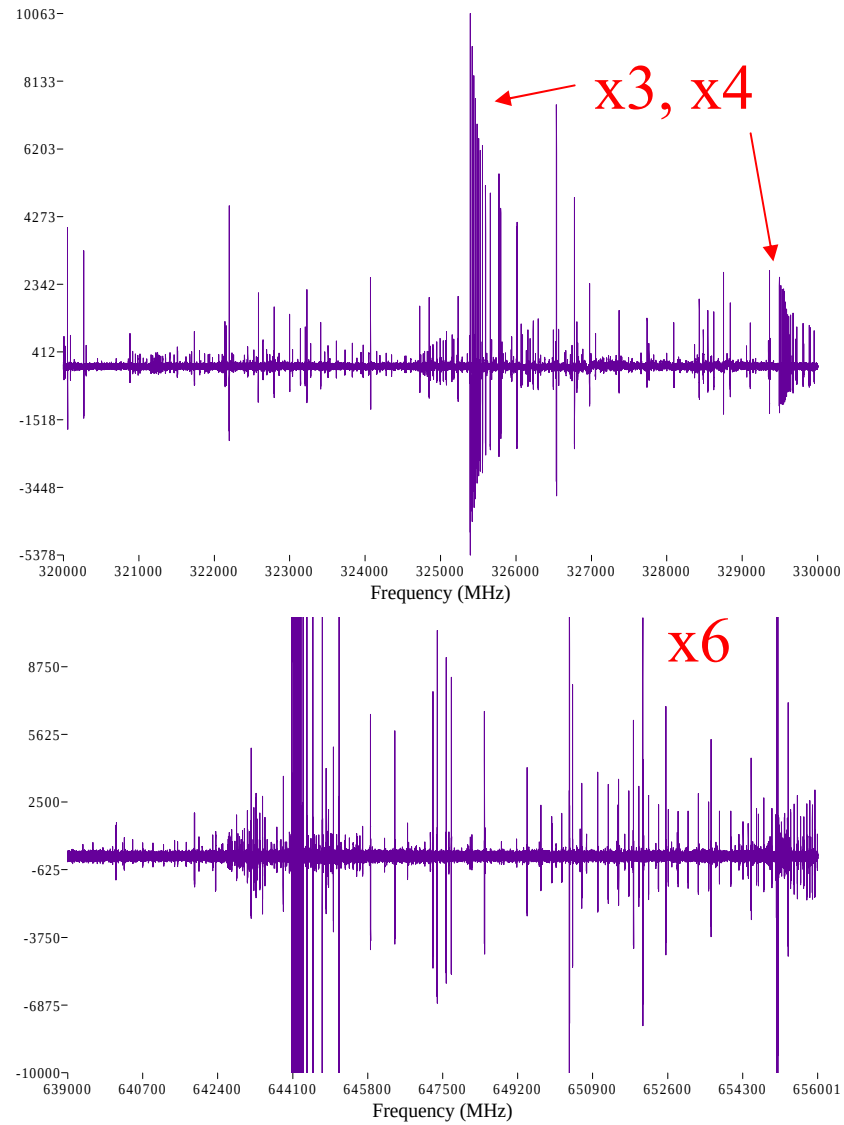

MLS 600 GHz Channel Linewidth Progress

Molecule	Frequency (GHz)	Air broadening (MHz/Torr)	Temp exponent	Current Accuracy	Priority
^{81}BrO	624.768	3.05	0.80	3%	1
	650.179	3.03	0.81	3%	1
$H^{35}Cl$	625.919	3.420	0.62	2%	1
O_3	625.372	2.99	0.75	4%	1
HO_2	649.702	3.71	0.2	6%	1
	660.486	3.51	0.63	4%	1
HOCl	635.870	-	-	-	2
ClO	649.451	2.782	0.86	3%	Done
SO_2	660.473	3.83	0.95	10%	2
	660.918	3.73	0.90	10%	2
CH_3CN	626.4	4.79	-		2
	660.7	4.81	-		2

O_3 is a dominant feature in the 240 GHz band

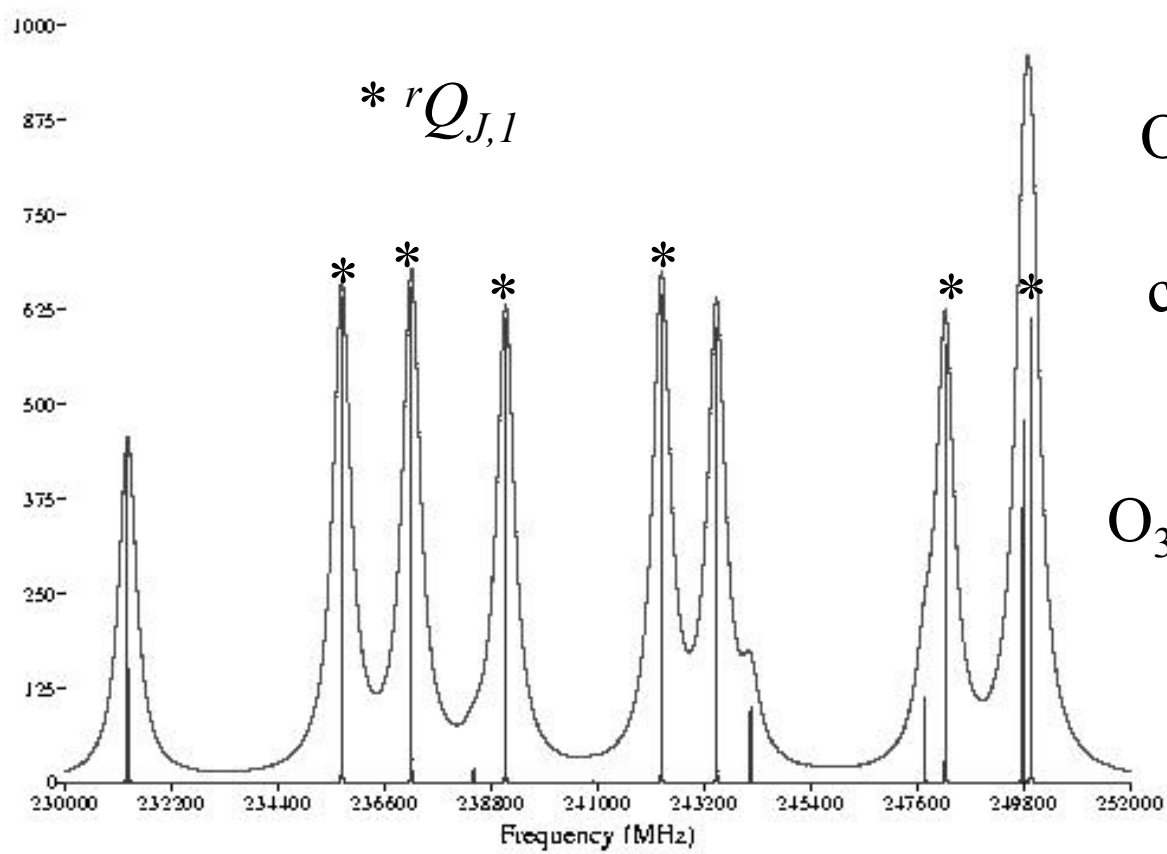

O_3 created in ozonizer is cryogenically trapped

O_3/O_2 mixture combined with buffer gas and flowed through cell

Measured and calculated values for γ_o(296 K) determined for O_3

γ_o ($K_a = 0$)

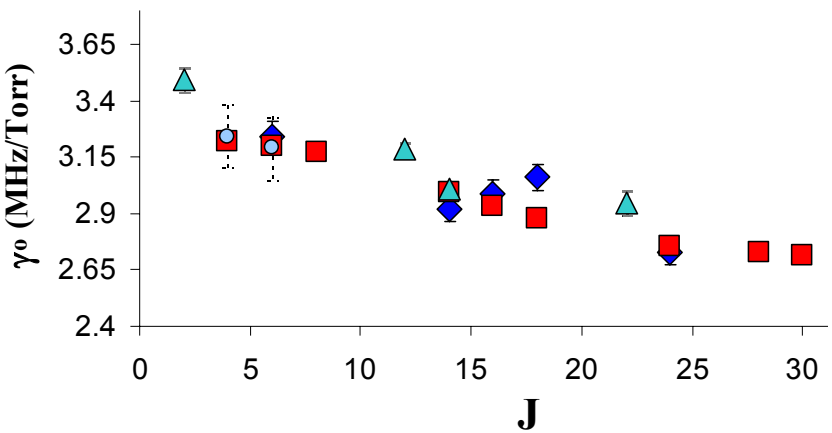

γ_o ($K_a = 1, J' = J$)

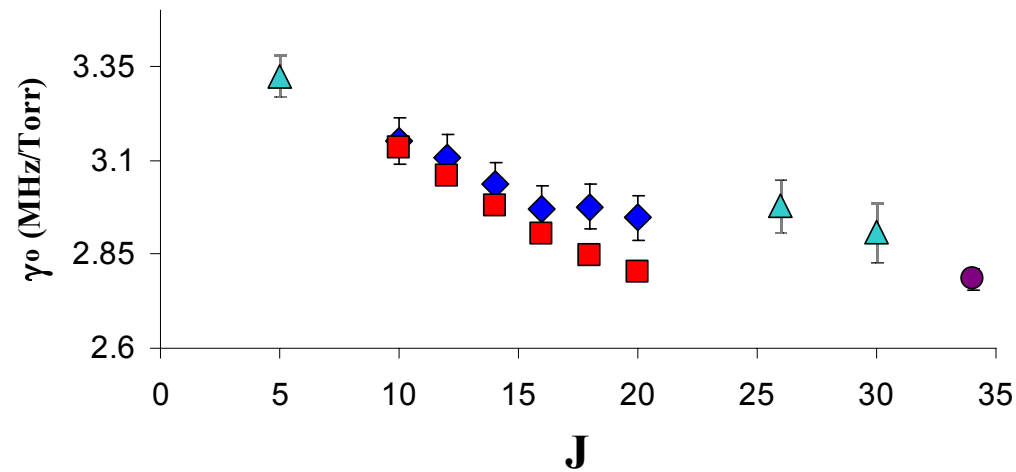

Measured rotational

- ● - Connor
- ◆ - this study
- ● - Priem,
- △ - ν_1 branch (Smith)
- ■ - Calculated rotational

J dependence of temperature exponents

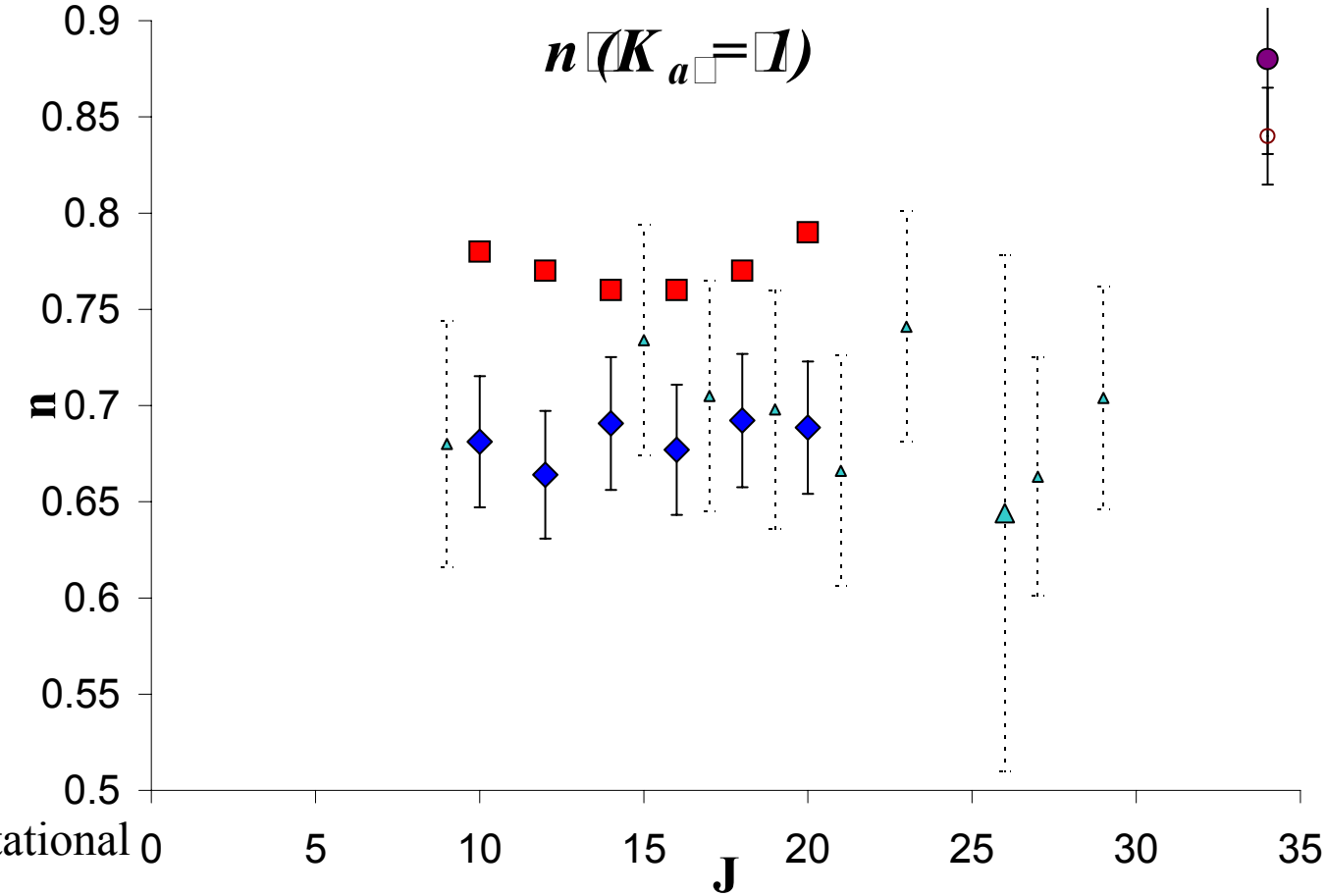

Measured rotational

- Connor
- this study
- Priem,

Δ -ν_1 branch (Smith)

- Calculated rotational

Carbon Monoxide Studies

- Pure gas in cylinder
- Medium - weak lines
- non-reactive but toxic
- sparse spectrum
- well studied in mm and infared

Carbon Monoxide

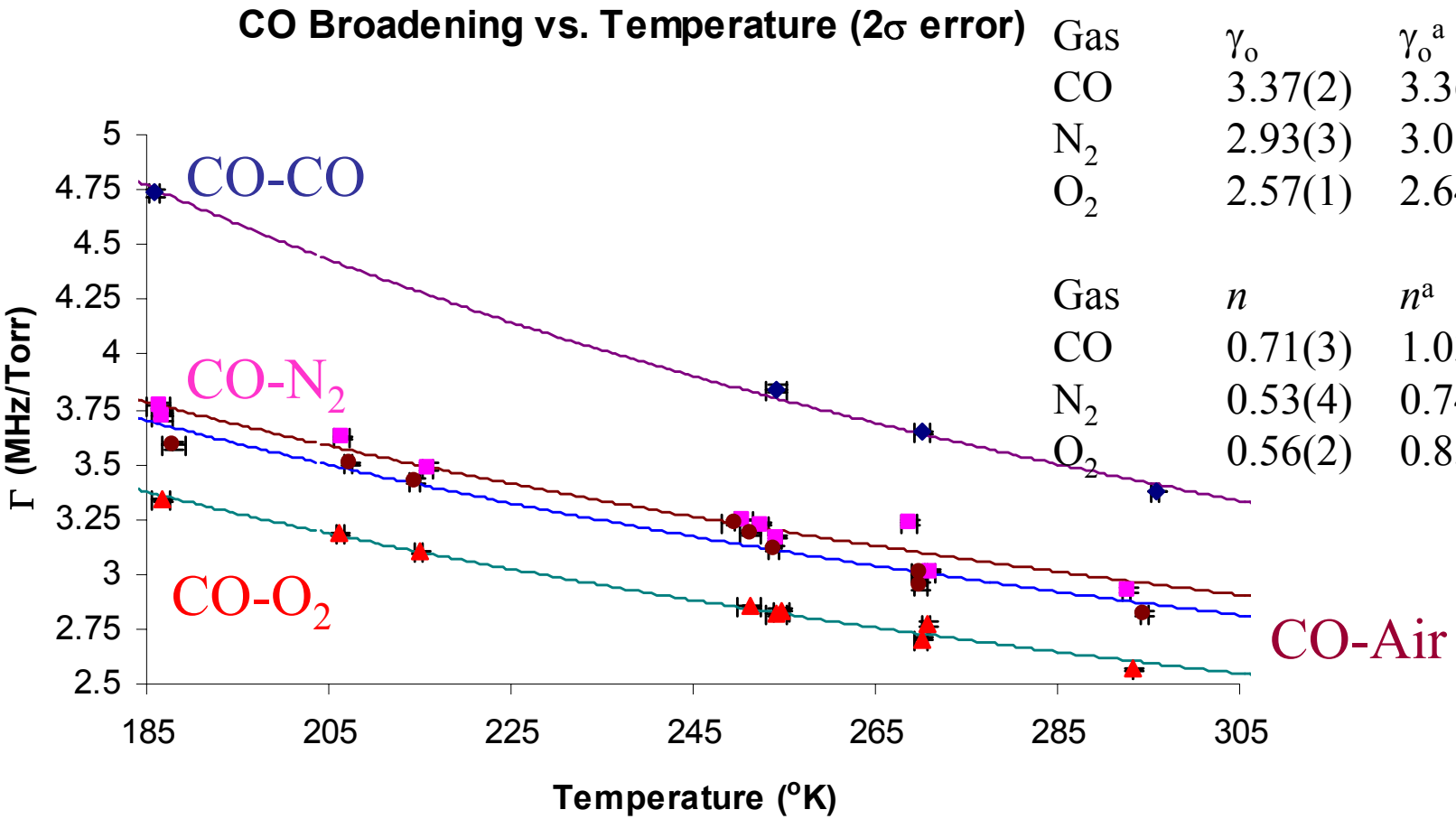

$J = 2 \leftarrow 1$

Gas	γ_o	γ_o[a]
CO	3.37(2)	3.36(7)
N_2	2.93(3)	3.01(5)
O_2	2.57(1)	2.64(5)

Gas	n	n[a]
CO	0.71(3)	1.03(10)
N_2	0.53(4)	0.74(8)
O_2	0.56(2)	0.85(9)

a. Semmoud and Colmont, *J. Mol. Spec.* **126**, 210-219, 1987.

Oxygen

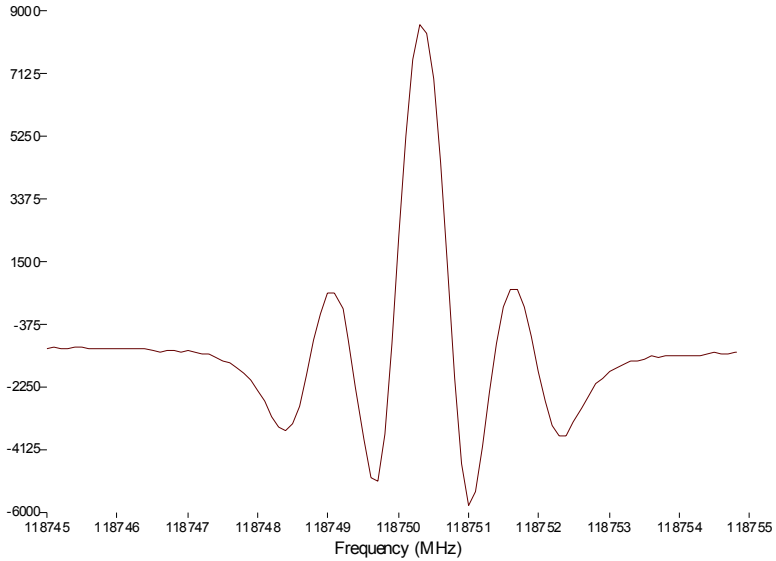

Oxygen 118.75 GHz Half-widths

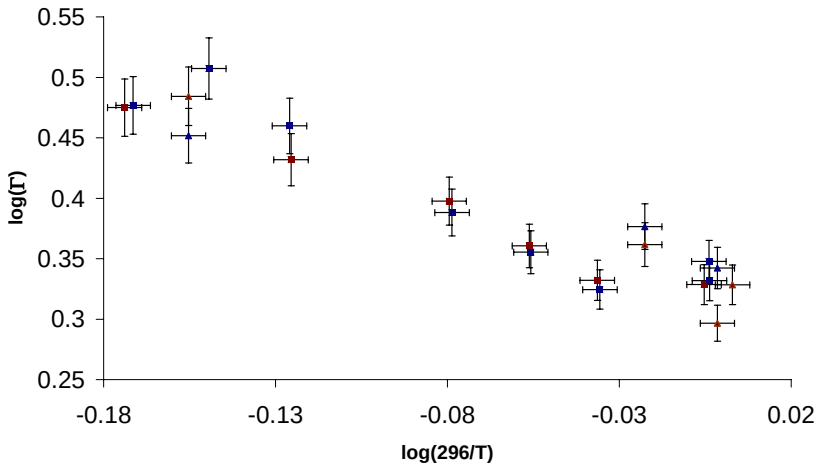

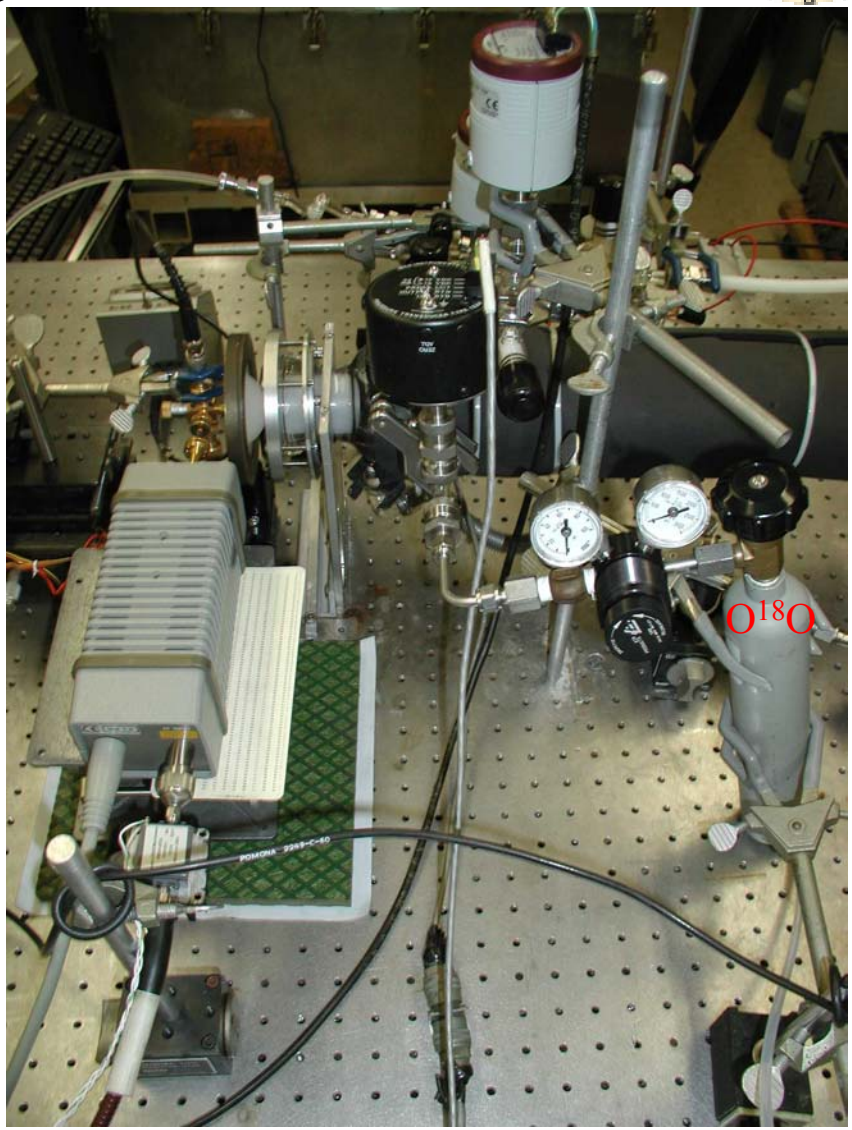

Hydrogen Cyanide

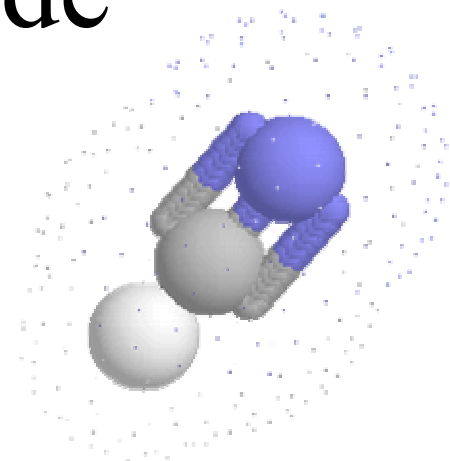

- Commercially available
- Gas mixture
  - specialty order, 10 ppm - 2% available
  - very dangerous!
  - Analogous to HCl experiment
- large dipole moment, few vibrational states
  - good for S/N

EOS MLS Low Frequency Requirements

Molecule	Frequency (GHz)	Air Broadening (MHz/Torr)	Temp. Exponent	Current Accuracy	Priority
CH_3CN	183.94	-	-	-	2
	202.3	6.06(11)	0.84(9)	~10%	2
CO	230.538	2.839(28)	0.548(45)	<3%	2
HCN	177.2612	-	-	-	2
$^{18}O^{16}O$	233.9462	-	-	-	1
O_3	231.2815	2.991(07)	0.703(08)	<2.2%	2
	235.7098	3.044(10)	0.655(10)	<2.5%	1
	237.1462	3.037(10)	0.693(10)	<2.6%	1
	239.0933	2.980(07)	0.692(08)	<2.2%	2
	242.3187	3.103(07)	0.663(08)	<2.1%	1
	243.4537	3.062(10)	0.685(14)	<2.9%	1
	244.1580	3.181(17)	0.749(18)	<3.8%	3
	247.7618	3.014(15)	0.685(14)	<3.2%	3
	248.1834	2.949(05)	0.680(05)	<1.8%	2
	249.7886	3.236(08)	0.674(09)	<2.3%	2
	249.9620	3.157(06)	0.675(07)	<2.1%	2
SO_2	200.2875				3

2.5 THz Sideband Spectrometer

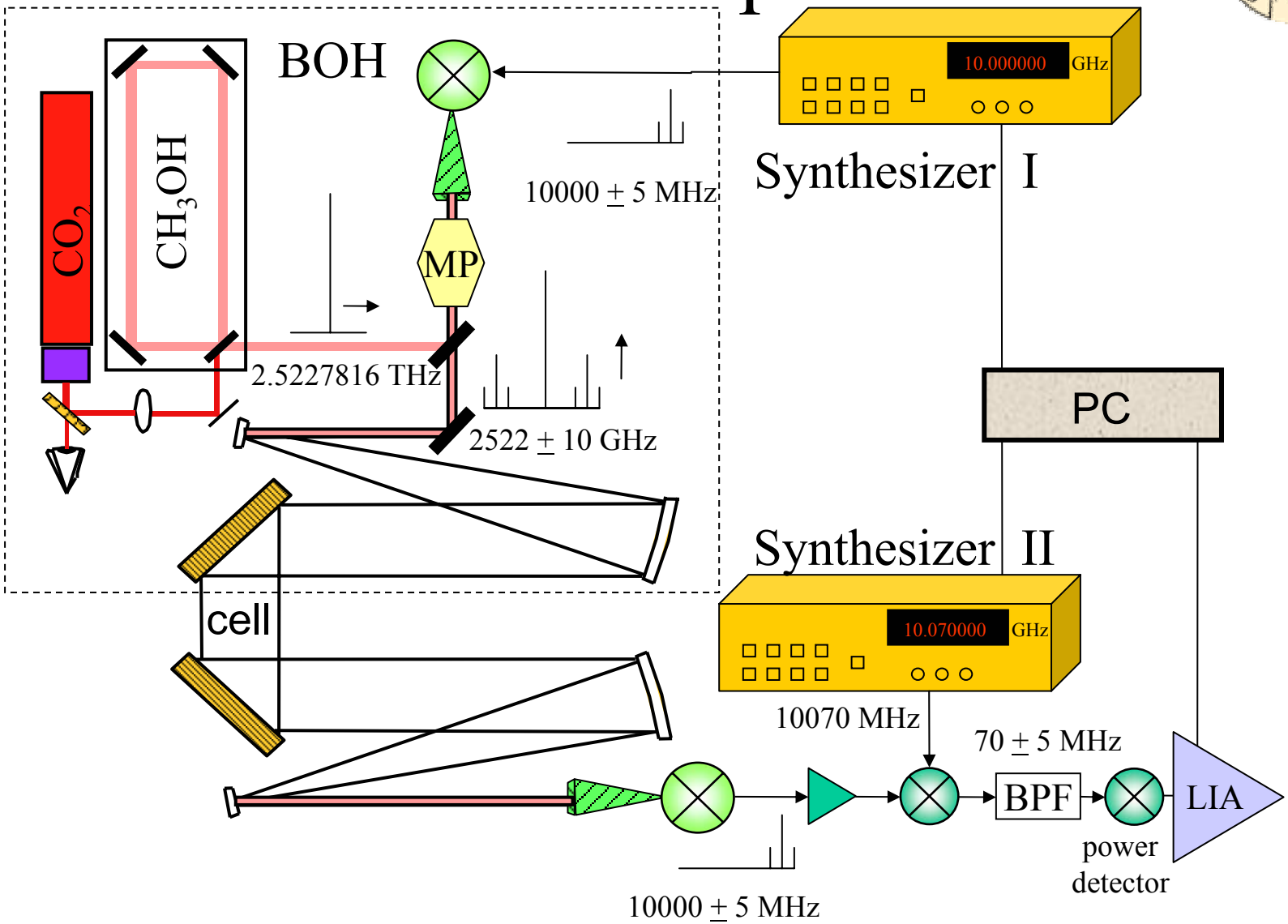

Linewidth Measurements Plan

DEC	JAN	FEB	MAR	APR	MAY	JUN	JUL	AUG	SEP
$O^{18}O$ →	CO	CH_3CN SO_2 HOCl	OH	O_3	H_2O	O_2 →		HNO_3	HCN
Static Cell		Flow cell	4” diameter flow cell					Static Cell	
x3		x6, x7	THz Instrument →					x2, x7	

Acknowledgements

- NASA – Code Y
  - Upper Atmospheric Research Program
  - EOS-Spectroscopy Program
- California Institute of Technology
  - Postdoctoral Scholar at JPL Program
- Jet Propulsion Laboratory
  - MLS Project and Team
  - Molecular Spectroscopy Group

Acetone

Ground State

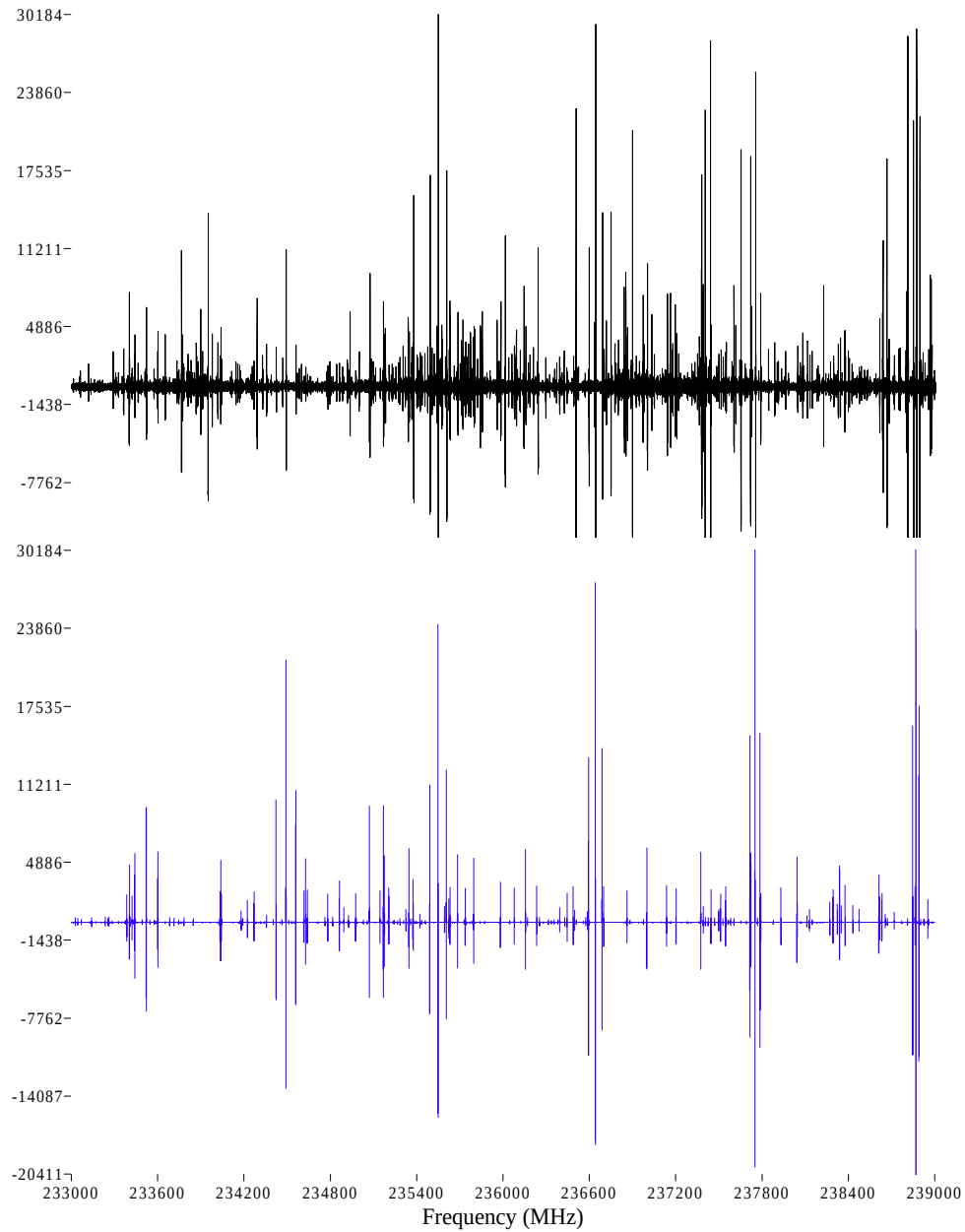

MEASUREMENTS OF THE DRY AND MOIST AIR CONTINUUM IN THE MICROWAVE REGION

MLS Meeting
Jet Propulsion Laboratory
December 11 - 12, 2002

Andrey Meshkov
Frank C. De Lucia
Ohio State University

OVERVIEW OF PRESENTATION

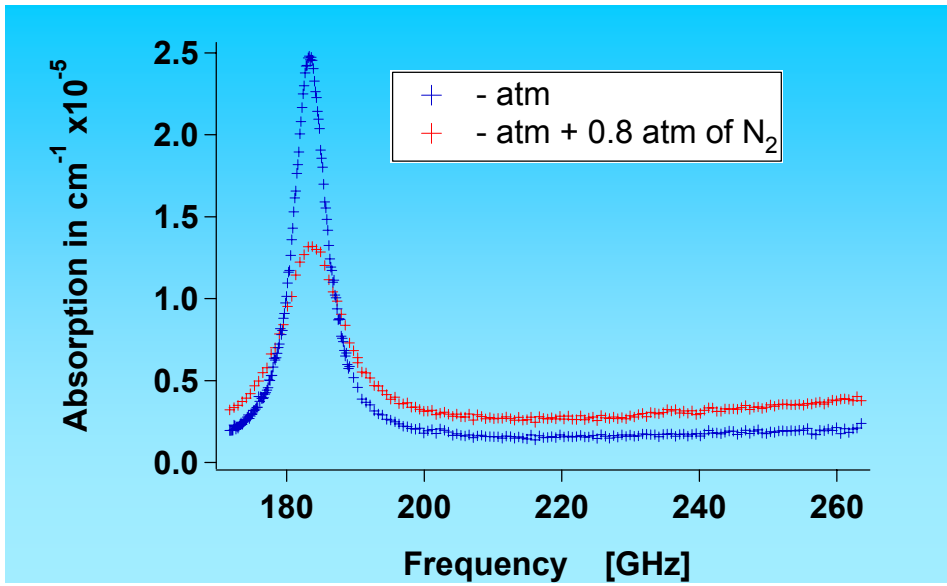

Frank De Lucia

- **Review of the Basic Problem**
- **The Experimental Approach**
- **Results to Date**
- **Plans and Strategies**

Andrey Meshkov

- **The Experimental Layout**
- **FASSST Ring Down vs. Cavity Q**
- **BWO Characteristics, FP Modes, and Measurement Strategies**
- **Statistical Limits**
- **Evaluation of Systematic Effects**

EXPERIMENTAL CONSIDERATIONS

Dry Air Continuum

- System must be able to measure small absorptions
- System must be able to test for other systematic contributions which might mask the dry air continuum

Moist Air Continuum

- Exchange of water between gas and surface

Want Direct Observation of Functional Dependence of Continua on Frequency, Pressure, and Temperature

dry air: $$\alpha(db/km) = 2.5 \bullet 10^{-11} \left(\frac{300}{T}\right)^{4.5} f^2 p^2$$

moist air: $$\alpha(db/km) = 2.5 \bullet 10^{-7} \left(\frac{300}{T}\right)^{2.5} f^2 pe + 9.8 \bullet 10^{-6} \left(\frac{300}{T}\right)^{5.5} f^2 e^2$$

FASSST RING DOWN SPECTROSCOPY

Traditional Measurement of Q:

About 6000 cavity modes in 90 GHz

High Q and need to measure small changes in Q require relatively slow frequency sweep and measurement

Measurement of FASSST Ring Down Time:

Look at the 6000 cavity modes in ~ 3 seconds

Well suited for the study and quantification of systematic and time varying effects

Increase in Statistical Noise Associated with Bandwidth:

Is this a problem?

CAVITY MODES IN A REAL SYSTEM

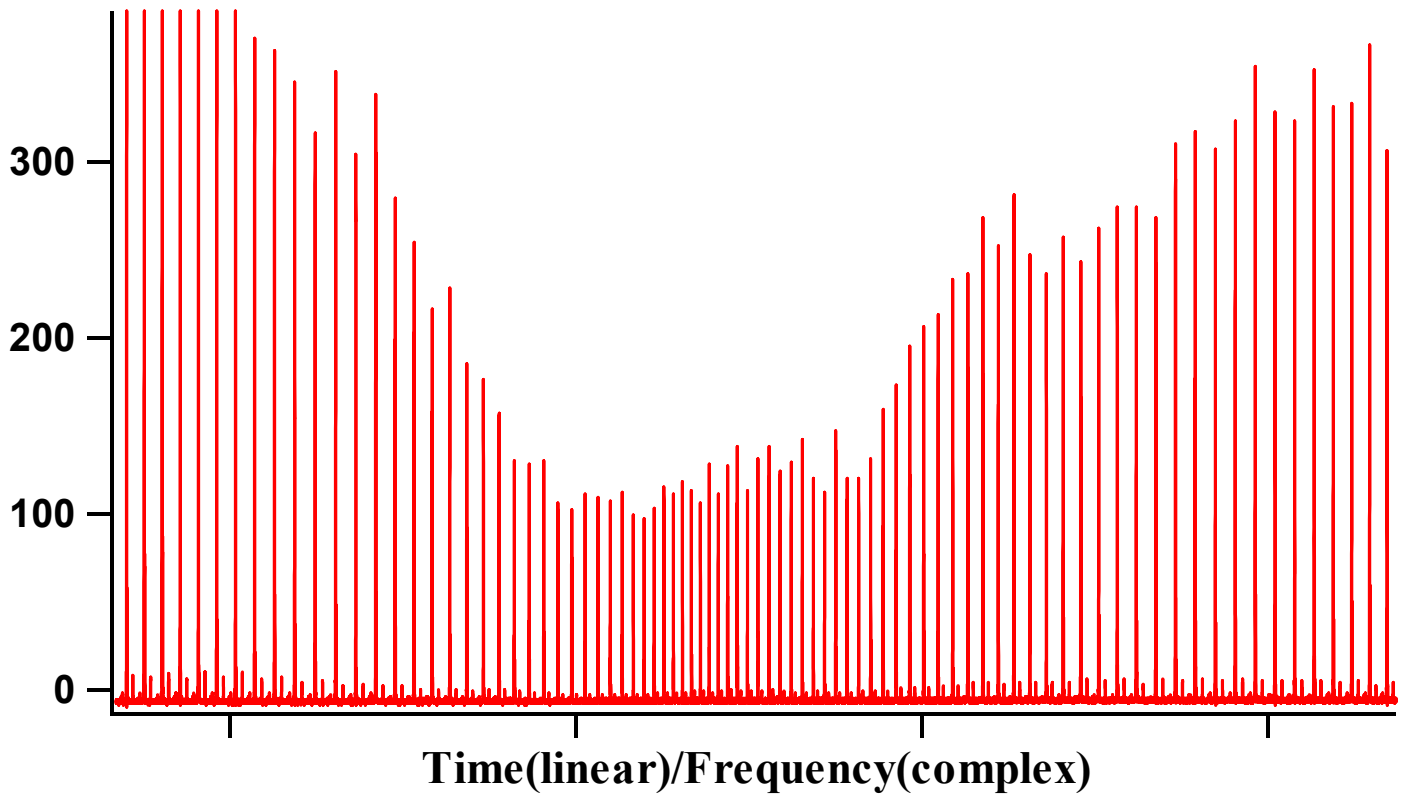

Nonlinear Frequency-Voltage Function of BWO modulates time between cavity modes

Higher Order Transverse Modes

Amplitude Variations

LOSS MECHANISIMS - IMPACT ON SUBTRACTION

Input/Output Coupling

-Standing waves

-Polarization effects

Internal Modes/Reflections

-Index of refraction effect

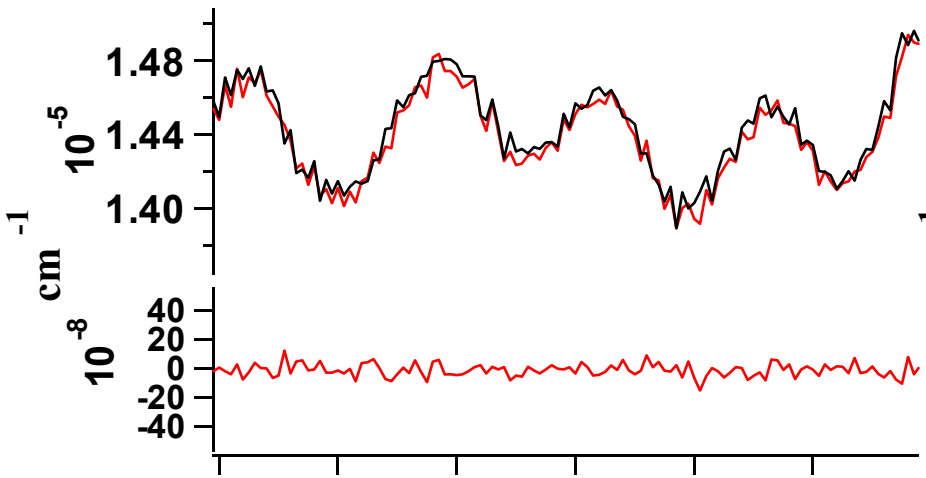

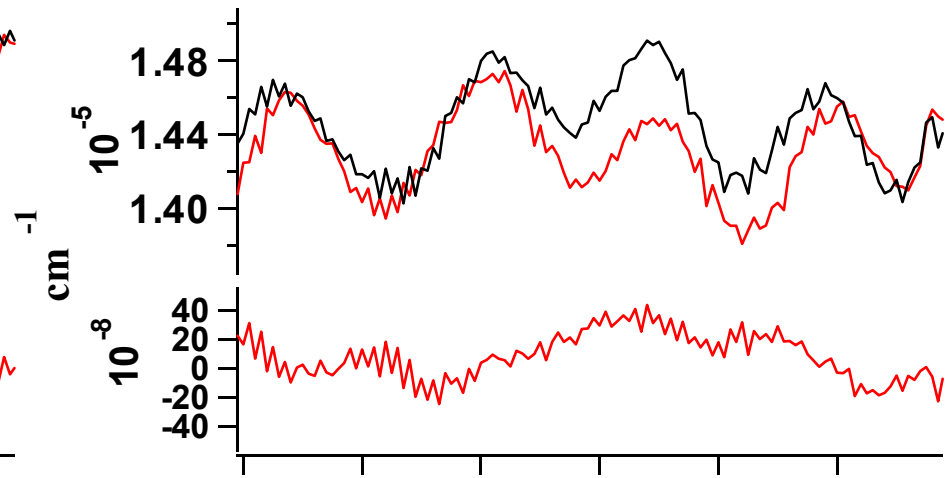

LOSS MECHANISIMS - SYSTEMATIC EFFECTS

Input beam splitter losses

-Coupling depends upon index of refraction

Output hole coupling losses

-Mode size depends upon index of refraction

Diffraction losses

-Mode size depends upon index of refraction

Reflectivity Losses

-Gas absorbed on mirrors

Block Diagram Of The Experiment

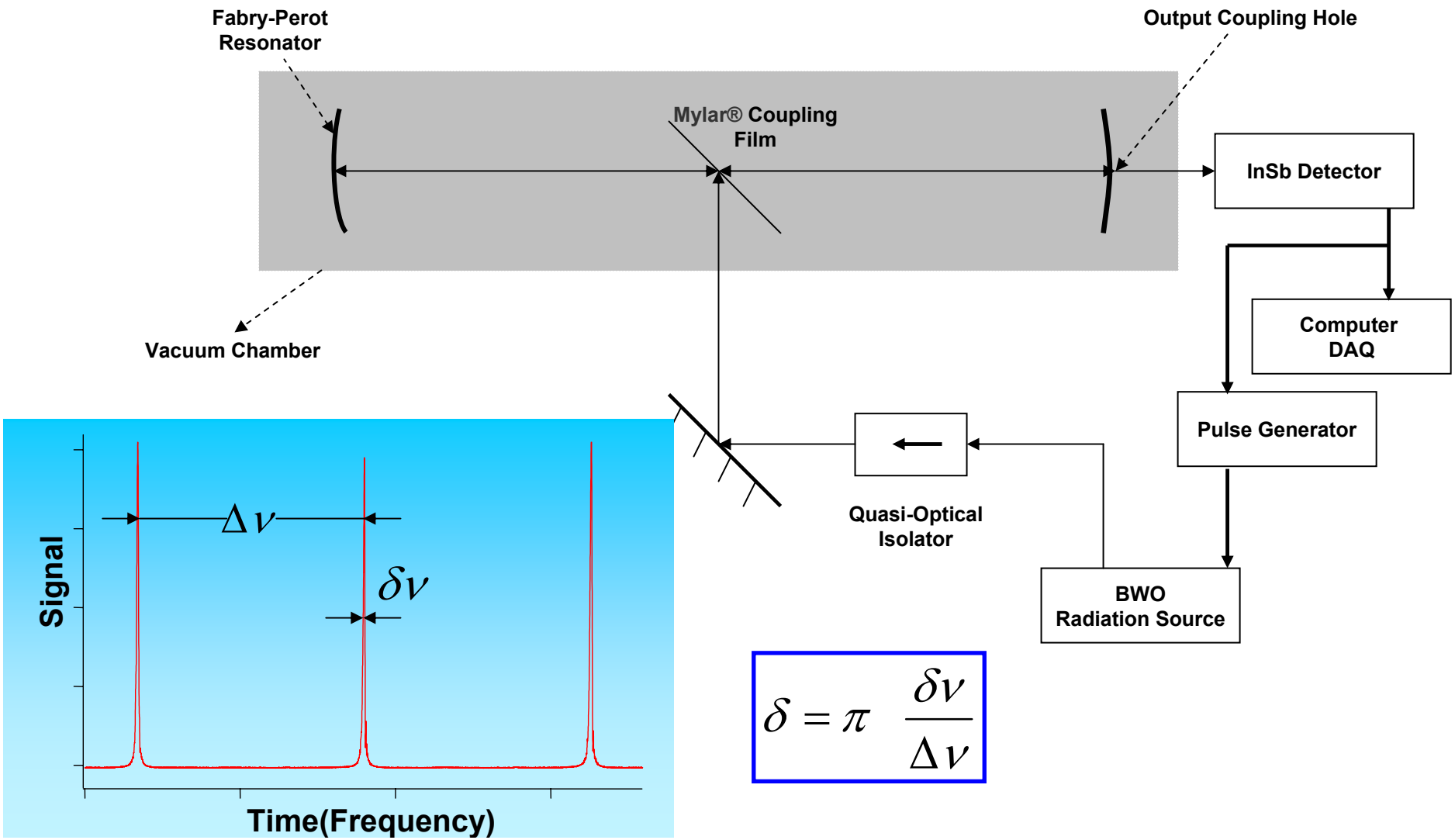

$$\delta = \pi \frac{\delta\nu}{\Delta\nu}$$

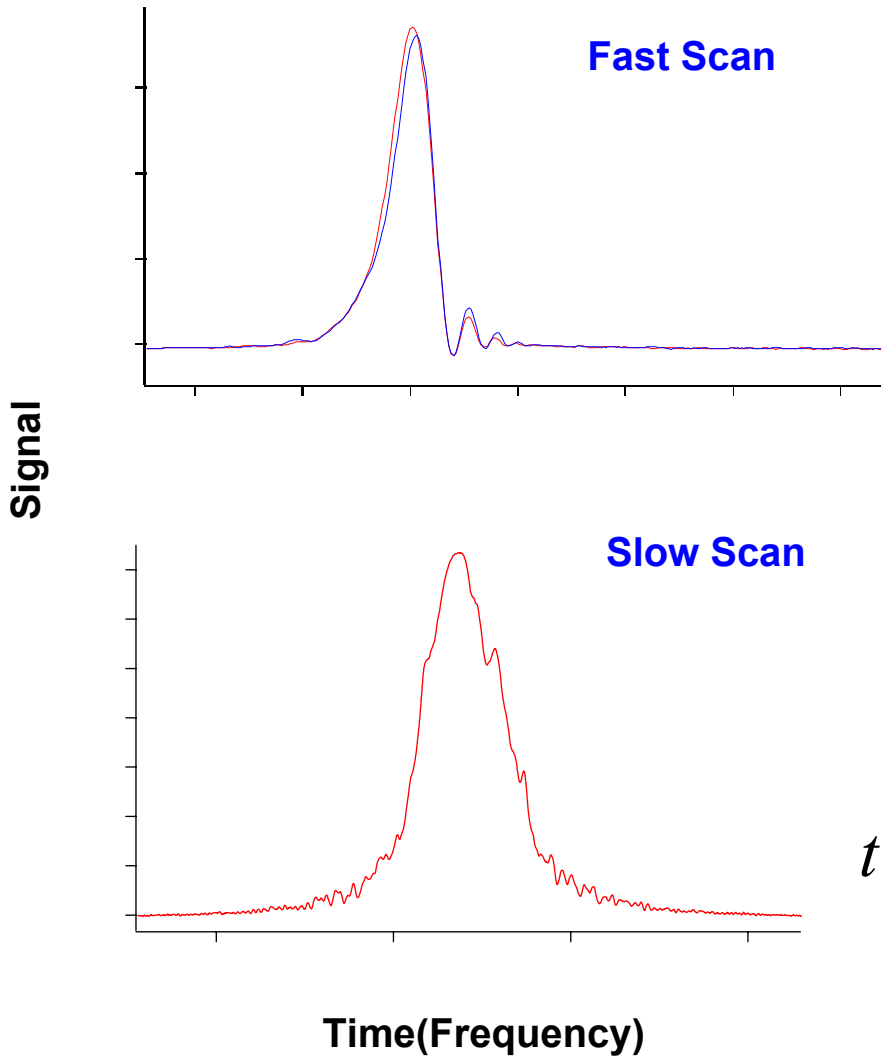

40 nS/pass (L=10m)

1% loss

20 ❍S/point -> 2mS/fringe

$$\delta\nu = 50kHz$$

$$t = \frac{90*10^9}{5*10^4} 2mS = 3600s = 1h$$

Ringdown

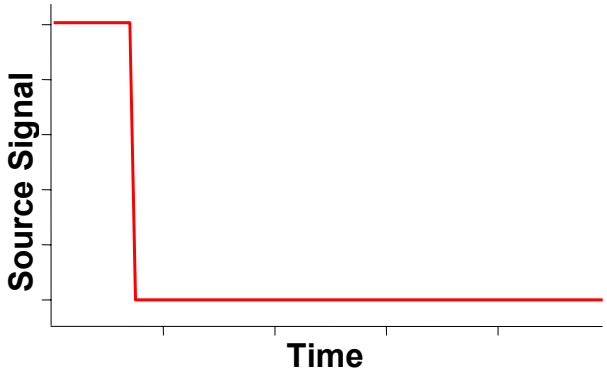

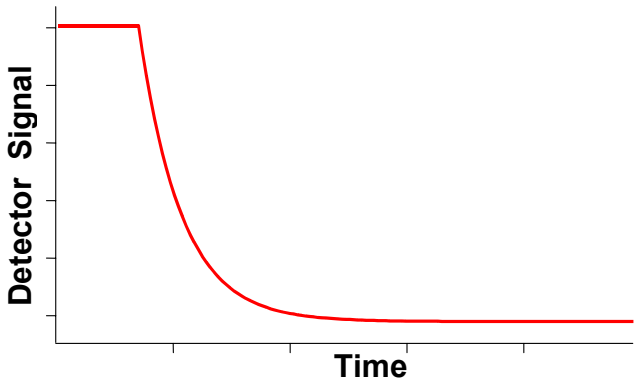

$$I = I_0 e^{-t/\tau}$$

$$\tau = \frac{t_r}{2\delta}$$

t_r - transit time for a round trip

δ - fractional power loss per pass

1% loss and 10m cavity:

$$\boxed{\tau = 1.7\mu S}$$

Triggering Scheme

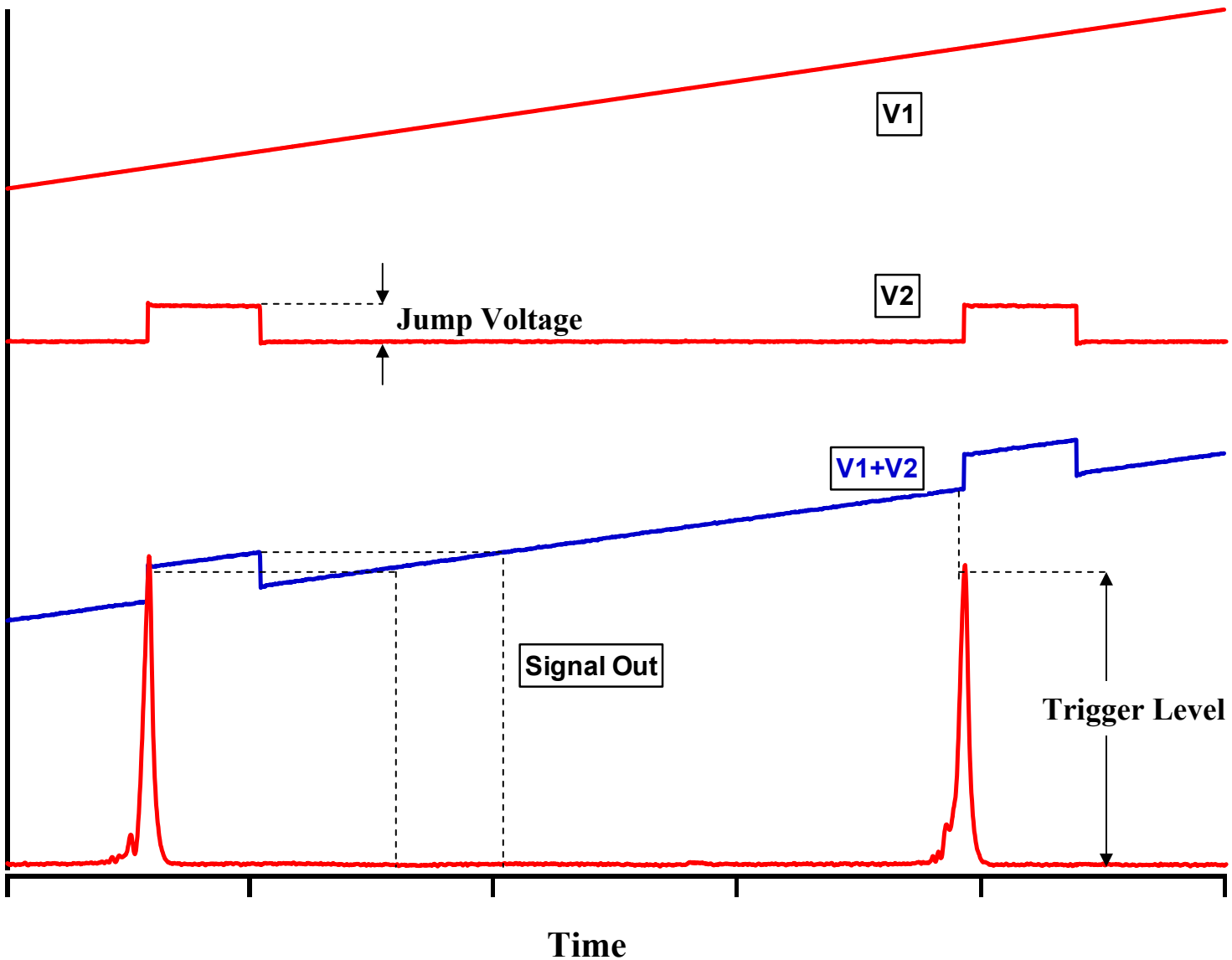

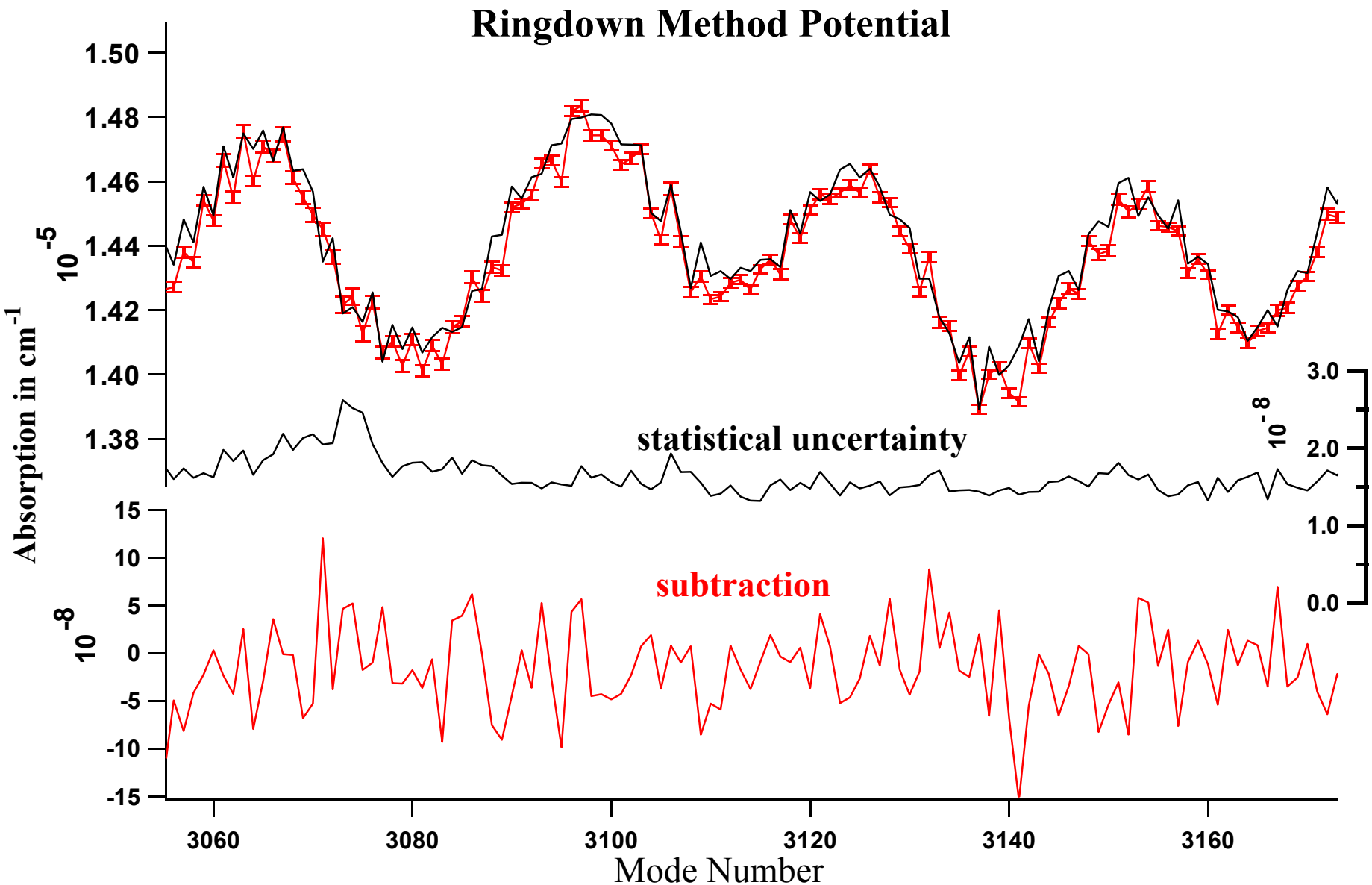
Ringdown Method Potential
Absorption in cm-1
10-5
1.50
1.48
1.46
1.44
1.42
1.40
1.38
statistical uncertainty
10-8
3.0
2.0
1.0
0.0
subtraction
10-8
15
10
5
0
-5
-10
-15
3060
3080
3100
3120
3140
3160
Mode Number

Real Life FP Modes

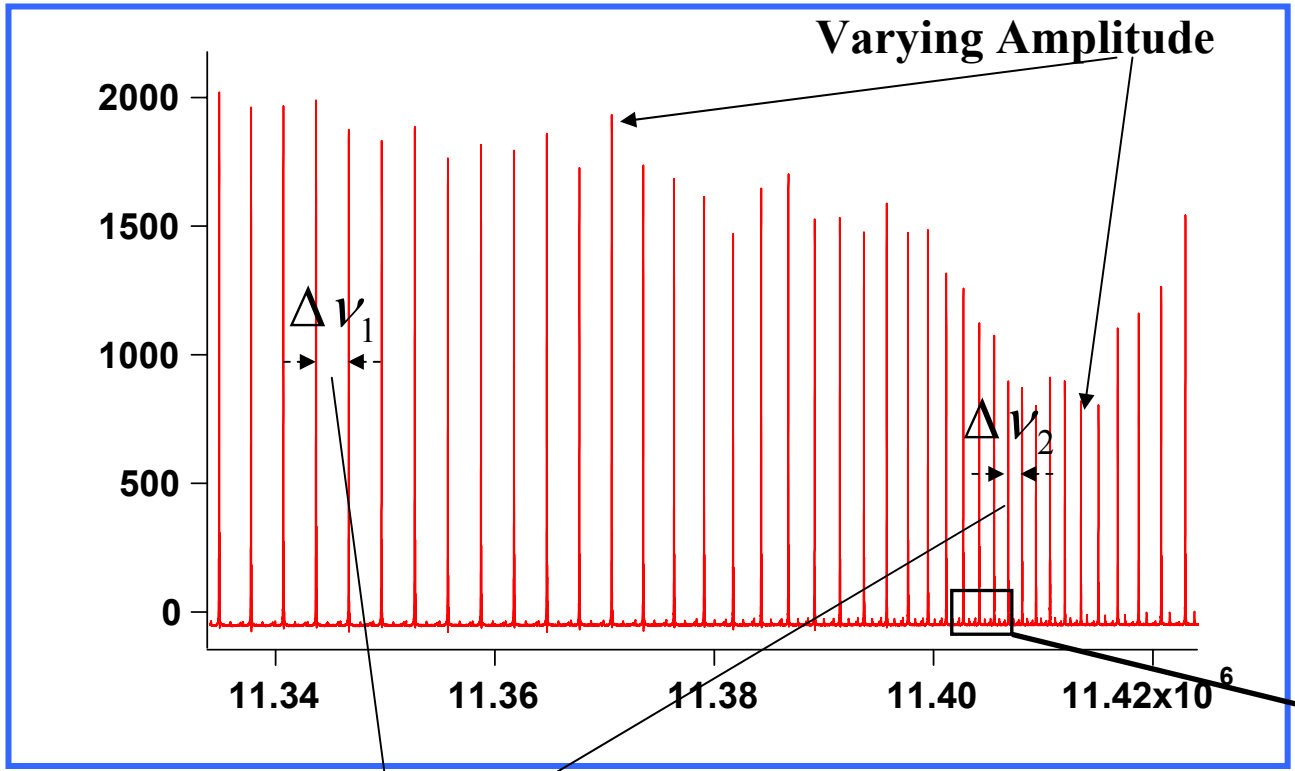

Varying mode spacing
(BWO physics related)

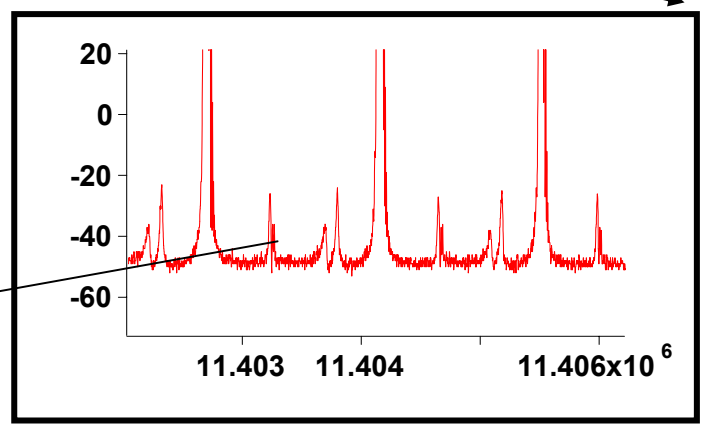

Higher Order FP Modes

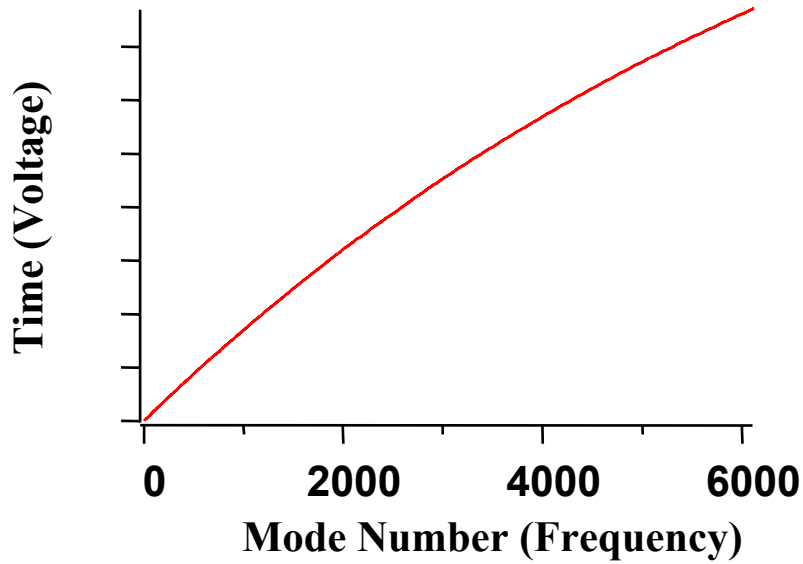

Large Scale
BWO
Frequency Voltage
Dependence

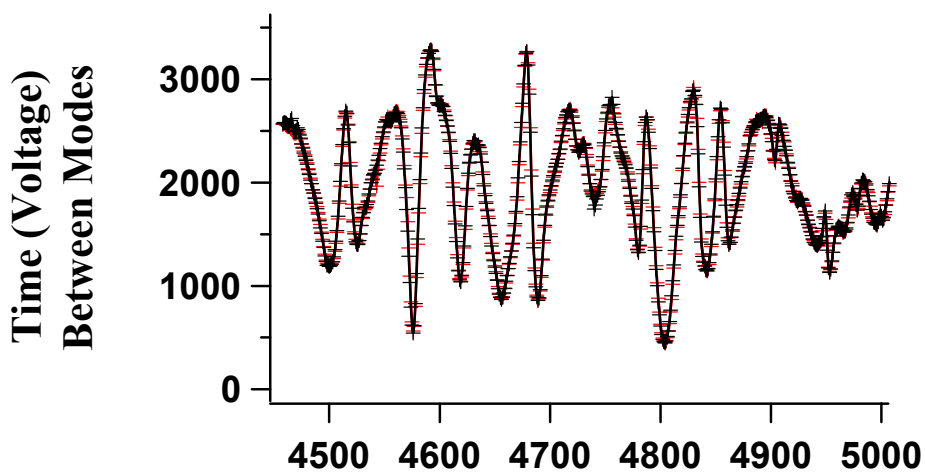

Small Scale

Two Consecutive
Scans

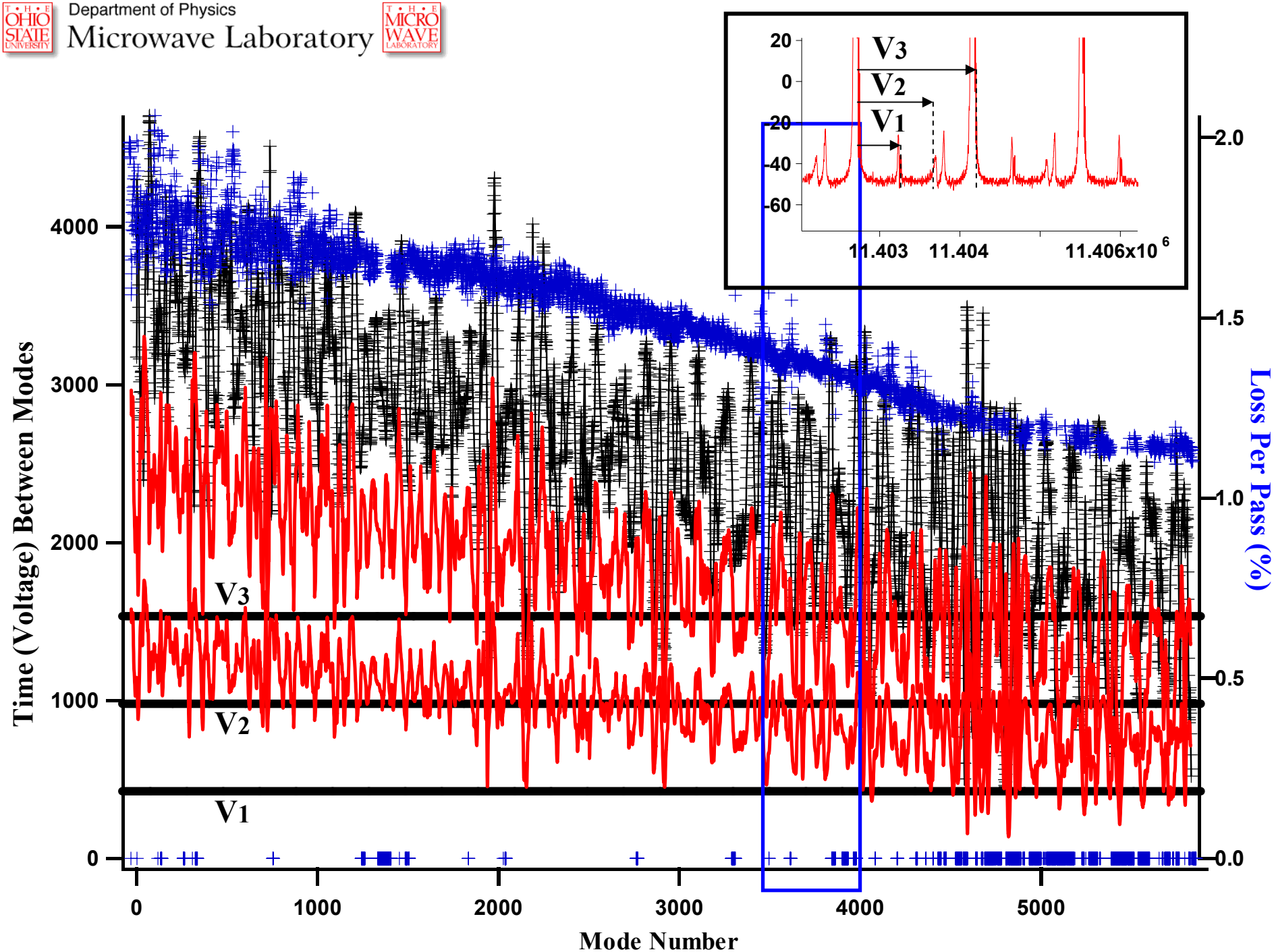
V3
V2
V1
20
0
-20
-40
-60
11.403
11.404
11.406x10 6
4000
3000
2000
1000
0
Time (Voltage) Between Modes
2.0
1.5
1.0
0.5
0.0
Loss Per Pass (%)
0
1000
2000
3000
4000
5000
Mode Number

Higher Order Modes Effect

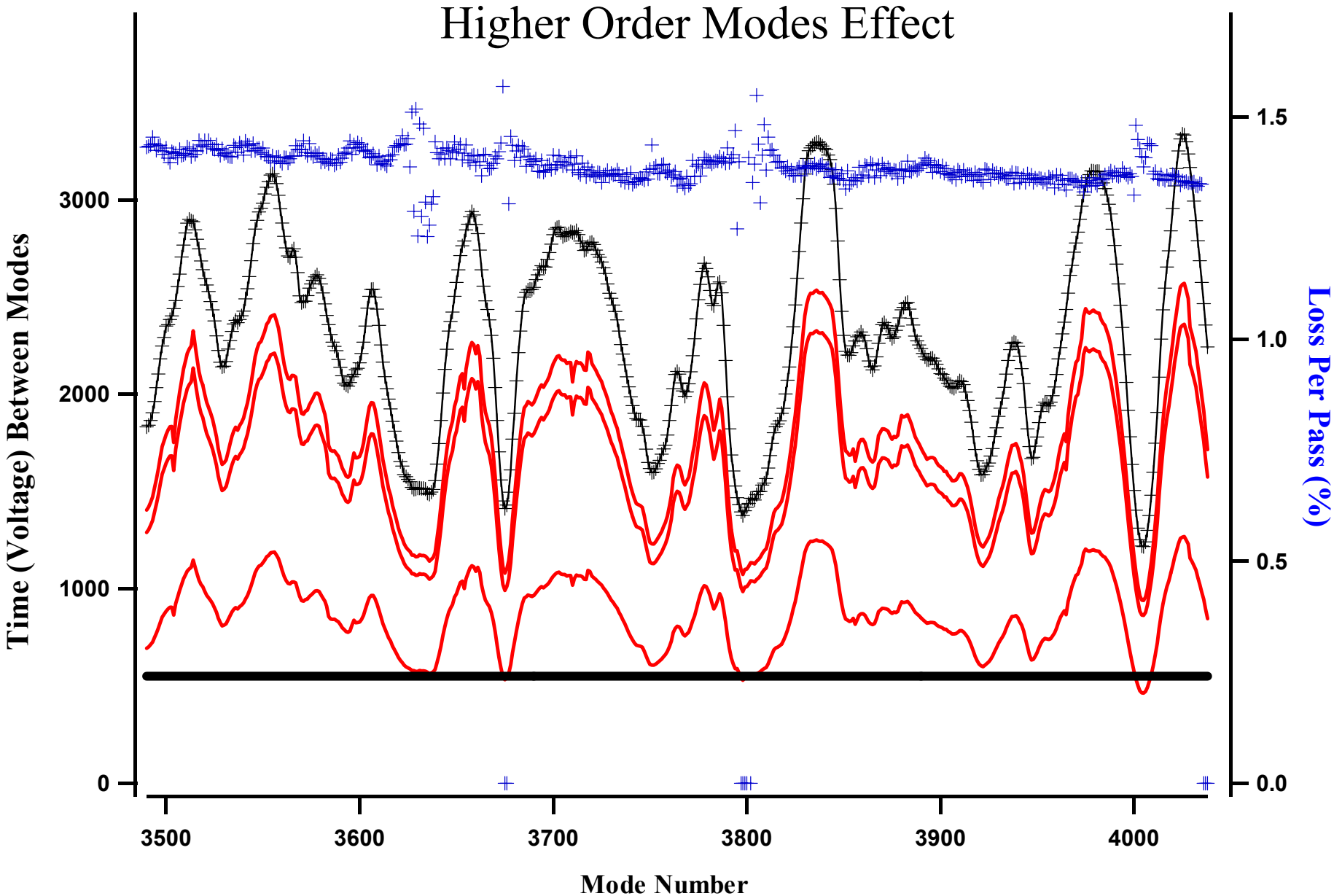

Solutions

Analog

time between a few consecutive FP modes determines the size of the trigger jump

Digital

changing trigger jump as we scan via GPIB controllable Pulse Generator

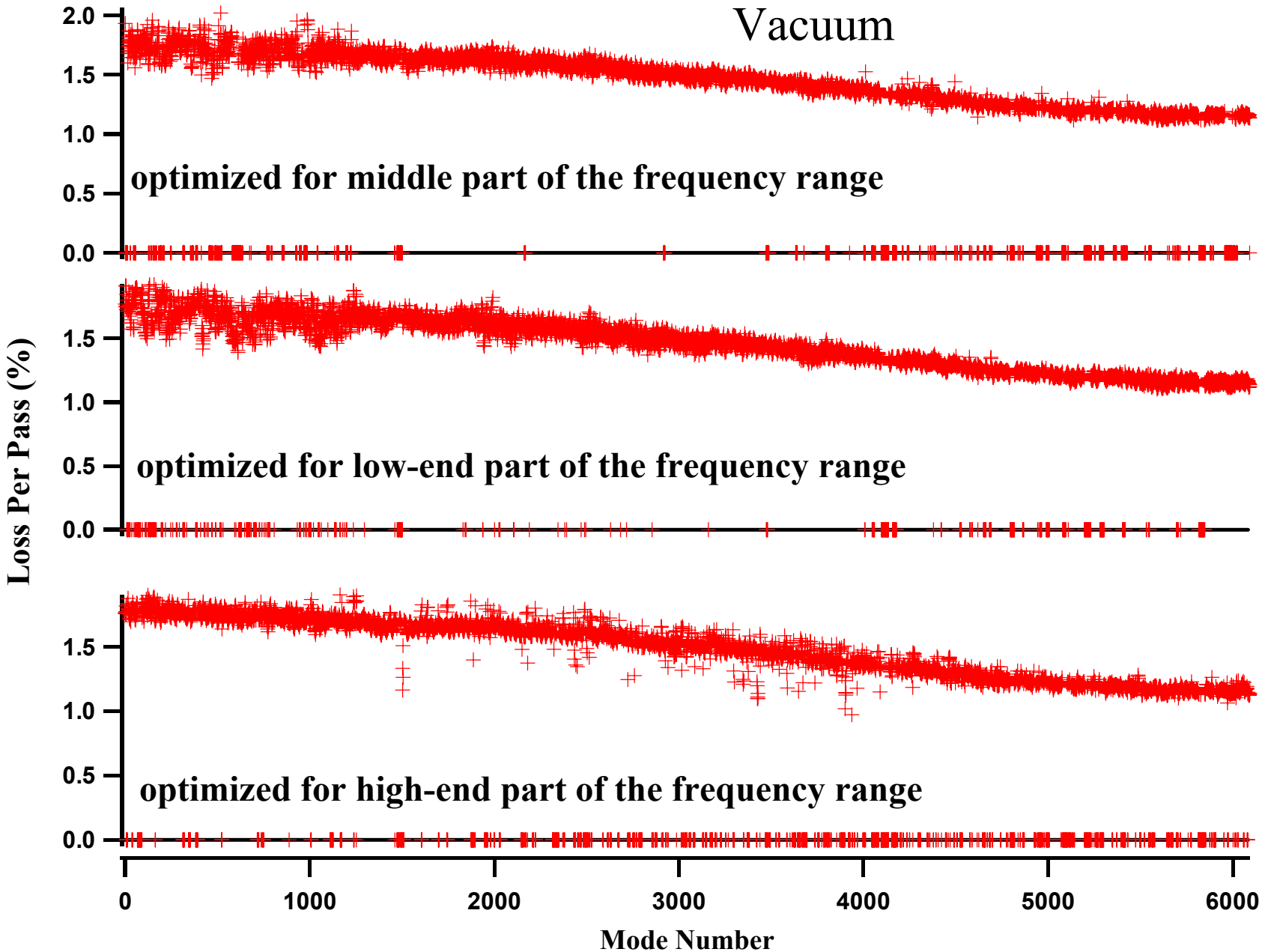
Vacuum
optimized for middle part of the frequency range
optimized for low-end part of the frequency range
optimized for high-end part of the frequency range
Loss Per Pass (%)
2.0
1.5
1.0
0.5
0.0
0
1000
2000
3000
4000
5000
6000
Mode Number

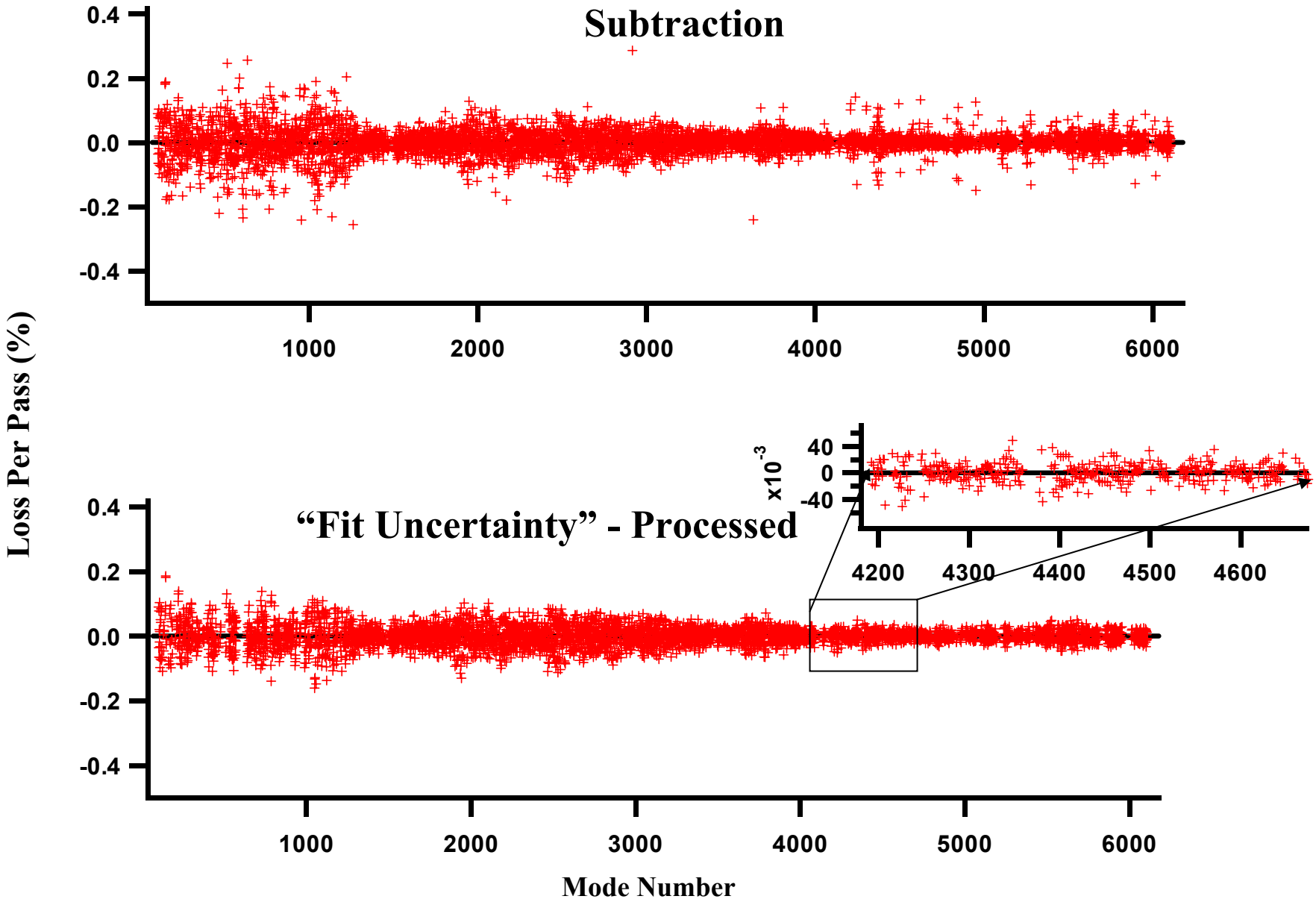
Subtraction
0.4
0.2
0.0
-0.2
-0.4
1000
2000
3000
4000
5000
6000
Loss Per Pass (%)
"Fit Uncertainty" - Processed
x10^-3
40
0
-40
4200
4300
4400
4500
4600
Mode Number

2 atm of Nitrogen

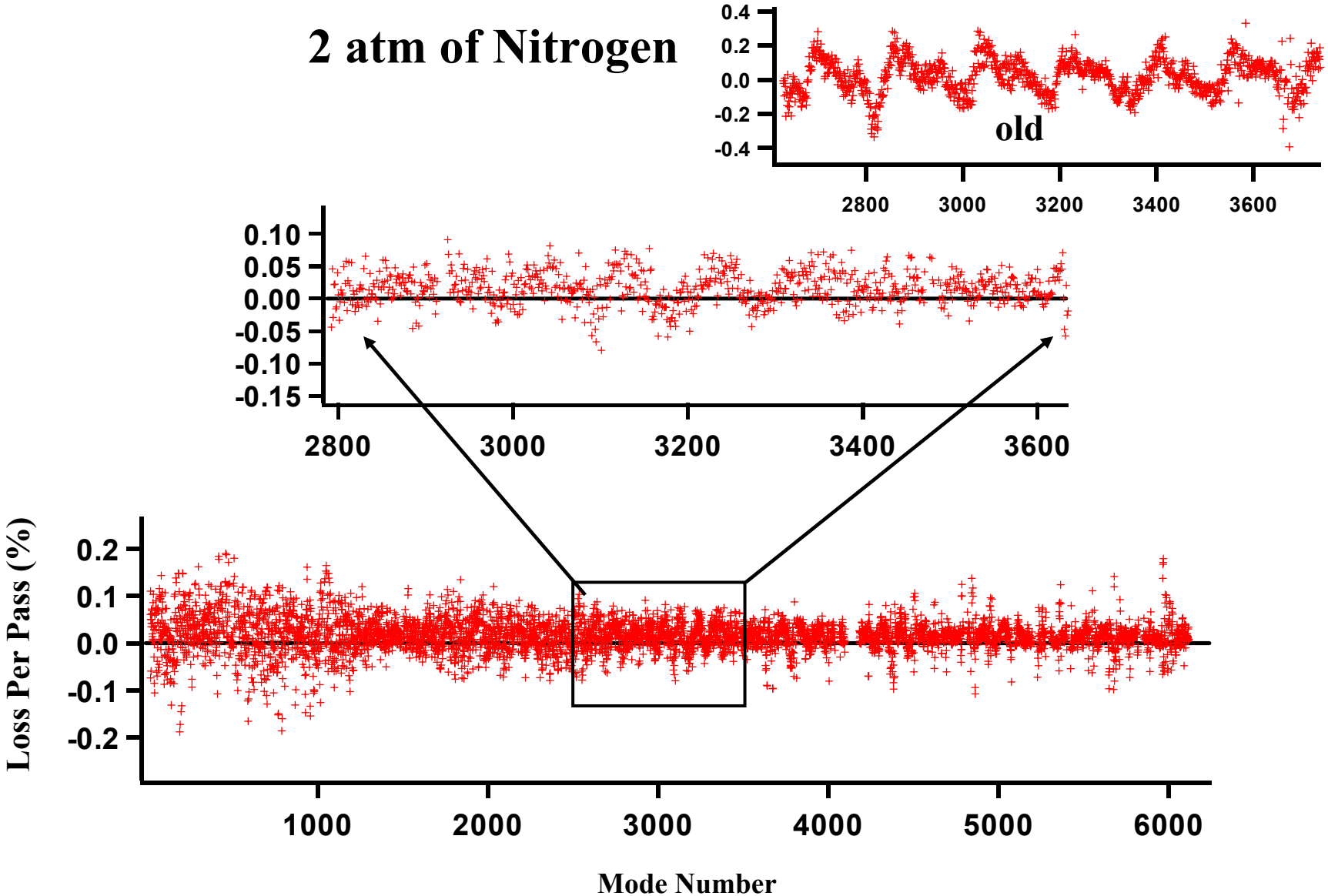

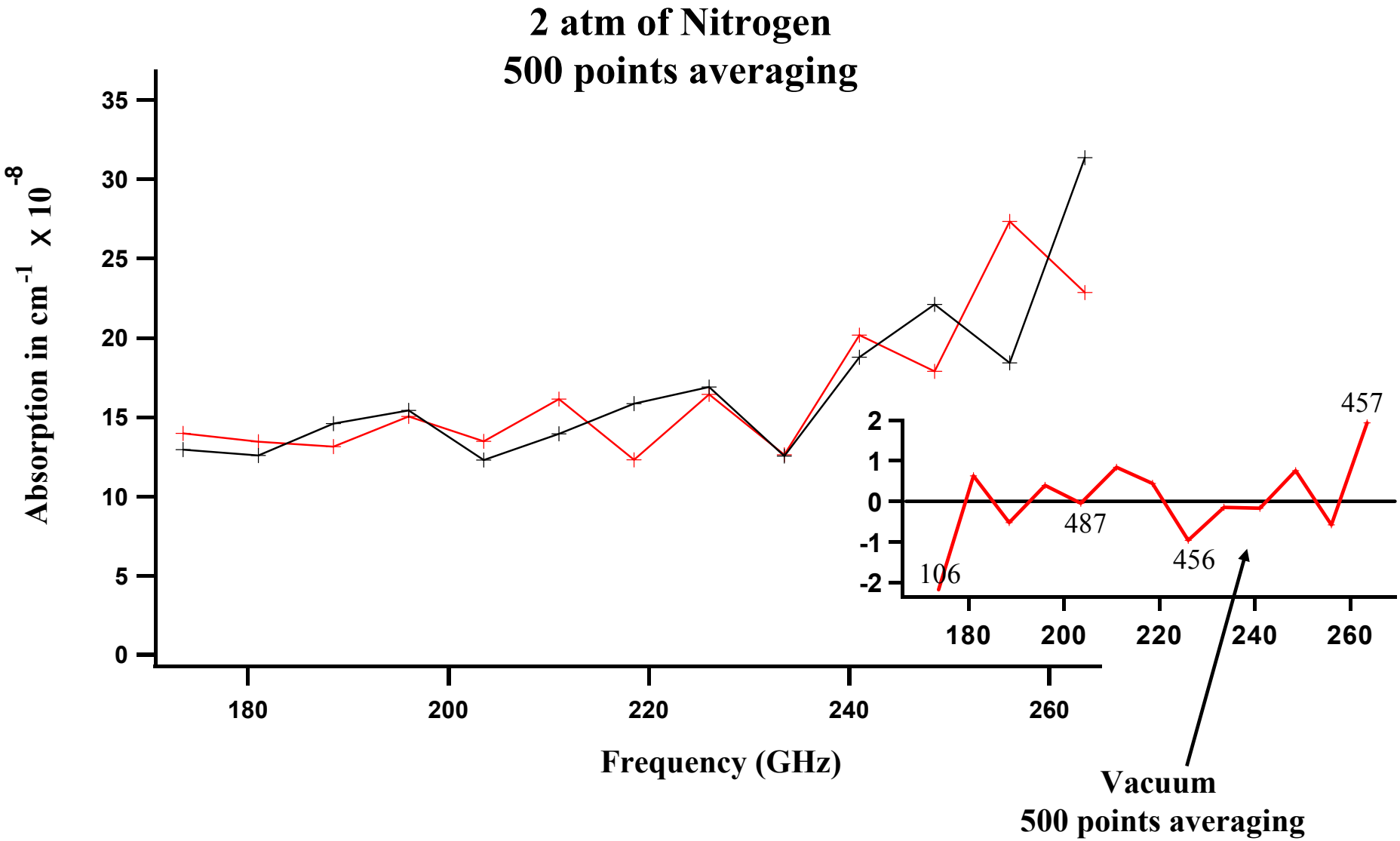
2 atm of Nitrogen
500 points averaging
Absorption in cm-1 X 10-8
35
30
25
20
15
10
5
0
180
200
220
240
260
Frequency (GHz)
2
1
0
-1
-2
106
487
456
457
Vacuum
500 points averaging

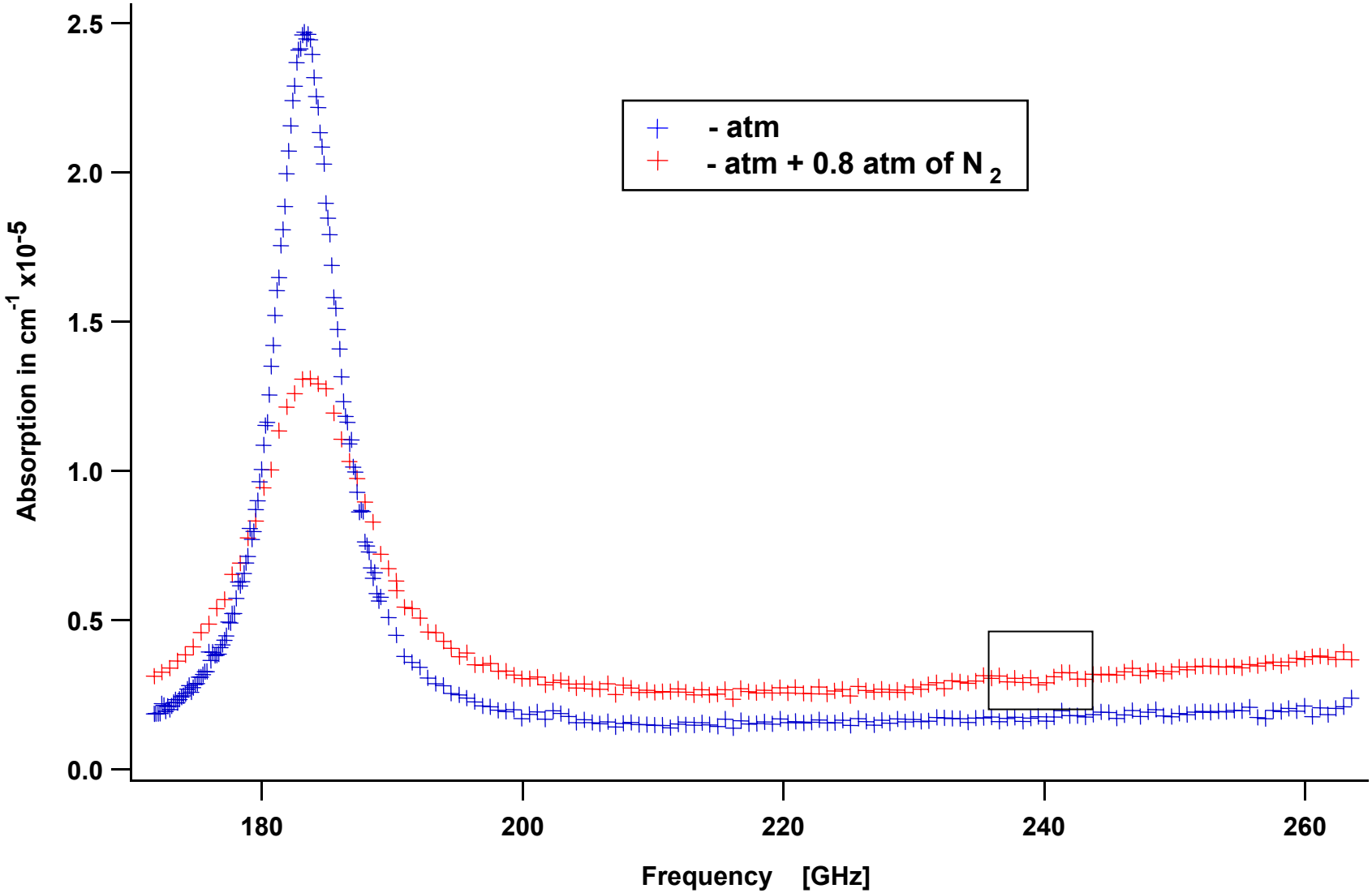
2.5
2.0
1.5
1.0
0.5
0.0
Absorption in cm-1 x10-5
180
200
220
240
260
Frequency [GHz]
- atm
- atm + 0.8 atm of N 2

SYSTEMATIC EFFECTS AND ERROR LIMITS

Water Vapor Concentration

- **-Dry Air Measurements**
- **-Moist Air Measurements**

Water and Other Gases Absorbed on Mirrors

Interference effects

PLANS AND TIME SCALES

Internal mode suppression
- should make atmosphere-vacuum have the same accuracy as vacuum-vacuum

Input & Output coupling
- increase EPL of the cavity by ~50%

Sweep Electronics
- AGC
- Linearization of sweep
- Sweep pause

Variable temperature control

Data runs: three parameter dimensions (P_{air}, P_{water}, T) plus the frequency dimension

Balloon measurements of continuum near 600 GHz

Robert Stachnik

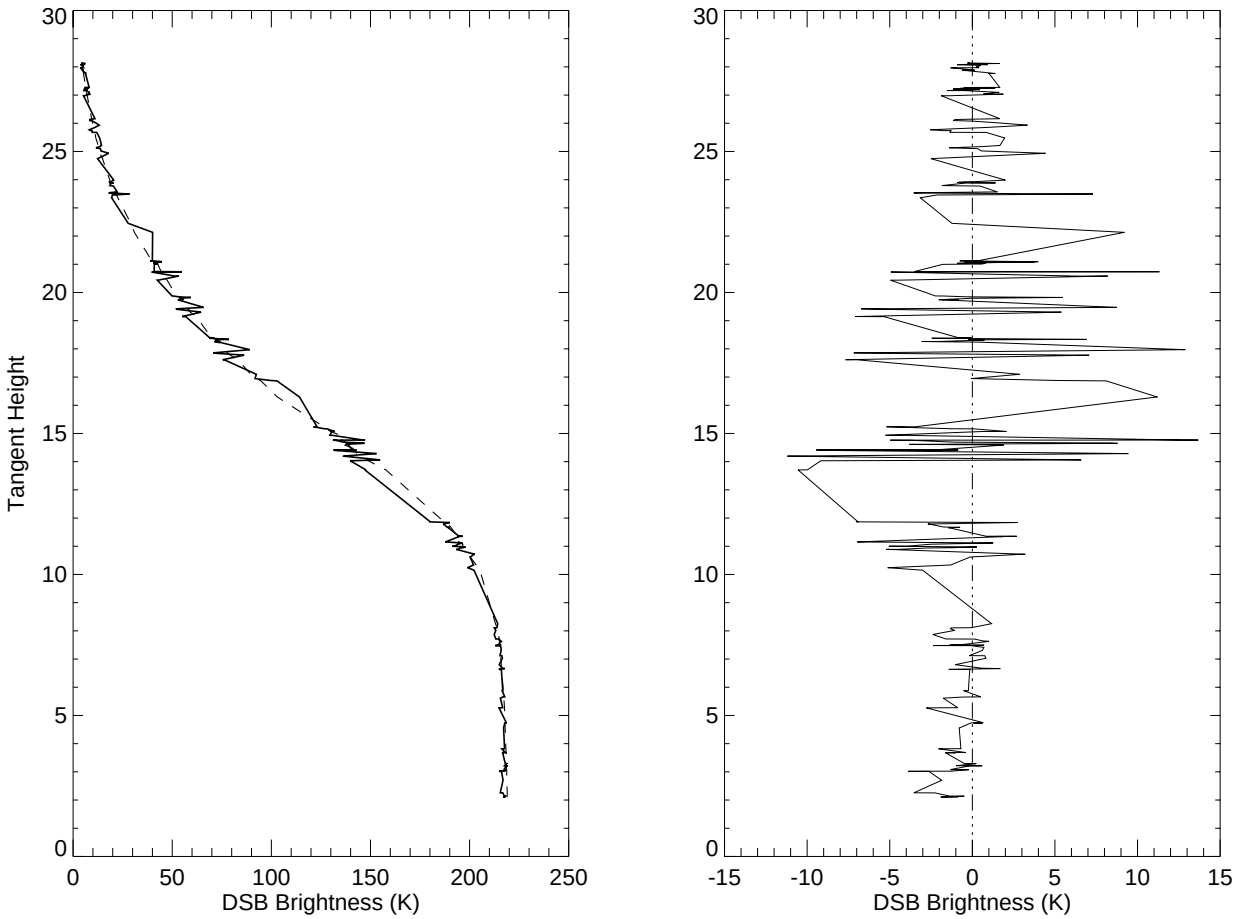

Figure 1: Measured (solid) and calculated (dashed) 640 GHz radiance versus tangent height from 6 successive limb scans from an SLS balloon flight on 20000315 from Kiruna, Sweden (left panel). Measured-calculated residual is plotted in the panel at right. Radiance calculation includes a H_2O 'continuum' cross section component $\beta = C_1\nu^2P^2(300/T)^{C_2}$, where C_1= 5.967e-16 and C_2=3.0 from the EOS MLS Forward Model TBD. 'Scatter' in the residual plot is largely due to balloon gondola (elevation) motion between limb scans.

EOS MLS 'forward model' meeting

Overall Instrument Status, Calibration Data for production processing

Robert F. Jarnot

December 11–12, 2002

OUTLINE

- Summary of instrument status at the time of the PER
- Summary of current instrument status
- Summary of radiometric and spectral calibration data status
  - ⇨ FOV status will be covered by Rick Cofield and/or Paul Stek in a subsequent presentation
  - ⇨ THz status will covered by Herb Pickett in a subsequent presentation

SUMMARY OF INSTRUMENT STATUS AT TIME OF PER, CONTINUED.

- At the time of the PER (March 2002) there were several anomalies that prevented EOS MLS from meeting its performance requirements:
  - ⇨ An odd-even MIF offset in all spectrometer channels,
  - ⇨ excess noise in the 12 Wide Filter channels,
  - ⇨ minor nonlinearity in many spectrometer bands/channels,
  - ⇨ excess phase noise in all GHz 1st. Local Oscillators,
  - ⇨ severe non-idealities in instrument radiometric response made it impossible to reliably measure relative sideband response,
  - ⇨ plots of T_{sys} showed elevated noise in the mid-band sections of all filterbanks, and
  - ⇨ the 'Blue Sky' data for R4 showed mysterious radiance 'bumps' in the center 11 channels of each FB25.

SUMMARY OF INSTRUMENT STATUS AT TIME OF PER

- The severity of these anomalies should not be underestimated. For example:
  - ⇨ Relative sideband sweeps, which for the GHz radiometers generate an 'atmospheric looking' signal of ∼1 GHz width, produced data with unpredictable channel-to-channel systematics up to ∼30 K.
  - ⇨ Tests which should have produced 'flat' spectra (Blue Sky test) were instead generating results with ∼0.5 K artifacts in the center portions of each band.
  - ⇨ Excess First LO phase noise was essentially 'destroying' high resolution DACS data.
- These causes of **all** of these problems were determined, and appropriate corrections implemented.
- This feat is not just a credit to those who identified the problems, but also to the small team who did a remarkable amount of work in a short time to implement the necessary fixes.

SUMMARY OF CURRENT INSTRUMENT STATUS

- Instrument Flight Software has significant loose ends and problems.
- Mechanism software (firmware) is not as robust as it should be:
  - Some mechanisms spontaneously enter 'high current' modes in which they continue to operate, but draw several Amps more current than they should.
  - We also anticipate having to 'tune' some mechanism parameters periodically in orbit.
- The GHz Antenna Scan Actuator has been repaired, but not replaced.
- One power supply needs replacing.
- The problem in FB10 (R4) of channels 20, 22 and 24 exhibiting excess noise has returned.
- SIF2 (the back-end IF electronics for Bands 2 to 6) has started to fail again.
  - This is particularly worrisome because all of the SIFs have been reworked by the manufacturer to overcome workmanship problems.

Calibration Data for production processing software

- EOS MLS calibrations have been completed on schedule.
  - ⇨ A *lot* of calibration data has been taken, and inspected using quick-look software.
  - ⇨ My initial assessment is that the quality of EOS MLS calibrations significantly surpasses that of UARS MLS in all areas.
- The schedule for analysis of these data, and delivery to Level 2, has been discussed with Bill Read, and appears consistent.
- Finally, and initial assessment of instrument performance versus requirements indicates that all important performance requirements are met.
  - ⇨ The *only* performance parameter that appears to not quite meet the letter of the requirements is that for noise in the outer two wide channels of R1B (Band 34), and even in this case the difference between requirements and actual performance is very minor (∼20%).

Pre-Ship Review

Verification of Science Requirements

Robert F. Jarnot

December 17–18, 2002

OUTLINE

- ❑ Summary GHz
- ❑ Requirements
- ❑ Checklist Status
- ❑ Radiometric Performance
- ❑ Requirements and Measured Noise Performance
  - ⇨ Plots of T_{sys} for all GHz bands
- ❑ Linearity
  - ⇨ Linearity Plots of Selected Bands
- ❑ Summary of Radiometric Performance Issues
- ❑ Spectral Performance
- ❑ Overall Summary
- ❑ THz performance verification covered in a subsequent presentation

SUMMARY

- At the time of the PER (March 2002) there were several anomalies that prevented EOS MLS from meeting all of its performance requirements:
  - ⇨ An odd-even MIF offset in all spectrometer channels,
  - ⇨ excess noise in the 12 Wide Filter channels,
  - ⇨ minor nonlinearity in many spectrometer channels,
  - ⇨ excess phase noise in all GHz 1st. Local Oscillators,
  - ⇨ severe non-idealities in instrument radiometric response made it impossible to reliably measure relative sideband response,
  - ⇨ plots of T_{sys} showed elevated noise in the mid-band sections of all filterbanks, and
  - ⇨ the 'Blue Sky' data for R4 showed mysterious radiance 'bumps' in the center 11 channels of each FB25.
- These causes of all of these problems have been determined, and appropriate corrections implemented.

REQUIREMENTS

- All performance requirements are taken from the 'Science Requirements on the EOS MLS Instrument and Data Processing Software' document (JPL D–14421), Revision 3.0
  - ⇨ Requirements are stated with results in this presentation
- An additional document, 'EOS MLS Flight Instrument Scientific Functional Verification and Calibration Checklist,' details all required verifications and calibrations.
- All Radiometric and Spectral requirements have been tested, results are outlined on the following pages.

Requirements Verification Checklist Summary

- All Local Oscillator and Filter Channel positions and widths have been verified:
  - ⇨ In addition, all filter channels have been shown to meet 'efficiency' requirements, and
  - ⇨ channel stability requirements are met with wide margins.
- All noise/sensitivity requirements have been tested:
  - ⇨ All requirements are met, except for some R1B Wide Filter channels which exhibit spectrally-varying noise $\sim 1.2\times$ requirements.
- Minor departures from ideal linearity have been measured in some channels:
  - ⇨ Some bandpass shape changes with signal power level have been observed. These effects require further study, but are not believed at this time to impact any measurement objectives.

RADIOMETRIC PERFORMANCE

Introduction:

- Sensitivity/noise are measured at the GHz Switching Mirror cavity Limb port
  - ⇨ this takes into account all optics/quasi-optics losses between the receivers and Switching Mirror Limb port
  - ⇨ sensitivity to limb radiances is slightly worse than presented below due to Antenna optical losses (reflectivities, scattering, . . .)
- Knowledge of Relative Sideband Response is required since all sensitivity requirements are levied in a single sideband.
- This presentation condenses a substantial amount of test data into just a few viewgraphs. It is inevitable that only the 'big picture' is presented here, with many details omitted.

RADIOMETRIC PERFORMANCE

Spectrally-Varying Allowable Noise Requirements:					Results:			
	T_{sys}	$\Delta I_{6\,MHz}$	$\Delta I_{96\,MHz}$	ΔI_{min}	T_{sys}	$\Delta I_{6\,MHz}$	$\Delta I_{96\,MHz}$	ΔI_{min}
R1A	1500 K	1.5 K	0.4 K	0.1 K	<1350 K	1.2 K	0.35 K	0.02 K
R1B	1500 K	1.5 K	0.4 K	0.1 K	<1400 K	1.3 K	0.40 K	0.02 K
R1BWF	1500 K	ΔI_{500} = 0.2 K		0.1 K	<2000 K	ΔI_{500} = 0.23 K		0.02 K
R2	4000 K	4 K	1 K	0.1 K	<3000 K	3.2 K	0.9 K	0.02 K
R2B5	4000 K	4 K	1 K	0.03 K	<2200 K	3 K	0.8 K	0.02 K
R3	4000 K	4 K	1 K	0.1 K	<3700 K	4 K	1 K	0.02 K
R3WF	4000 K	ΔI_{500} = 0.4 K		0.1 K	<4000 K	ΔI_{500} = 0.4 K		0.02 K
R4	12000 K	12 K	3 K	0.1 K	<12000 K	10 K	3 K	0.1 K

- Measured Relative Sideband responses are between 1:1 and 0.8:1 (u/l)
  – requirements are met, with exception of R1B Wide Filters.
- Measured ΔI_{min} based on ~5 hours each of signal and reference, include all spectrometer channels, and are pk–pk values. Requirements need demonstration to only 1 hour of integration time.

RADIOMETRIC PERFORMANCE

Requirements for Spectrally-Averaged Noise:	Results:
The allowable 1σ noise in the spectrally-averaged component *of the radiance from each radiometer (ssb, after calibration, average value over all channels of the radiometer) measured in an individual 0.17 s integration period is* $4\times10^{-4}\times T_{sys}$ *for all GHz radiometers.*	R1A: 1.9E-4$\times T_{sys}$ R1B: similar to R1A R1WF: 2.2E-4$\times T_{sys}$ R2:1.2 – 1.6E-4$\times T_{sys}$ R3: 0.9 – 2.4E-4 $\times T_{sys}$ R4: 2.2E-4 $\times T_{sys}$

- The noise levels indicated above are dependent upon the calibration sequence and calibration algorithms.
- The results above were derived using the nominal in-flight calibration sequence and algorithms with a Calibration Window of 6 MAFs.
- Requirements for spectrally-averaged noise are met.

Radiometric Performance: T_{sys} for 25 channel Filterbanks

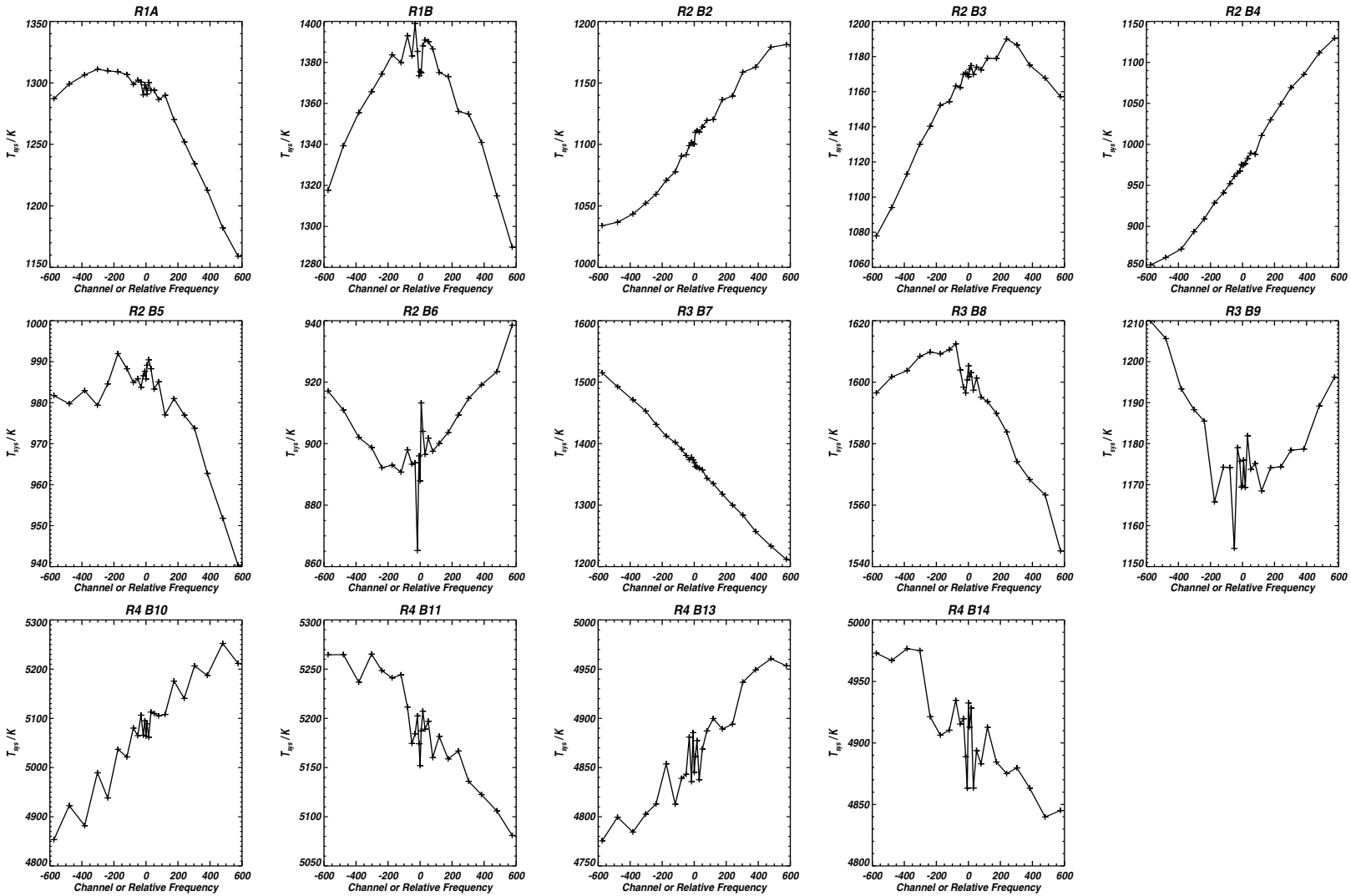

Radiometric Performance: T_{sys} for Mid-Band and Wide Filters

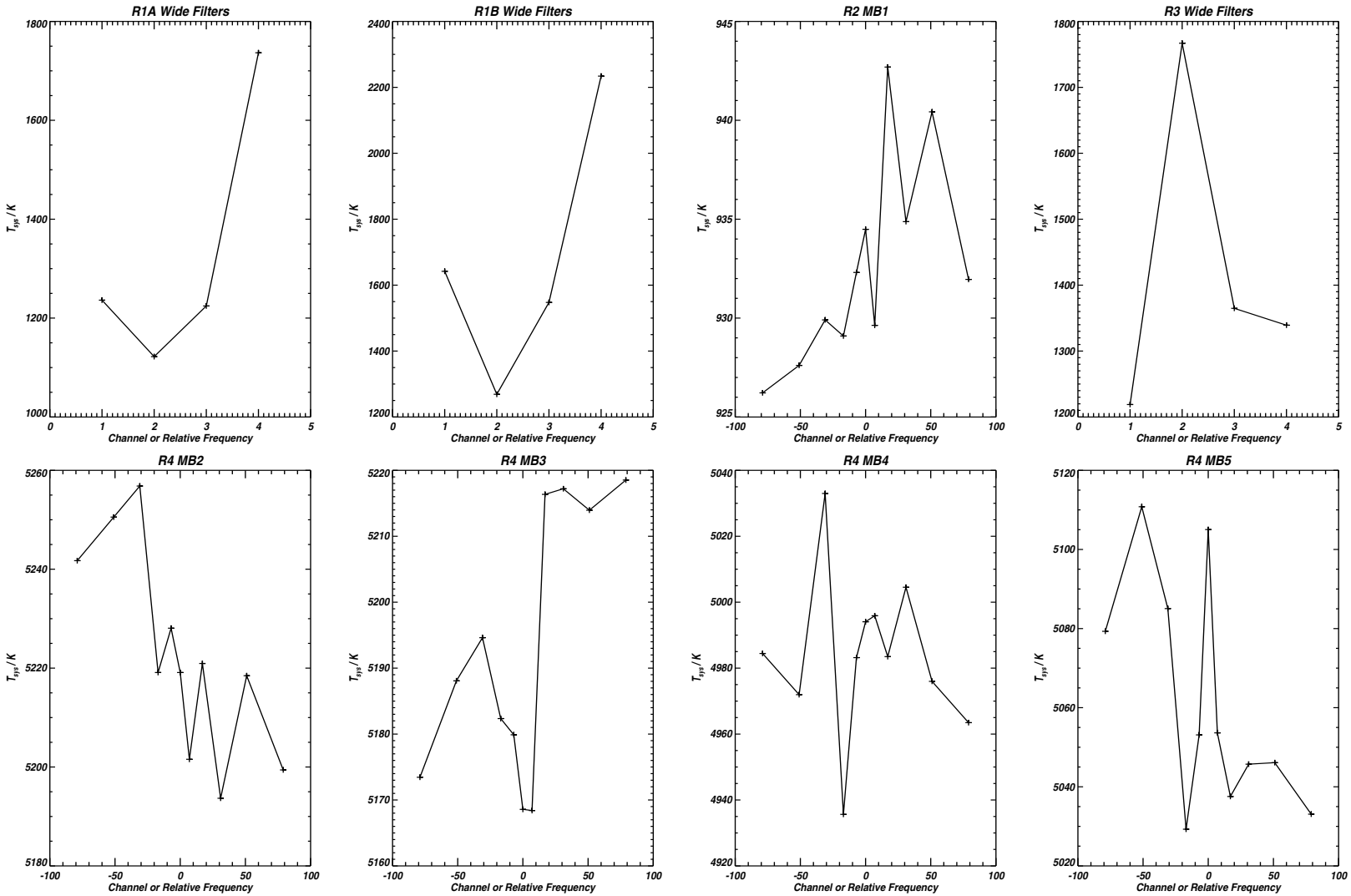

RADIOMETRIC PERFORMANCE

Linearity must be considered in two distinct ways:

- *Integral Linearity:* the large scale variation of 'Counts' versus scene radiance
  - ⇨ non-idealities in this realm map directly into radiometric gain errors
- *Differential Linearity:* the channel-to-channel calibrated radiance variations as the scene temperature moves between the reference temperatures (Space and internal Target)
  - ⇨ these are the more important linearity errors since they add spectral artifacts to the measured radiances
- Linearity data samples from all radiometers are presented on the following pages

Linearity Performance: R1B

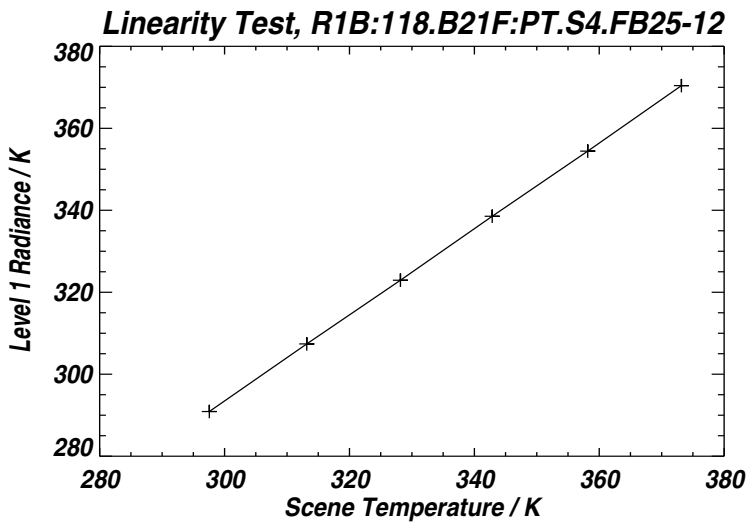

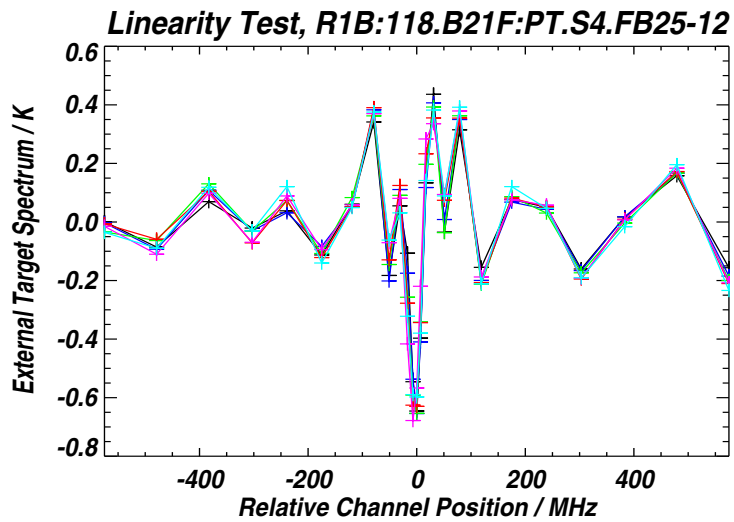

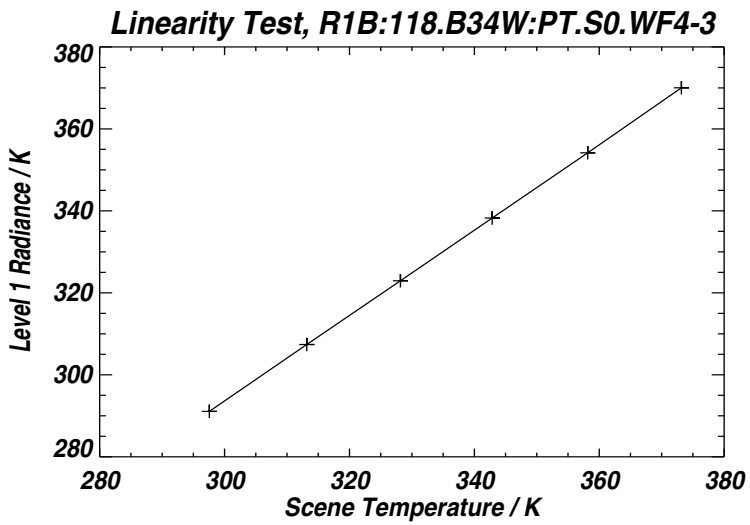

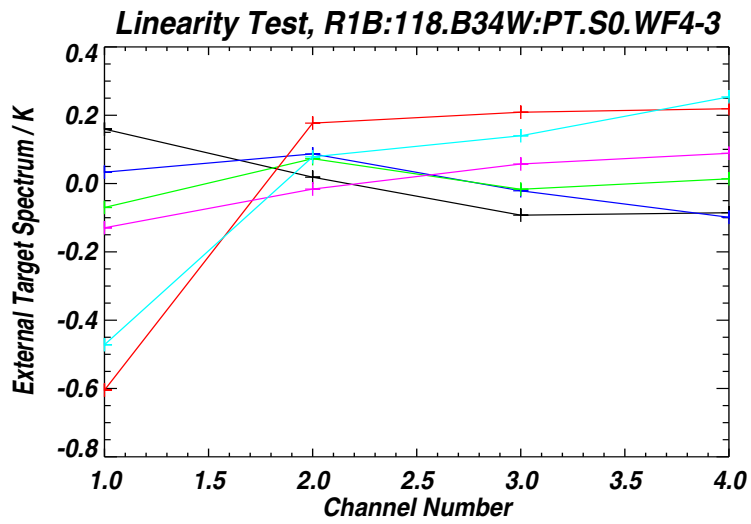

Linearity Performance: R2, B2 and B6

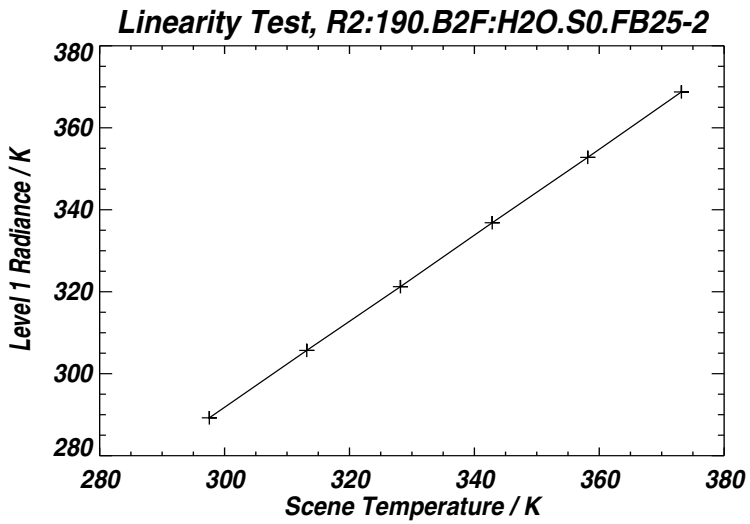

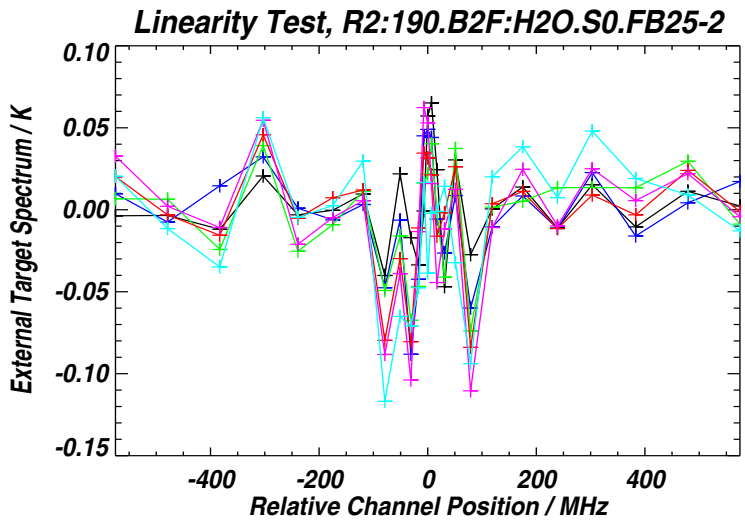

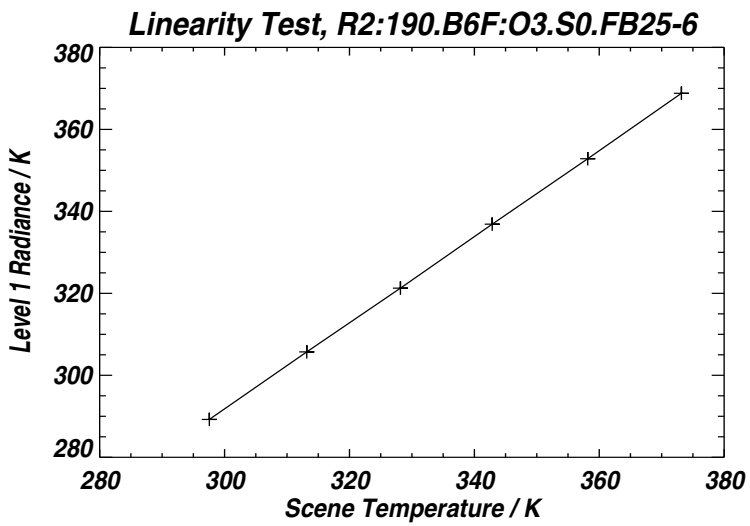

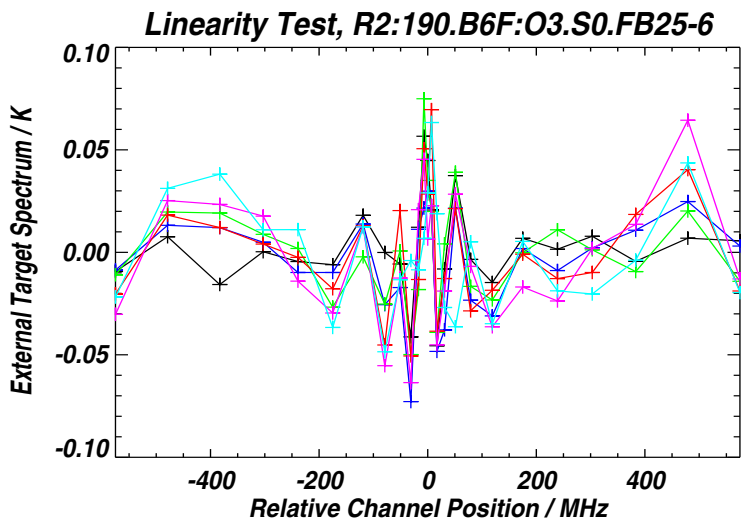

Linearity Performance: R3, B7 and B33

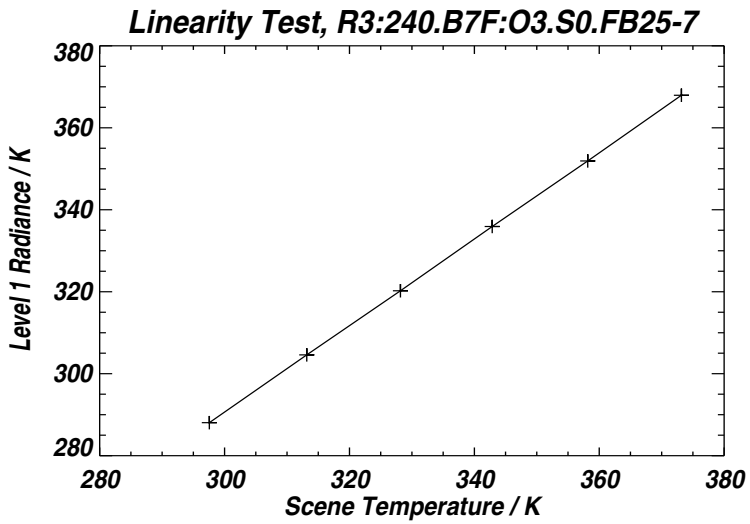

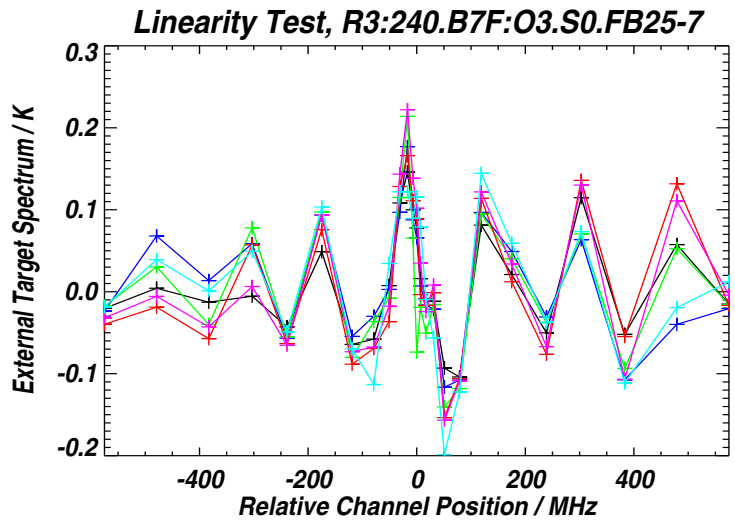

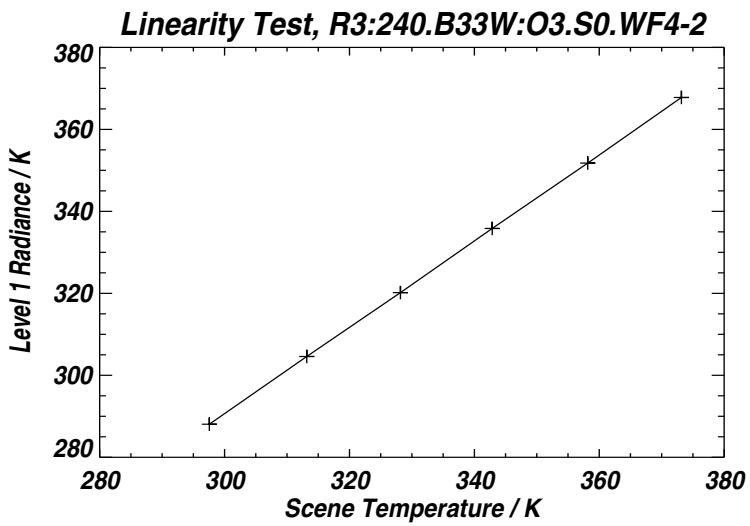

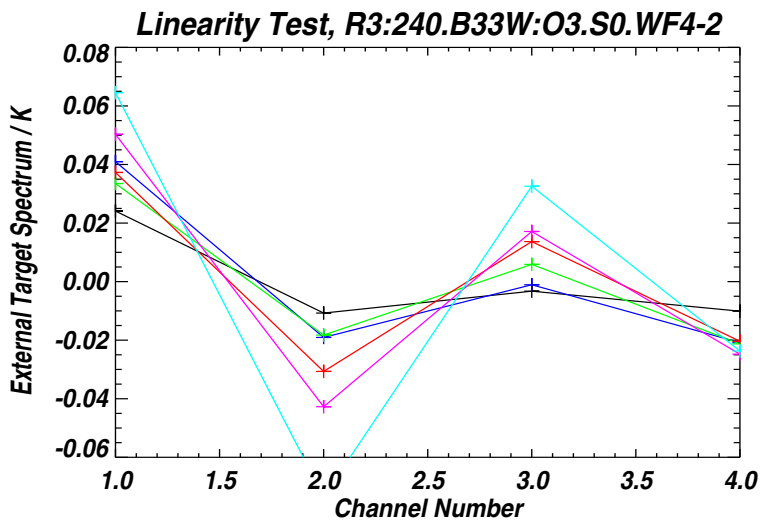

Linearity Performance: R4, B10 and B14

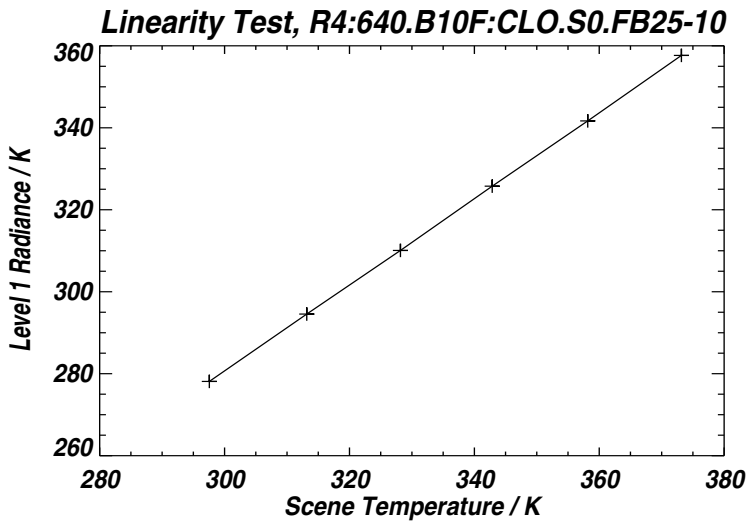

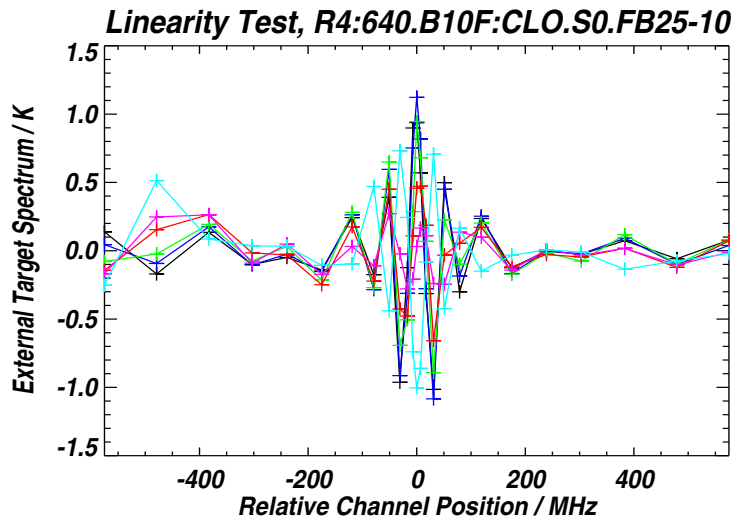

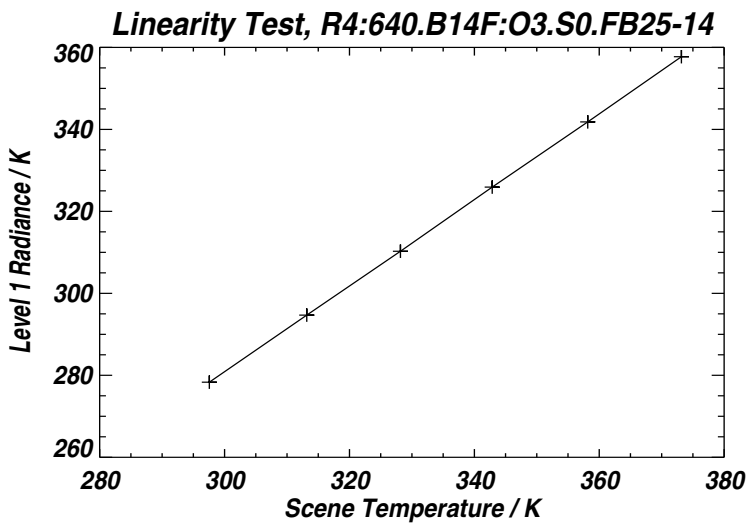

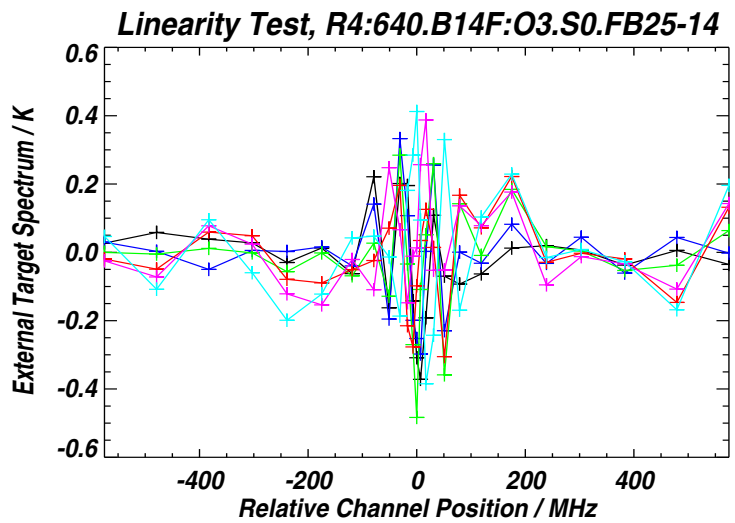

RADIOMETRIC PERFORMANCE

Summary of linearity data:

- Integral Linearity is very good in all bands.
- Differential Nonlinearity effects are evident in several 11 and 25-channel Filterbanks, but at sufficiently low levels not to be a problem.
- The clearest evidence of nonlinearity appears in the data from all three Wide Filter sets. These nonlinearity characteristics are highly repeatable, and discussions with Nathaniel Livesey indicate that the observed behavior will not be a problem for Level 2 processing.
- Data from the other bands are very similar to those presented here.

SPECTRAL PERFORMANCE

- All channel and LO positions have been verified.
- Master Oscillator frequency monitoring results predict 1 part in 10^{-8} drift over 5 years (requirement is $<6\times10^{-8}$).
- All bands have been swept with a Fabry-Pérot for relative sideband determination.
- All channels have been swept (end-to-end) in both sidebands (except R1A/B which are single-sideband implementations).
  - ⇨ All FilterBank Switch permutations have been swept.
  - ⇨ In bands with significant standing waves introduced by the sweeper (R1 and R4), all sweeps were performed twice (source in nominal and $\lambda/4$ shifted positions).
  - ⇨ R1 sweeps were performed in the test cart (not Nearfield) configuration to move the source away from the Space Port.

SPECTRAL PERFORMANCE, CONTINUED.

- Front-end sweep data have been examined for spectral responses in extraneous regions.
- Fabry-Pérot (Relative Sideband) sweep data have been similarly scrutinized.
- Key spectral regions have been explicitly targeted with the Front-end sweep apparatus to search for unwanted spectral responses.
  - ⇨ No sensitivity in untargetted spectral regions has been observed.
- Spectral performance requirements are met.

DIGITAL AUTOCORRELATOR SPECTROMETERS

- Radiometric performance requirements are met:
  - ⇨ Measured noise is at the levels expected for a 2-bit digital autocorrelator with the chosen threshold levels and encoding scheme (Padin).
- Spectral performance meets requirements:
  - ⇨ Channel positions and overall passband shapes have been measured.
- Correct operation in compressed and uncompressed Science Data modes has been verified.

SUMMARY

- All radiometric performance requirements are met except:
  - ⇨ Spectrally-varying noise in the R1B Wide Filter channels is up to $\sim 1.2\times$ requirements, and
  - ⇨ minor nonlinearity needs further evaluation, but does not appear to be a problem at this time.
- Instrument spectral performance meets requirements.
- From the Radiometric and Spectral performance viewpoint, the instrument is ready for shipment.

EOS MLS 'forward model' meeting

Instrument Data for Level 1 Software

Robert F. Jarnot

December 11–12, 2002

CATEGORIES

- Diagnostic/Engineering
- Radiometric Calibration
- Pointing
  - ⇨ See Table 4.2 of the Level 1 ATBD (included at the end of this presentation) for further details.

Diagnostic/Engineering

- R_0, C_l, C_h, a, b, c, d, e, f (EU to temperature conversions)
  - ⇨ All data available.

Radiometric Calibration

- B_i, τ, $S_g(f)$ (Noise bandwidths, integration time, PSD)
- ρ, η (optics reflectivities, efficiencies, baffle transmissions)
  - ⇨ All data available. Analysis required.

Pointing

- **E**, **D** (Rotation matrices, Instrument-to-S/C, S/C-to-IRU)
  - ⇨ Data to be obtained at TRW. See FOV presentation.

Table of Level 1 parameters (from ATBD):

Table 4.2: Summary of parameters required by Level 1 software. PRD is an abbreviation for Platinum Resistance Device, the type of temperature sensor used to monitor the ambient calibration targets. IRU is the abbreviation for Inertial Reference Unit, the spacecraft attitude determination system.

Symbol	Units	Description	Purpose
B_i	Hz	Noise bandwidth of each filter channel	Radiometric noise determination
τ	s	Integration time	Radiometric noise determination
$S_g(f)$	$\mathrm{W\,Hz^{-\frac{1}{2}}}$	Post detector noise power spectral density for each radiometer	Absolute radiance uncertainties
r'_l, r'_u	–	Relative sideband responses from mixer to switching mirror	Radiometric calibration
ρ_r^k	–	Reflectivity of antenna element k	Antenna emission (radiance) determination
$\eta_{i,s}^{AA}$	–	Antenna beam efficiencies	Limb port to limb radiance conversion
$\eta_{i,s}^{MX}$	–	Baffle transmissions	Radiometric calibration
$\eta_{i,s}^{k}$	–	Optical transmission of antenna reflector k	Radiometric calibration
ϵ_r	–	Calibration target emissivities	Target radiance determination
$\mathrm{d}\alpha$	$\mathrm{K^{-1}}$	Pointing thermal coefficients	Absolute pointing. These coefficients are combined with measured MLS structural temperatures to determine thermal distortions
α, ϵ	$^\circ\,\mathrm{Count^{-1}}$	Encoder coefficients	Conversion of encoder counts to pointing angles
$\mathbf{E}$	–	Rotation matrices from instrument to spacecraft reference cubes	Absolute pointing determination
$\mathbf{D}$	–	Rotation matrix from spacecraft reference cube to IRU reference frame	Absolute pointing determination
$\mathbf{E}^T$, $\mathbf{D}^T$	$\mathrm{K^{-1}}$	Thermal coefficients of $\mathbf{E}$ and $\mathbf{D}$	Absolute pointing. These coefficients are combined with spacecraft thermal data to correct for thermal distortions in spacecraft structure between MLS and the IRU.
$\mathrm{R_0}$	Ω	0 C resistances of individual PRD temperature sensors	Determination of cal target temperatures
$\mathrm{C_l}, \mathrm{C_h}$	Ω, V	Engineering Data Hybrid internal calibration values	Conversion of engineering data "counts" to engineering units
a, b	–	PRD conversion coefficients	Conversion of PRD resistance into inferred temperature
c, d, e, f	–	Thermistor conversion coefficients	Conversion of thermistor resistance into inferred temperature

EOS MLS 'forward model' meeting

GHz radiometric and spectral data for forward model

Robert F. Jarnot

December 11–12, 2002

SUMMARY

- All necessary radiometric and spectral data have been acquired.
- Data quality is very good to excellent.
- I have included the Pre-Ship Review presentations to illustrate some of these data.

Pre-Ship Review

GHz Radiometric and Spectral Calibration Status

Robert F. Jarnot

December 17–18, 2002

OUTLINE

- ❑ Radiometric Calibration Requirements
- ❑ Radiometric Calibration
- ❑ Relative Sideband Response
- ❑ Calibration Targets
- ❑ Spectral and FOV Calibration Requirements
- ❑ Spectral Calibration
- ❑ Summary

Documentation and Requirements

- The EOS MLS Calibration Plan (JPL D–15189, EOS MLS DRL 018) presents the plan for calibration of this instrument
  - ⇨ All calibrations leverage experience gained with calibration of UARS MLS, the only significant changes being in the method chosen for GHz antenna FOV calibration (Near-Field versus Far-Field), and the more sophisticated switching and data analysis used in the relative sideband response measurements.
  - ⇨ In addition, all Radiometric and Spectral Calibrations were performed with the external test equipment tightly synchronized to the instrument. This afforded an order of magnitude time savings compared to the prior UARS equivalent measurements, and noticeably improved data quality.
- Calibration requirements are taken from the 'Science Requirements on the EOS MLS Instrument and Data Processing Software' document (JPL D–14421), Revision 3.0
- All GHz Calibrations were successfully performed as per the Plan, and within the proposed schedule.

Requirements

Radiometric Calibration:

- *Radiometric calibration shall be performed and provide the means to convert the output of each instrument data channel to the total amount of power received by that channel through the MLS antenna*
- *The systematic uncertainty (i.e. not including the estimated contributions of random noise) in the absolute value of the atmospheric/Earth radiances measured through each spectral channel shall be less than 3 K (at the 90% confidence level)*
- *The systematic uncertainty (i.e. not including the estimated contributions of random noise) in the spectrally-varying component of the atmospheric/Earth radiances, measured from one channel or filter to another throughout a given radiometer, shall be less than 1% or $\Delta I_{\mathrm{min}}/3$, where ΔI_{min} for each spectral region is given in Table 3.2–2*

RADIOMETRIC CALIBRATION

- The most important Radiometric Calibration parameters (as used by Level 1 Data Processing software) are provided by FOV Calibration, and are described in the next presentation.
  - ⇨ FOV-related parameters include Switching Mirror cavity baffle transmissions, Antenna reflector reflectivities, emissivities and scattering parameters.
- Relative sideband response is required by Level 2 (retrieval) software in order to interpret the measured radiances correctly.
- We require knowledge of internal Calibration Target emissivity, but there is only a weak dependence on this knowledge since most of the small spillover (radiance seen from outside the Calibration Target baffles) is at approximately the same temperature as the calibration Targets themselves.
- Calibration parameters are required for the PRD (temperature monitors) on the Calibration Targets, and for the electronics which read the PRD resistances.

Relative Sideband Response

Relative sideband response is measured using a Fabry-Pérot to sweep through both sidebands of each radiometer:

- Two sets of grids are required (90 and 200 lpi) to sweep all radiometers.
- The GHz switching mirror provides an ambient view every Major Frame (MAF), and
- external switching mirrors provide LN_2 views every MAF (before and after the Fabry-Pérot).
- These calibration views provide periodic gain calibration, and allow the use of Level 1 software to process the Fabry-Pérot data directly into radiances.
- The switching mirror behind the Fabry-Pérot provides both ambient and LN_2 views for each grid separation:
  - ⇨ This eliminates the effect of the standing waves introduced by the Fabry-Pérot.
- Preliminary analyses indicate satisfactory sideband performance in all GHz receivers.
- A schematic and picture of the sideband measurement setup, and some quick-look FM data, are presented on the following pages.

Relative Sideband Response Measurement System

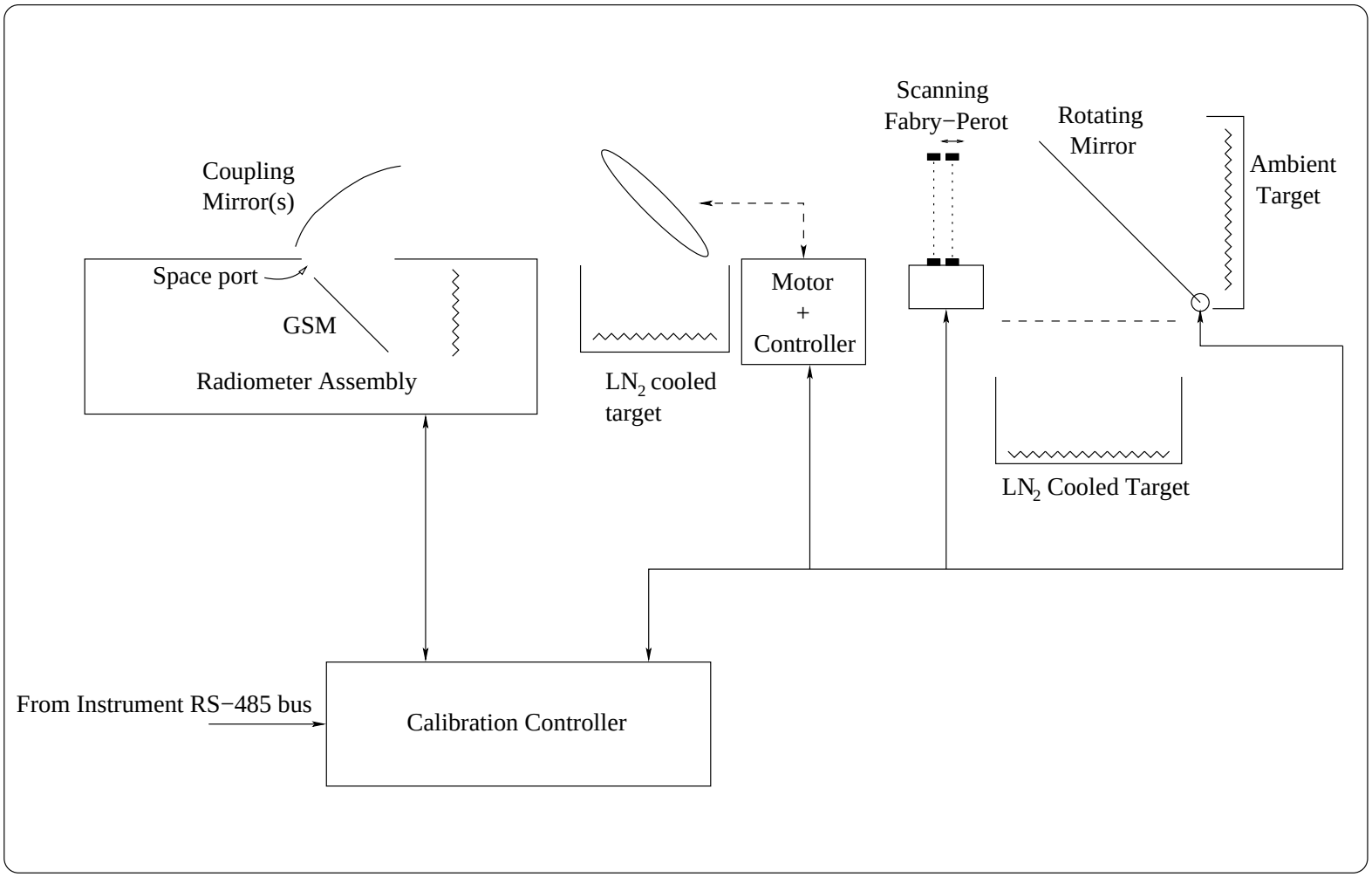

Relative Sideband Response Measurement Timing (R4)

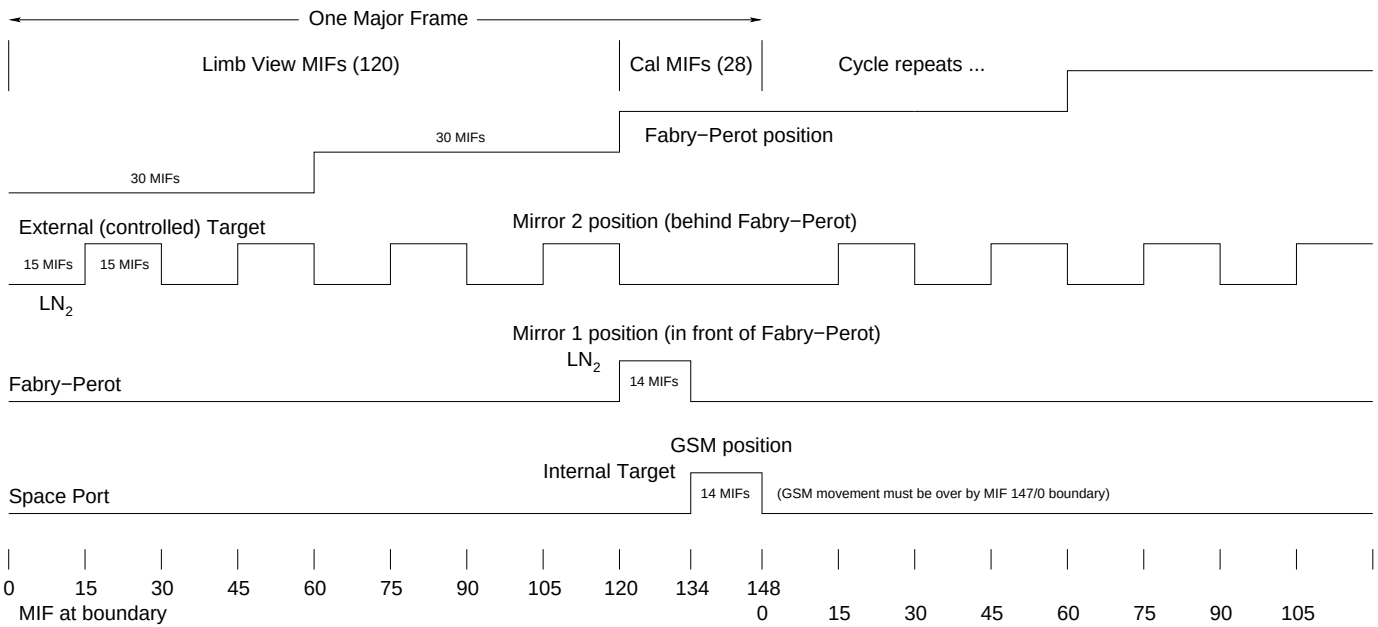

GSM: @MIF 134 move to Internal Target. @MIF 145 move to Space Port. This motion must end prior to start of next MAF.

External Mirror 1: @MIF 120 move to LN2 view. @ MIF 134 move to Fabry−Perot view.

External Mirror 2: @MIFs 30, 60, 90 and 120 move to LN2 view. @MIFs 15, 45, 75 and 105 move to External (controlled) Target view.

Fabry−Perot movements are steps taking place starting at MIFS 30 and 90.

The following Level 1 overrides assume that the GSM and external switching mirrors perform their sequences exactly as indicated above, and that motions take 3 MIFs (or less) to complete (for all mirrors and Fabry−Perot).

Level 1 overrides: (approximate)

T = MIFs 137..144. Use actual temperature of Internal Target in data processing.

S = MIFs 122..133. Assume 80 K temperature for LN2 view.

L = remaining MIFs, which should be views through the Fabry−Perot as follows:

To LN2: MIFs 3..14, 33..44, 63..74 and 93..104. Assume T is stable (80 K).

To external target. MIFs 18..29, 48..59, 78..89 and 108..119. Assume temperature is stable (30 C).

The remaining MIFs should all be Discards (due to mirror/FP movement).

/users/jarnot/texinput/figures/FPsequence_2.fig

Relative Sideband Response, continued

FM Relative Sideband Sweep, Band 2 (R2) 10 μm steps

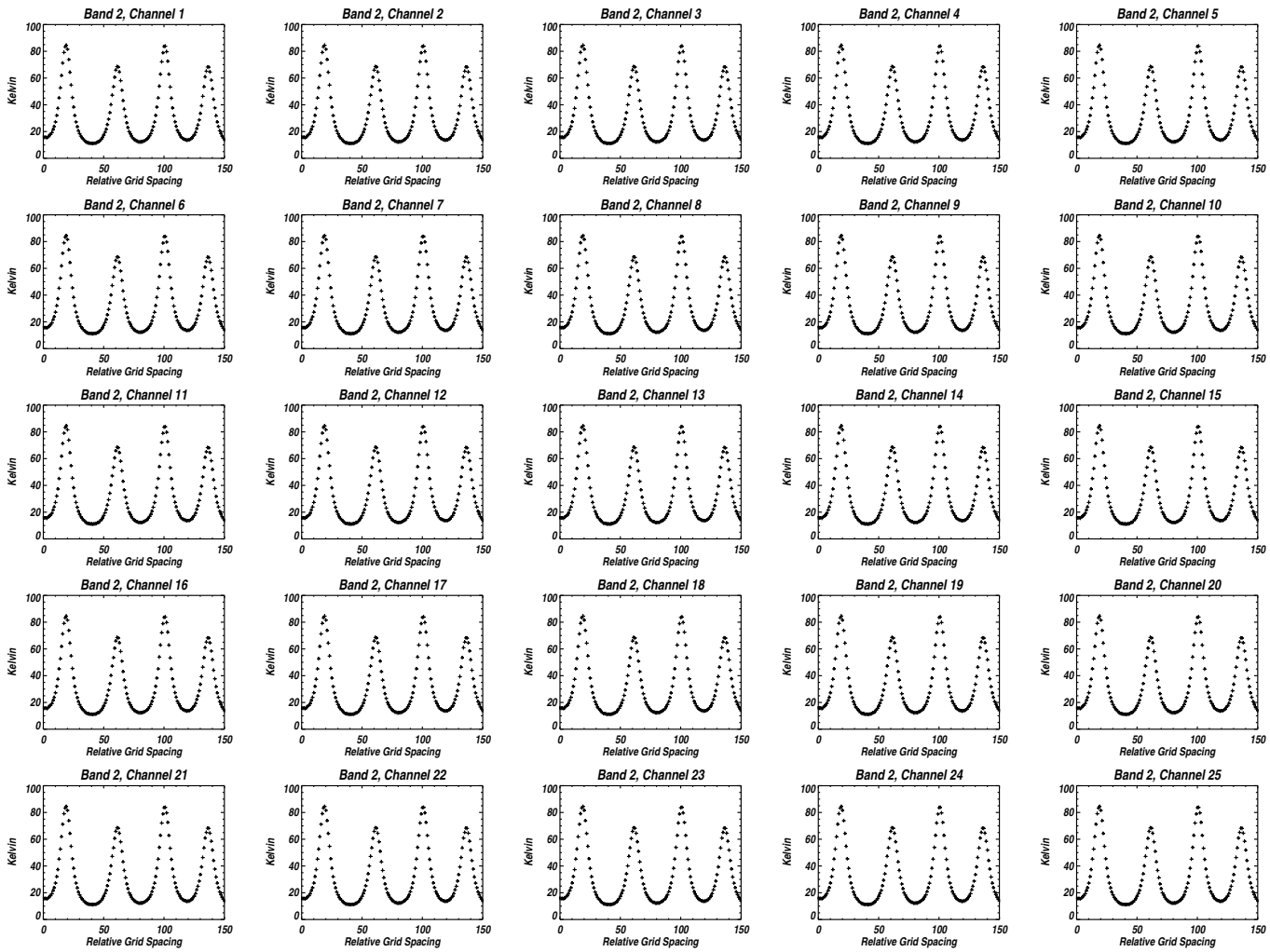

FM Relative Sideband Sweep, Band 6 (R2) 10 μm steps

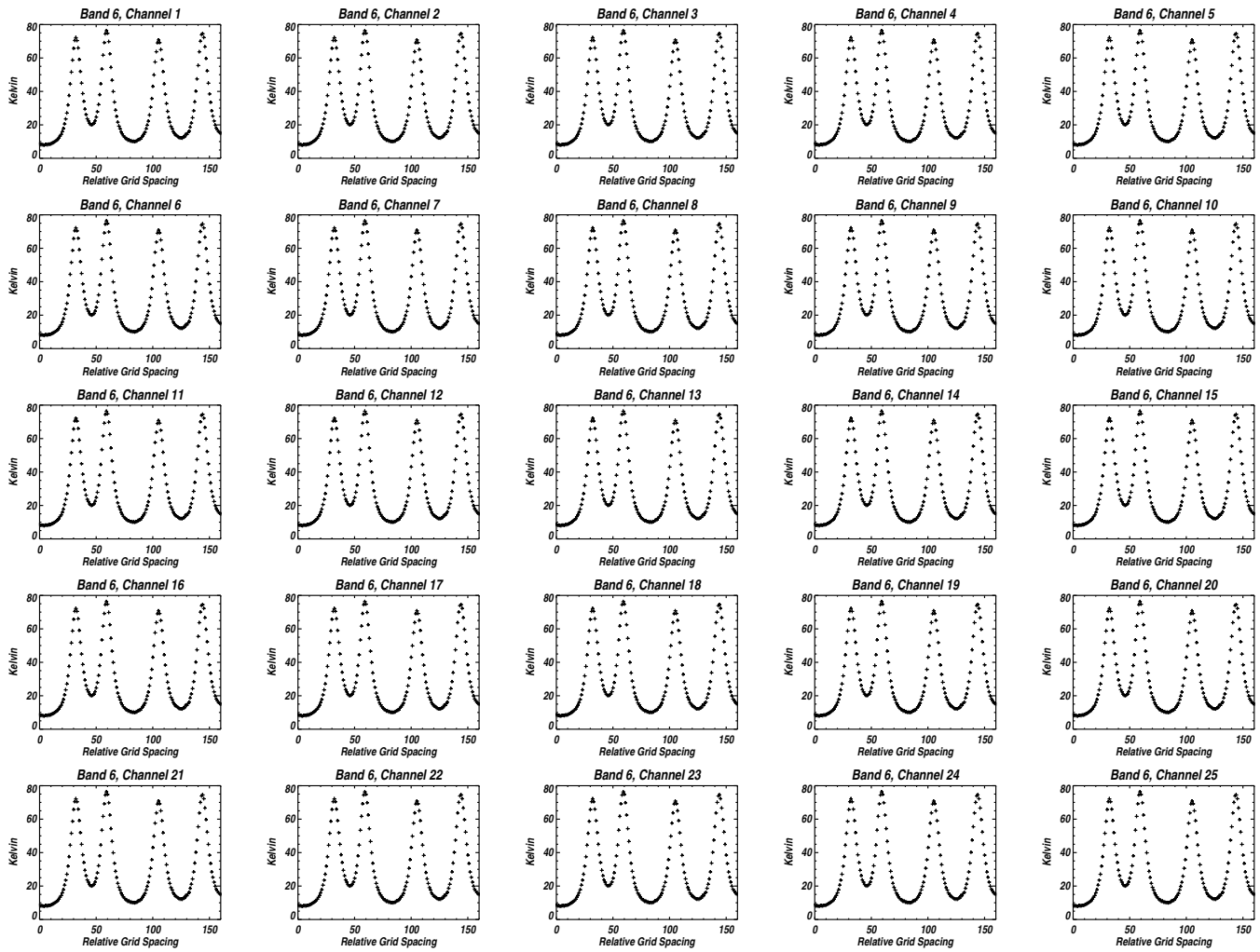

FM Relative Sideband Sweep, Band 7 (R3) 10 μm steps

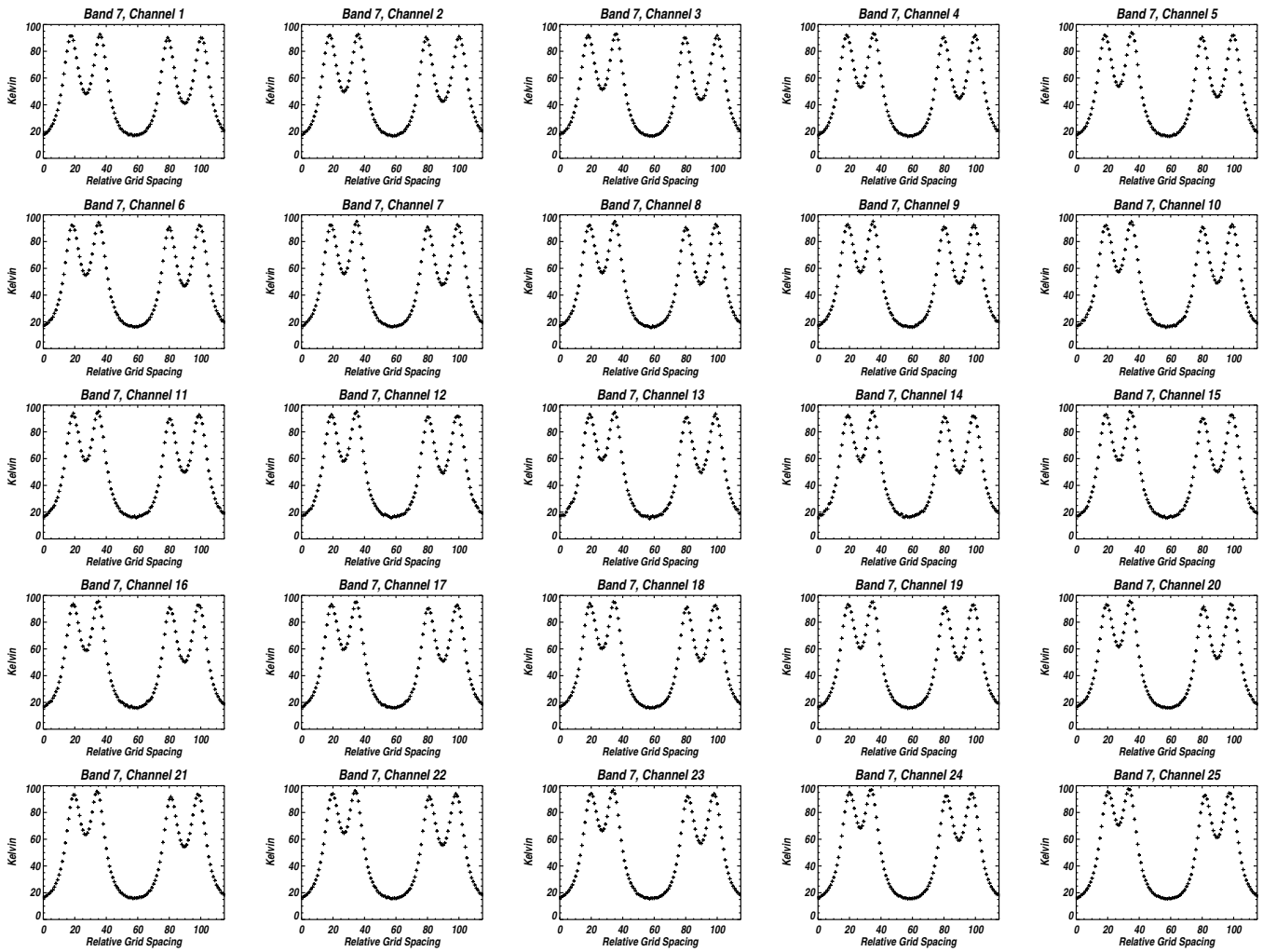

FM Relative Sideband Sweep, Band 9 (R3) 10 μm steps

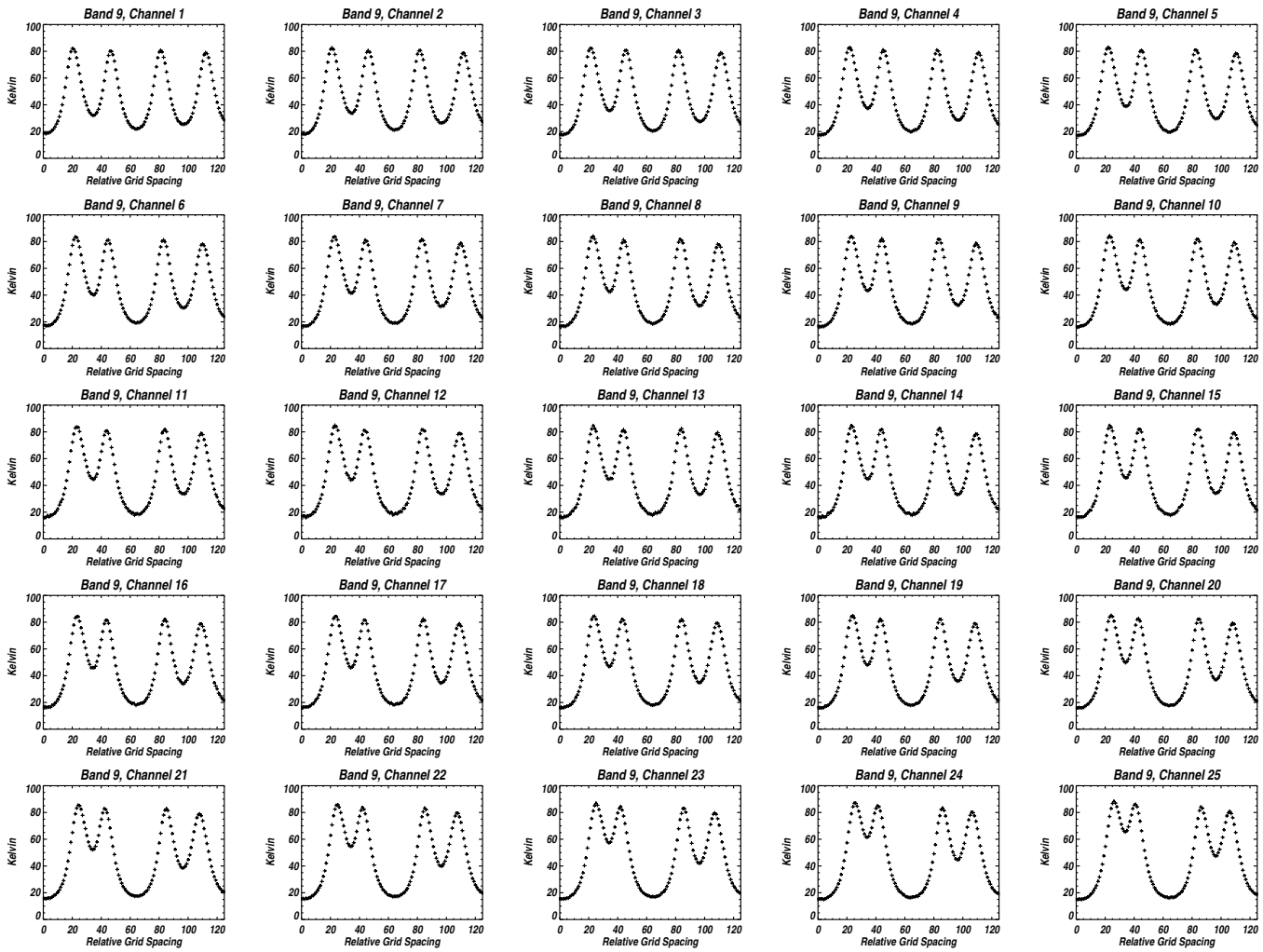

FM Relative Sideband Sweep, Band 10 (R4) 2 μm steps

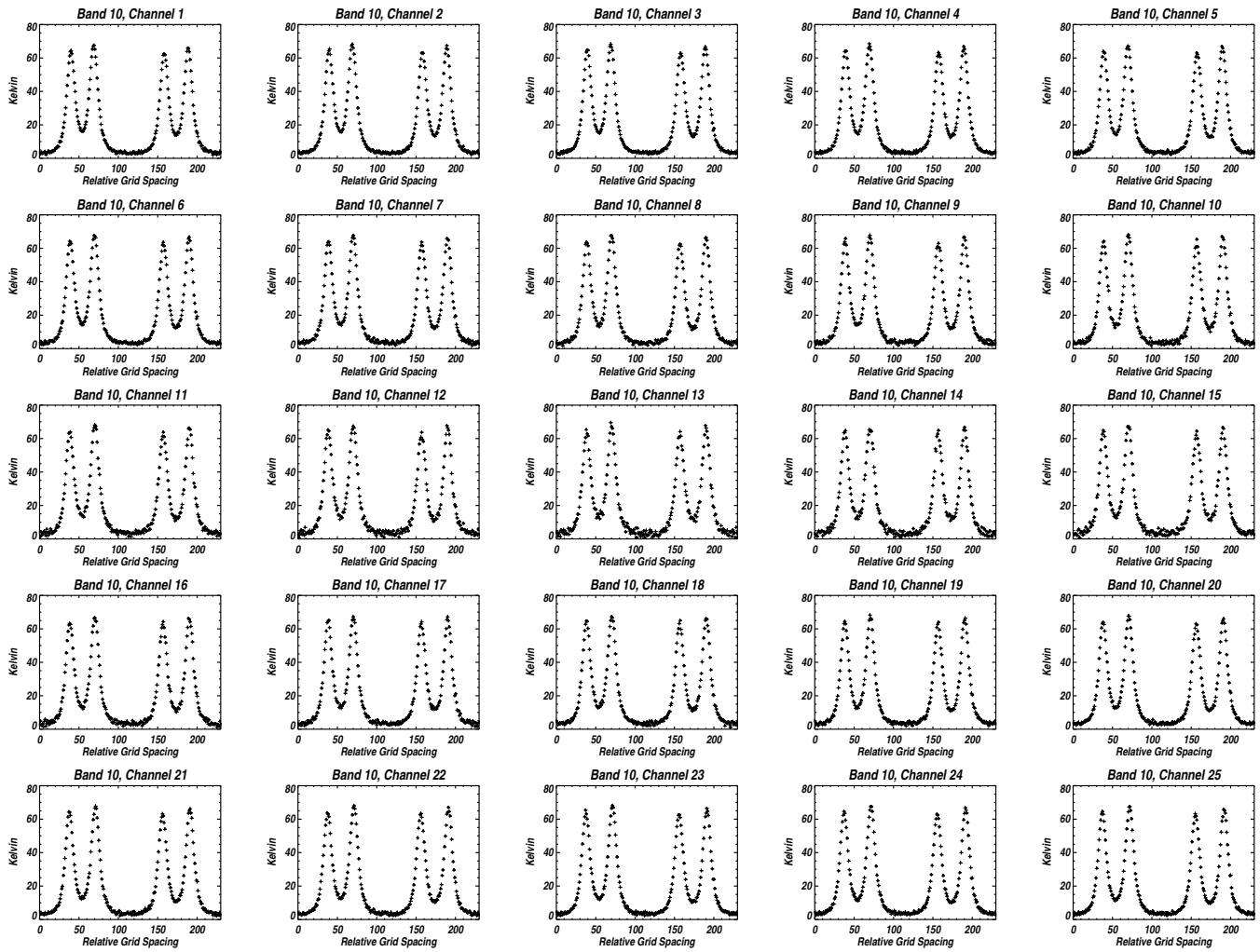

FM Relative Sideband Sweep, Band 14 (R4) 2 μm steps

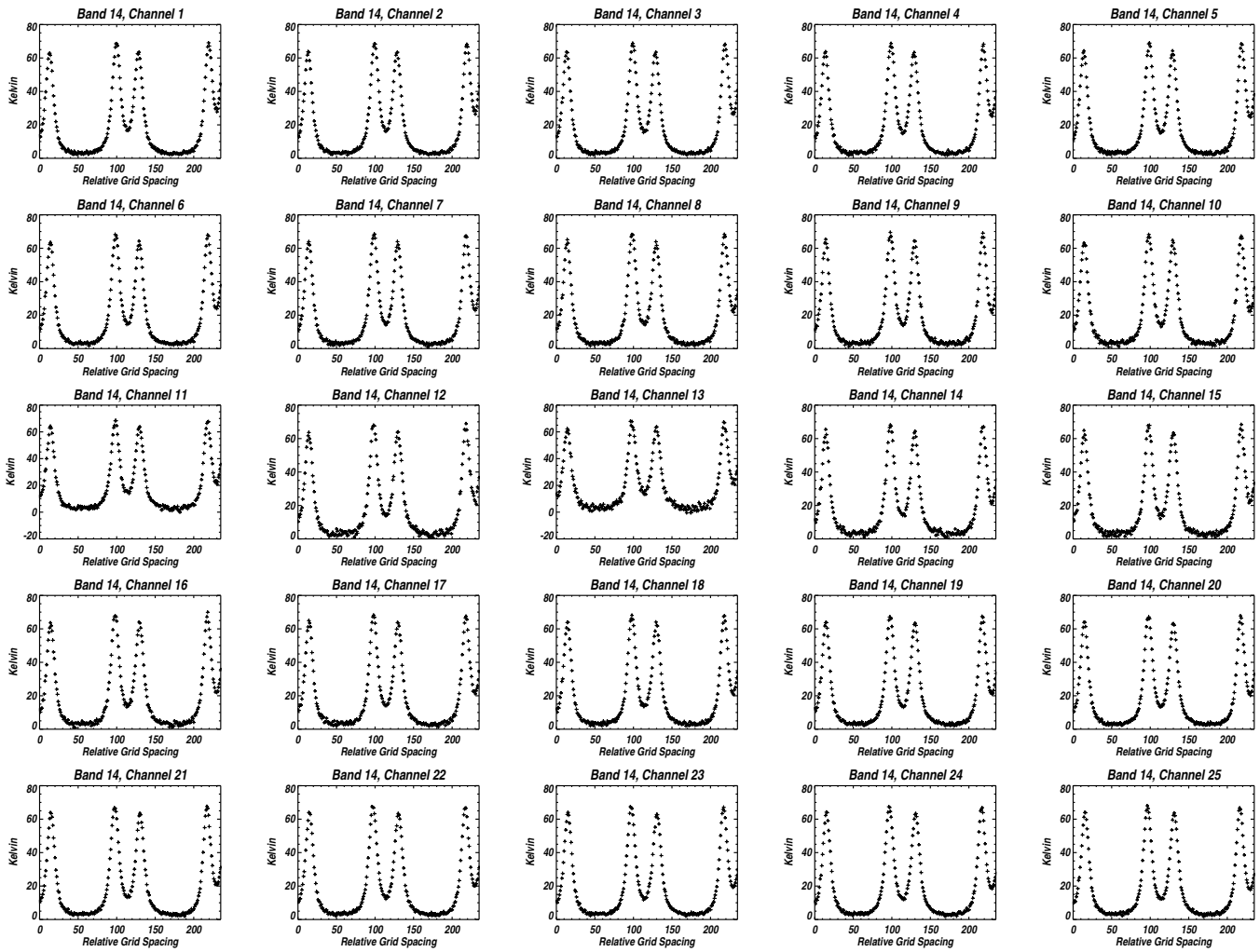

CALIBRATION TARGETS

- Calibration Target emissivity (as a function of frequency, polarization) was measured as part of the Calibration Target fabrication task.
  - ⇨ Performance is satisfactory, and
  - ⇨ The Blue Sky test has shown that these standing waves are not scan-dependent
- All necessary engineering calibration data (PRD 0°C resistances, Engineering Data Hybrid internal calibration resistances) are in hand.

REQUIREMENTS

Spectral and FOV Calibration:

- *Spectral and FOV calibration shall be performed and provide the instrument relative response as a function of frequency and angle for each channel*
- *The systematic uncertainty (i.e. not including the estimated contributions of random noise) in the absolute value of the atmospheric/Earth radiances measured through each spectral channel shall be less than 3 K (at the 90% confidence level)*
- *The systematic uncertainty (i.e. not including the estimated contributions of random noise) in the spectrally-varying component of the atmospheric/Earth radiances, measured from one channel or filter to another throughout a given radiometer, shall be less than 1% or $\Delta I_{\min}/3$, where $\Delta I_{\min}$ for each spectral region is given in Table 3.2–2*

SPECTRAL CALIBRATION

- The primary method of spectral calibration is to sweep all receivers (in both sidebands) with a fundamental source:
  - This provides direct end-to-end calibration.
  - Source power remains constant to all intents and purposes across the bandwidth of even the broadest channels.
  - Measurements have been made in all GHz channels, in both sidebands (except the single-sideband R1 radiometers), and with all combinations of FilterBank Switch settings.
  - For bands with significant standing waves in the RF setup (R1 and R4), all measurements have been made with the source in a nominal and $\frac{\lambda}{4}$-shifted position.
- A schematic and picture of the sweep setup, and some quick-look FM data, are presented on the following pages.

Front-End Sweeper Schematic

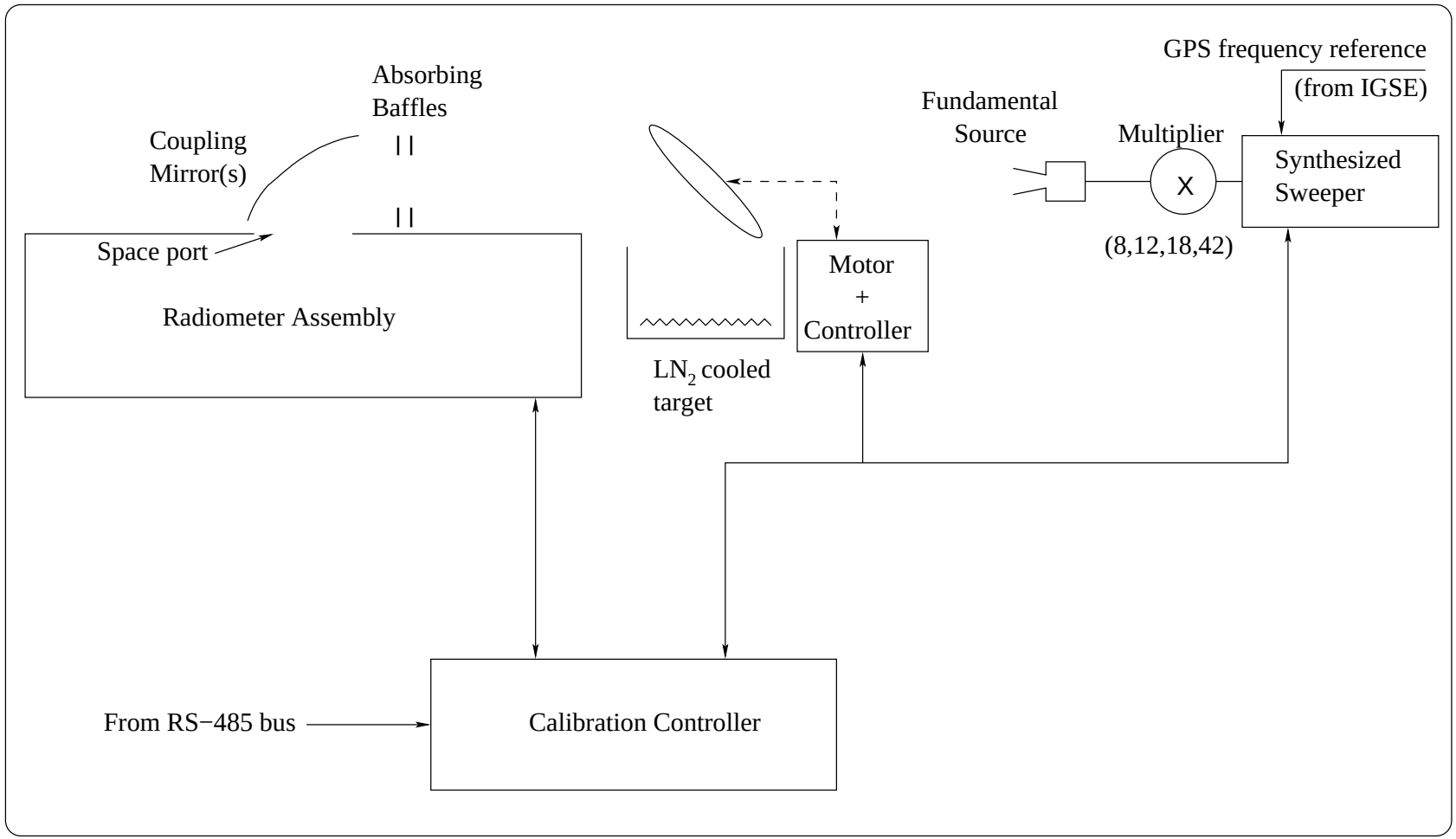

Front-End Sweeper, continued

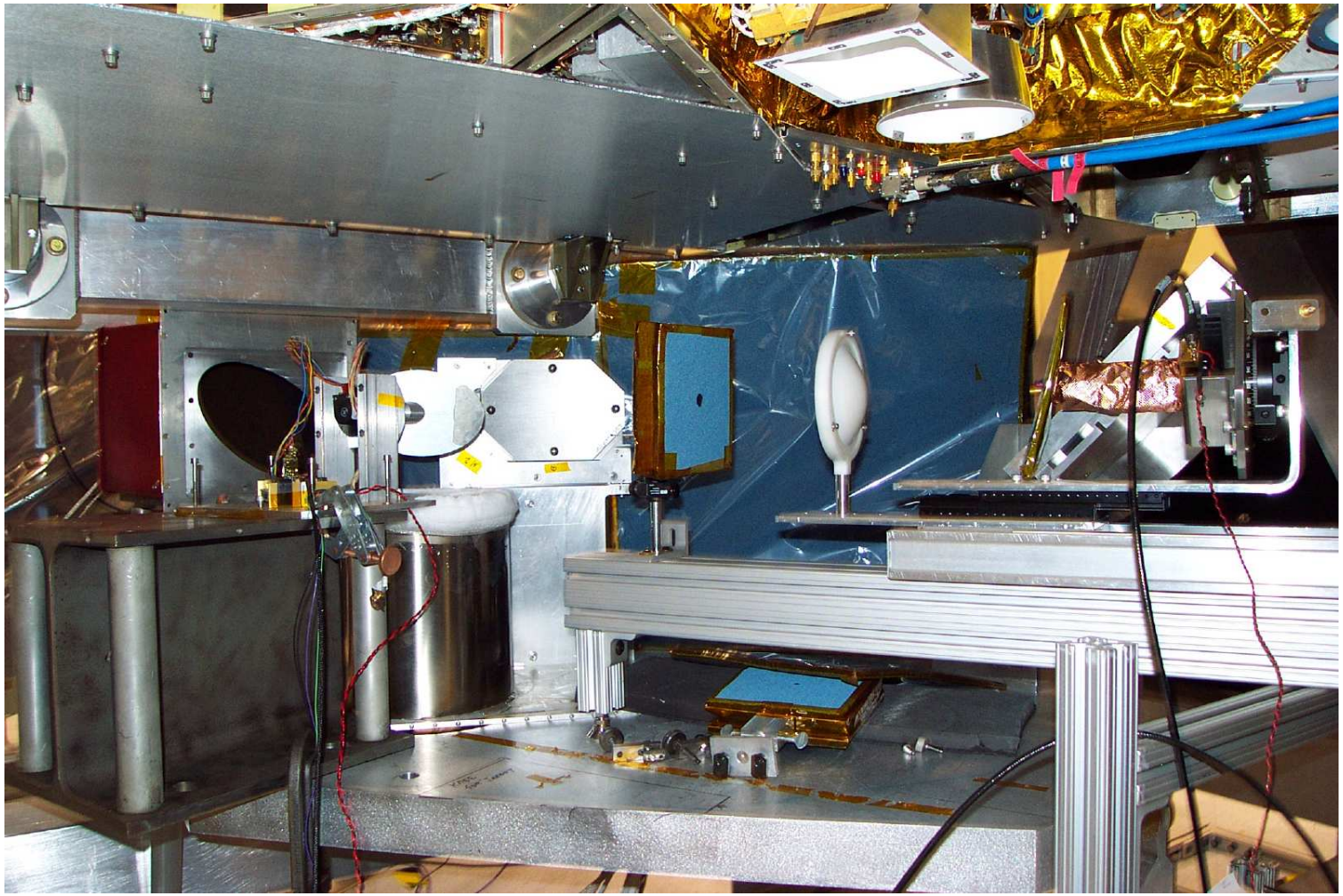

Spectral Calibration – End-to-End Spectral Sweeps, R1

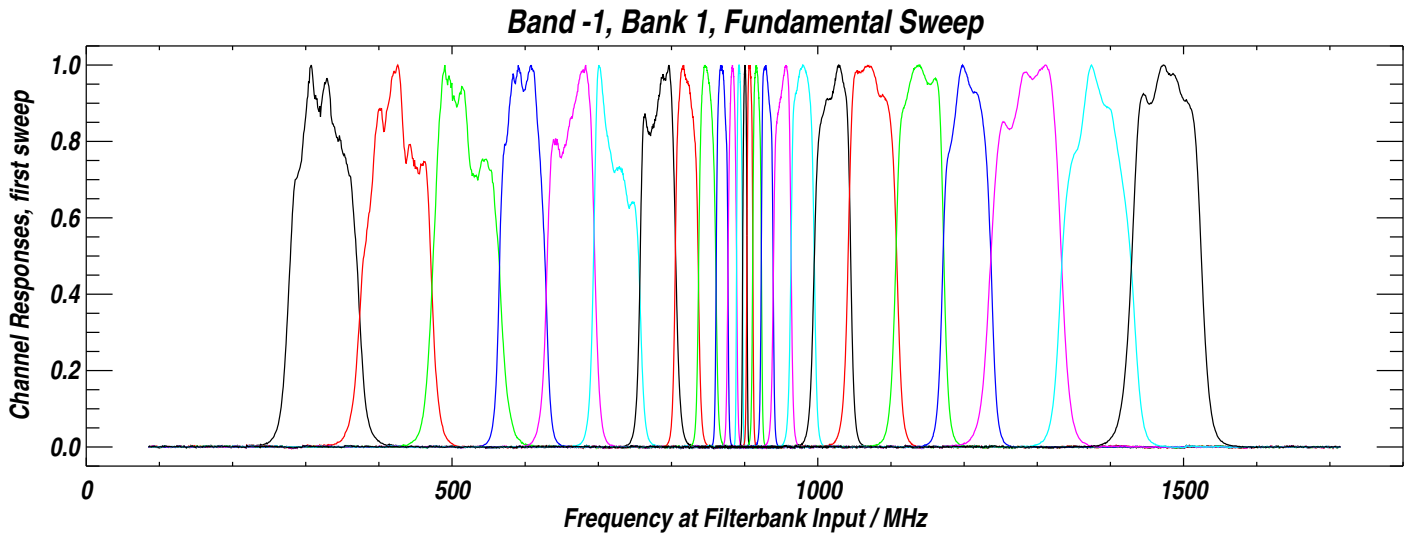

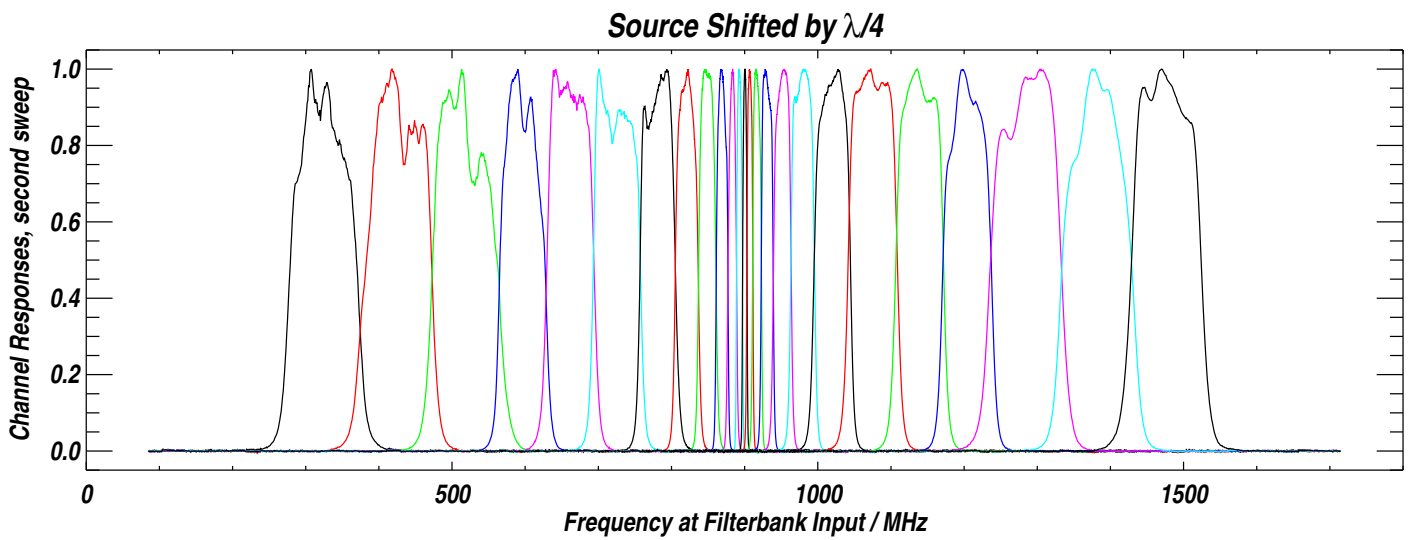

Spectral Calibration – End-to-End Spectral Sweeps, R1

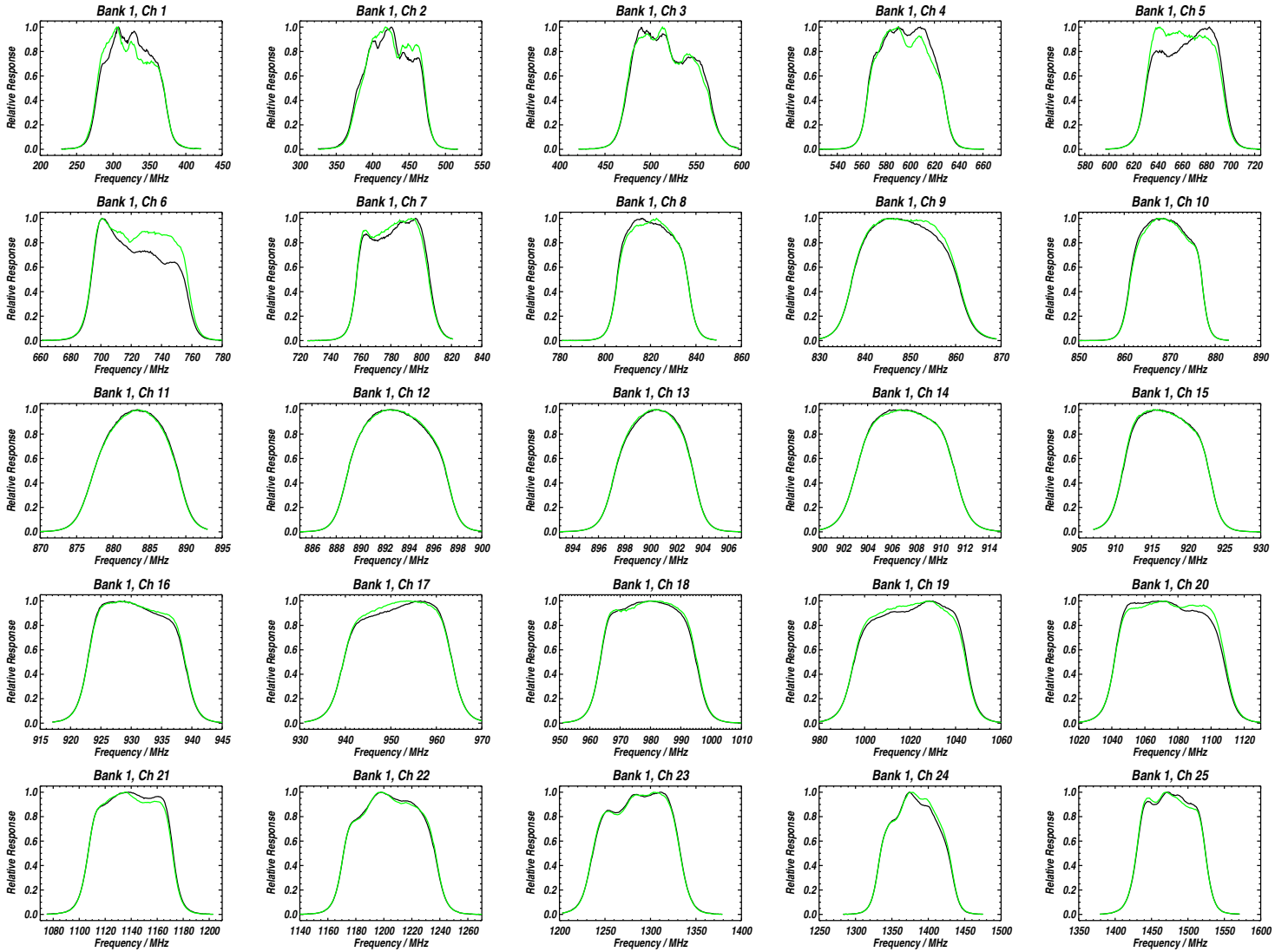

Spectral Calibration – End-to-End Spectral Sweeps, R2, B2

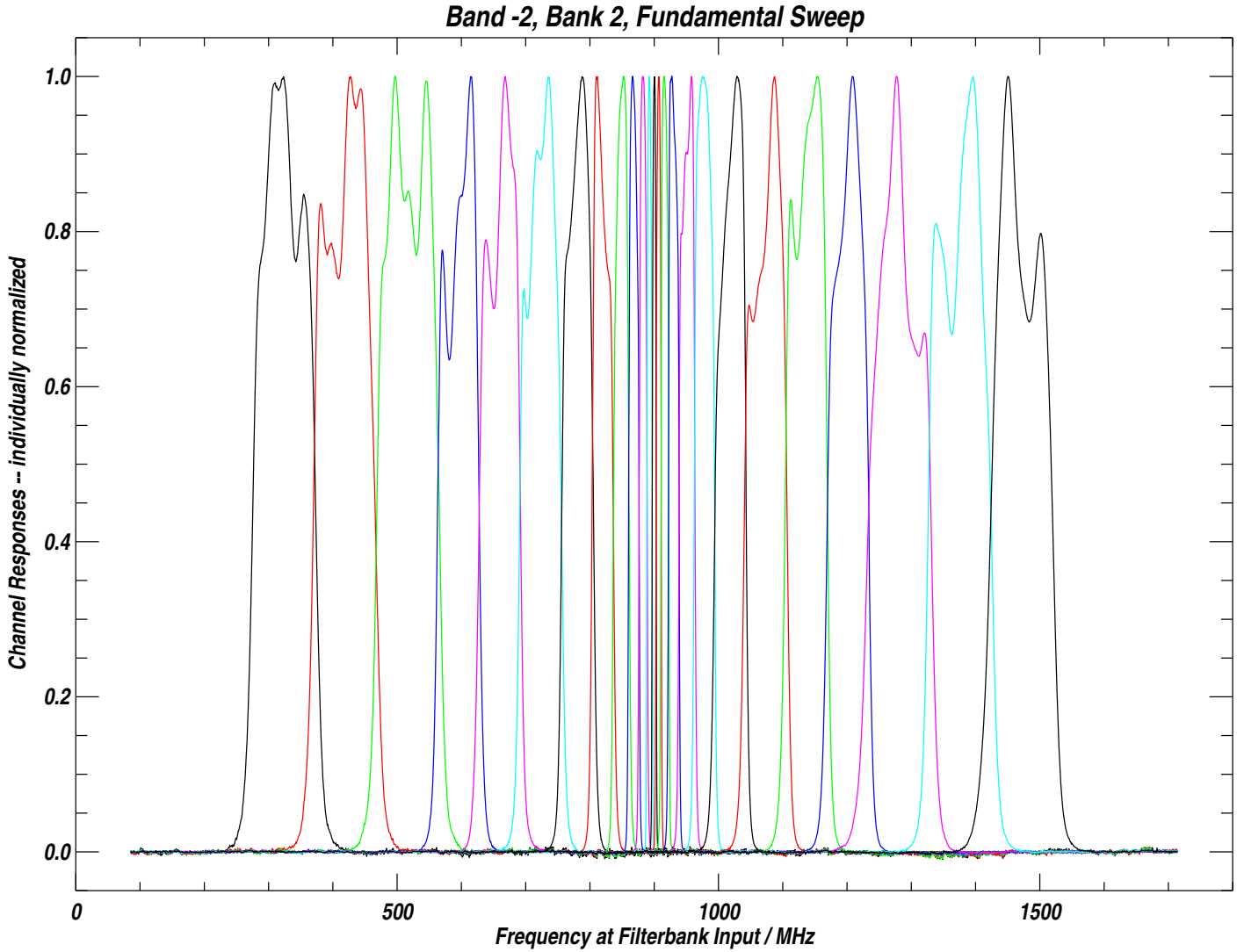

Spectral Calibration – End-to-End Spectral Sweeps, R2, B2

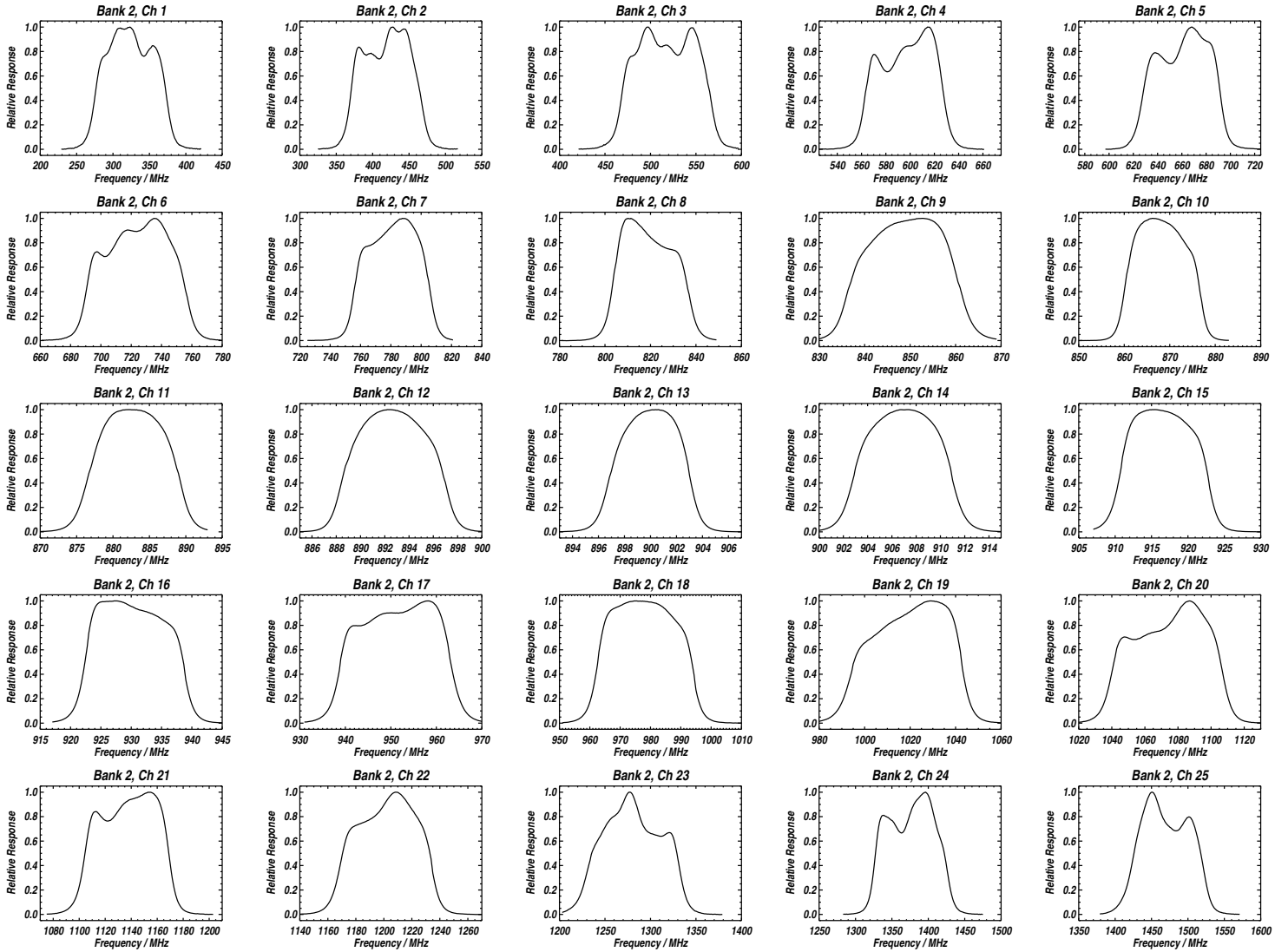

Spectral Calibration – End-to-End Spectral Sweeps, R2, B6

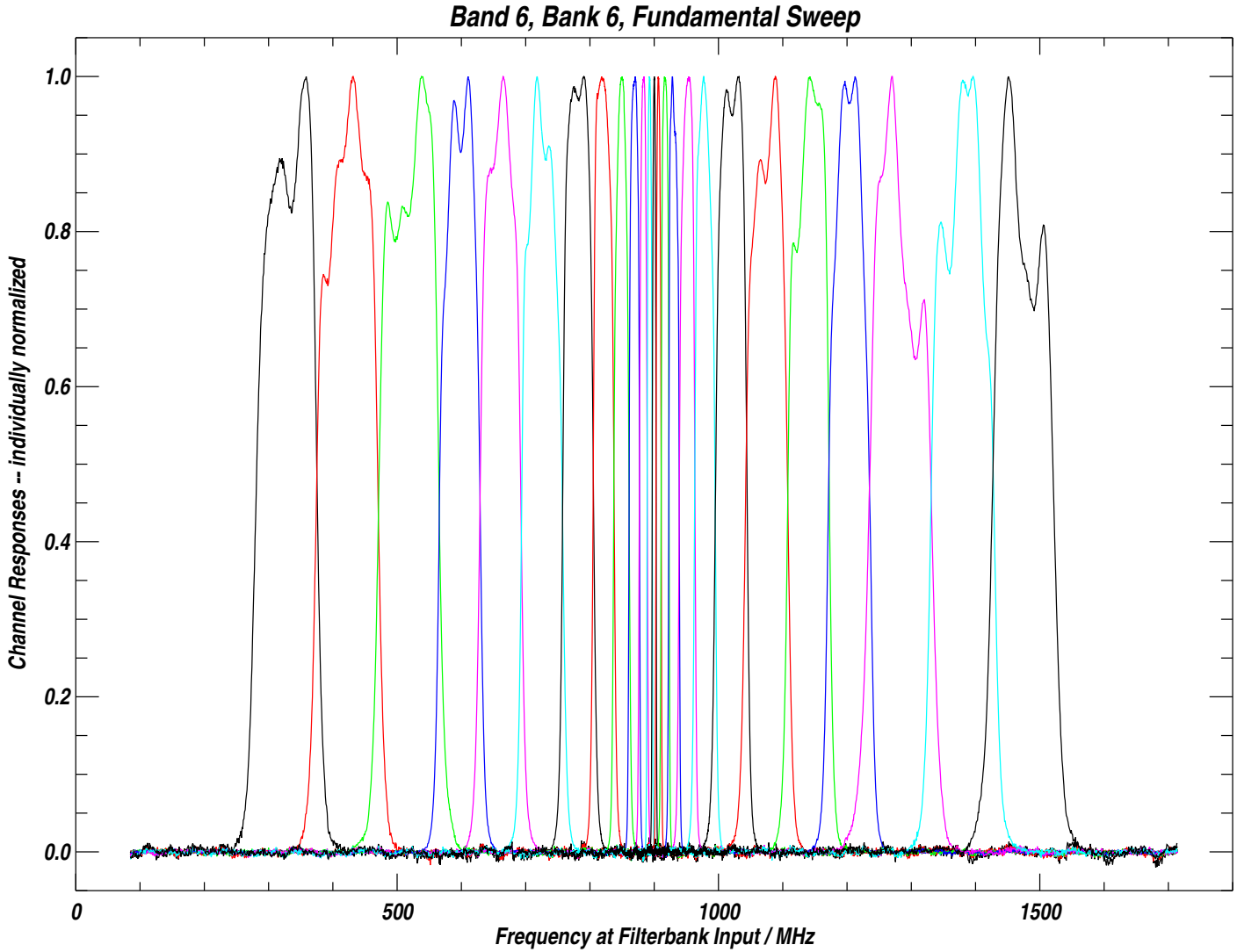

Spectral Calibration – End-to-End Spectral Sweeps, R2, B6

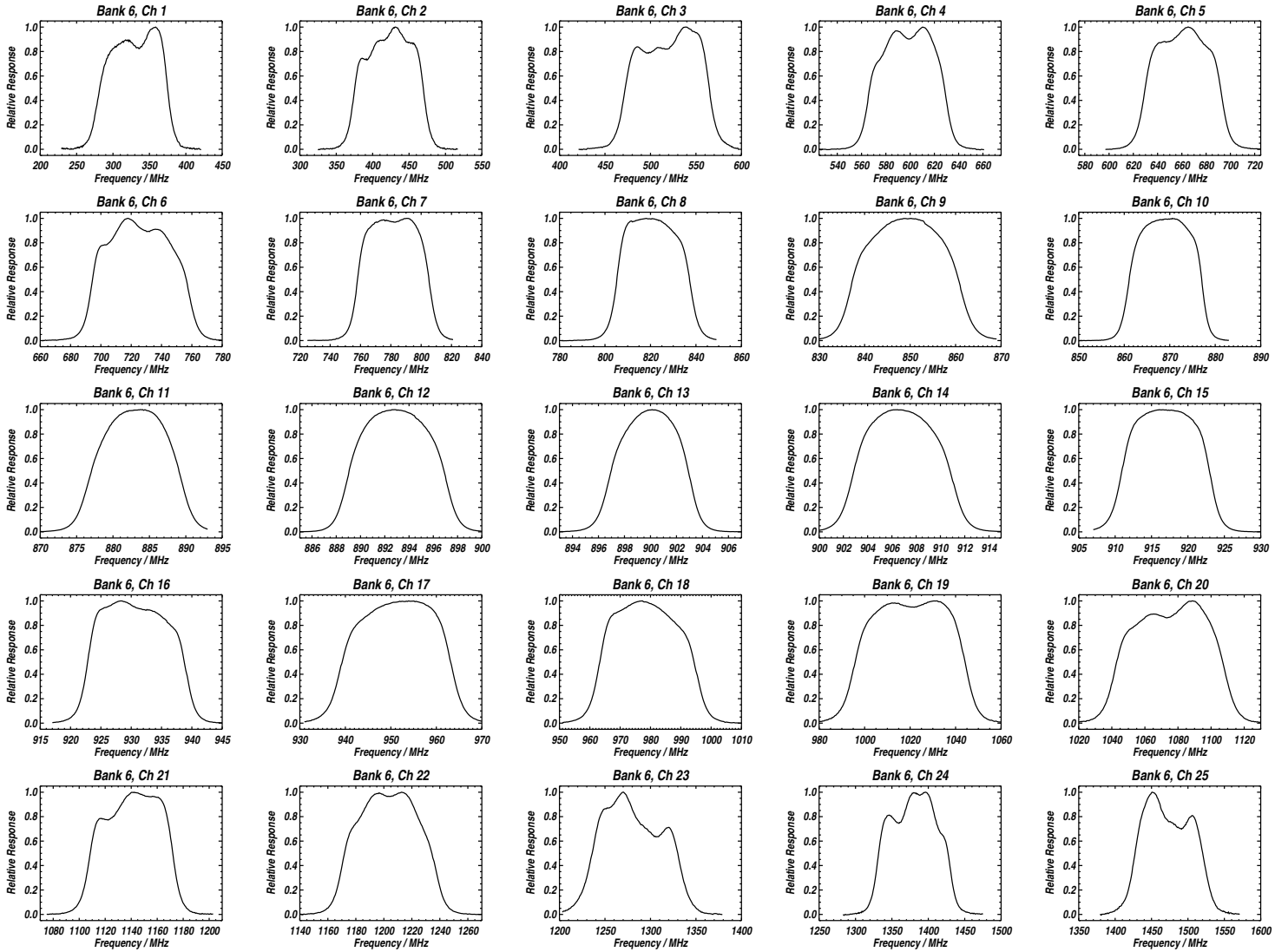

Spectral Calibration – End-to-End Spectral Sweeps, R3, B7

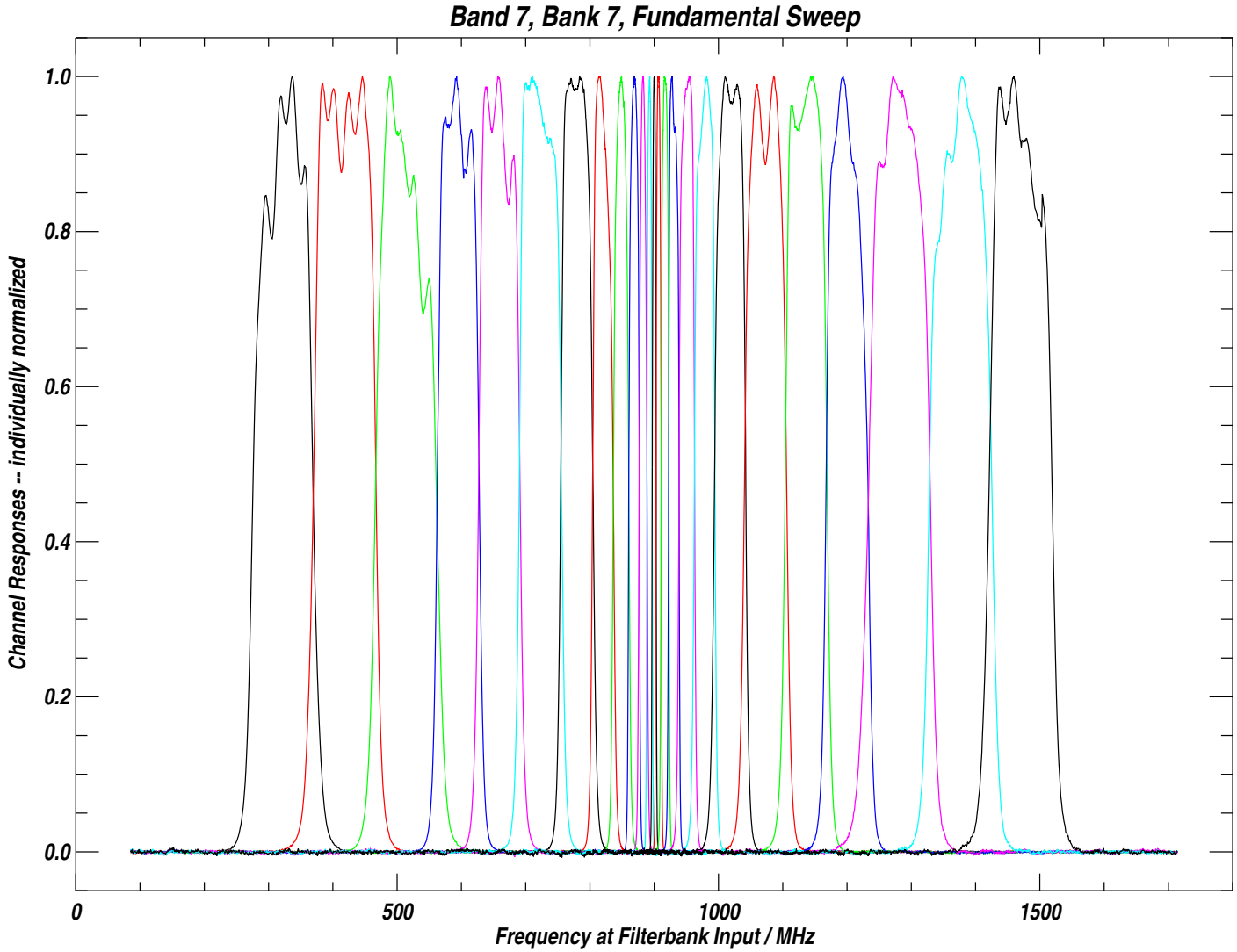

Spectral Calibration – End-to-End Spectral Sweeps, R3, B7

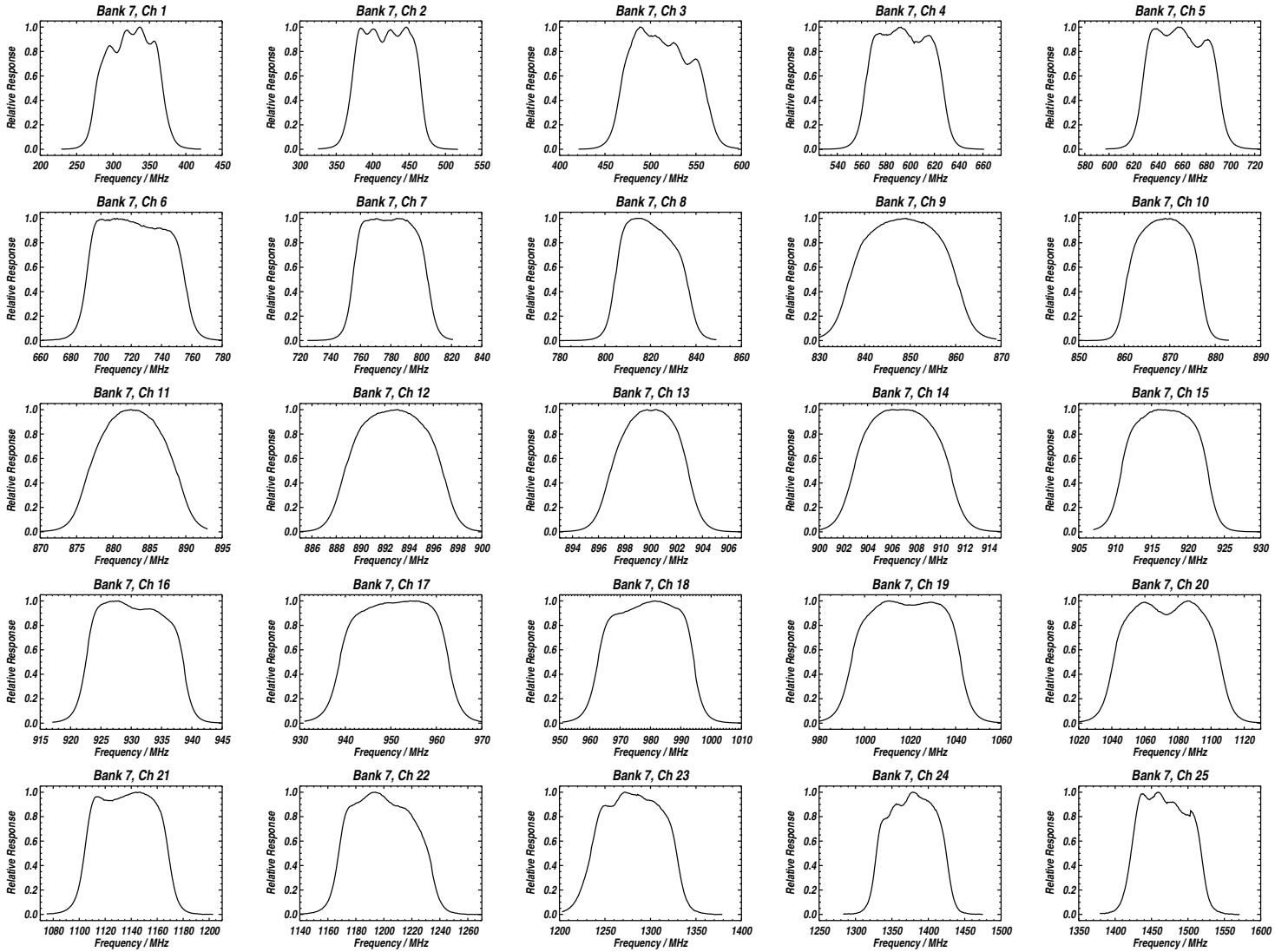

Spectral Calibration – End-to-End Spectral Sweeps, R3, B9

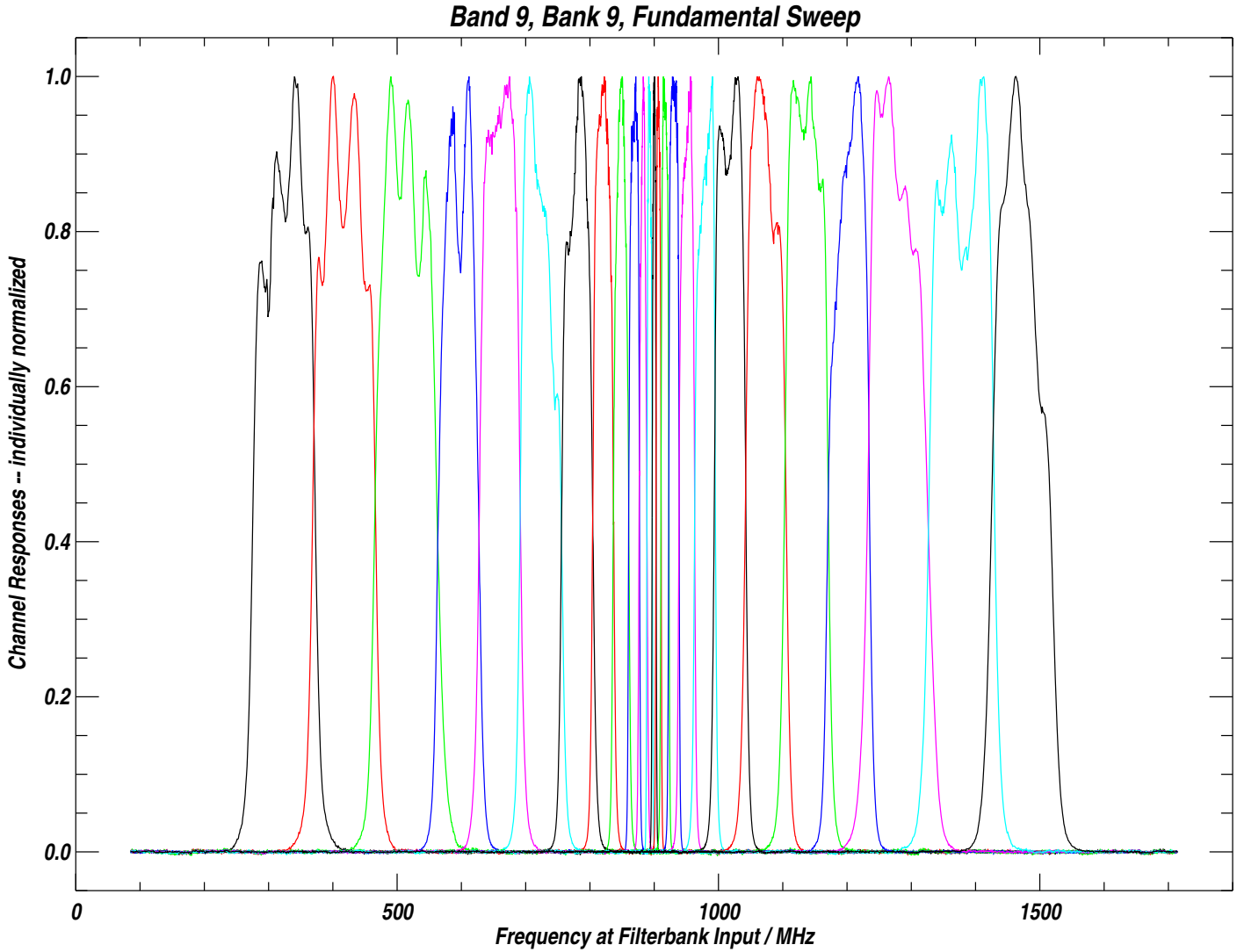

Spectral Calibration – End-to-End Spectral Sweeps, R3, B9

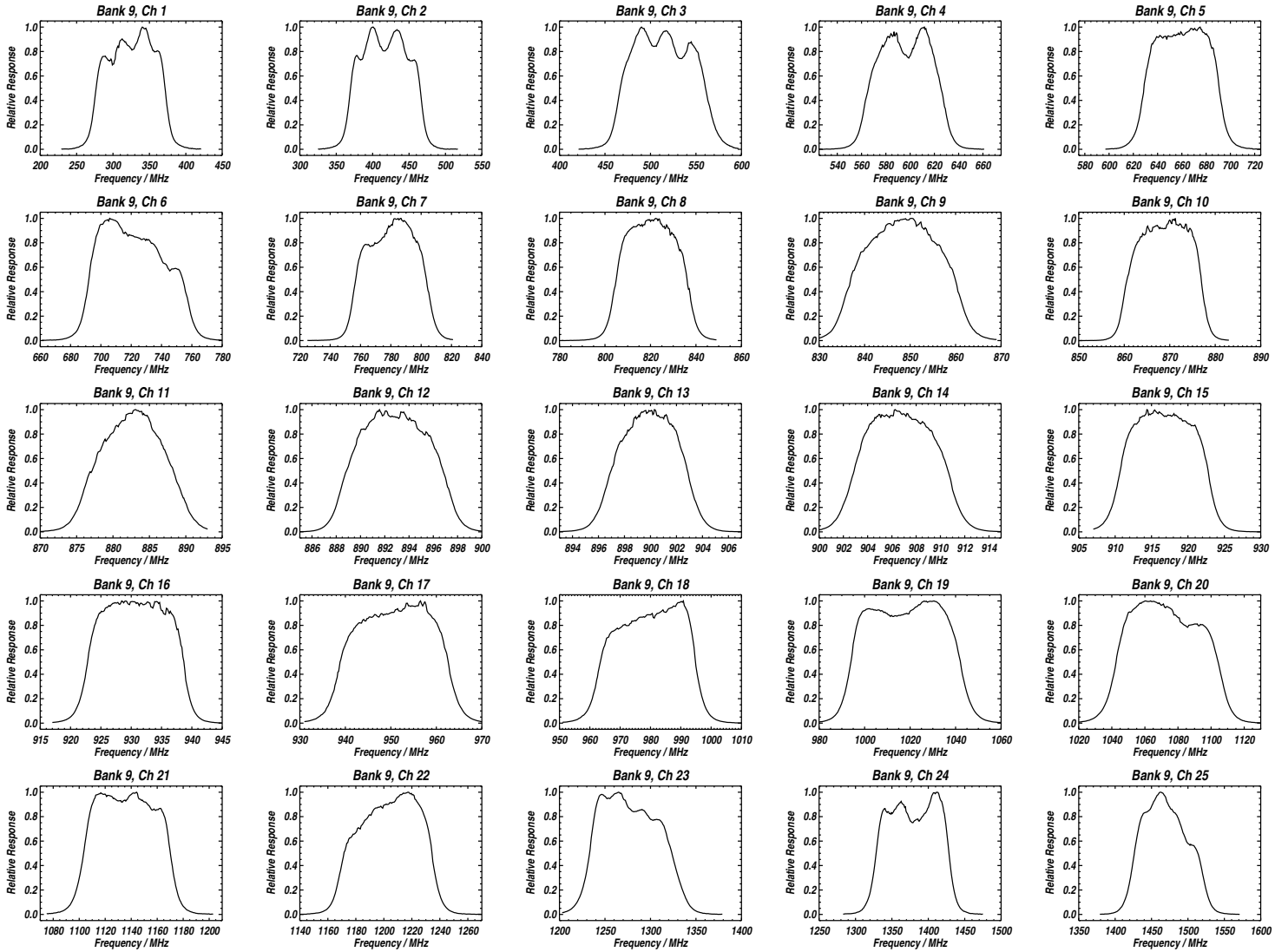

Spectral Calibration – End-to-End Spectral Sweeps, R4, B10

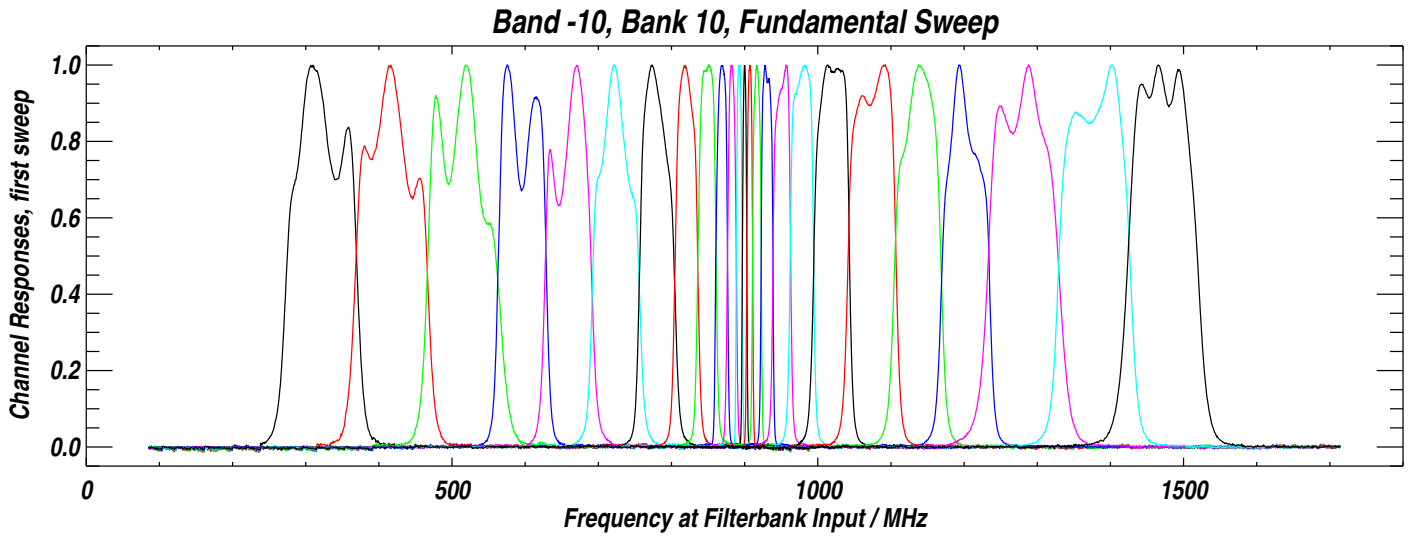

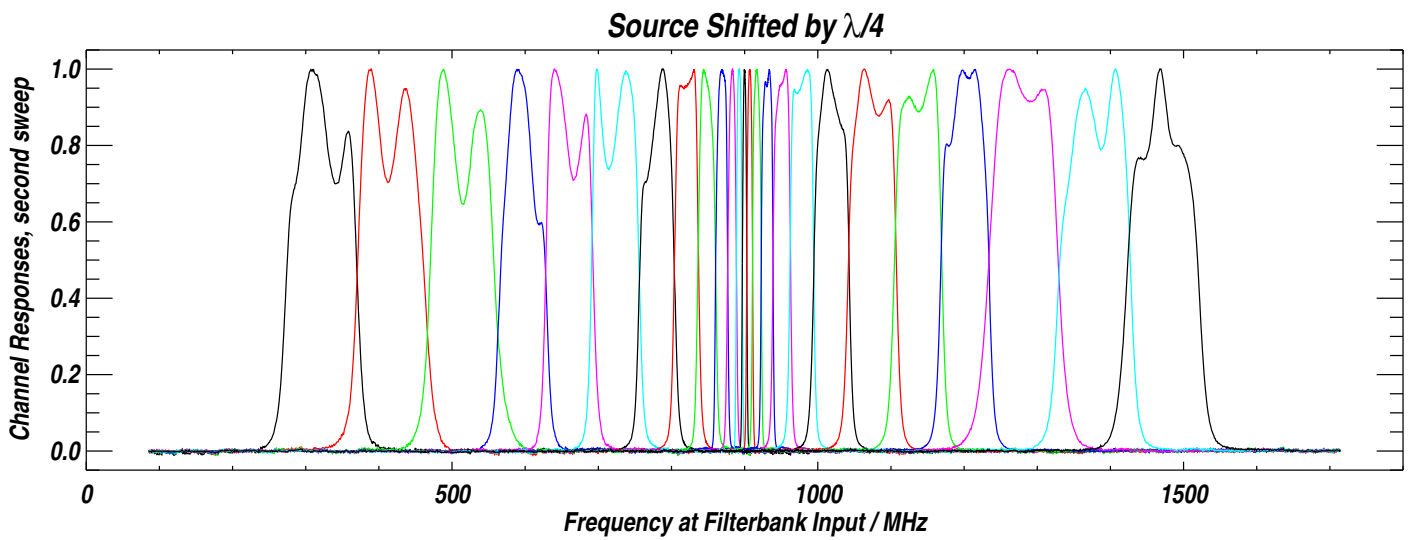

Spectral Calibration – End-to-End Spectral Sweeps, R4, B10

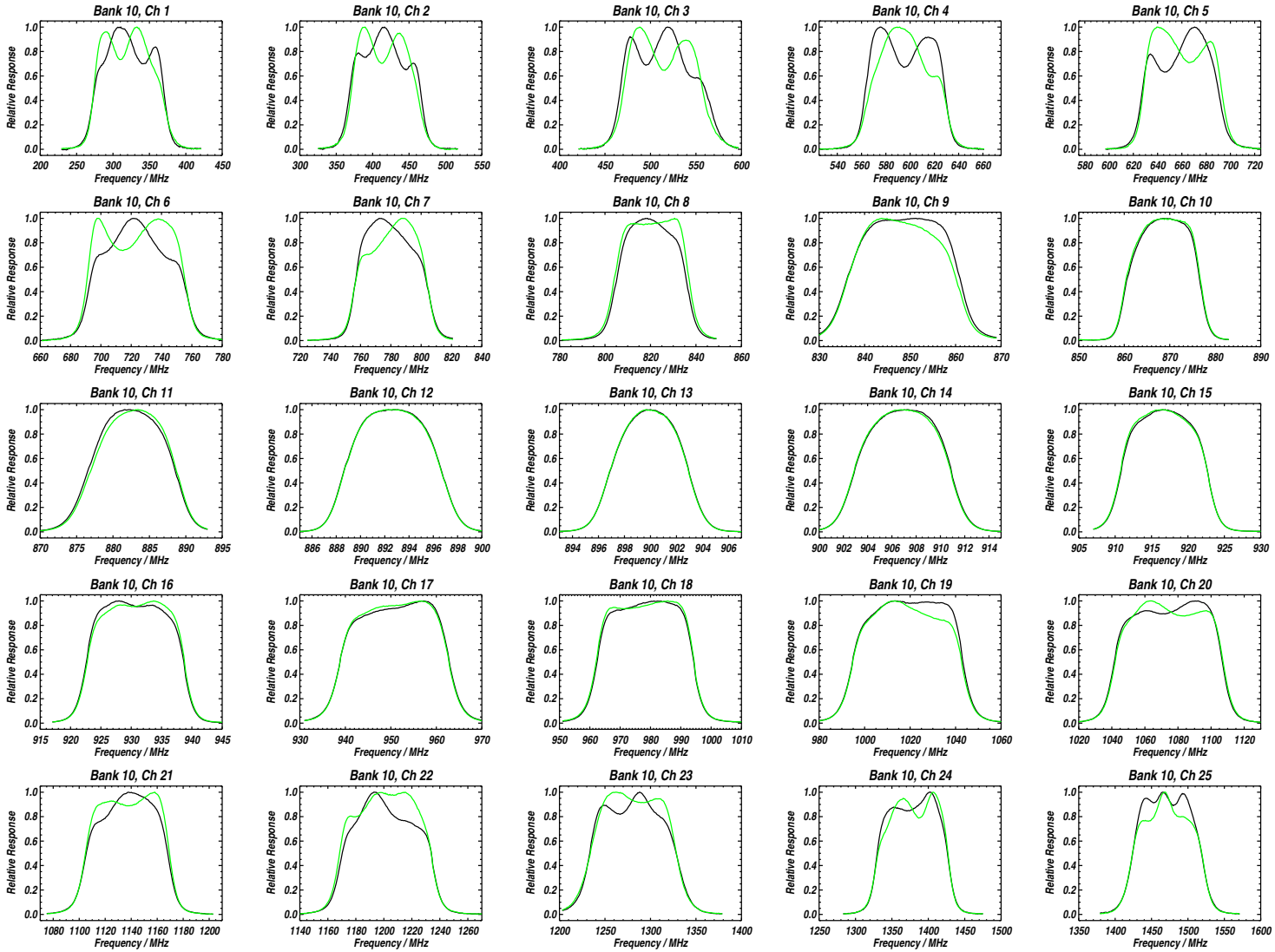

Spectral Calibration – End-to-End Spectral Sweeps, R4, B14

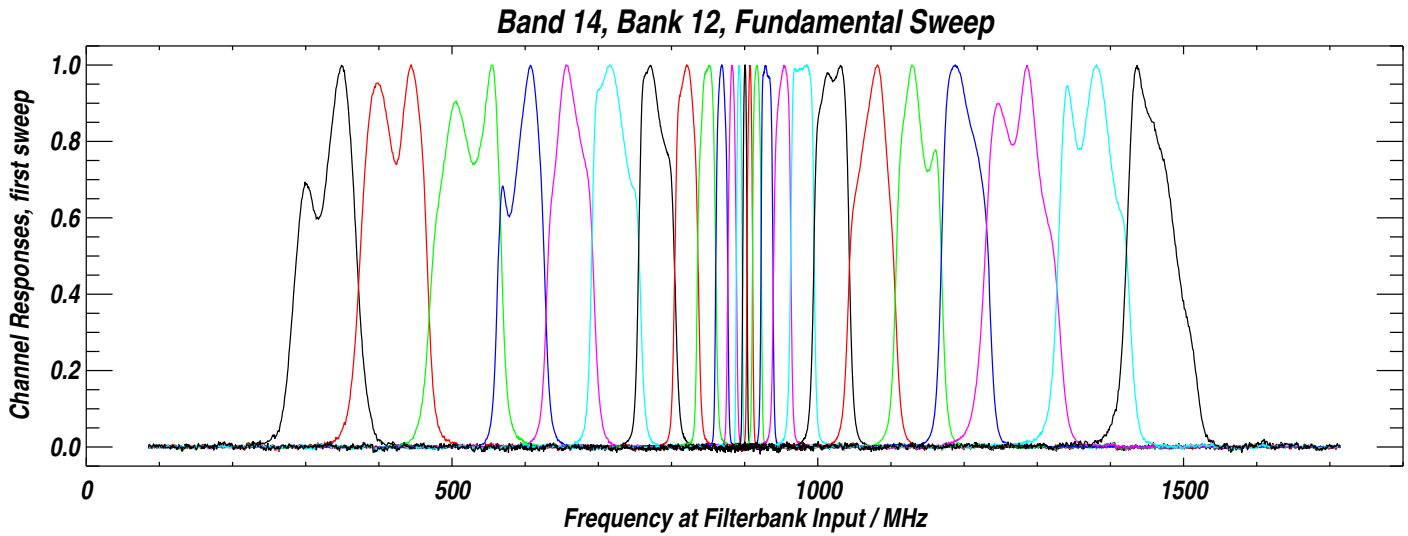

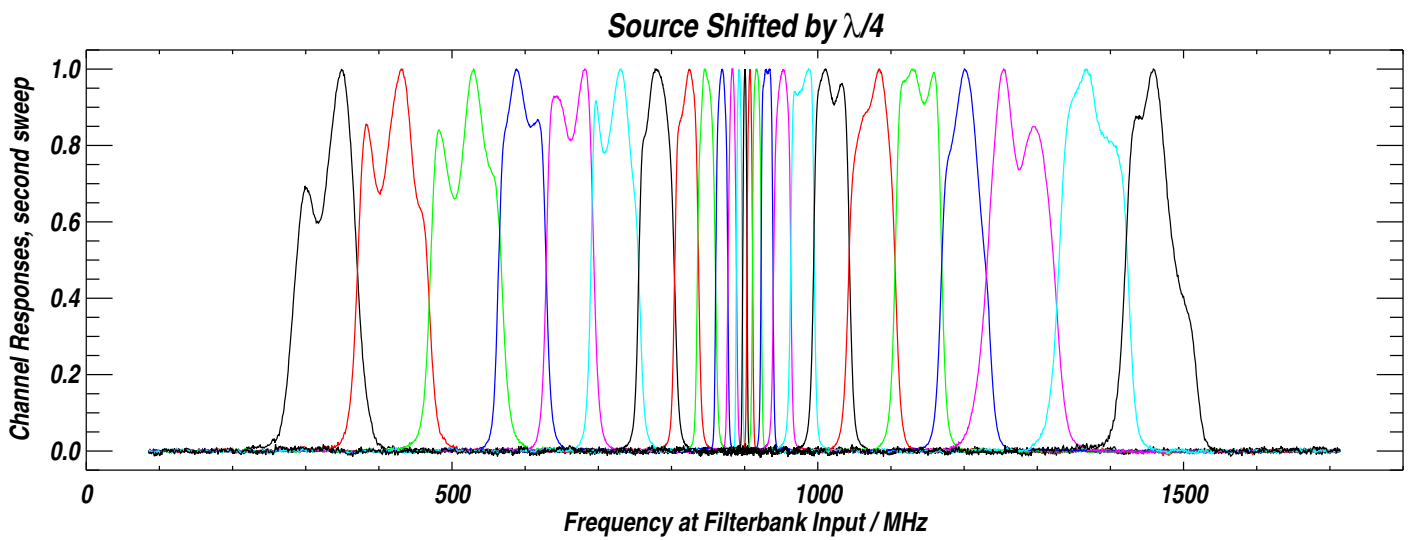

Spectral Calibration – End-to-End Spectral Sweeps, R4, B14

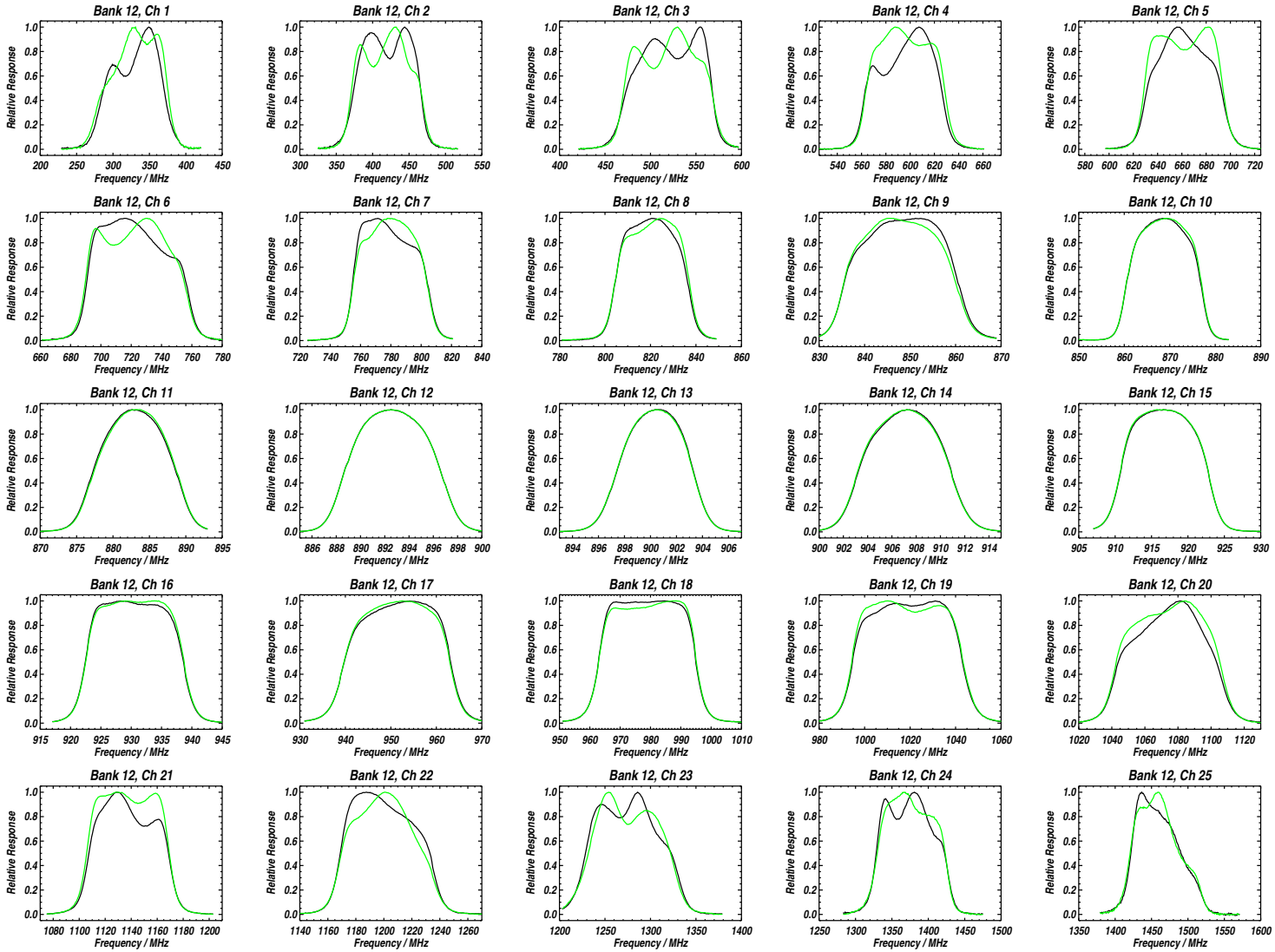

SUMMARY

- All GHz radiometric and spectral calibrations have been completed.
- The quantity of calibration data is substantial, and it will take many months to fully analyze.
  - ⇨ Quick-look software was used in 'real time' to rapidly verify adequate data quality.
- My preliminary assessment of calibration data quality is that it substantially surpasses the corresponding UARS data, and that all calibration requirements will be met.

GHz FOV Calibration

Richard E. Cofield
Paul C. Stek

Outline

1. Measurement technique (Stek)
    1. Concept
    2. Mechanical setup
    3. RF equipment
    4. Optical alignment
    5. Measurements
    6. Example data and discussion of errors
2. Data analysis (Cofield)

Near Field FOV Measurement

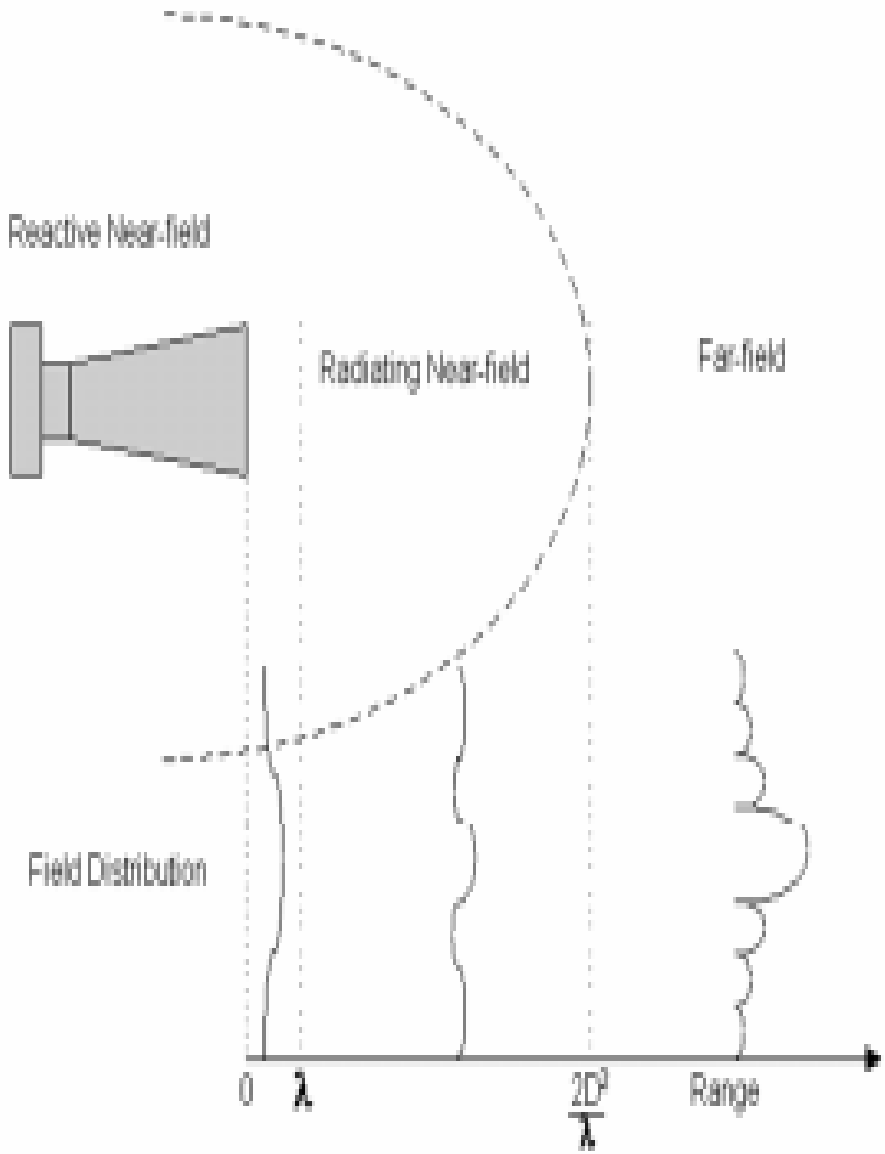

- Measure Phase and Amplitude over surface in front of Antenna
- Project to far field (basically a Fourier Transform)
- Measurement in clean room.
  - Eliminate contamination problems
  - Reduce setup time
  - Allows assembly and calibration to continue between tests
- Works at 640 GHz
- Need high thermal stability, very planer scanner, very stable reference cable.

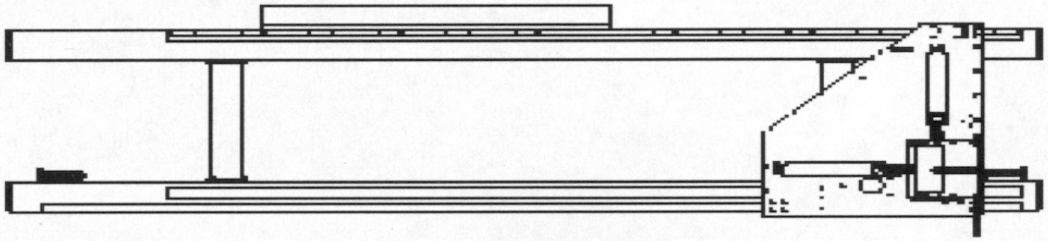

TOP VIEW

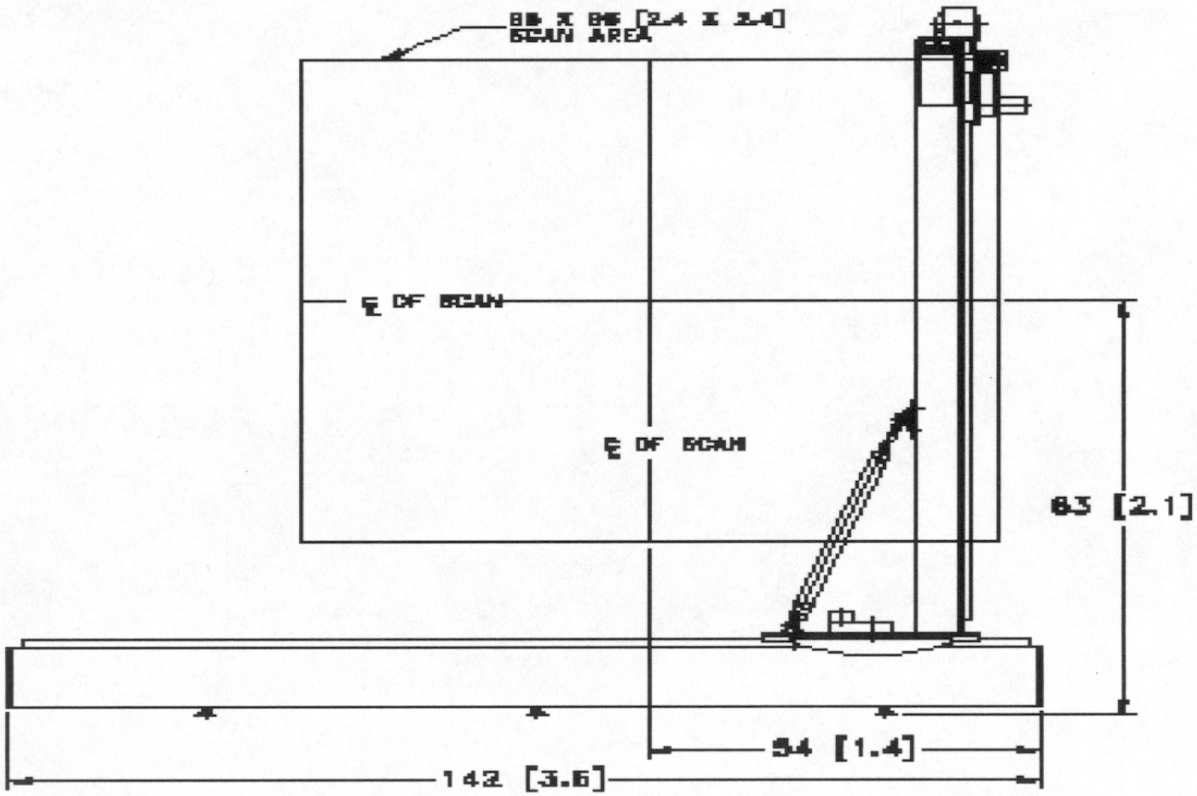

FRONT VIEW

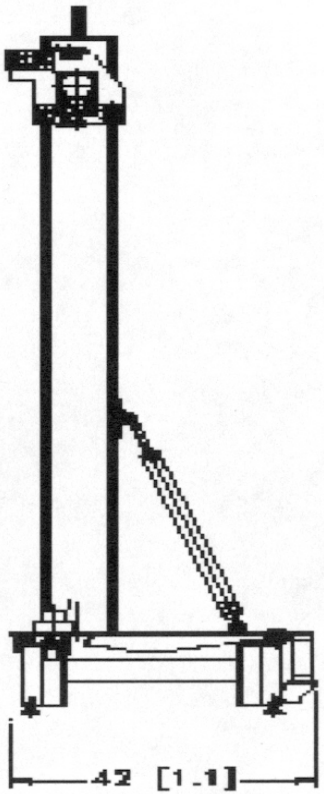

SIDE VIEW

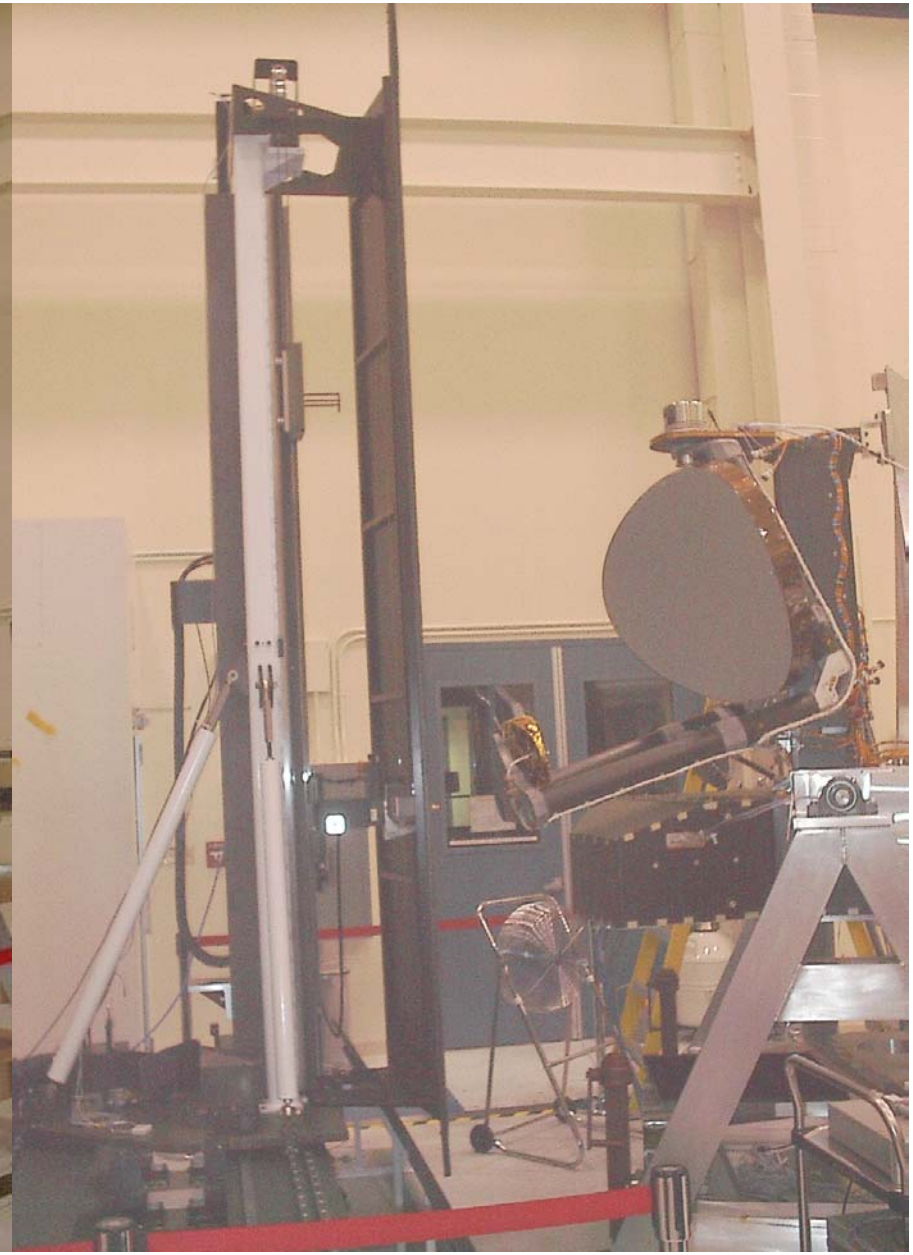

Optical Alignment

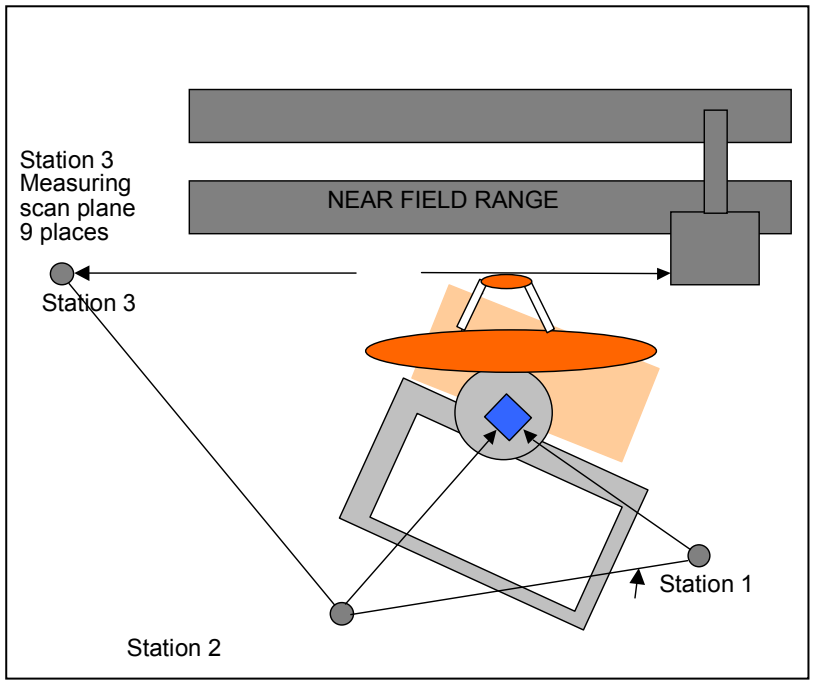

- Measure angle of scan plane at turning station
- Measure alignment cube to turning station
- Read encoder for antenna position
- Primary pointing measurement is relative to 234 GHz beam pattern

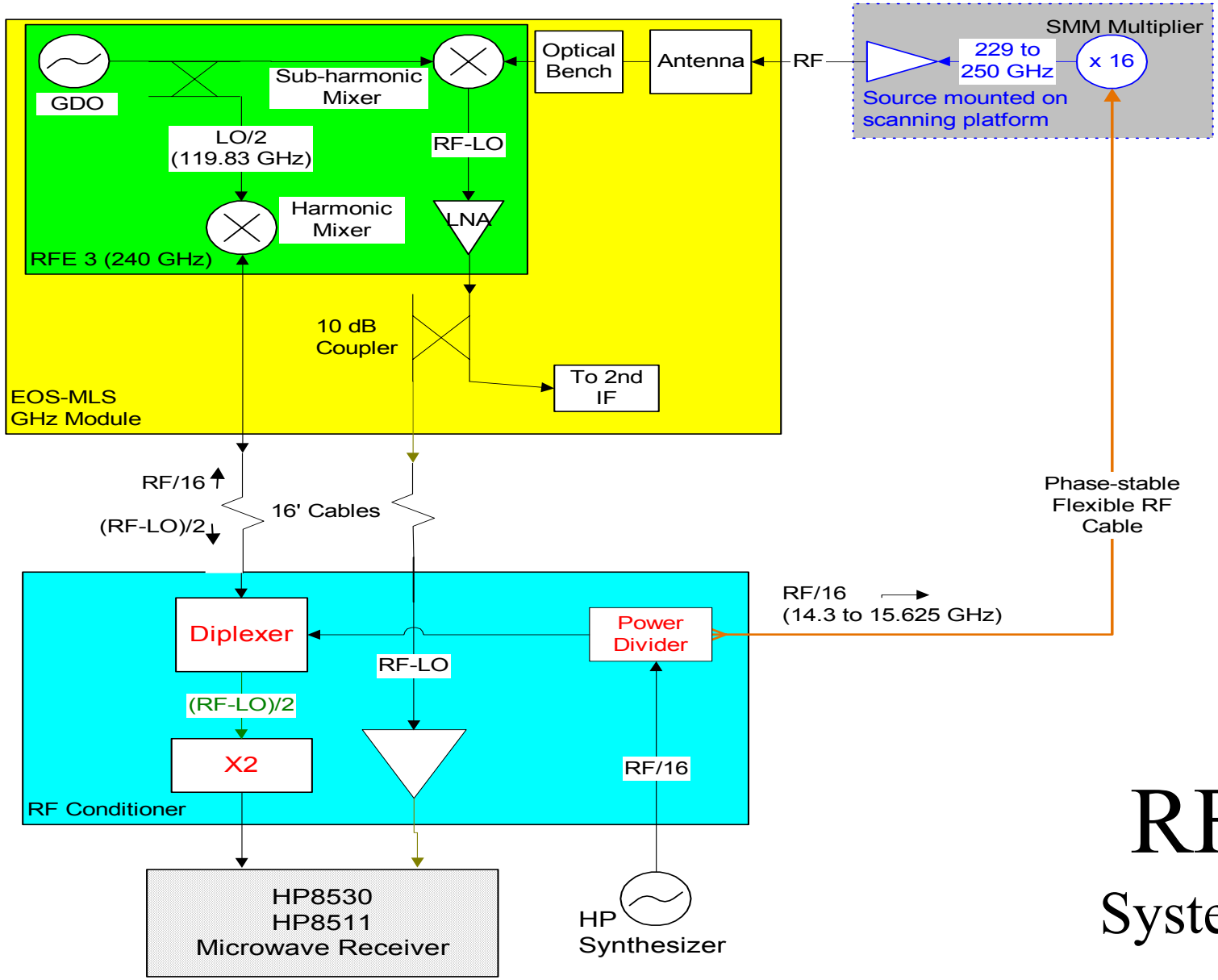
GDO
Sub-harmonic Mixer
LO/2 (119.83 GHz)
RF-LO
Harmonic Mixer
LNA
RFE 3 (240 GHz)
Optical Bench
Antenna
RF
SMM Multiplier
229 to 250 GHz
x 16
Source mounted on scanning platform
10 dB Coupler
To 2nd IF
EOS-MLS GHz Module
RF/16
(RF-LO)/2
16' Cables
Phase-stable Flexible RF Cable
Diplexer
RF-LO
Power Divider
RF/16 (14.3 to 15.625 GHz)
(RF-LO)/2
X2
RF/16
RF Conditioner
HP8530 HP8511 Microwave Receiver
HP Synthesizer

RF System

Near Field Patterns

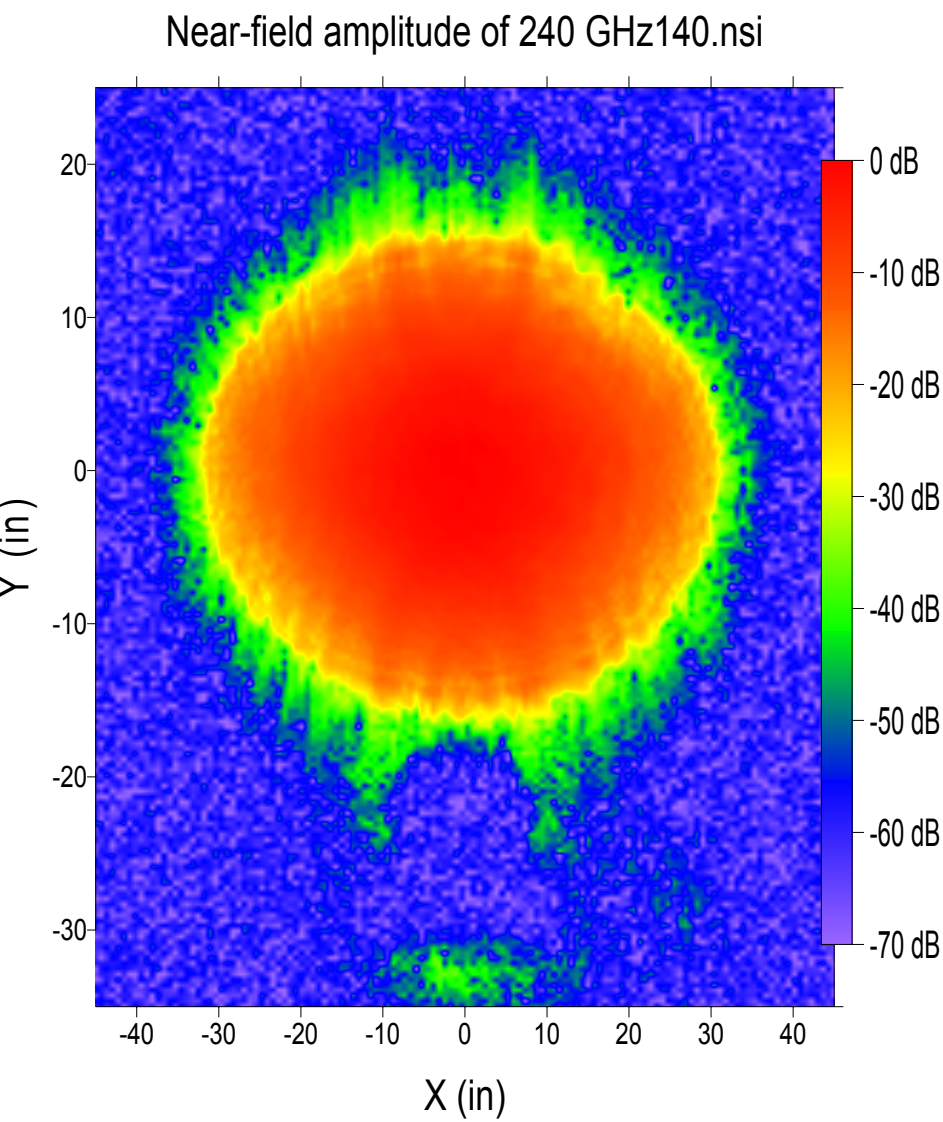

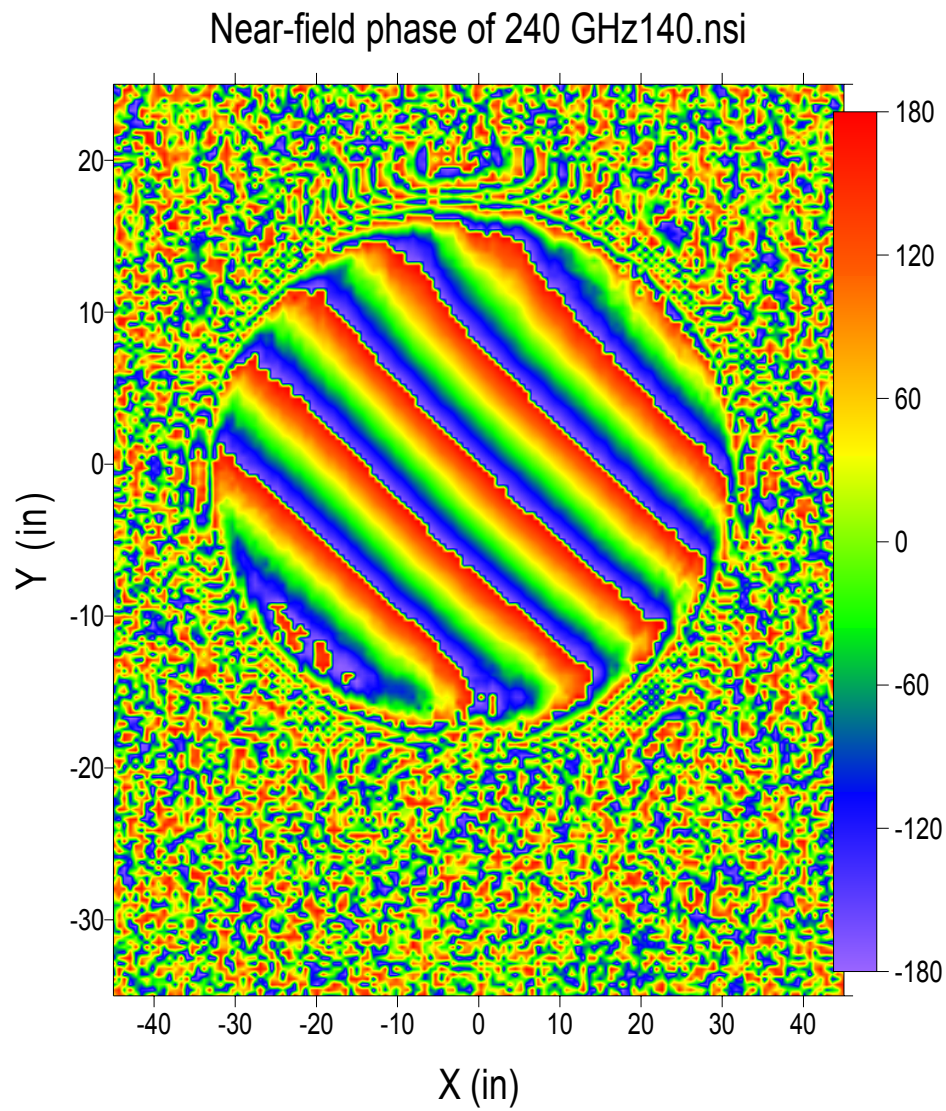

Far Field Patterns

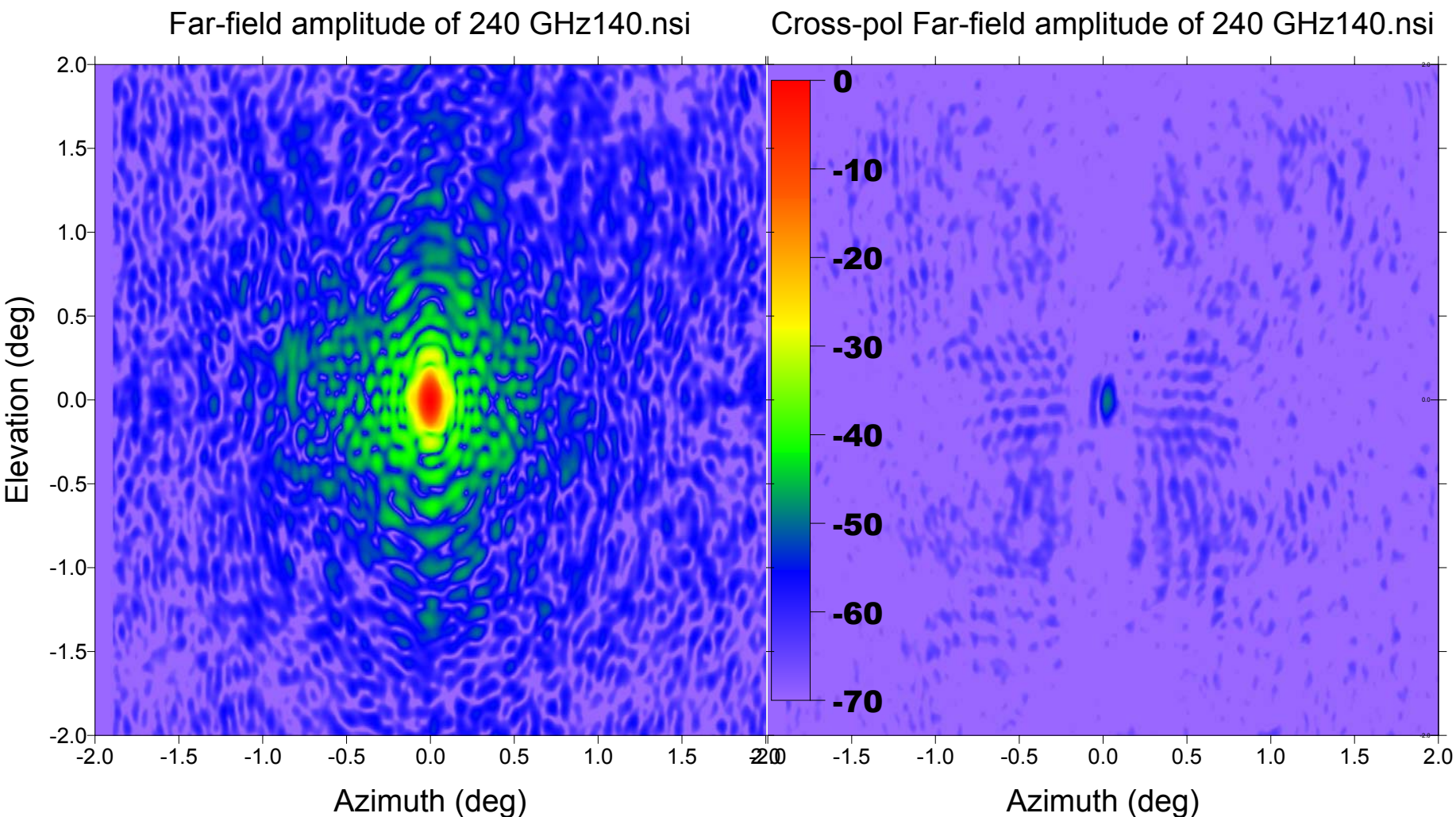

Far Field Patterns (continued)

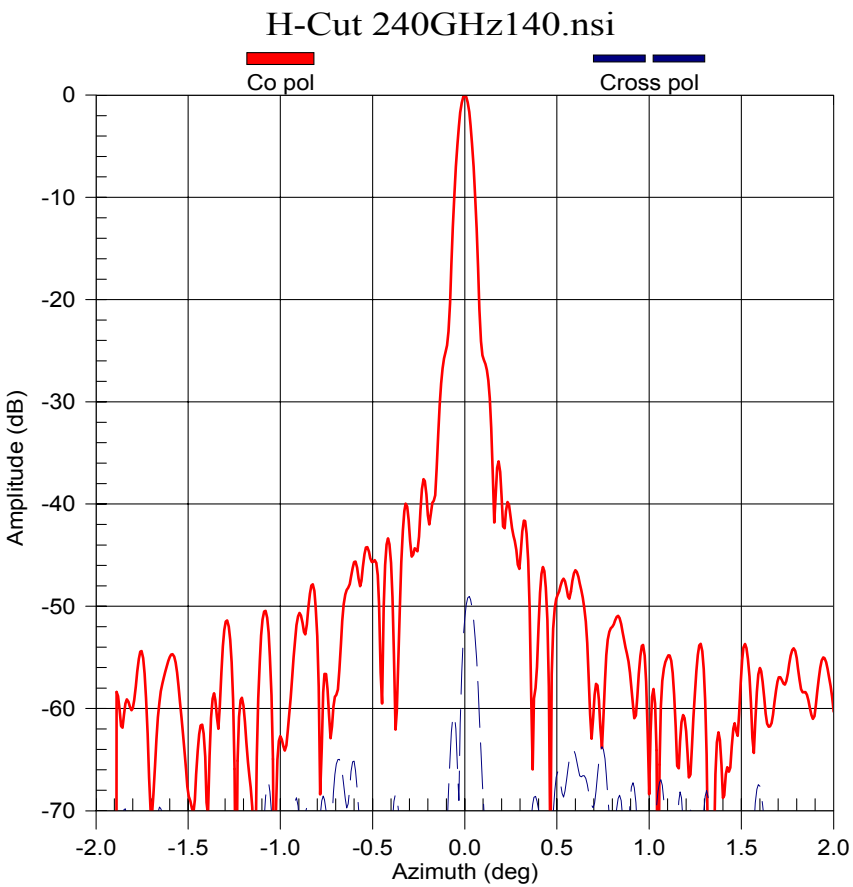

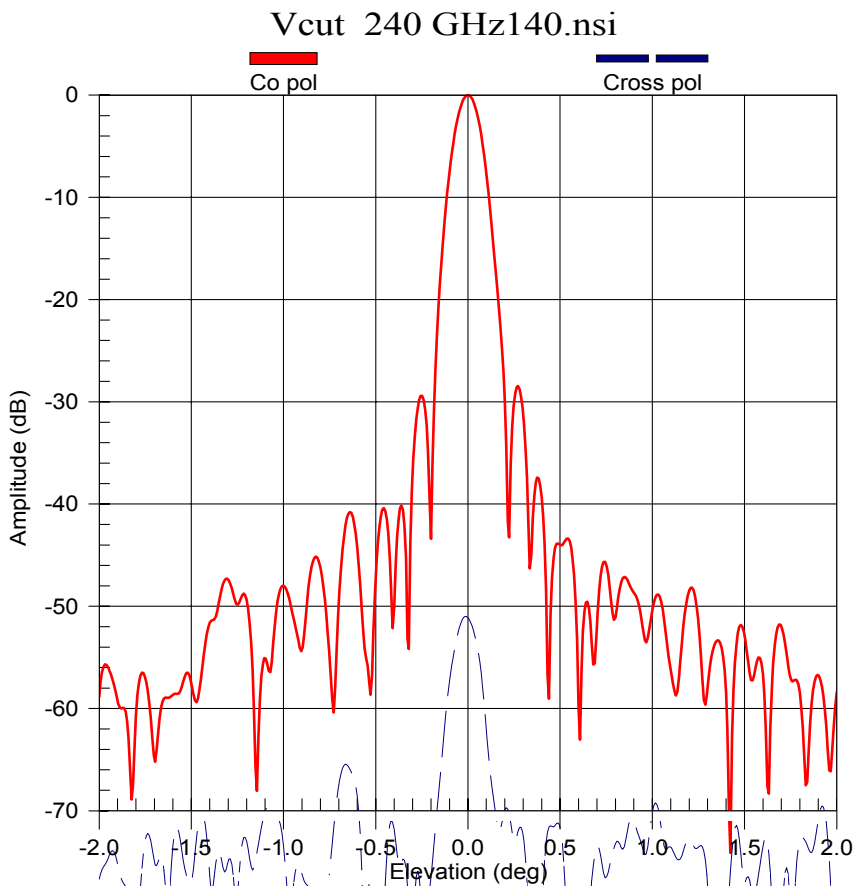

R1A Near Field

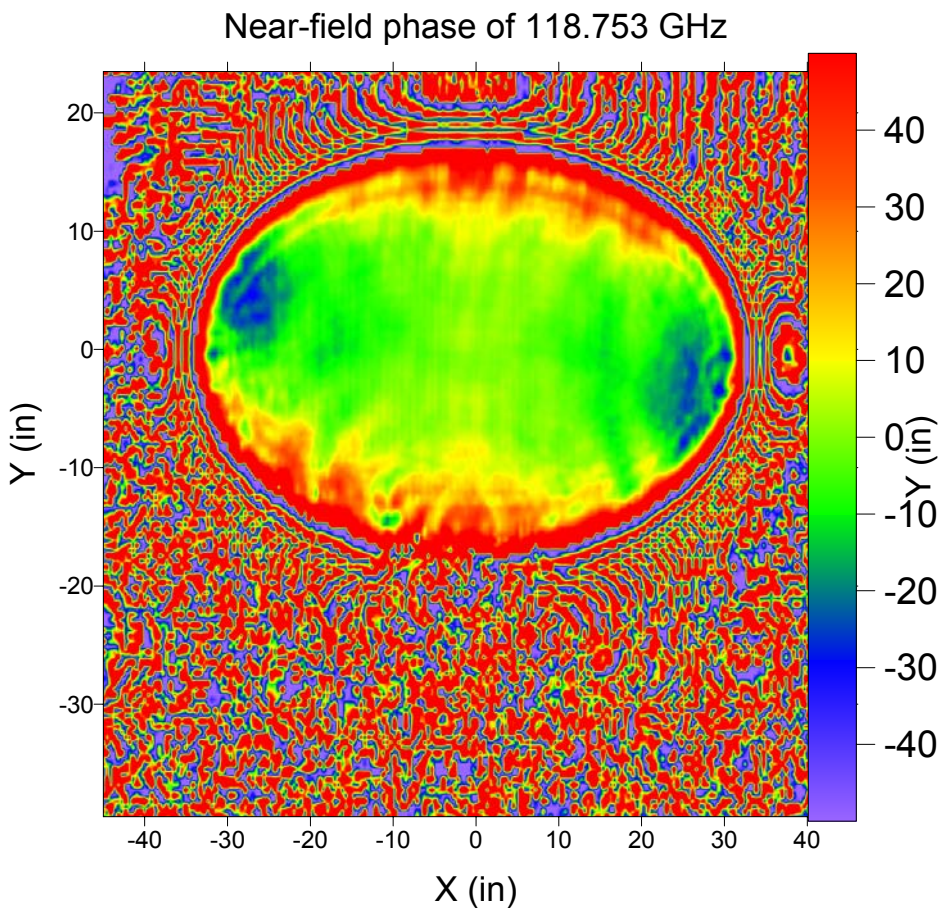

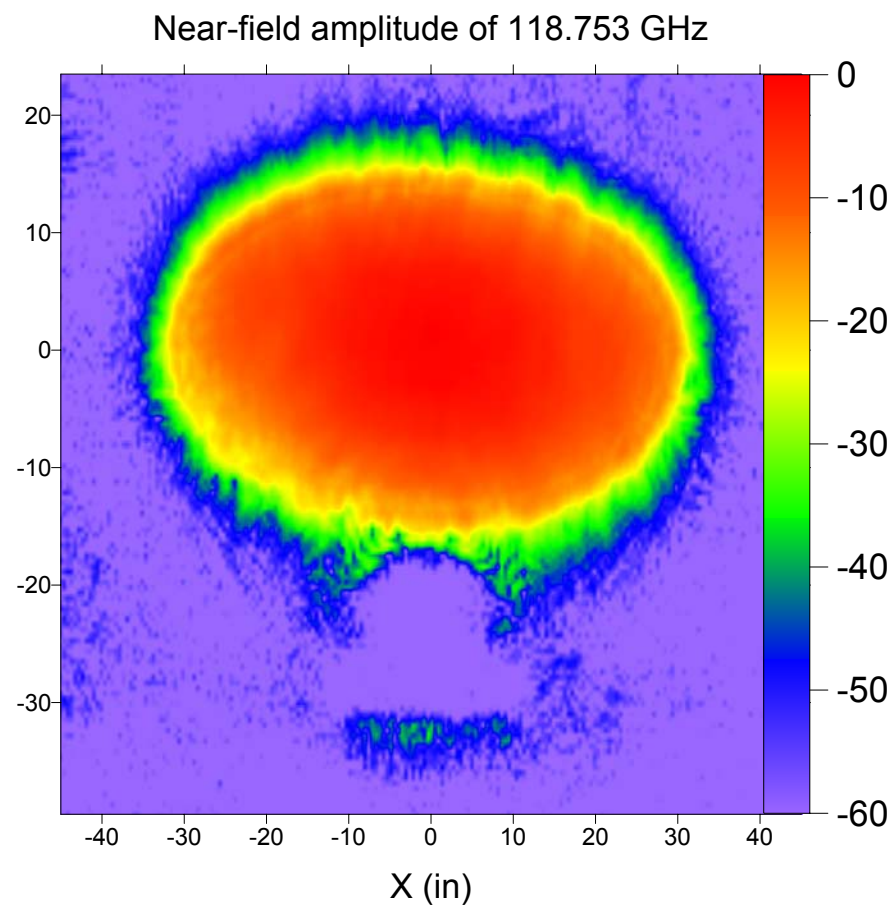

R1A Far Field

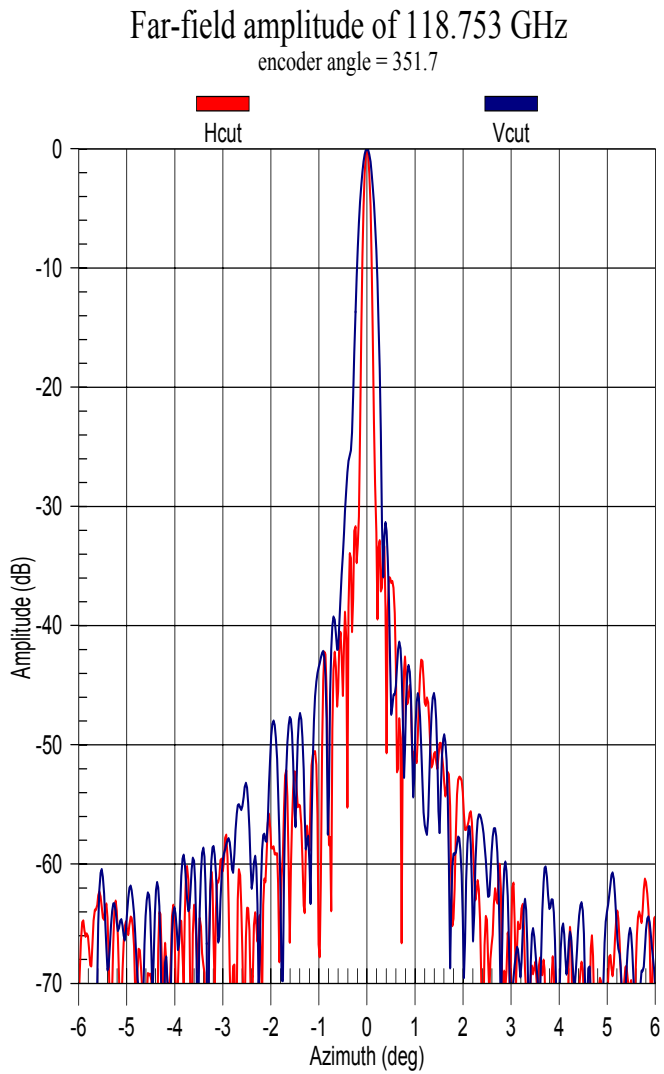

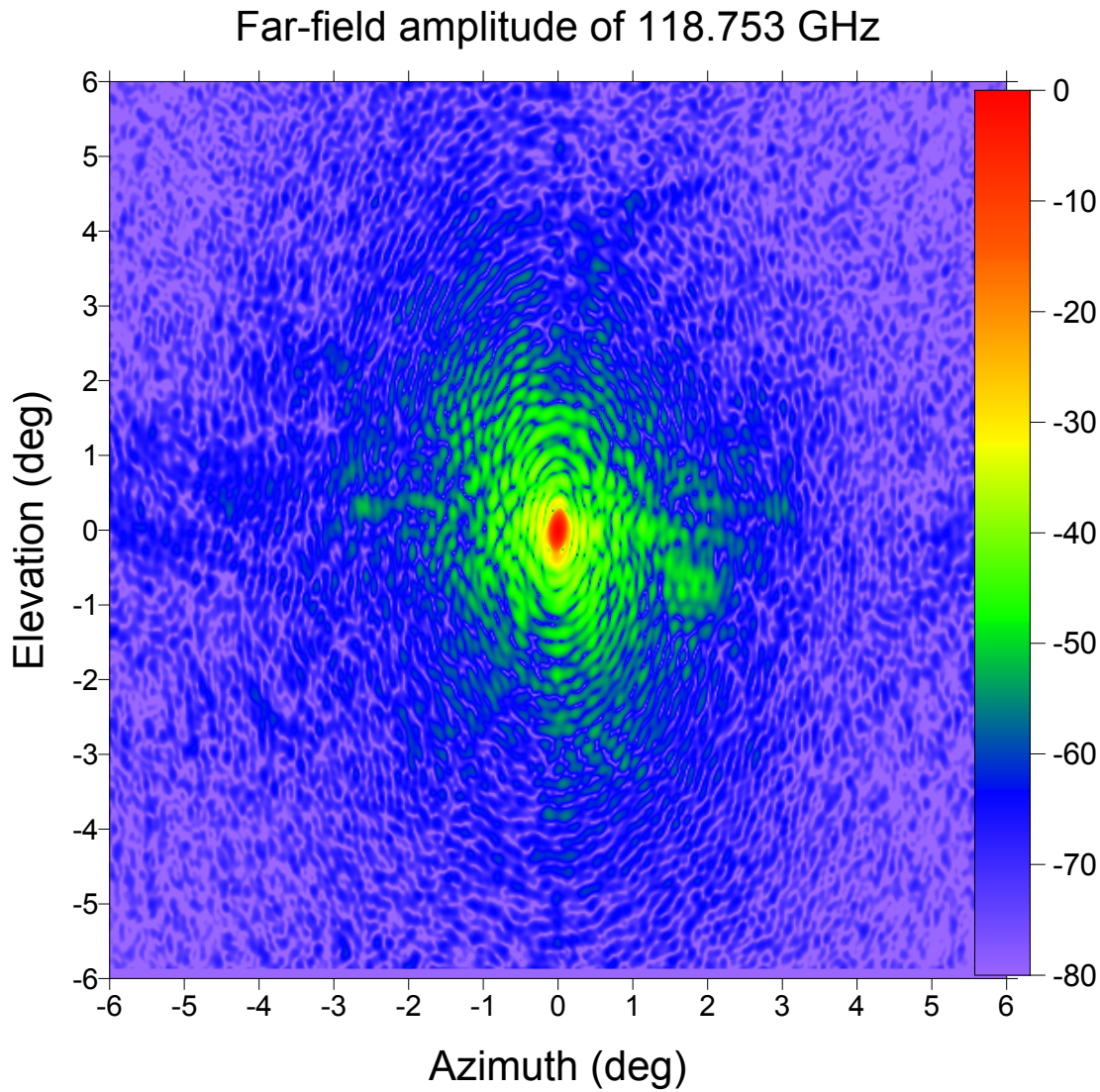

R1A co-alignment

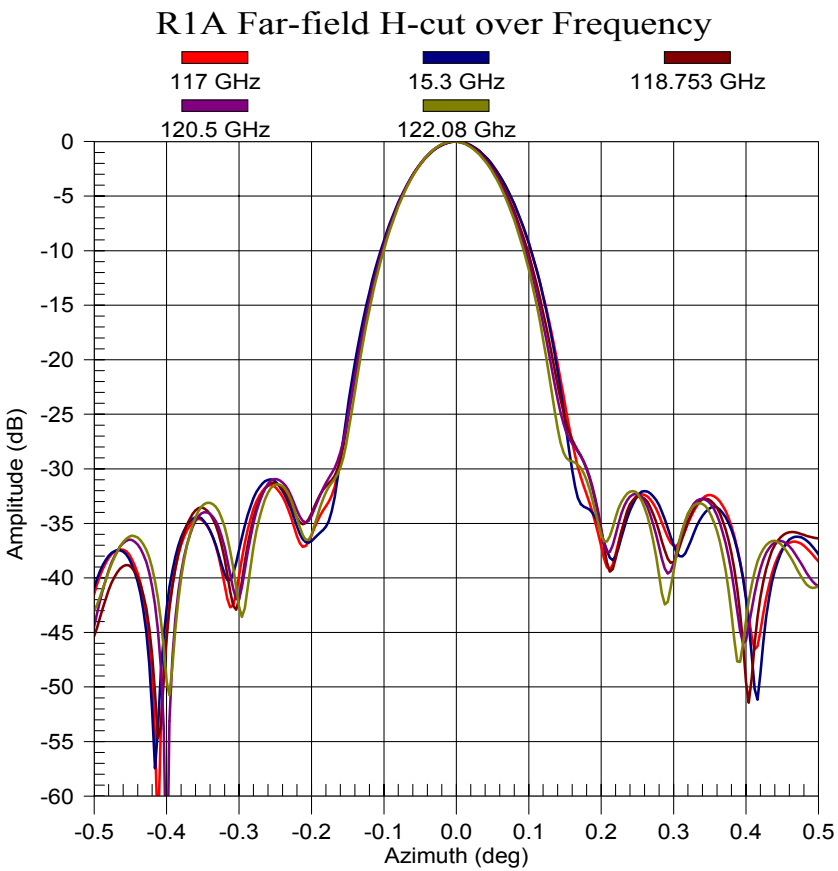

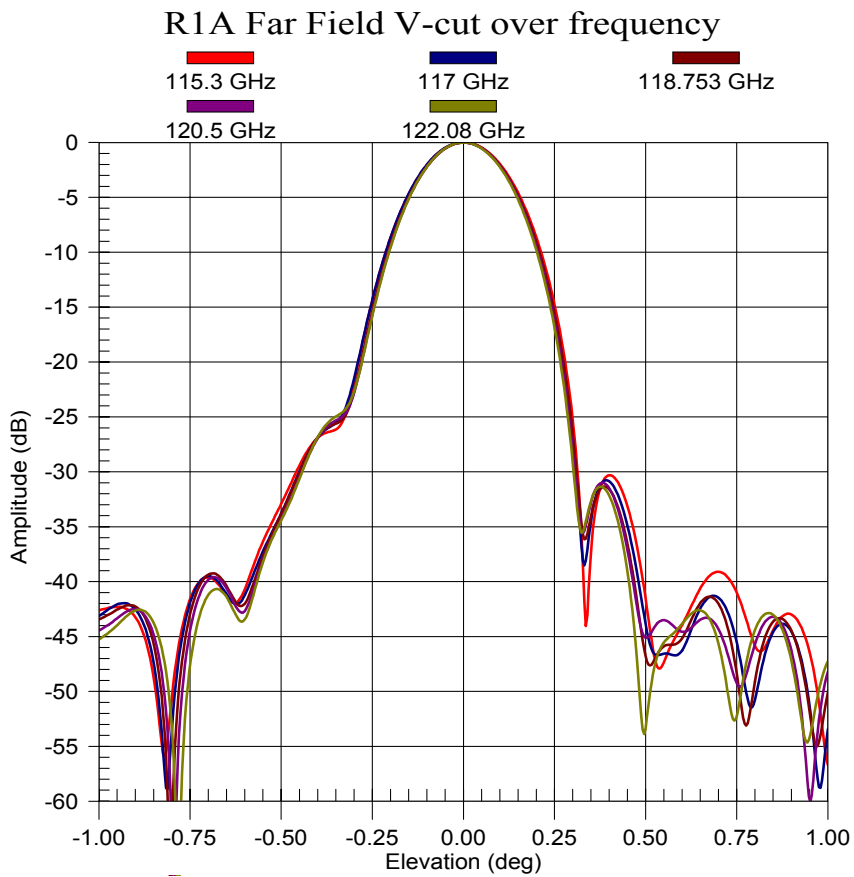

R1A Far Field Variation Over Scan Angle

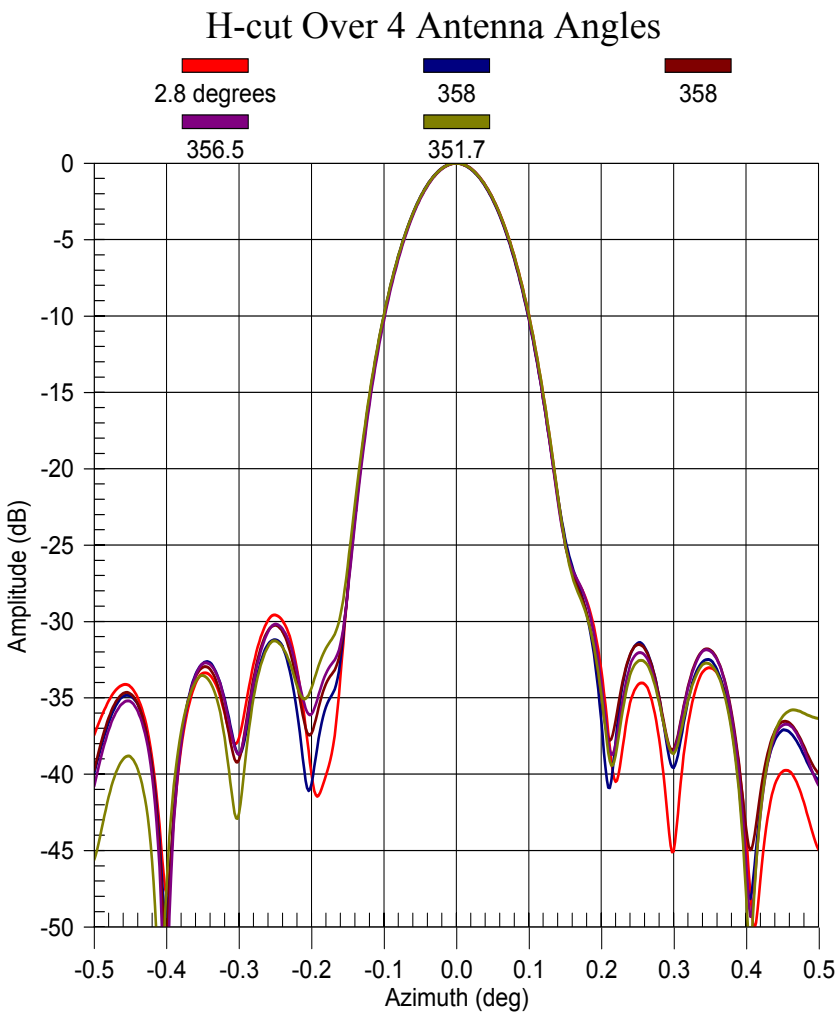

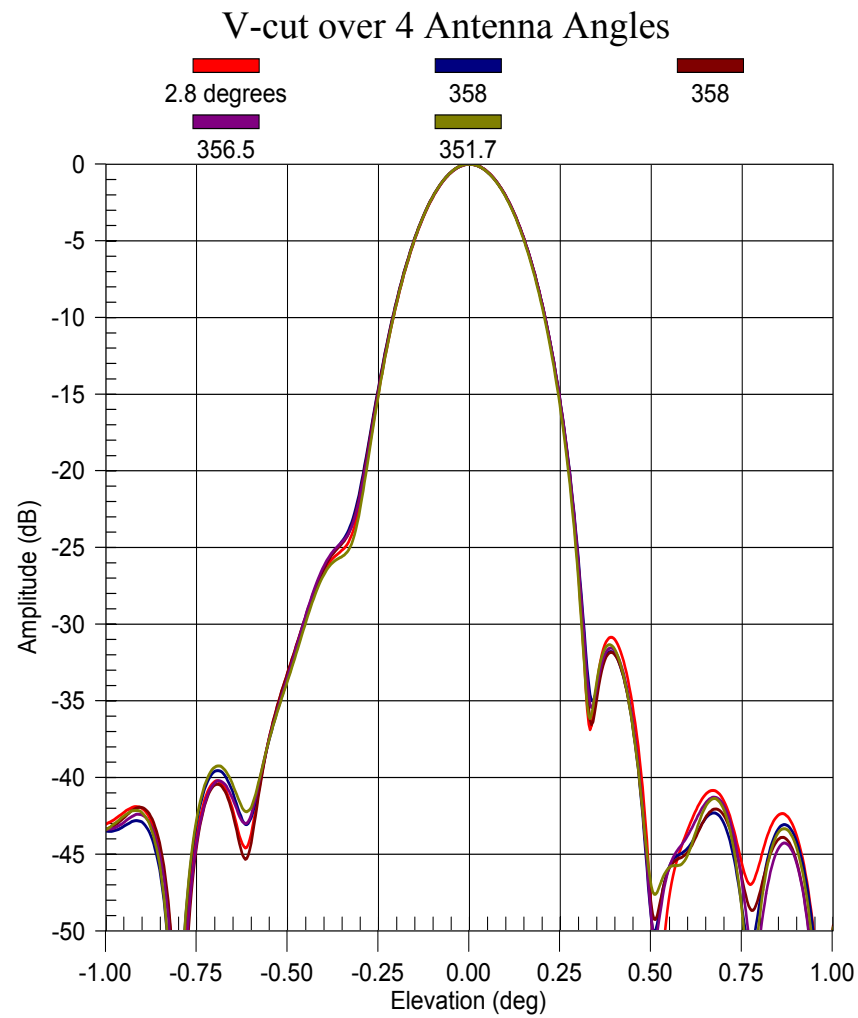

R1B Near Field

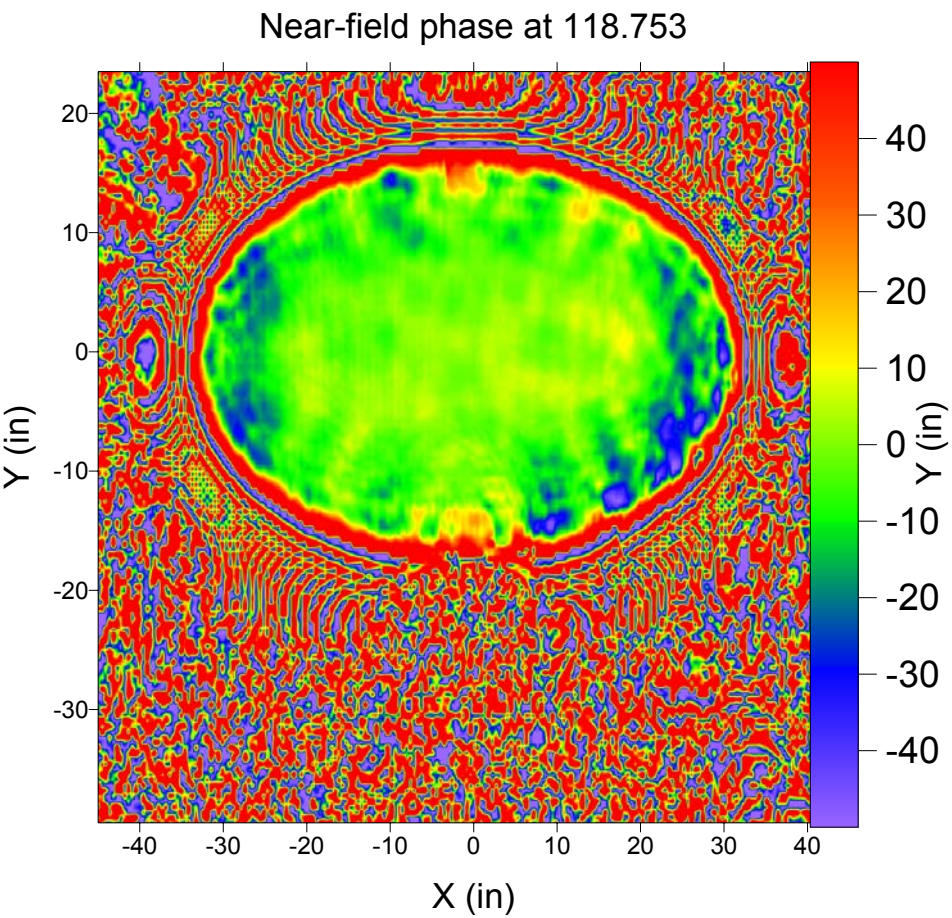

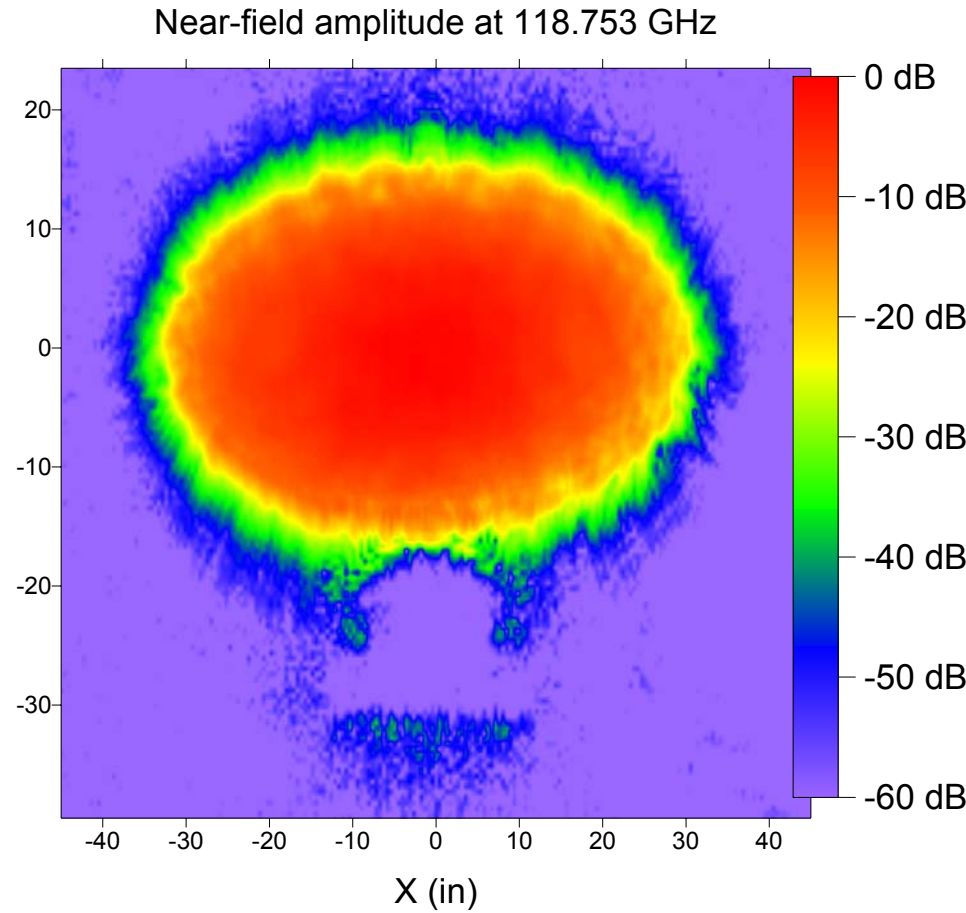

R1B Far Field

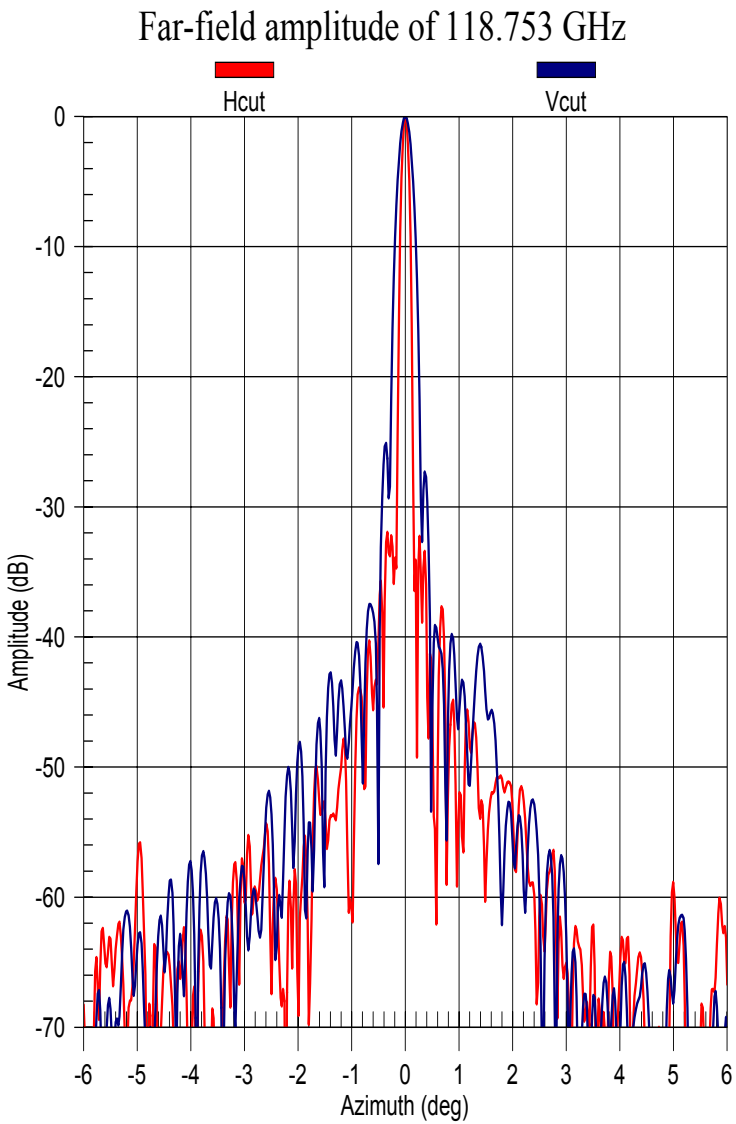

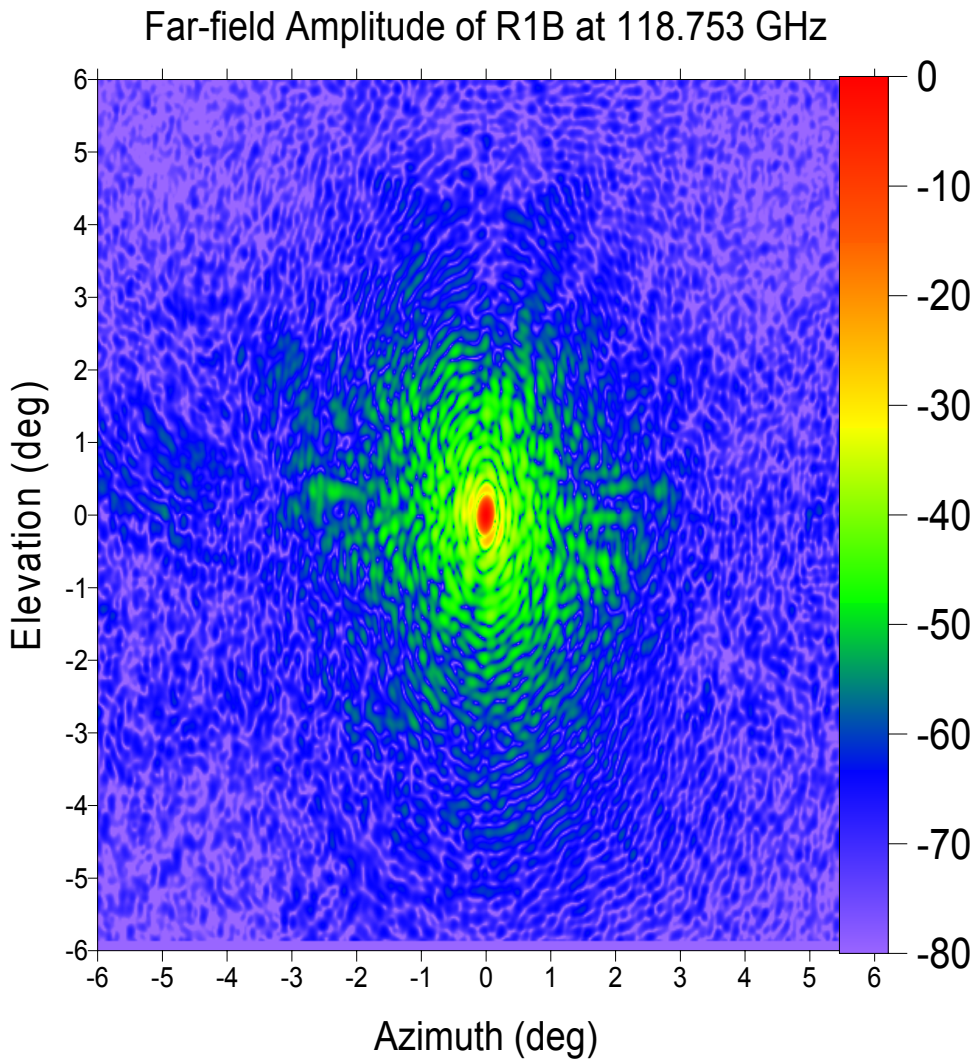

R1B Co-alignment

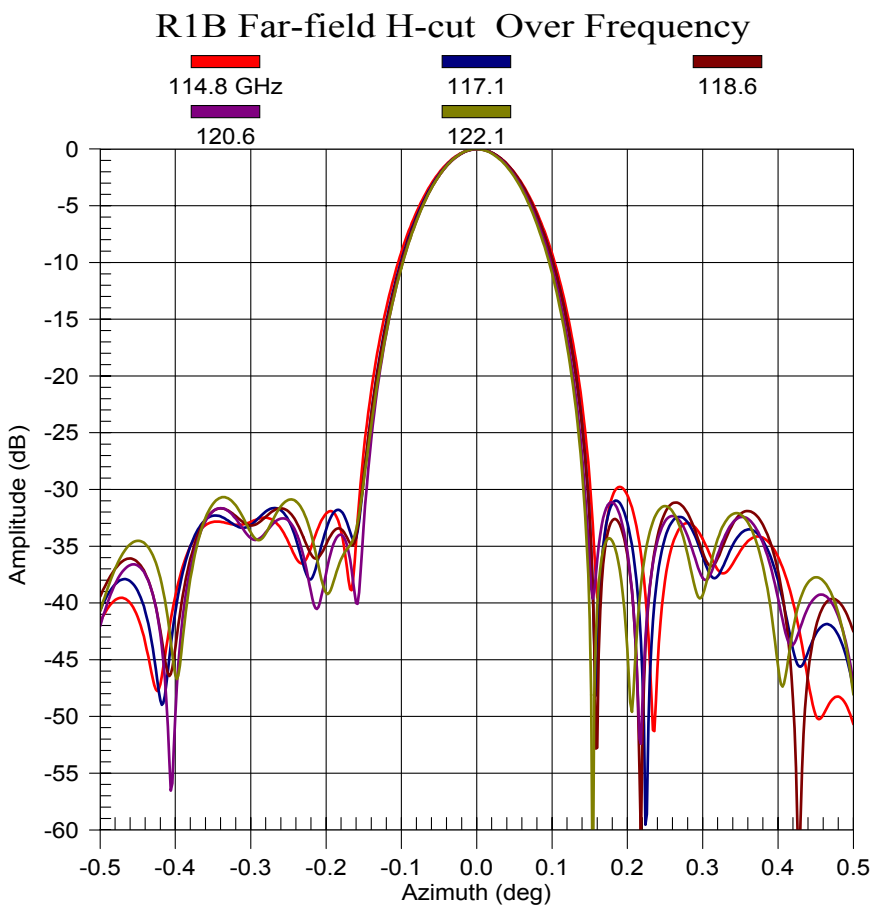

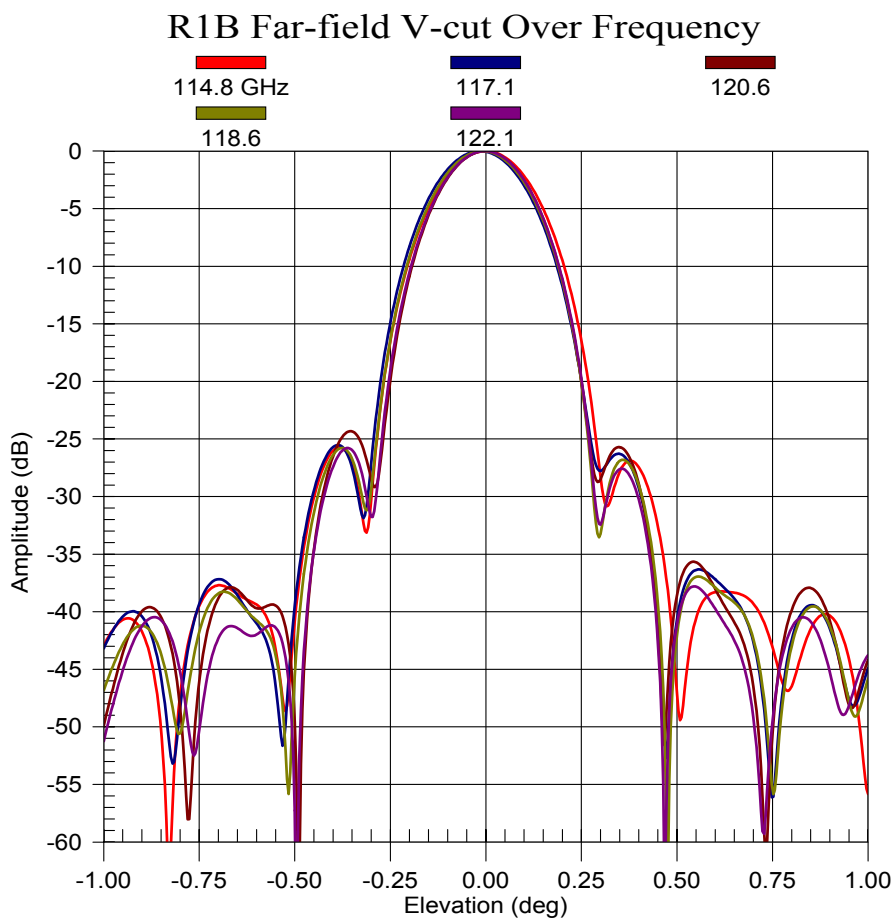

R1B Far Field Variation over Scan Angle

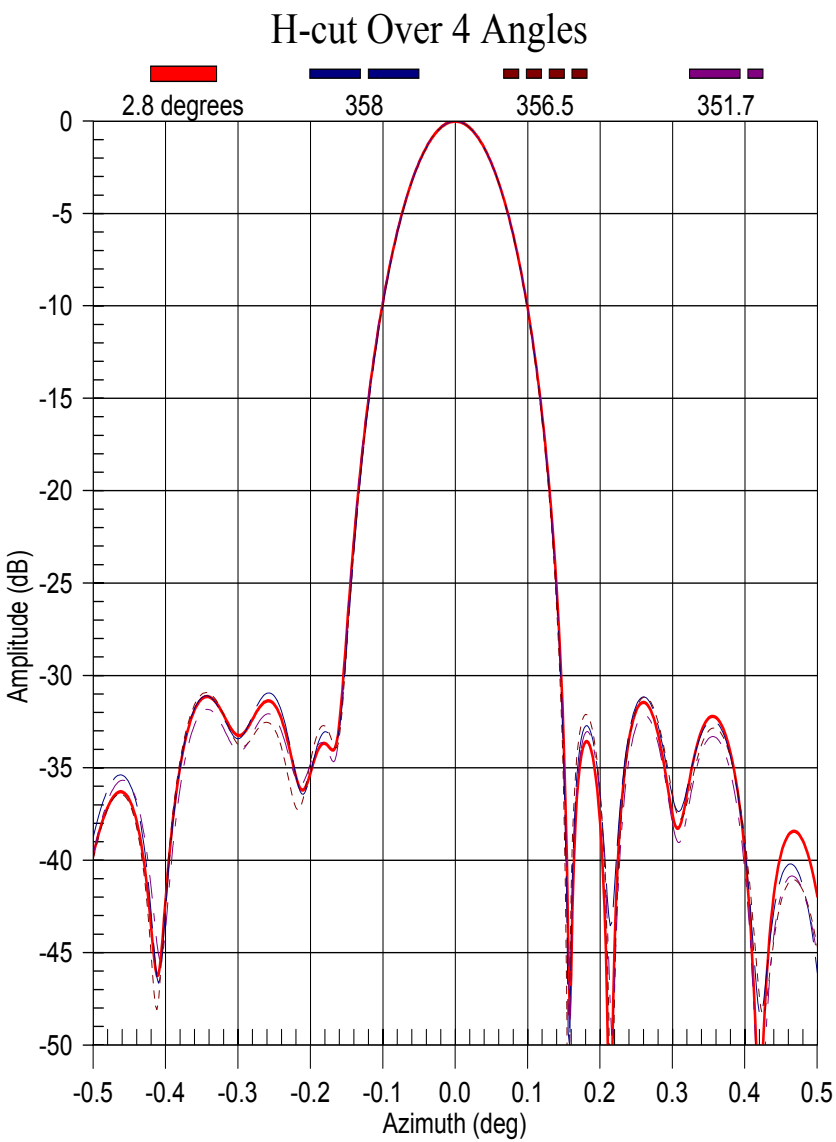

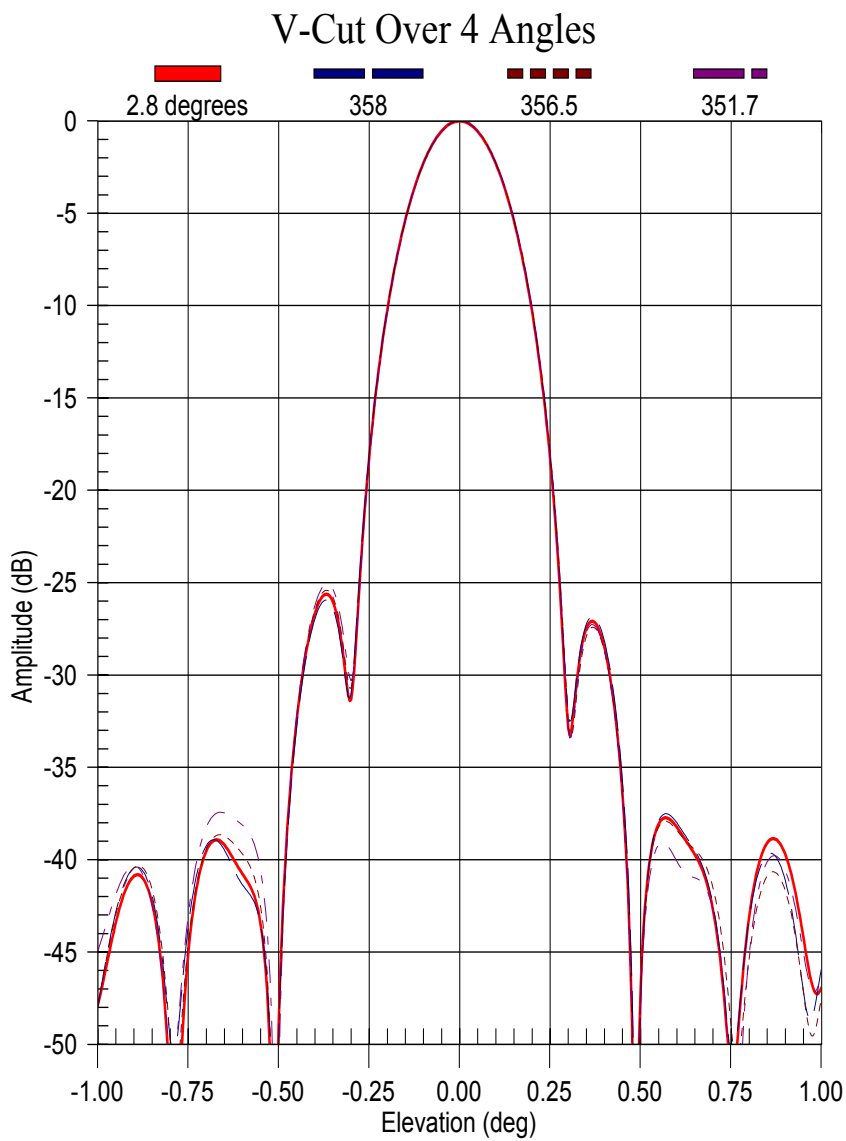

R2 Near Field

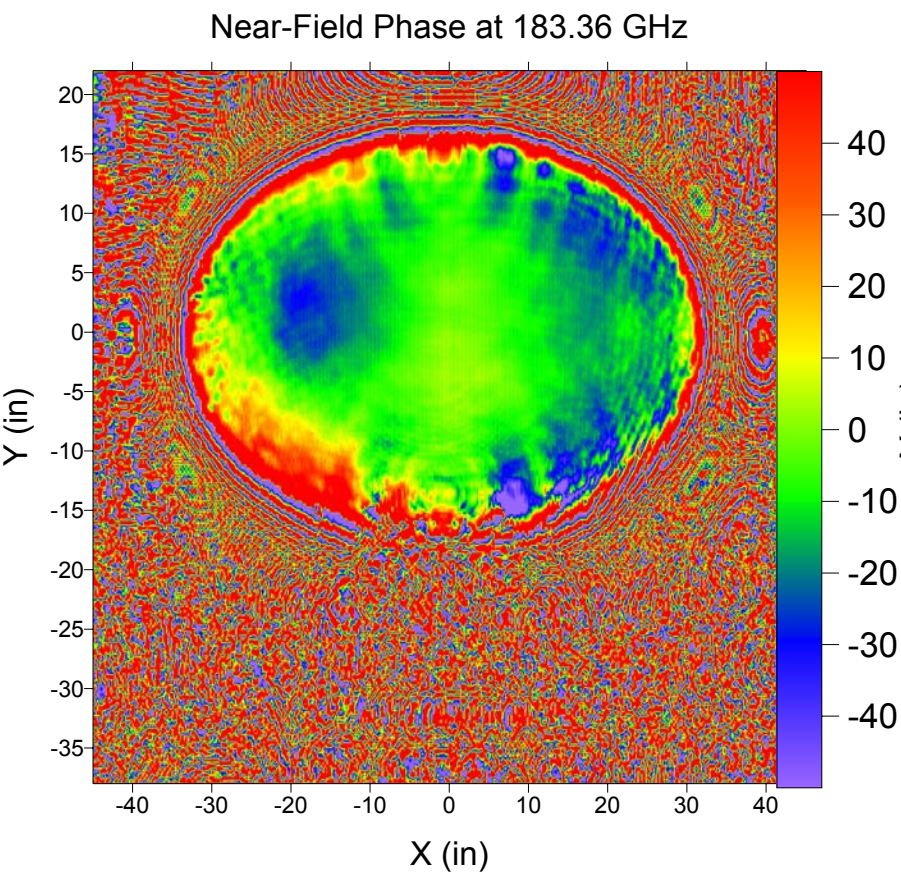

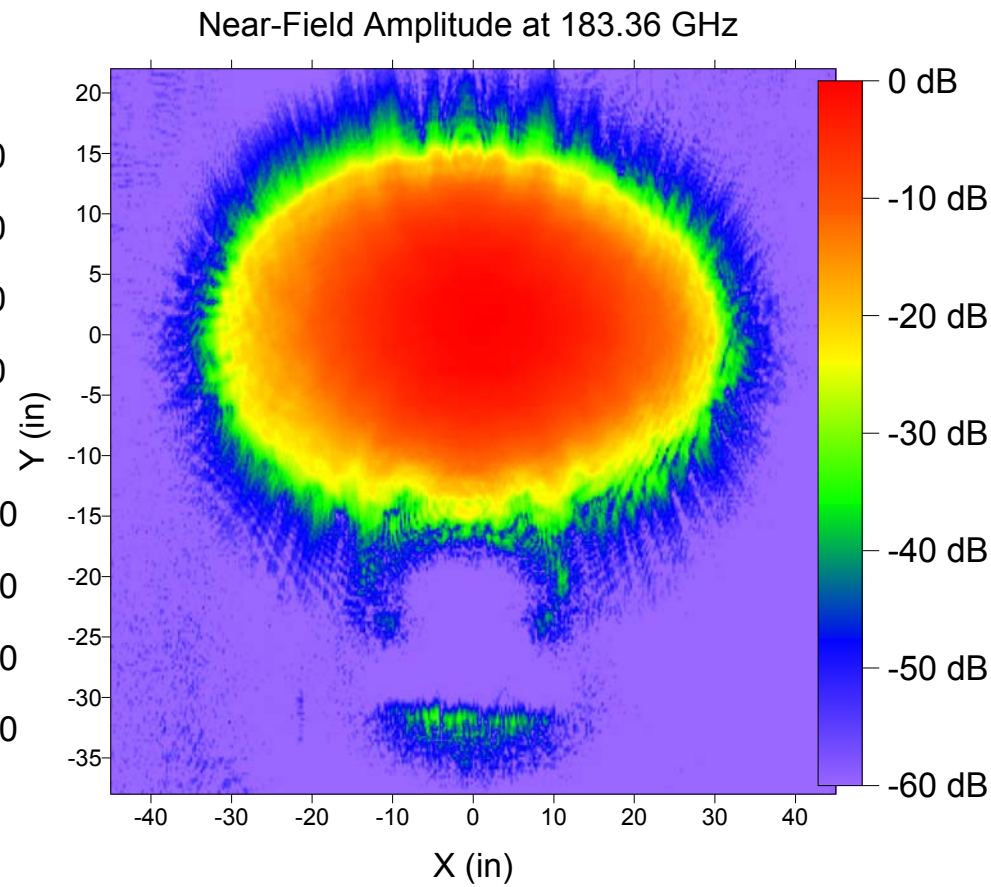

R2 Far Field

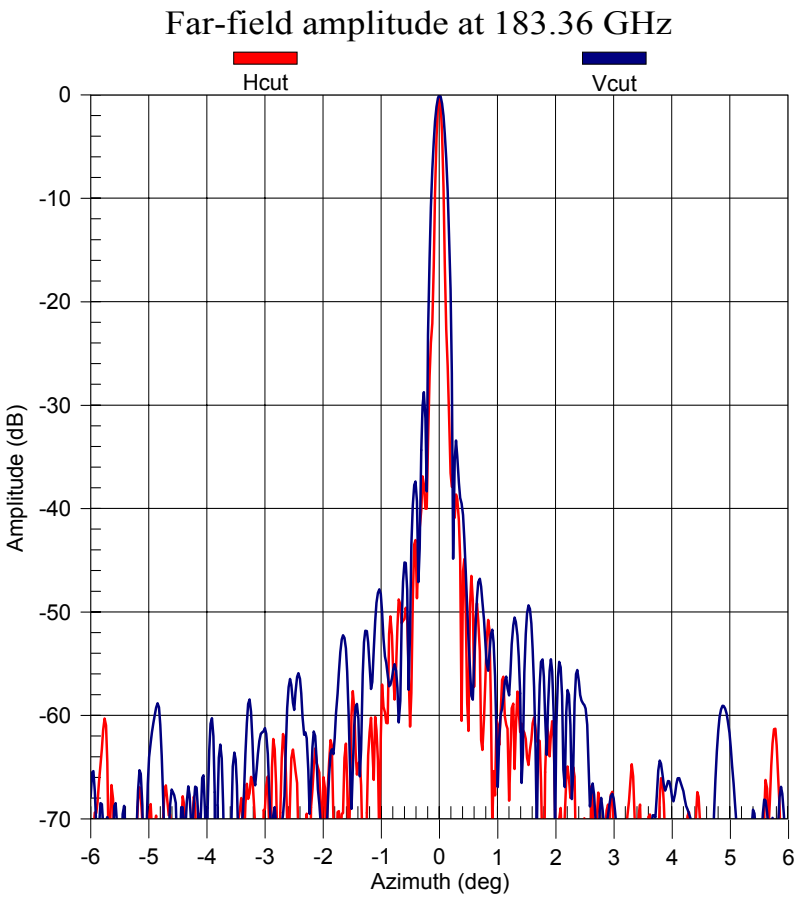
Far-field amplitude at 183.36 GHz
Hcut
Vcut
Amplitude (dB)
0
-10
-20
-30
-40
-50
-60
-70
-6
-5
-4
-3
-2
-1
0
1
2
3
4
5
6
Azimuth (deg)

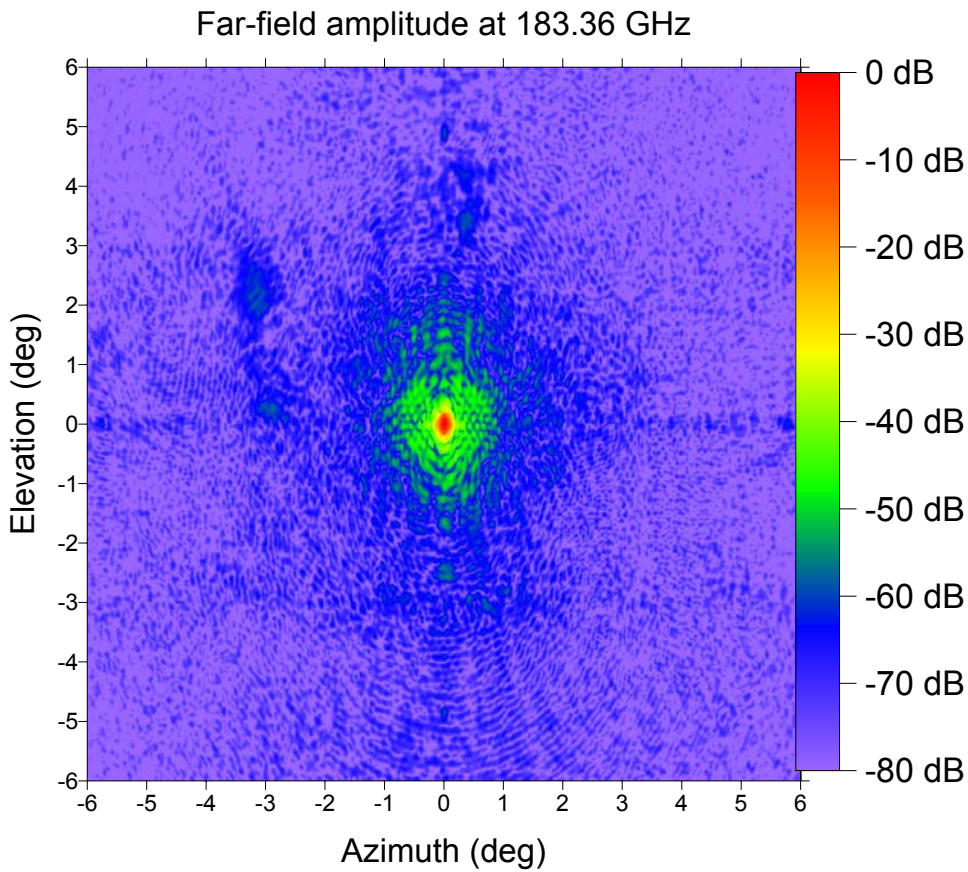
Far-field amplitude at 183.36 GHz
Elevation (deg)
Azimuth (deg)
-6
-5
-4
-3
-2
-1
0
1
2
3
4
5
6
0 dB
-10 dB
-20 dB
-30 dB
-40 dB
-50 dB
-60 dB
-70 dB
-80 dB

R3 Near Field

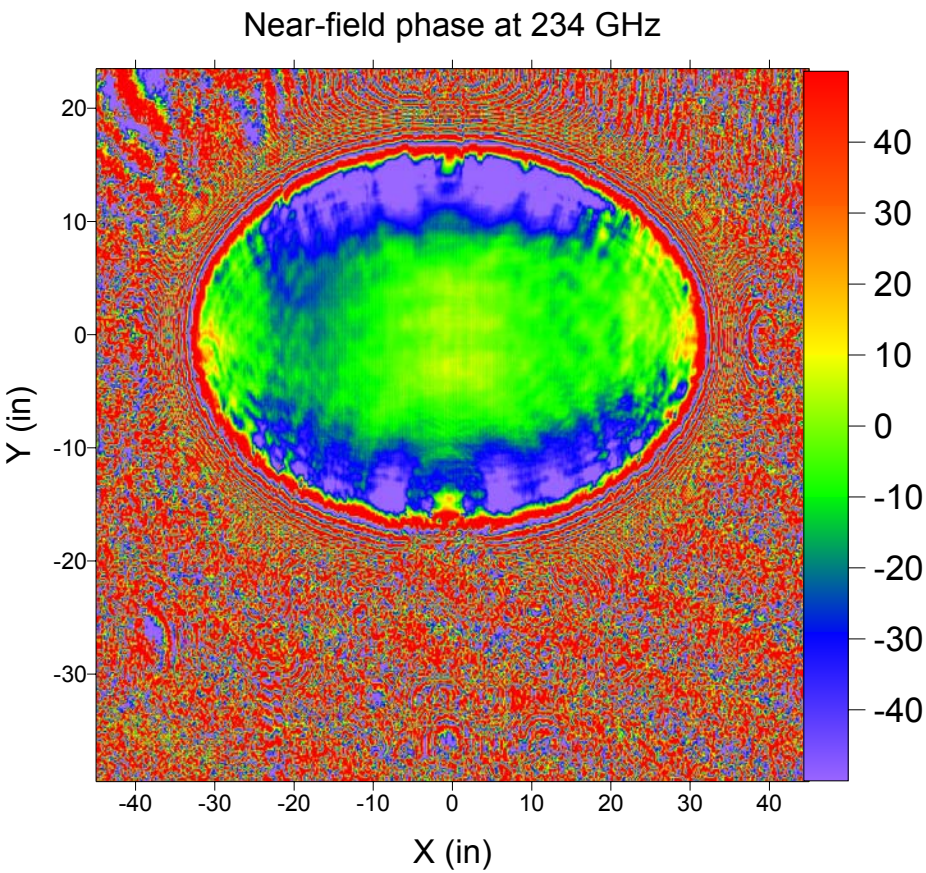

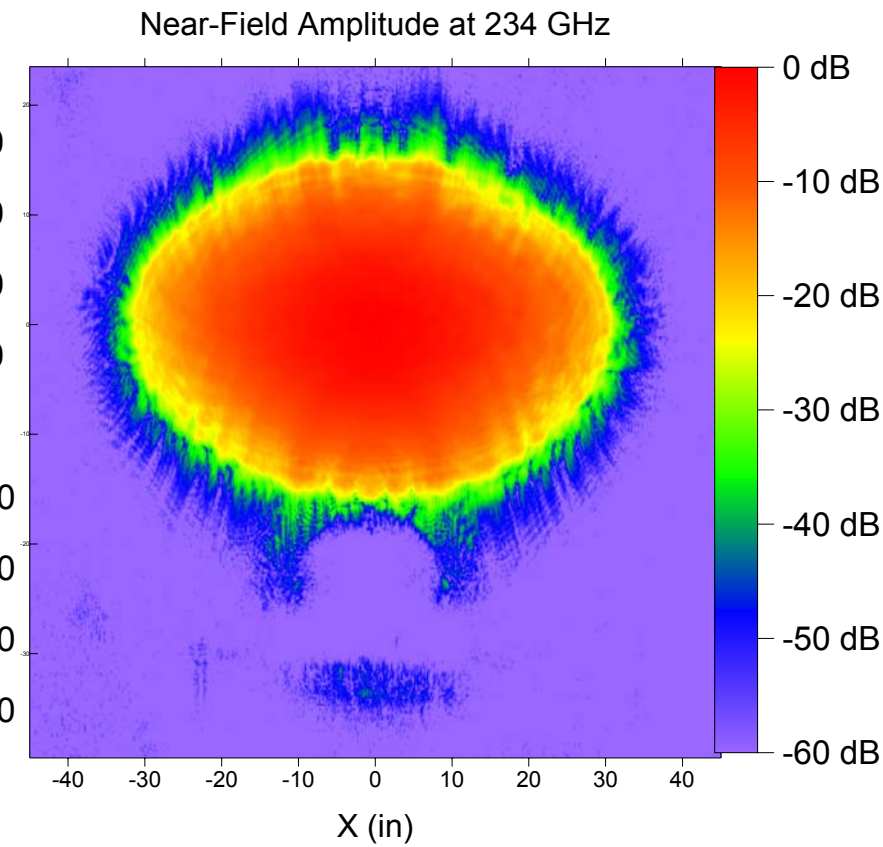

R3 Far Field

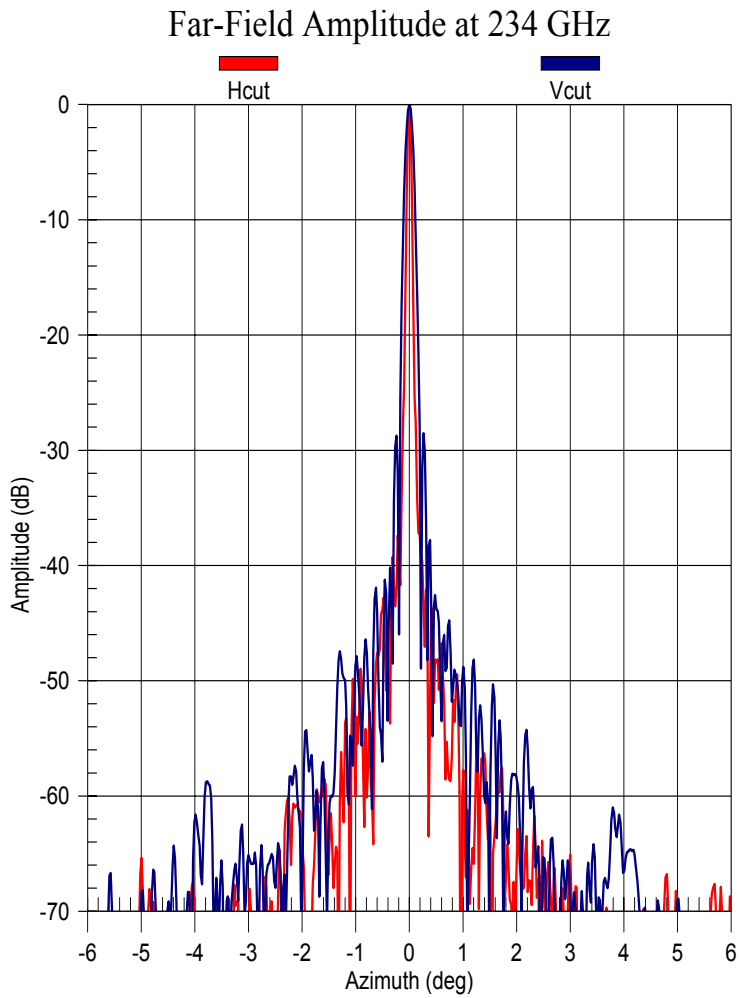
Far-Field Amplitude at 234 GHz
Hcut
Vcut
Amplitude (dB)
0
-10
-20
-30
-40
-50
-60
-70
-6 -5 -4 -3 -2 -1 0 1 2 3 4 5 6
Azimuth (deg)

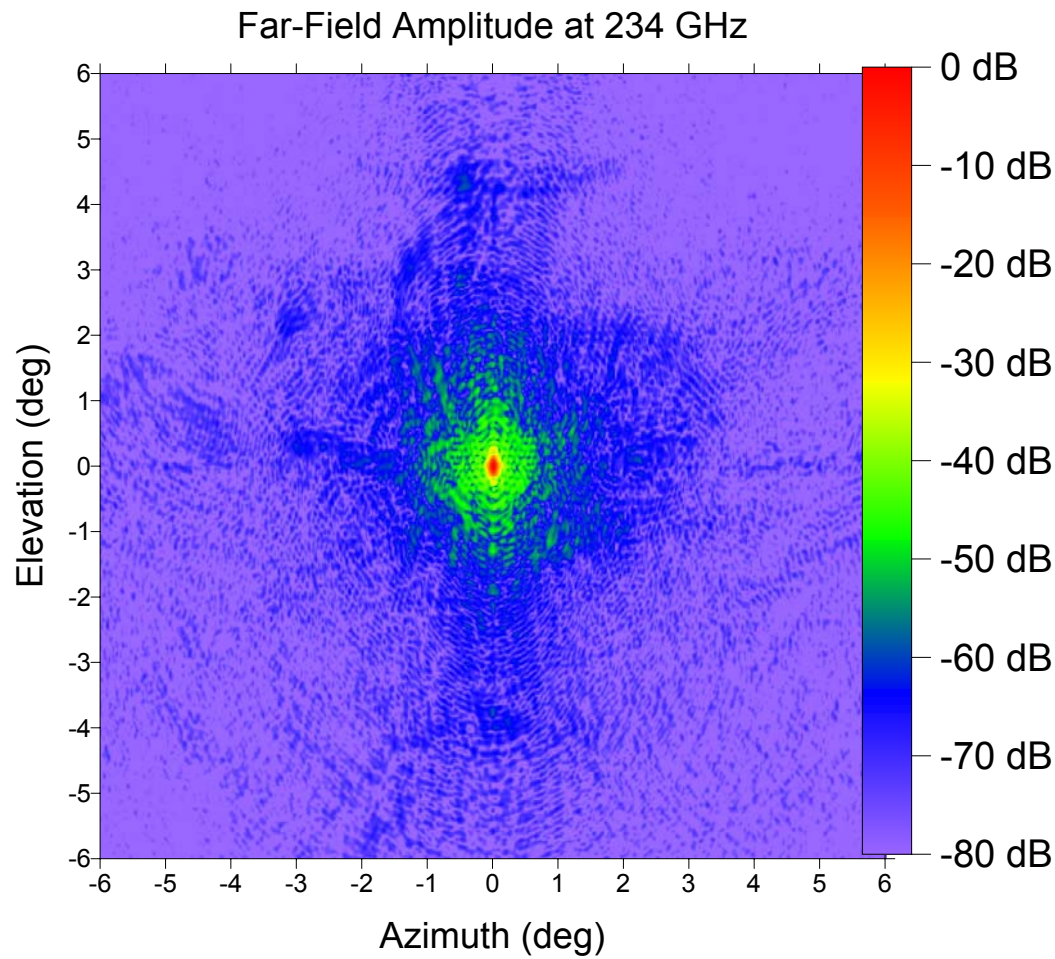
Far-Field Amplitude at 234 GHz
Elevation (deg)
6 5 4 3 2 1 0 -1 -2 -3 -4 -5 -6
-6 -5 -4 -3 -2 -1 0 1 2 3 4 5 6
Azimuth (deg)
0 dB
-10 dB
-20 dB
-30 dB
-40 dB
-50 dB
-60 dB
-70 dB
-80 dB

R4 Near Field

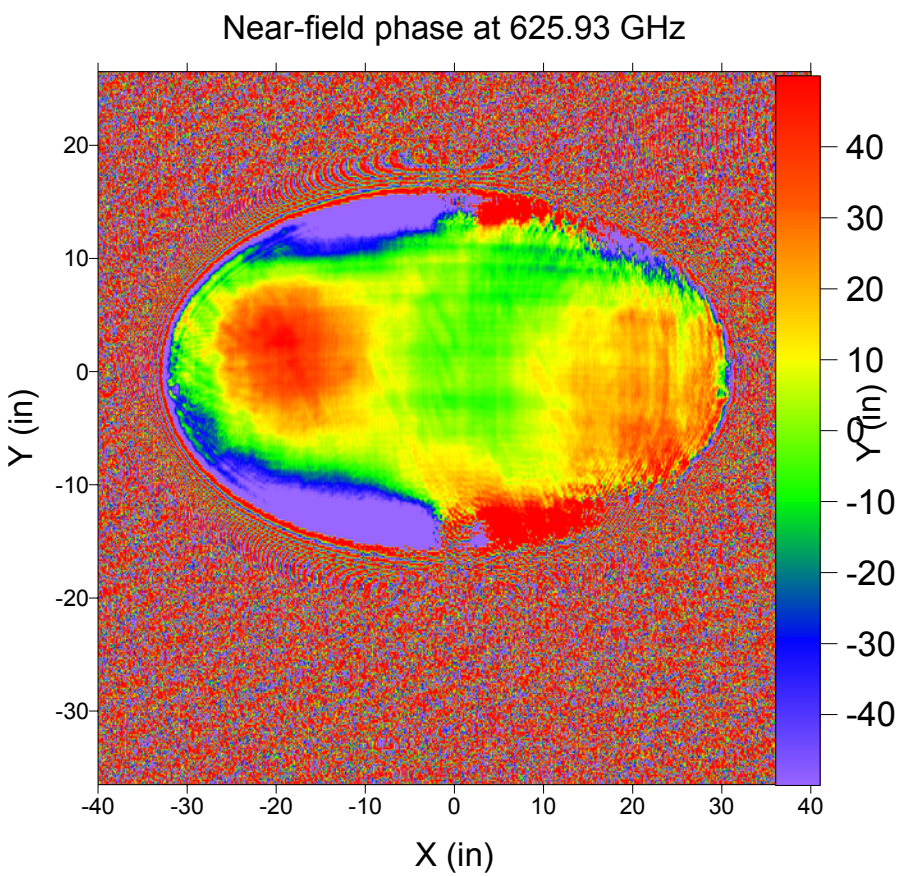

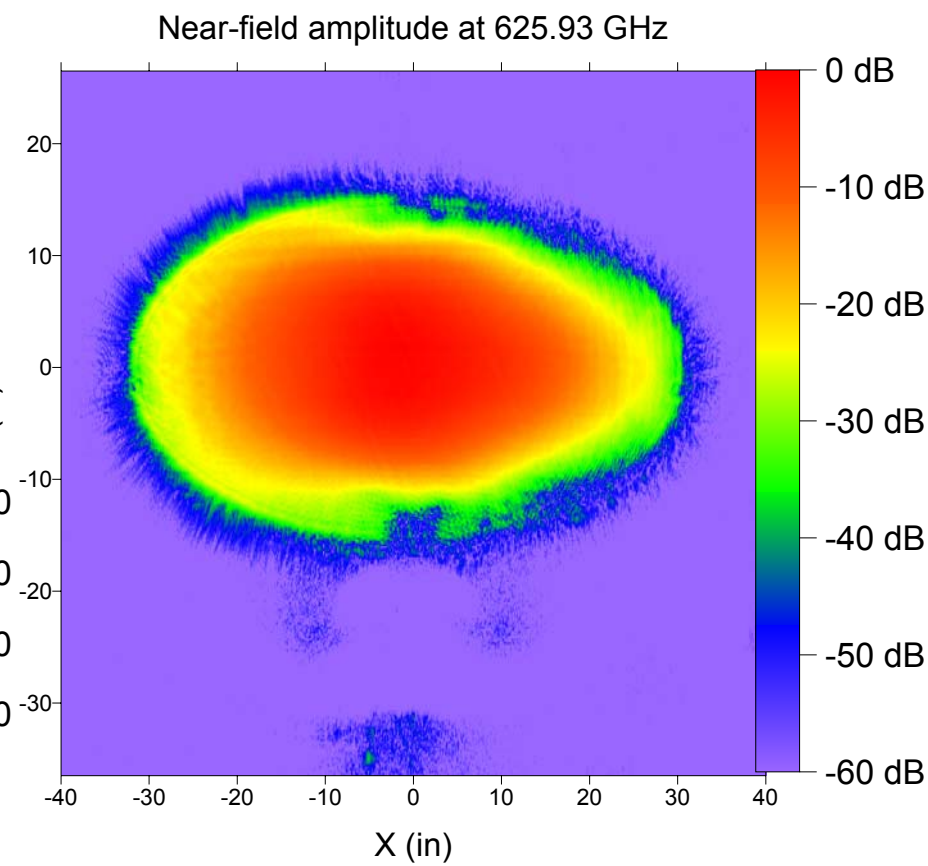

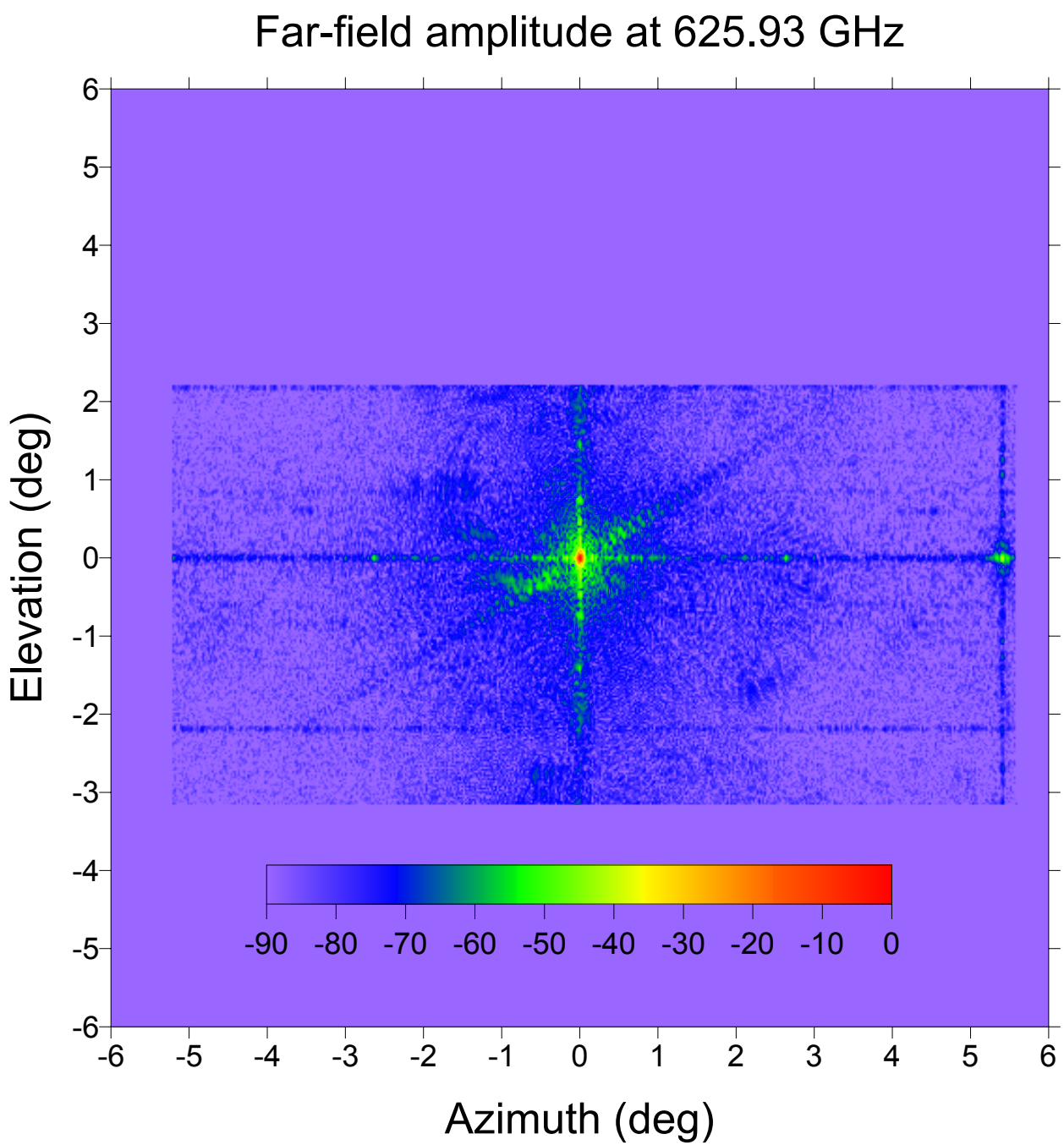
Far-field amplitude at 625.93 GHz
Elevation (deg)
Azimuth (deg)
6
5
4
3
2
1
0
-1
-2
-3
-4
-5
-6
-6 -5 -4 -3 -2 -1 0 1 2 3 4 5 6
-90 -80 -70 -60 -50 -40 -30 -20 -10 0

Cut Just Off Axis

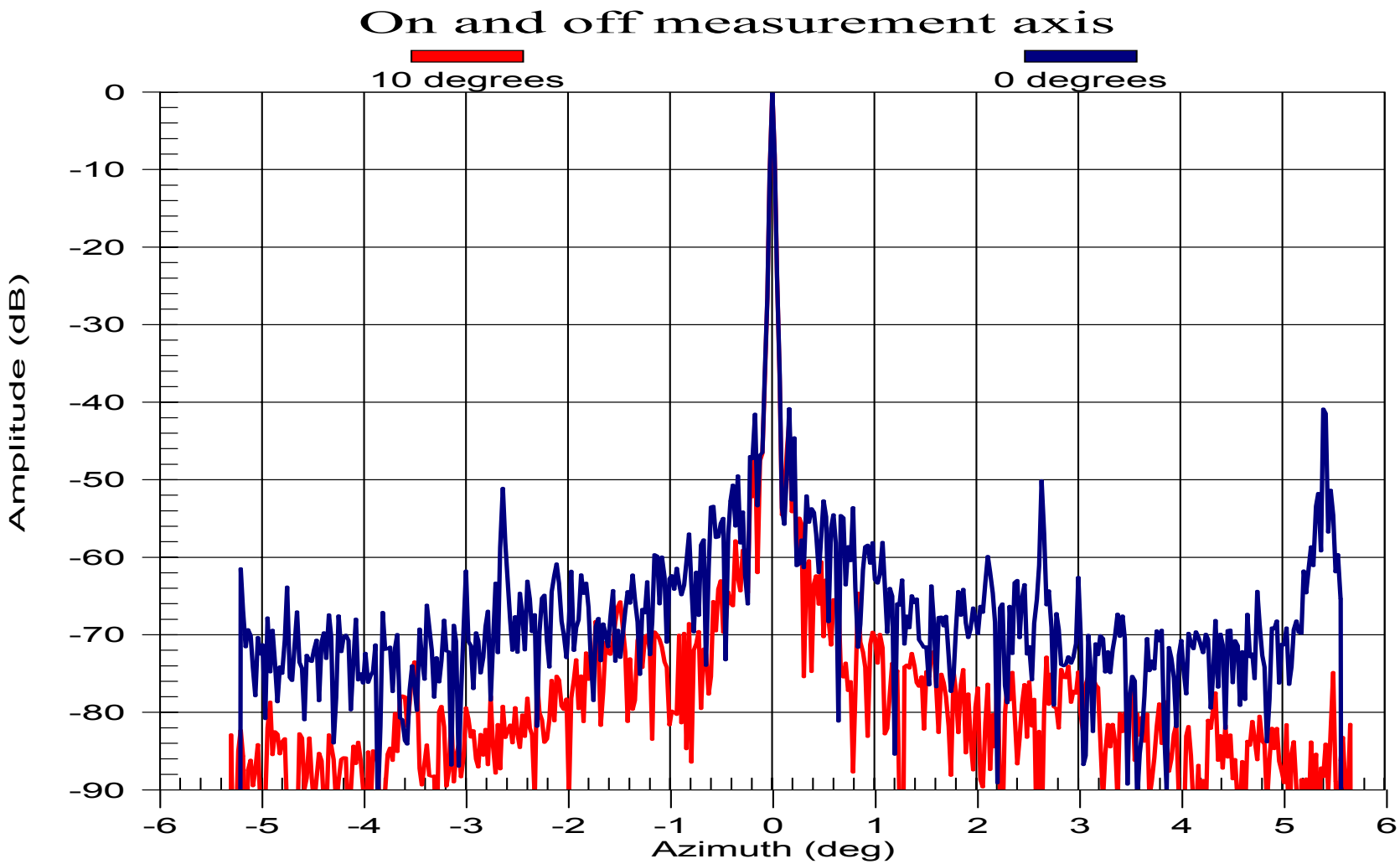

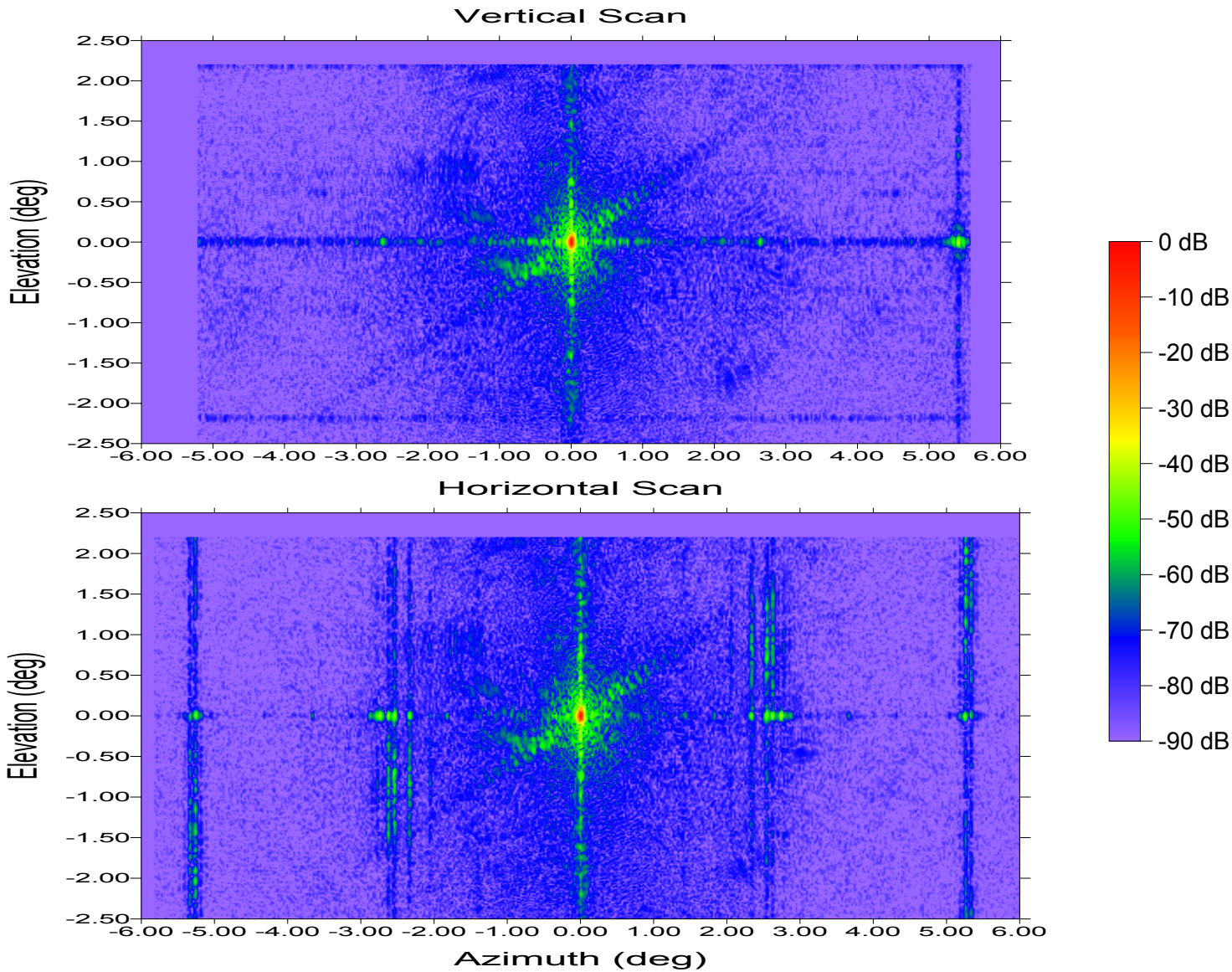
Vertical Scan
Elevation (deg)
2.50
2.00
1.50
1.00
0.50
0.00
-0.50
-1.00
-1.50
-2.00
-2.50
-6.00 -5.00 -4.00 -3.00 -2.00 -1.00 0.00 1.00 2.00 3.00 4.00 5.00 6.00
Horizontal Scan
Elevation (deg)
Azimuth (deg)
0 dB
-10 dB
-20 dB
-30 dB
-40 dB
-50 dB
-60 dB
-70 dB
-80 dB
-90 dB

Pre-Ship Forward Model Meeting

GHz FOV Calibration

Richard E. Cofield
Paul C. Stek

December 11-12, 2002

GHz FOV Calibration

Overview

- Verify FOV Performance unchanged through Env. Tests
- Results from definitive FOV calibration
  - Update pointing, HPBW, Beam Efficiency
  - Scan angle and frequency dependences
  - Compliance with calibration requirements
- Analyses to be performed for calibration report
- Conclusions

FOV Requirements

- Requirements from Science Requirements Document (SRD: JPL D-14421, Rev 3.0)
- Performance requirements
  - §3.5.1 HPBW and Beam Efficiencies
  - §3.5.2 FOV coincidence R1A,R1B,R2,R3,R4
    - R5 coincidence to GHz radiometers pending determination of module shims and measurement of module cubes to spacecraft reference.
  - §3.5.3-4 FOV boresight placement and knowledge; scan plane to orbit
    - measurements complete to module cubes and mounts; pending verification of mount-to-spacecraft reference.
  - *Following material shows all performance requirements are met.*
- §3.5.1 FOV Calibration Requirement
  - *Definitive calibration dataset is adequate to prove that calibration requirement is met; details to appear in Calibration Report.*

GHz FOV Calibration

HPBW and Beam Efficiency - Results

Requirements in SRD §3.5.1

		HPBW Vertical / °		HPBW Horizontal / °		Beam Efficiency within 2.5xHPBW	
		Required	**Measured**	***Required***	**Measured**	***Required***	**Measured**
118 GHz	**R1A**	*≤0.123*	[0.107,0.118]	*≤0.283*	[0.227,0.245]	*≥0.95*	[0.978,0.987]
	R1B	*≤0.123*	[0.111,0.119]	*≤0.283*	[0.220,0.236]	*≥0.95*	[0.980,0.982]
190 GHz	**R2**	*≤0.085*	[0.074,0.084]	*≤0.189*	[0.147,0.168]	*≥0.95*	[0.959,0.980]
240 GHz	**R3**	*≤0.066*	[0.058,0.064]	*≤0.189*	[0.116,0.126]	*≥0.95*	[0.962,0.973]
640 GHz	**R4**	*≤0.028*	[0.0252,0.0271]	*≤0.189*	[0.0528,0.0572]	*≥0.95*	[0.962,0.967]

Requirements are met.

GHz FOV Calibration

dFOV Coincidence - Results

Requirements in SRD §3.5.2

Limb Vertical	R1A	R1B	R2	R3	R4
Requirement:		*coincident within 0.025 °*			
meas.dθ / °	≡0	0.015	0.005	0.020	0.011
3σ / °	-	<0.003	<0.003	<0.003	<0.003
Δ from PER		0.0030	-0.0005	0.0043	0.0018

Limb Horizontal	R1A	R1B	R2	R3	R4
Requirement:		*coincident within 0.05 °*			
meas.dϕ / °	≡0	0.009	-0.006	0.010	0.006
3σ / °	-	<0.015*	<0.003	<0.003	<0.003
Δ from PER		-0.0009	0.0020	0.0007	-0.0002

θ,ϕ are spherical polar angles in GHz cube frame

*Large IF dependence of R1B Limb H dFOV is under investigation

Requirements are met as shown in following plots.

GHz FOV Calibration

dFOV Coincidence – footprints at limb tangent point for four different scan angles and various IFs

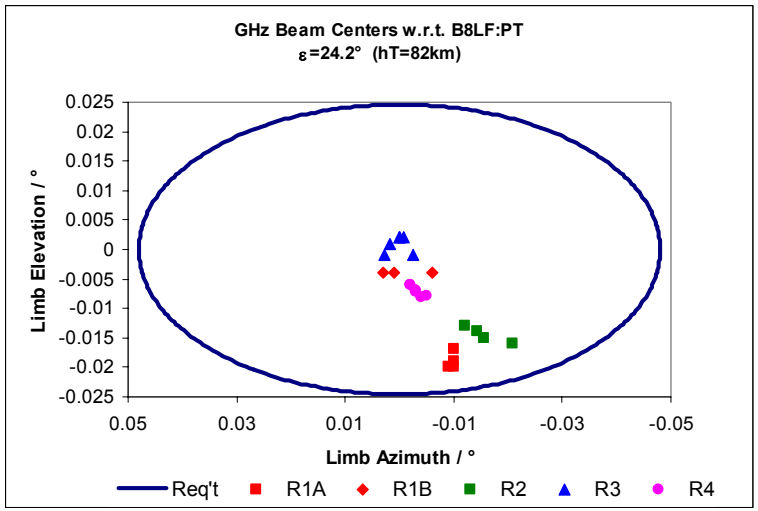

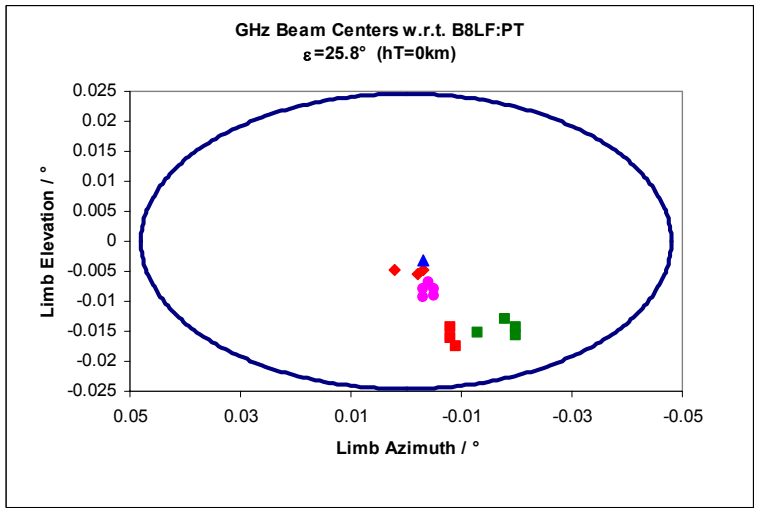

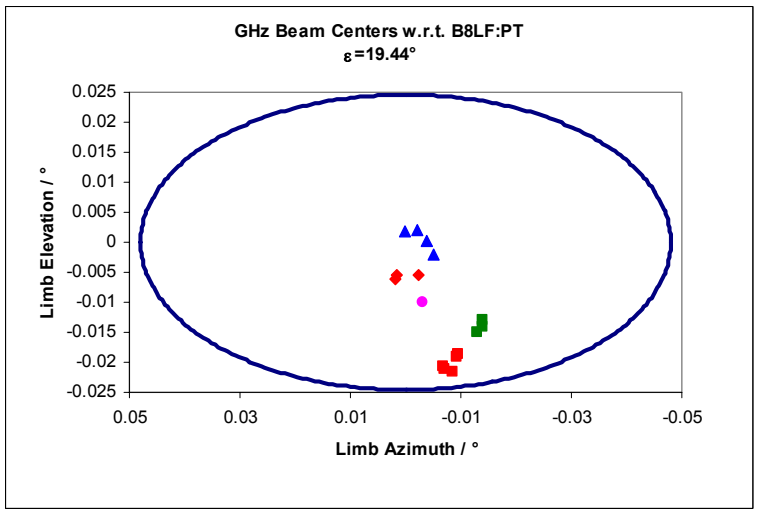

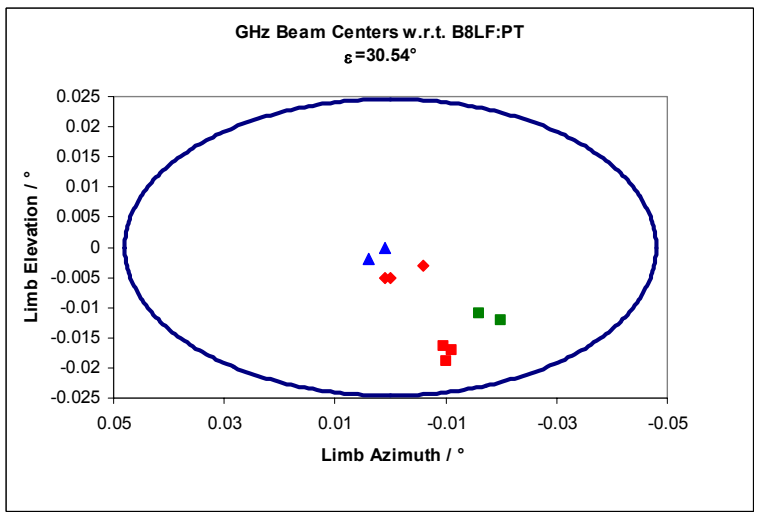

GHz FOV Calibration

Alignment Transformations

Entries in Tables 3.5.5-1a and b of Interface Control Document (TRW D26475 Rev.D) show compliance with alignment budget and establish shims between modules and observatory to meet SRD § 3.5.3.

			θxyz
GHz mounts to GHz Cube			/arcsec
0.9999997	-0.0003153	-0.0007003	-701.0
0.0003176	0.9999942	0.0033982	-144.5
0.0006992	-0.0033985	0.9999940	65.5

GHz mounts to B8LF:PT FOV			Yaw,Pitch,Roll / °
-0.0011029	0.9999962	0.0025098	90.06319
-0.4099517	-0.0027414	0.9121031	-0.14380
0.9121065	-0.0000230	0.4099532	65.79802

			θxyz
THz mounts to THz cube			/arcsec
0.9999777	-0.0046549	-0.0047956	-365.0
0.0046633	0.9999876	0.0017474	-989.2
0.0047874	-0.0017697	0.9999870	961.9

THz mounts to FOV direction measured 4-5 Dec.2002; data reduction TBD.

Changes in alignment angles through environmental test:

<30 arcsec for GHz, 74 arcsec for THz module: *meet 180arcsec allocation for Launch Vibration.*

Following will complete ICD tables before delivery:

- Error estimates
- Explanatory figure
- Y,P,R conversion to θx,θy,θz
- cube-to-boresight transformations derived from those given here.

GHz FOV Calibration

Calibration Requirement

- FOV Calibration Requirement [SRD §3.7.2]
- *The FOV response of the instrument shall be characterized sufficiently that its uncertainty does not introduce uncertainties in the forward model calculation of atmospheric/Earth radiances which, at the 90% confidence level, exceed:*
  - *3~Kelvin in the absolute value of the atmospheric/Earth radiances measured through each GHz spectral channel, and*
  - *1% or $\Delta I_{min}/3$, where $\Delta I_{min}/3$ is in Table 3.2-2 of the Science Requirements Document, in the spectrally-varying component of the atmospheric/Earth radiances measured from one channel or filter to another throughout a given radiometer.*

- Ancillary requirements for radiometric and spectral calibrations, imposed by in-flight calibration using Switching Mirror (GHz only):
  - Antenna Ohmic Loss
  - Baffle Transmissions
- Requirements are flowed down in Calibration Plan §4 and Appendix D.

GHz FOV Calibration

Baffle Transmissions and Antenna Reflectivities

- Transmissions calculated by propagating RFE patterns to ports (in near field) and integrating over port outlines
- Radiometric measurement of antenna ohmic reflectivities was described in PER. Similar surface treatments and UARS experience justify using Primary Reflector losses for all 3 antenna reflectors.

	R1A	R1B	R2	R3	R4
η **Limb**	0.99598	0.99344	0.99889	0.99929	0.99789
η **Space**	0.99587	0.99317	0.99890	0.99928	0.99788
(L-S)	0.00011	0.00027	-0.00001	0.00001	0.00001
ρ^1_r	0.99621		0.99736	0.99449	0.98819

- Transmissions will be re-calculated by band for delivery to the forward model. Ohmic reflectivities unchanged since PER.

GHz FOV Calibration

EOS MLS on Near-Field Test Range

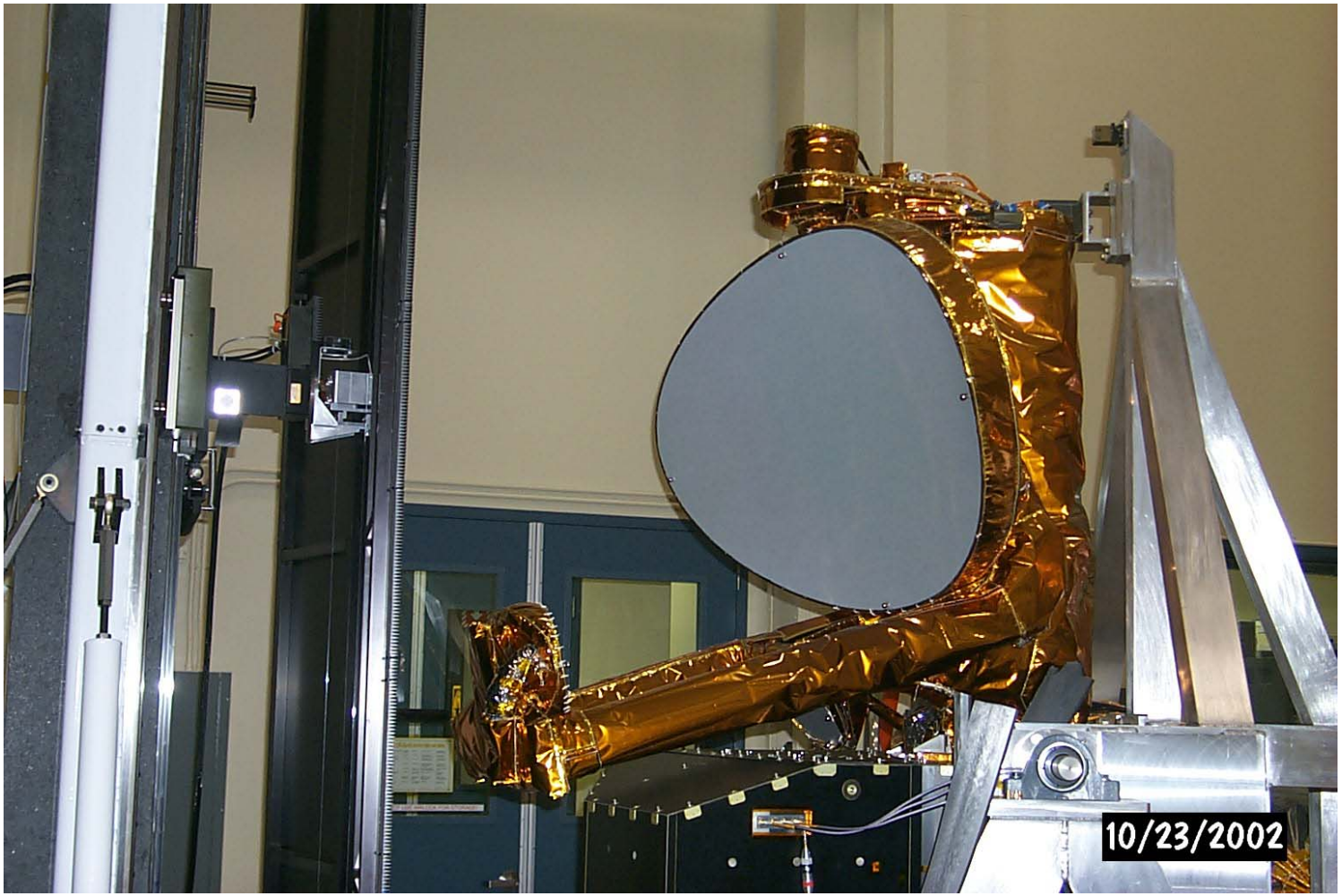

GHz FOV Calibration

Frequencies and Scan Angles Measured

- Pre-/post-environmental test comparison
  - R1A,B: 115.3, 118.8, 122.0 GHz
  - R2: 177.3, 183.3, 206.1 GHz
  - R3: 230.5, 233.9, 249.5 GHz
  - R4: 624.8, 649.5, 651.9, 660.0 GHz
- Definitive FOV calibration: same plus
  - R1A,B: 116.8, 118.1, 119.5, 120.8 GHz
  - R2: 181.6, 201.0, 204.4 GHz
  - R3: 243.6, 235.6, 245.4, 248.8 GHz
  - R4: 625.9, 633.5, 635.9 GHz
- Scan angles for definitive FOV calibration:
  - 19.4 °,24.2 °,25.8 °,30.5° from xy plane

GHz FOV Calibration

R4 FOV Repeatability through Environmental Tests

Limb V

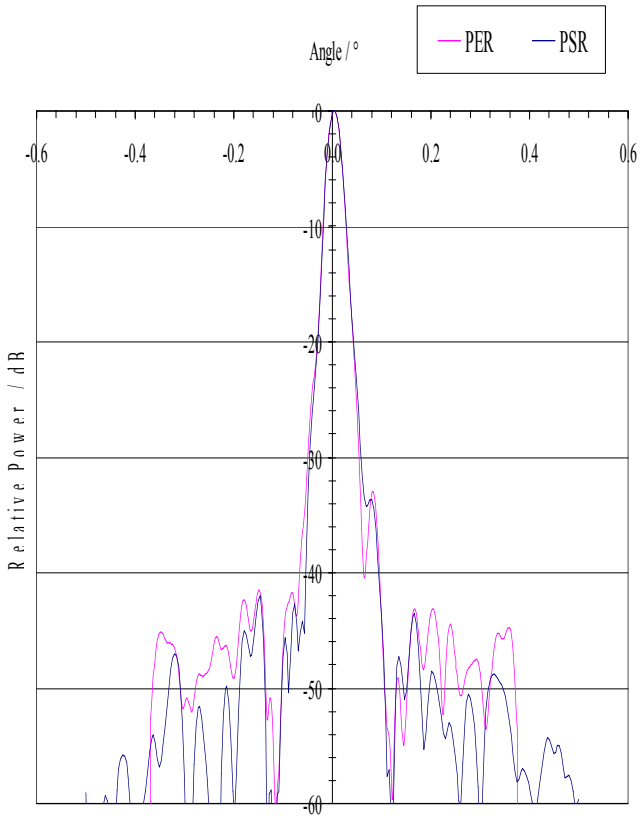

Limb H

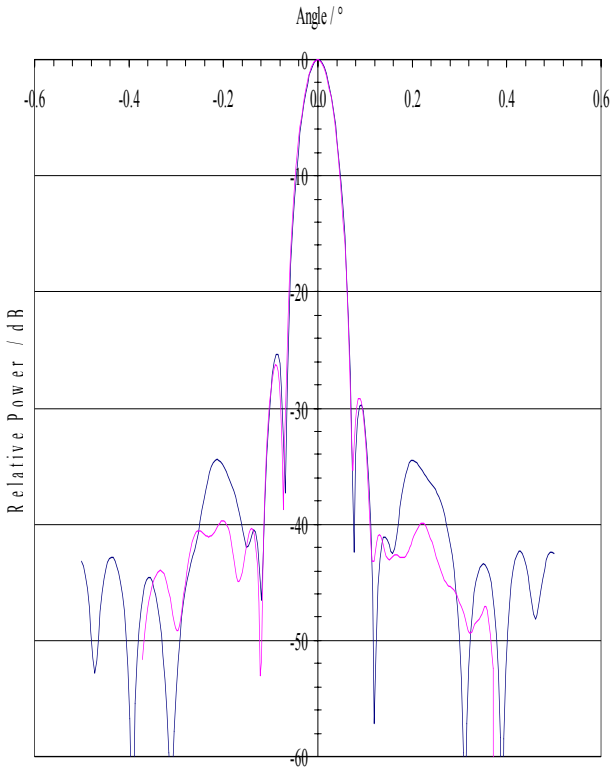

Sidelobe differences due to test equipment artifacts will be removed in delivered FOV functions.

GHz FOV Calibration

R4 FOV Variation with IF

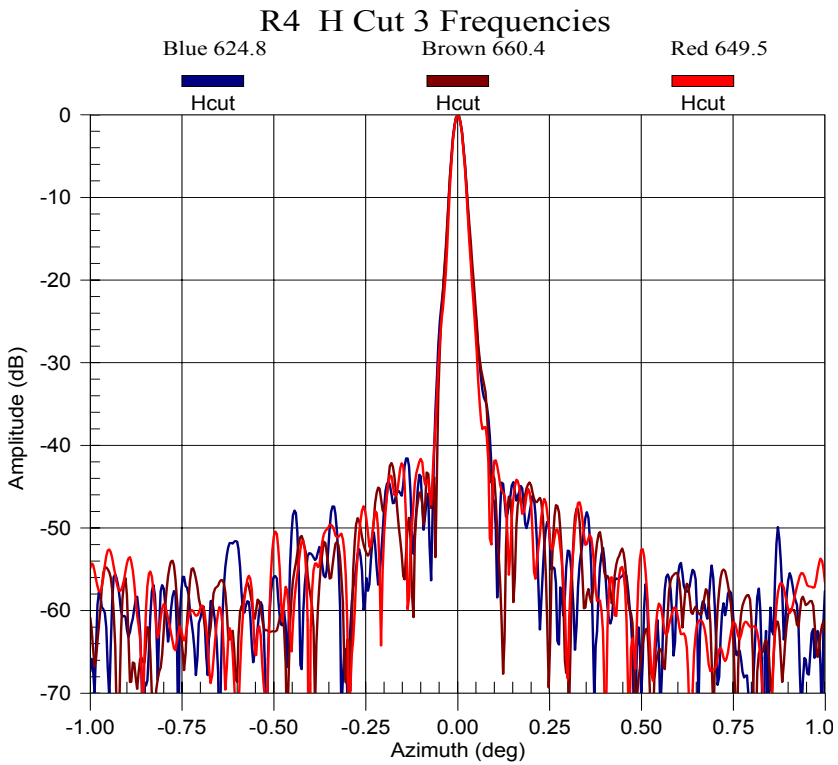

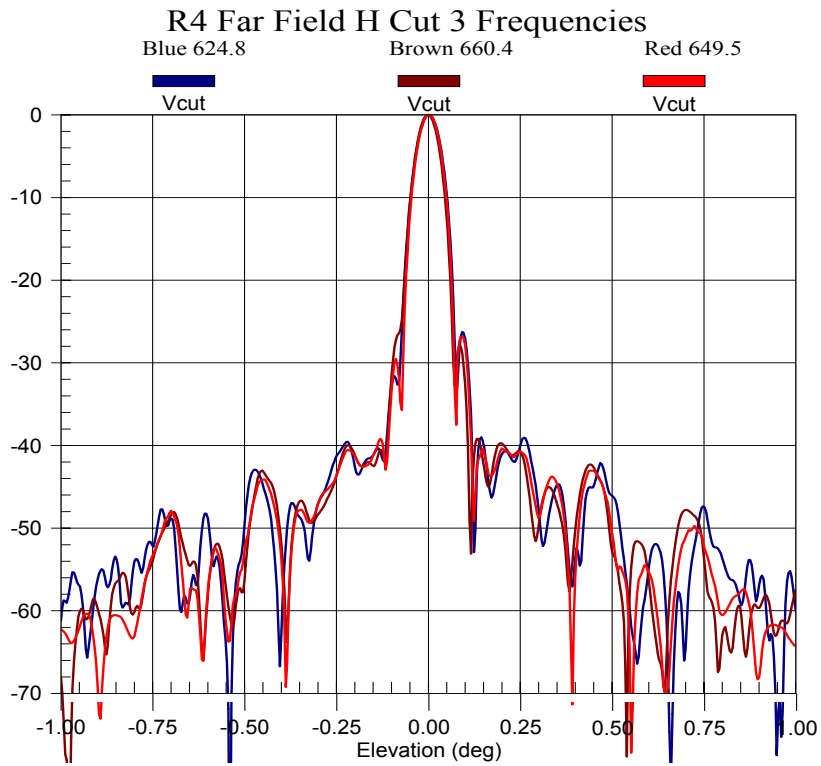

Variations with IF are similarly small for R1-R3.

GHz FOV Calibration

R3 FOV Variation with Scan Angle

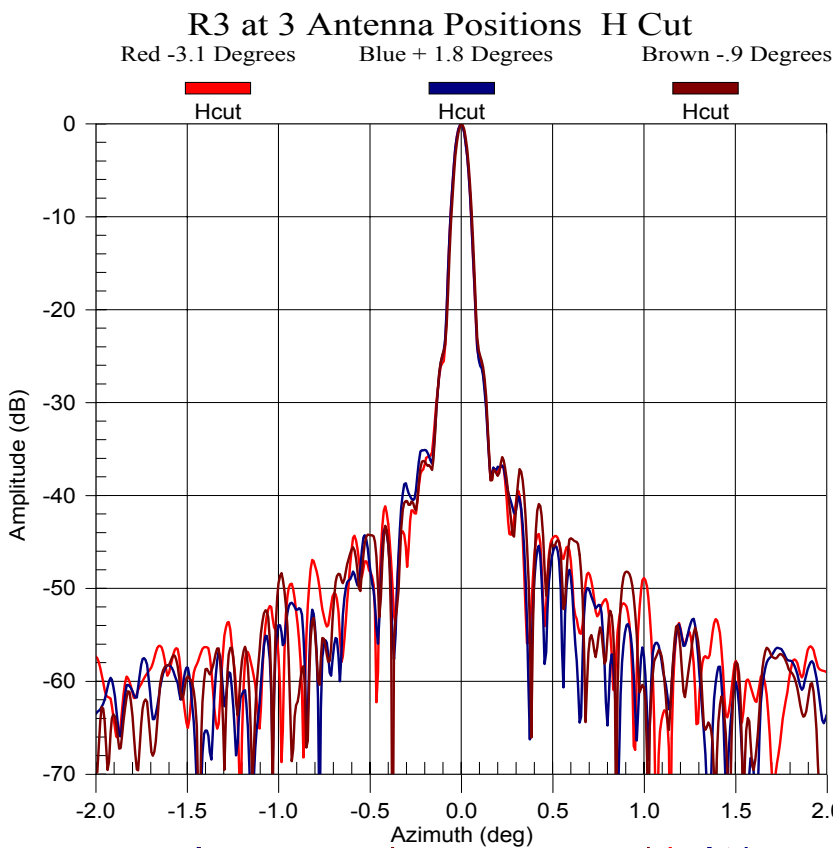

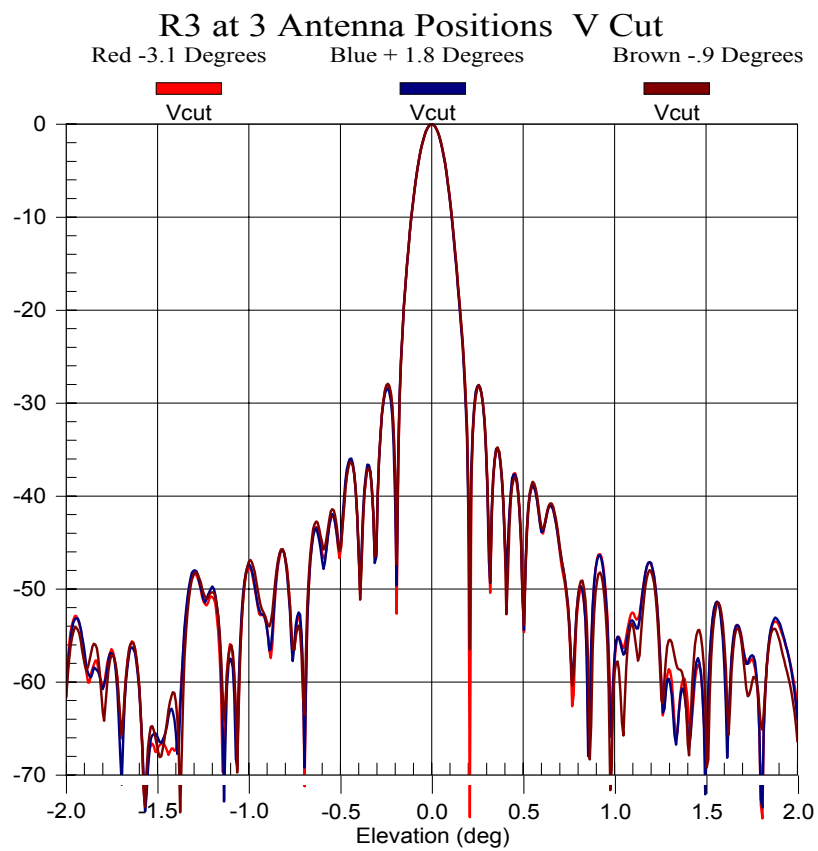

Patterns overlaid at boresight; theodolite and Encoder data included previously.

FOV variation with scan angle meets performance requirements and is expected to meet calibration requirement when treated as an FOV knowledge error component.

GHz FOV Calibration

Collapsed FOVs
(deliverables to forward model)

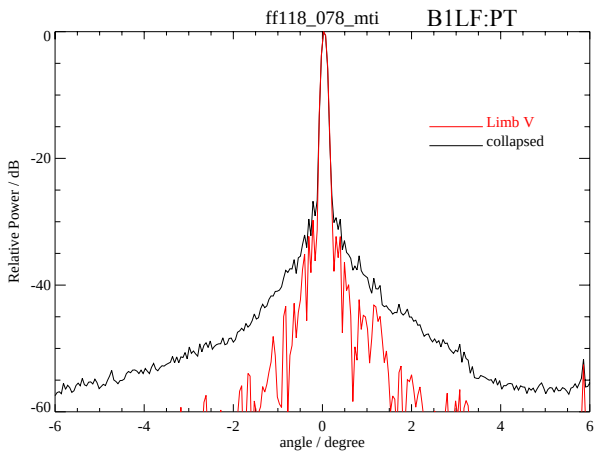

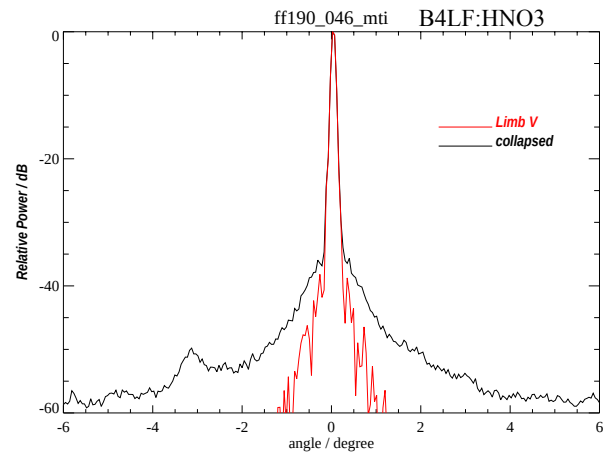

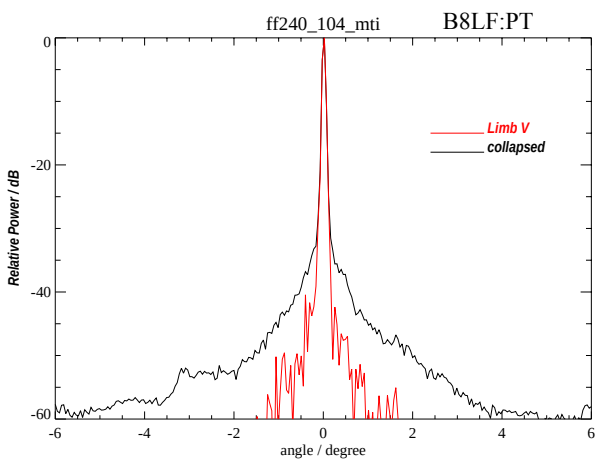

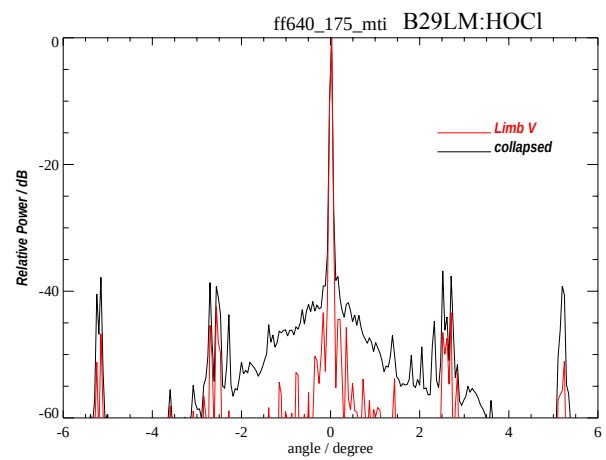

Spikes in R4 are due to test equipment artifacts and will be removed for Cal. Report.

GHz FOV Calibration

Method to Prove Compliance with FOV Calibration Requirement

- Radiance kernels $T_B(h_T)$ have been computed with a forward model, for convolution with far-field patterns .
- Measured FOVs are perturbed within bounds established by a grid of known frequencies and scan positions; then convolved radiances are tested against SRD requirements. This validates previous estimates of numbers of frequencies and scan positions to be measured.
- Patterns are measured over a small fraction of 4π solid angle (±0.1 radian≈5.7° semi-cone) about boresights of GHz FOVs. Analytical models provide bounds on envelope of sidelobes outside these ranges.

- Compliance matrix will be completed in Calibration Report.

Remaining Issues to be resolved in Calibration Report

- Complete reconciliation of NFR patterns with analytical models and subsystem performance data.
- Deliver FOV calibration datasets and error estimates to science team.
  - Team has used pre-environmental patterns during last 9 months of software development.
- Repeatability tests show R4 tripler changeout would have minor effect on R4 FOV calibration. Worst-case changes can be accounted for by limited subsystem characterization (RFE patterns) before delivery for integration on AURA observatory .

Deliverables to Forward Model

- Patterns, FOV directions, antenna losses and efficiencies were discussed above.

- Quantities related to polarization:
  - Cross-polarized aperture fields are much lower than in UARS (<-30 dB w.r.t. || pol…perhaps due to location of polarizing grid).
  - Relative phase of || and ⊥ pol patterns (each a complex function) could not be measured on either Near Field nor Far-Field (feed pattern) Ranges. These numbers will be calculated from horn pattern models and propagated to the far field in deriving $G_{||}$, $G_{\perp}$, $G_{|}$ and $G_{\circ}$.
  - Polarization angle ξ was measured for all bands in definitive calibration; final numbers await characterization of the near-field probes.

- Scan dependences of FOVs are small enough to be treated as contributors to FOV knowledge error, i.e. we expect to include them and still meet the FOV calibration requirement.

GHz FOV Calibration

Conclusions

- Changes in FOV through environmental tests are all within allocations, and performance requirements continue to be met.
- Science team has reviewed FOV calibration deliverables:
  - Pre-Environmental dataset has been adequate for forward model calculations since its delivery May 2002.
- FOV Calibration dataset is complete and of sufficient quality to prove that calibration requirement is met.
- GHz module is ready to ship without further system FOV calibration.

Pre-Ship Review

THz Performance and Calibration

Verification of THz Science Requirements

Herbert M. Pickett

JPL

December 17-18, 2002

THz Performance and Calibration

Overview

- Radiometric Accuracy Considerations
- Radiometric Calibration
- Sideband Sensitivity Calibration
- Single Sideband Sensitivity
  - Double sideband performance measured with loads at two temperatures
  - Correct double sideband performance to single sideband sensitivity based on sideband measurements
- FOV Calibration
- FOV-related performance requirement verification

Note: Verification of THz Science Requirements described during description of performance calibration

THz Performance and Calibration

Radiometric Accuracy Considerations

- No radiometric correction for insertion losses are needed since Scan Switching Mirror is first optical surface
- No space-view baffle correction is needed since space view is from same port as limb view
  - Aperture in THz module is oversized in the vertical by $\pm 6^{o}$ compared with 2.8^{o} difference in scan angle between space view and view to surface of the Earth
- Ambient calibration target has paint with measured 94% THz absorptivity for single reflection
  - Ribbed mechanical design assures at least 2 reflections giving 99.6% emissivity and meets requirements
  - Target is oversized with respect to the primary to avoid additional corrections
- Cannot measure of linearity in the THz module
  - Infer from GHz measurements of backend linearity
  - Linearity of Response is less of an issue because T_{sys} is larger (300 K DSB signal is 2% of total filterbank signal)

Radiometric Calibration in Level 1 Processing

- Use data from an entire 'orbit' (~100 min) to fit space views and calibration target views to radiometric gain (counts/K) and local oscillator power derivative (counts/mW)
  - Local oscillator (GLLO) variations can be large compared with radiance variation and can vary on timescales smaller than a MAF (24.67 sec)
  - Mixer bias voltage reported by laser telemetry each MIF is a good surrogate for GLLO power and is the quantity used in the fit
  - Counts are corrected to average GLLO power and then divided by radiometric gain to give an intermediate result that has a large offset
- Using data for each MAF, fit the offset for the calibrations to their brightness temperature using a quadratic fit to nearby calibrations
  - Similar to GHz except that GLLO re-optimize events break the continuity of the offset every 5 min and the fit has to be restricted to calibrations that are part of the same continuous GLLO segment
- Level 1 processing procedure has been tested and validated during I&T

THz Performance and Calibration

Example of Radiometric Calibration

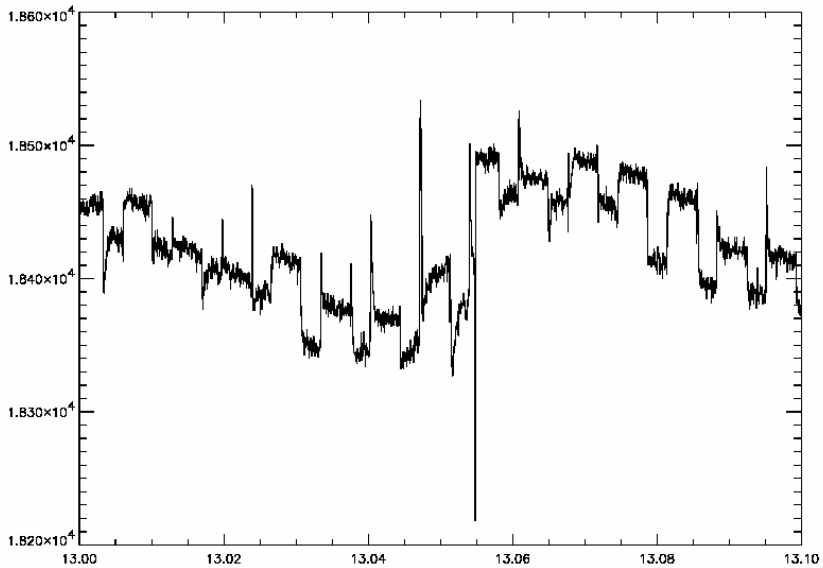

Raw Counts

Calibrated Radiance (K)

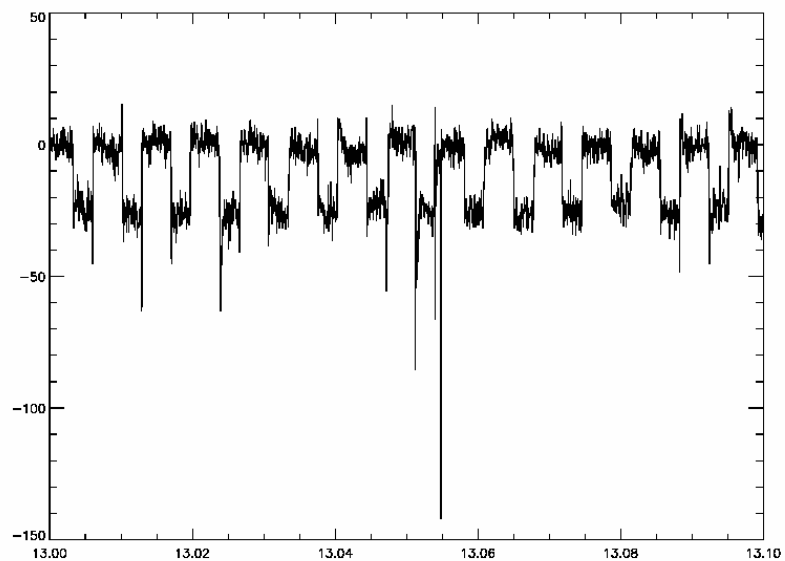

Test Configurations

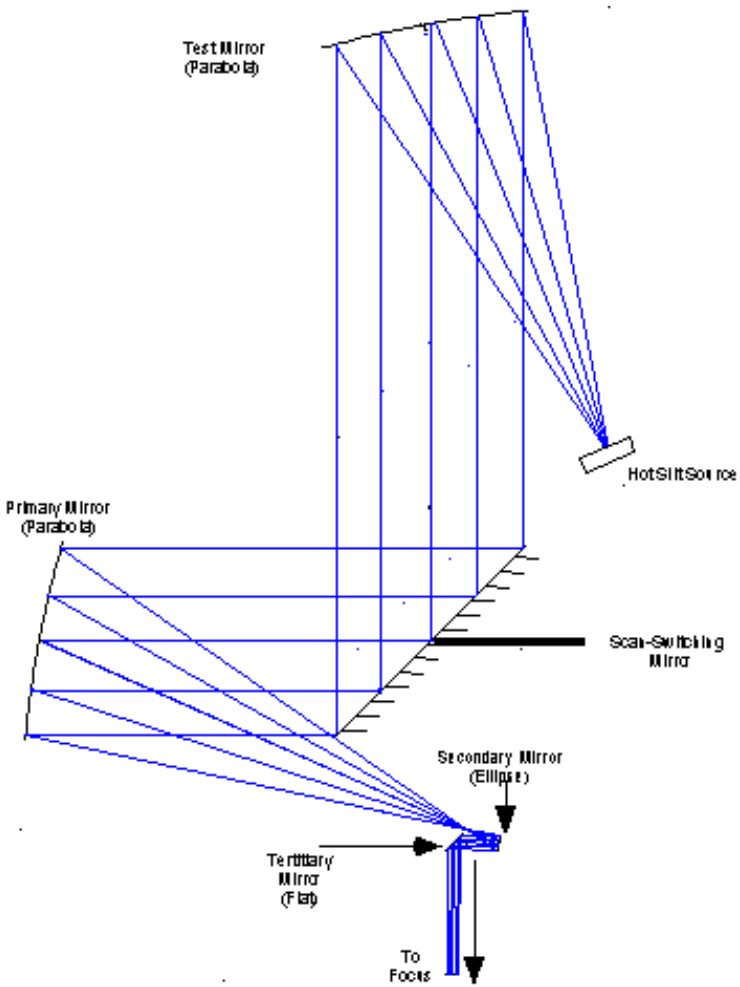

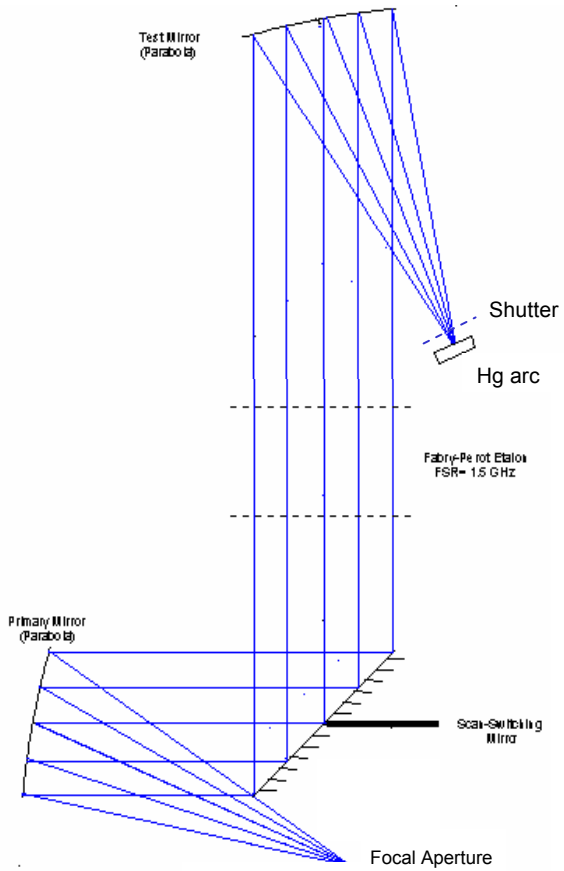

Sideband Calibration Method

- Uses FILOS Fabry-Perot Etalon that has a free spectral range of 1500 MHz and a width of 12 MHz and can be scanned over more than a wavelength with an accuracy of 3 MHz
- Measure 5 sec with shutter open, 5 sec with shutter closed, step Fabry-Perot separation by 0.5 μm, repeat once, then move to ambient target for 2 sec, re-lock LLO if needed and repeat for 193 steps.
- Correct signal power variation using ambient target
- Take difference of shutter open/close averages

THz Performance and Calibration

Raw Sideband Data

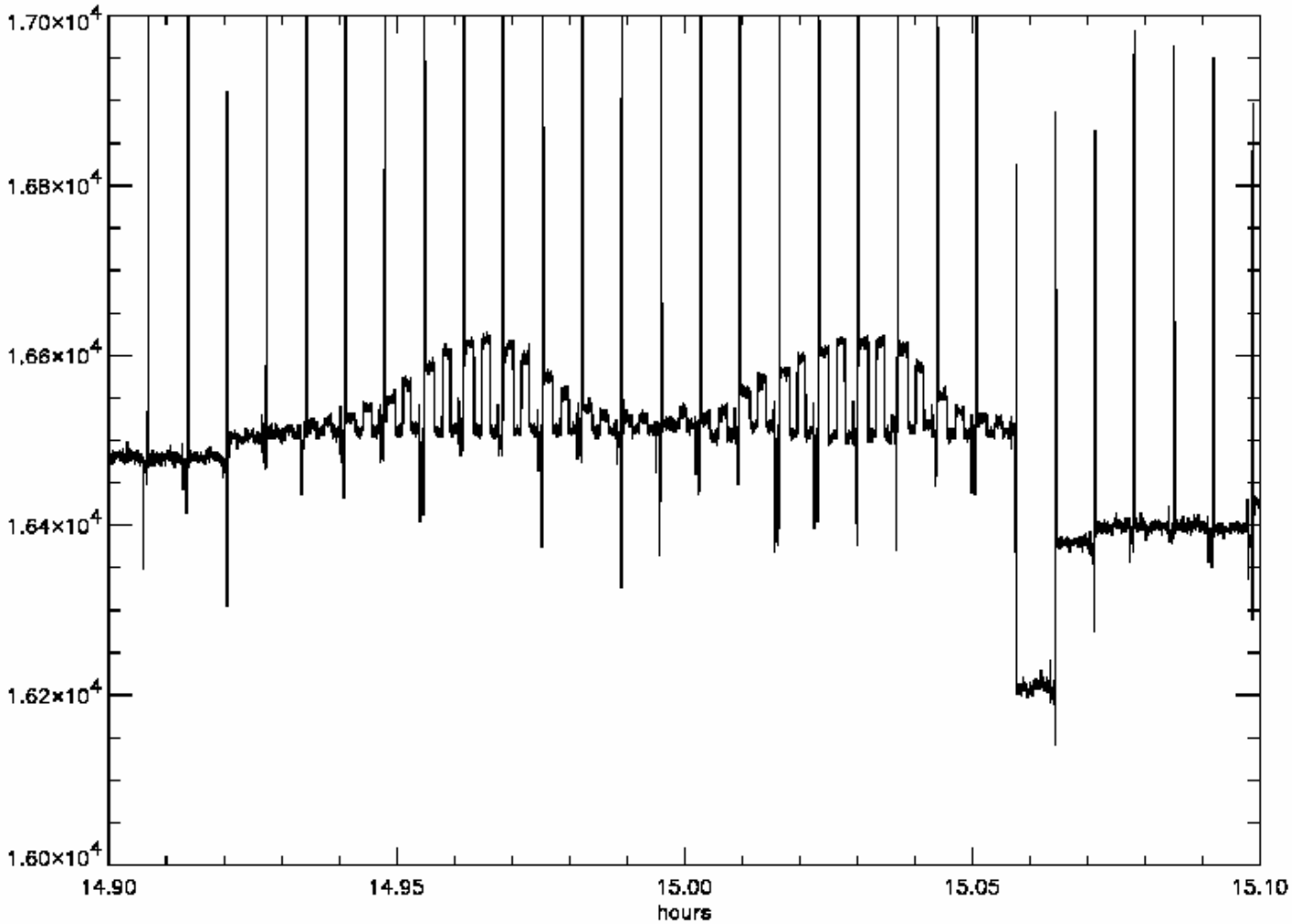

Sideband Fitting Program

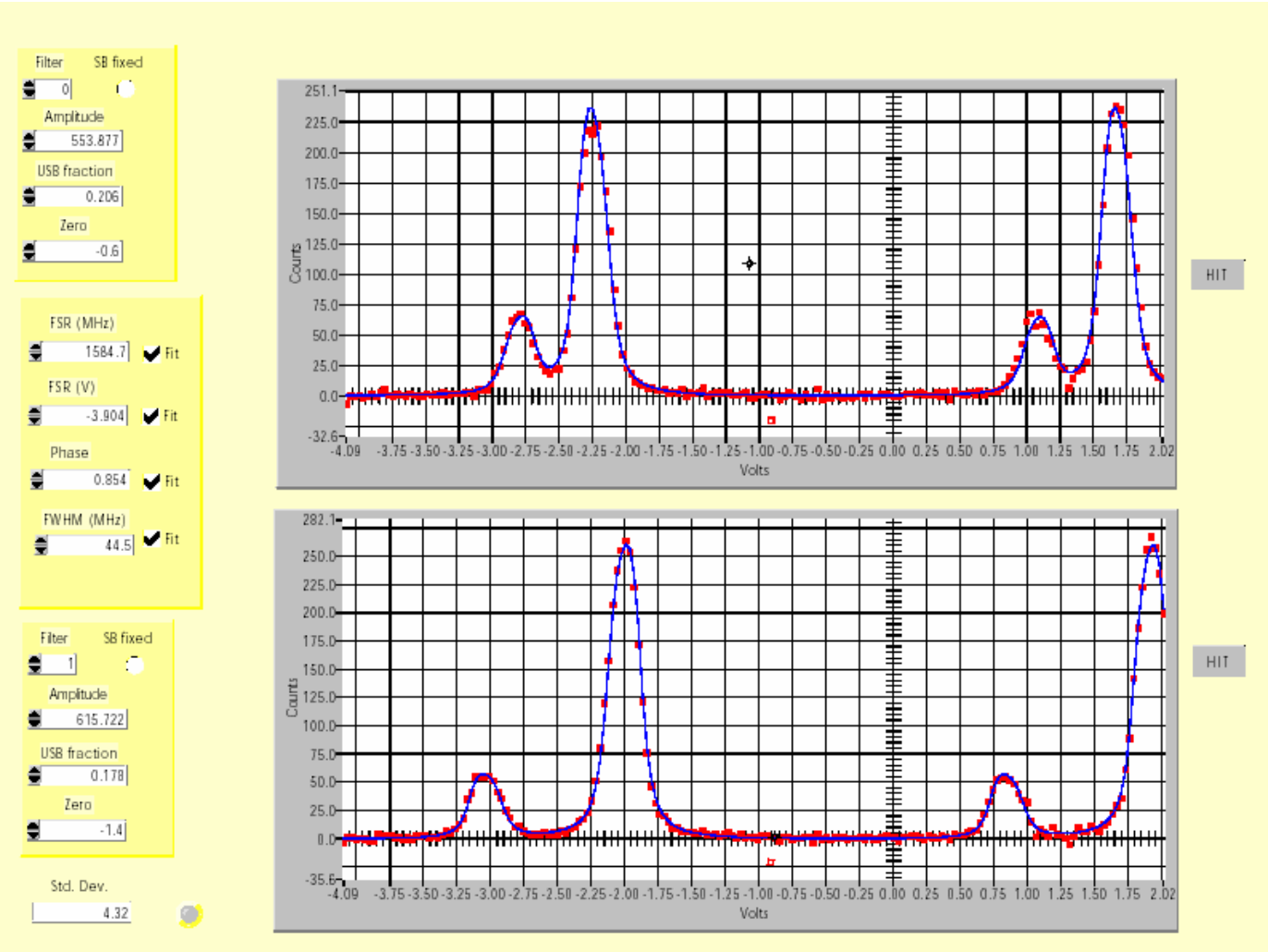

THz Performance and Calibration

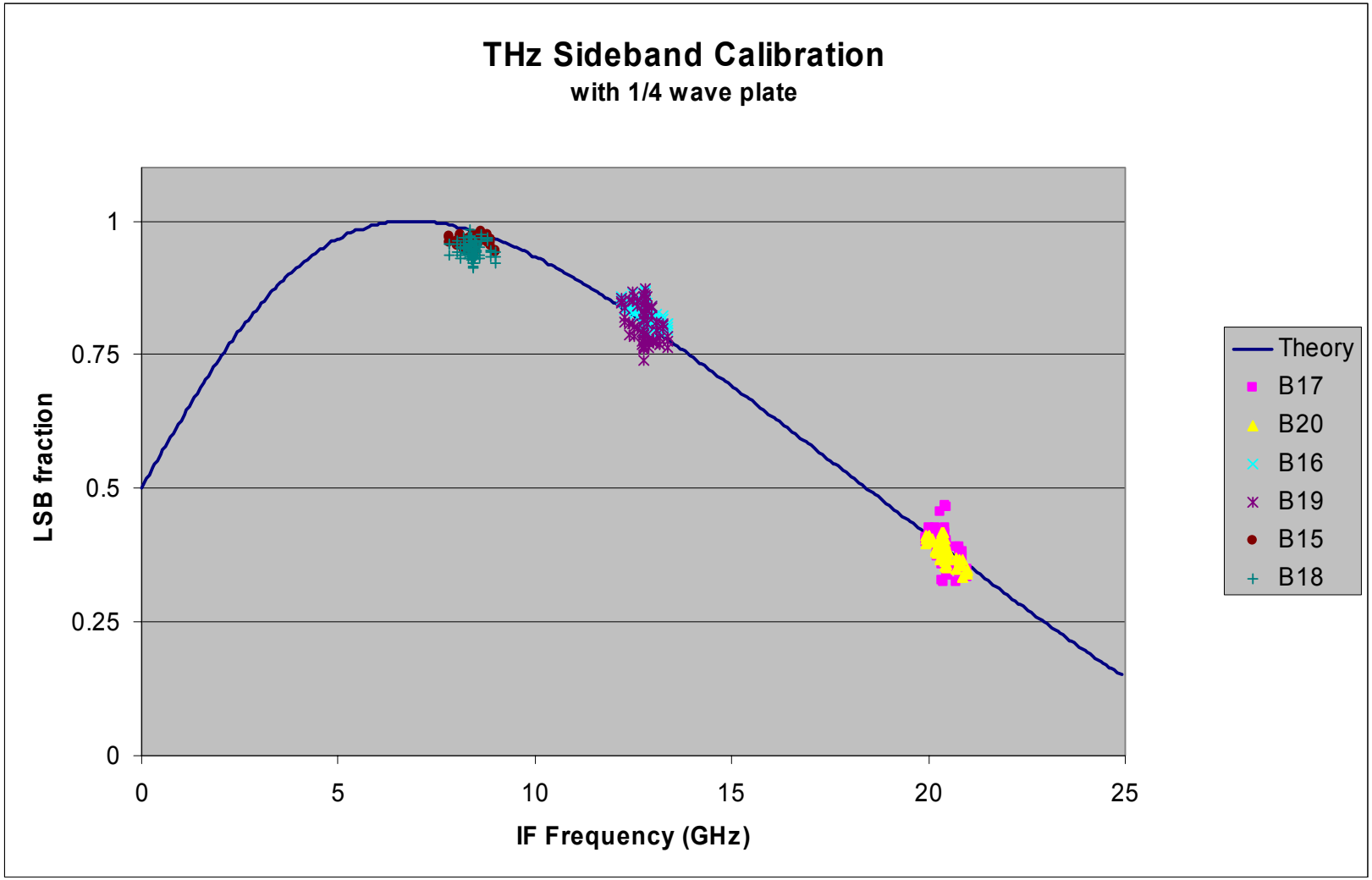

THz Performance and Calibration

Zoom in On Sideband Result with ¼ Wave Plate

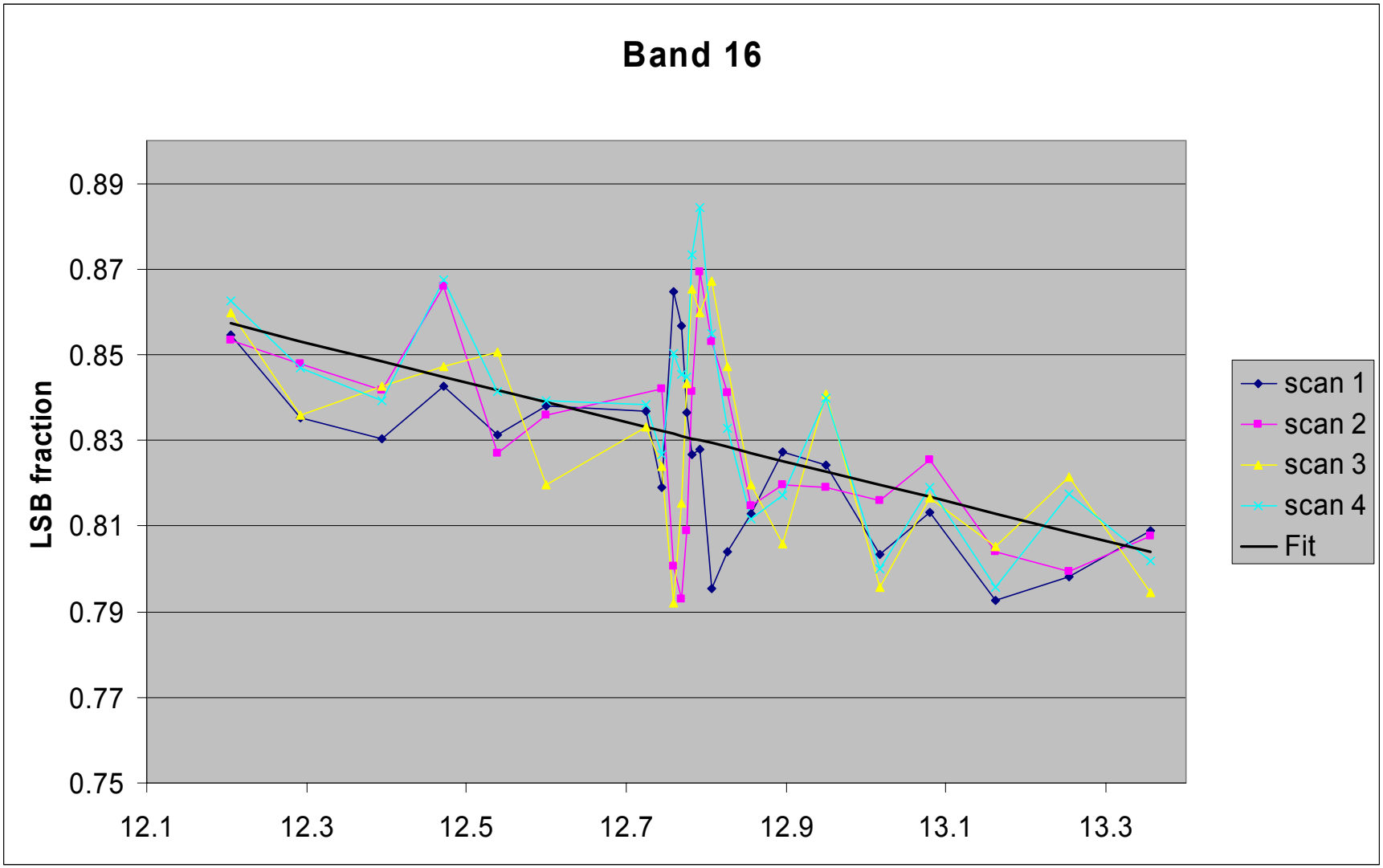

THz Performance and Calibration

Summary of Sideband Results

Band	LSB fraction	RMS error	slope * GHz	RMS error
Band 15 (OHa-H)	0.960	0.0010	-0.0053	0.0038
Band 18 (OHa-V)	0.948	0.0017	-0.0027	0.0066
Band 16 (OHb-H)	0.831	0.0019	-0.0463	0.0067
Band 19 (OHb-V)	0.812	0.0032	-0.0473	0.0113
Band 17 (O2-H)	0.390	0.0031	-0.0620	0.0123
Band 20 (O2-V)	0.383	0.0016	-0.0619	0.0064

- Analysis:
  - Fit Center Band Sideband Fraction and Slope
  - Center fraction and slope is given above along with estimated error
- ¼ wave plate used to suppress standing wave is essential
  - No evidence of 200 MHz standing wave previously observed
  - Scatter at center of the band due to radiometric noise and sparse scan sampling
- Sideband errors scale with radiance
  - Contribution to pointing and high altitude OH scales with fractional error
  - Contribution to low altitude OH scales with fractional error X 5
- Sideband measurement uncertainty better than 0.4%

THz Performance and Calibration

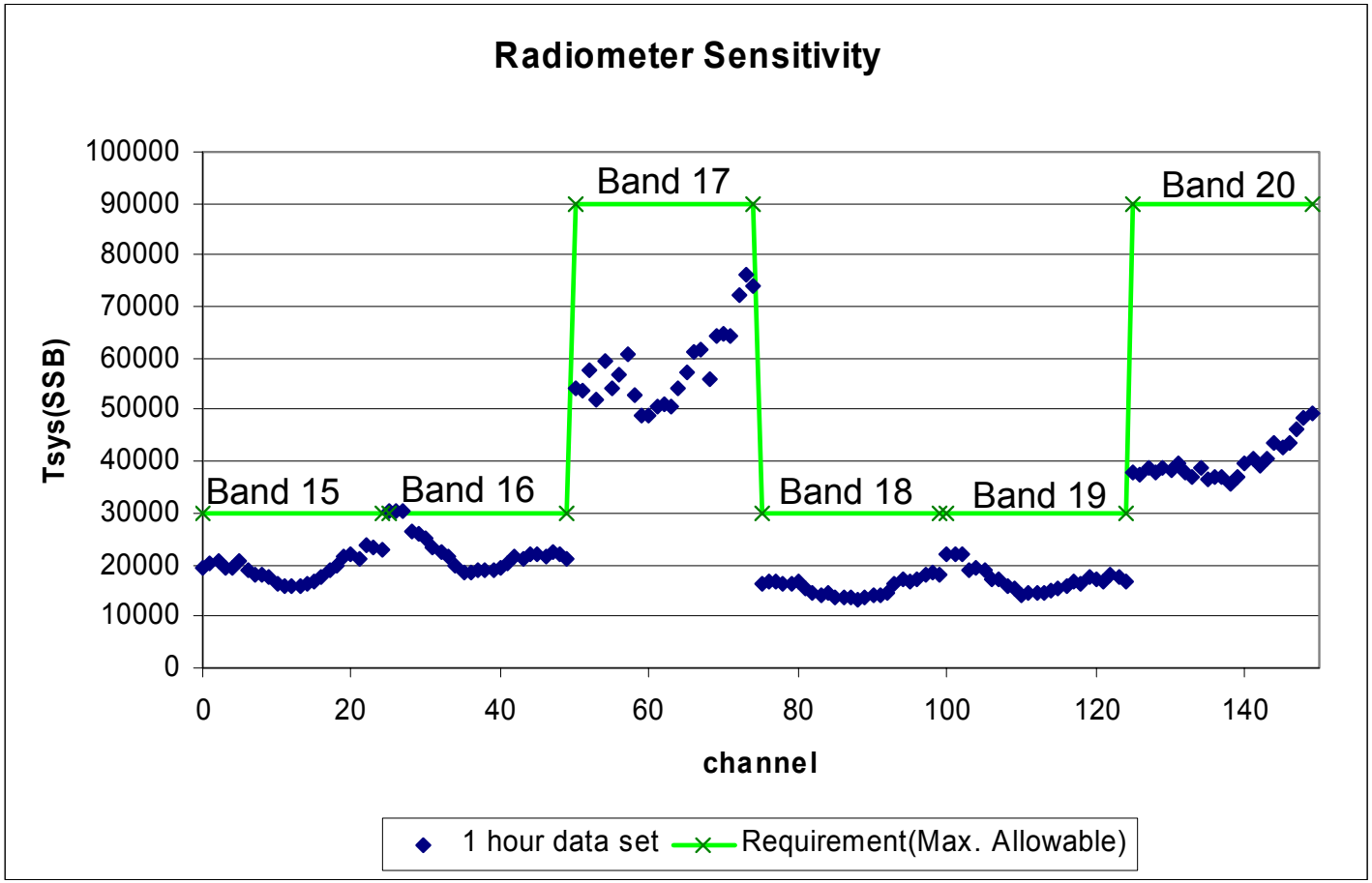

All THz Radiometers meet T_{sys} and ΔI_{min} Requirements (data taken on 12/08/2002)

FOV Calibration

- Measurement Technique:
  - FOV Determined from Compact Range with Incoherent Hg Arc Source
    - Uses a 0.216 mm slit (0.0206^o angular extent)
    - Measure 3 overlapping one dimensional patterns of ~1° extent for ± 1.3^o total
    - Each pattern includes an ambient target view and a view at the boresight angle
- Analysis:
  - Observed pattern can be deconvolved with the slit function and with the averaging effect of the continuous scan using the Fourier transform of the pattern
  - The Fourier transform is the one-dimensional autocorrelation function of the aperture field distribution
  - Can truncate to ± primary diameter and check for power outside the limits
  - Slit is chosen so that its sinc has no zeros and only decays to 0.45
  - Pattern is sampled at 0.01^o intervals so that the Fourier transform extends beyond the primary diameter
  - Use of a continuous scan at this sample interval produces a second sinc that decays to 0.82

THz Performance and Calibration

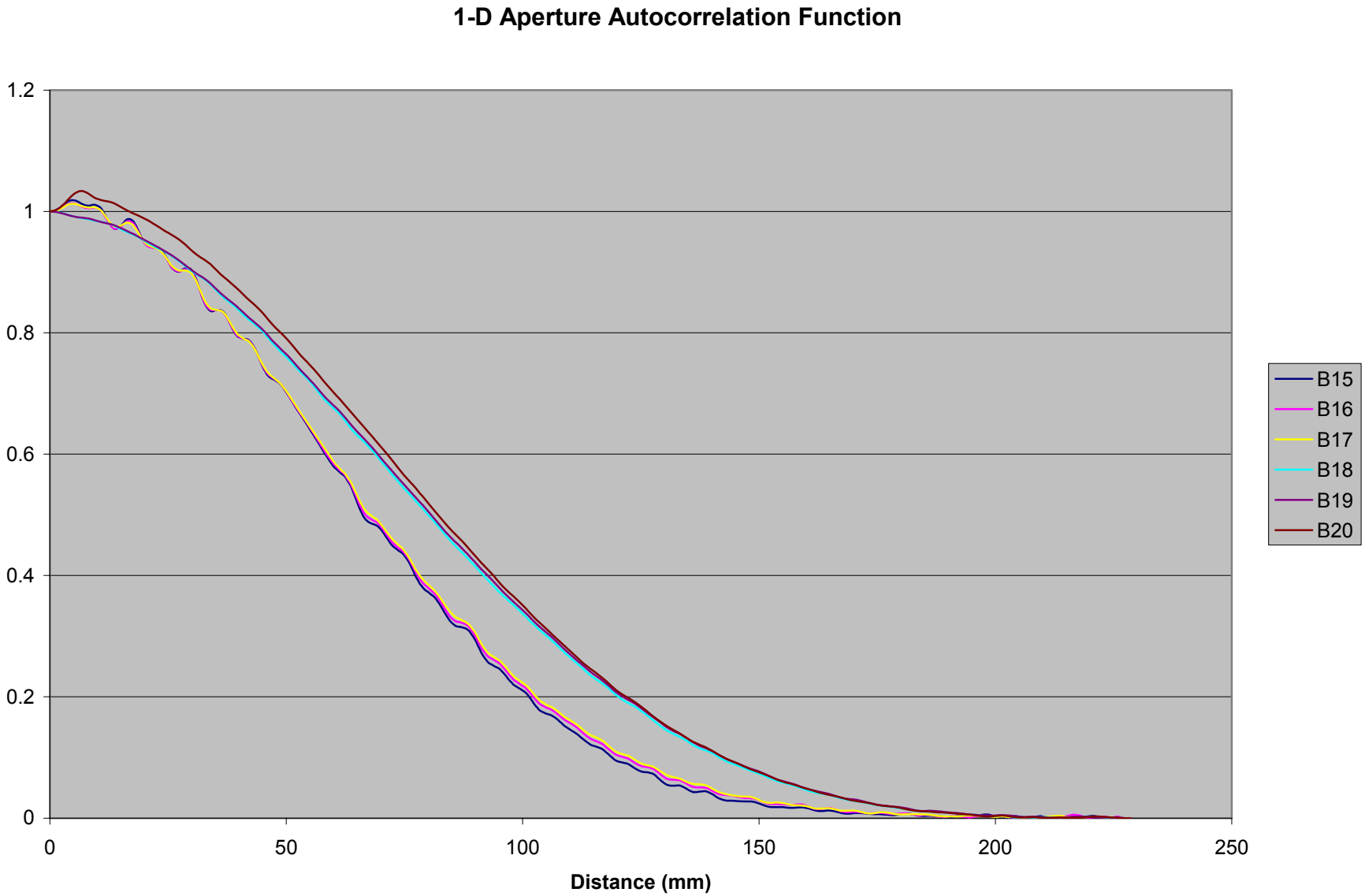

THz Performance and Calibration

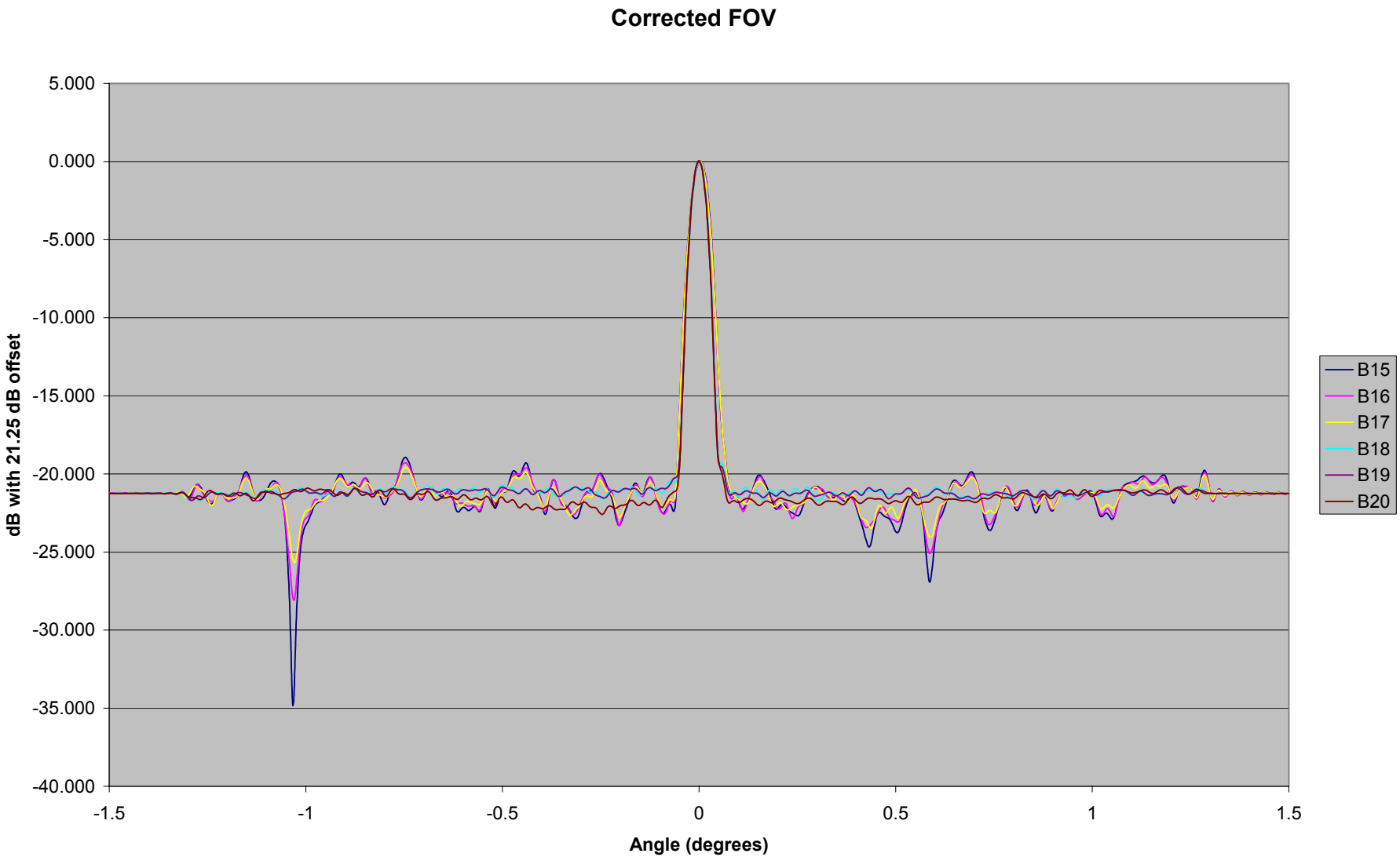

THz Performance and Calibration

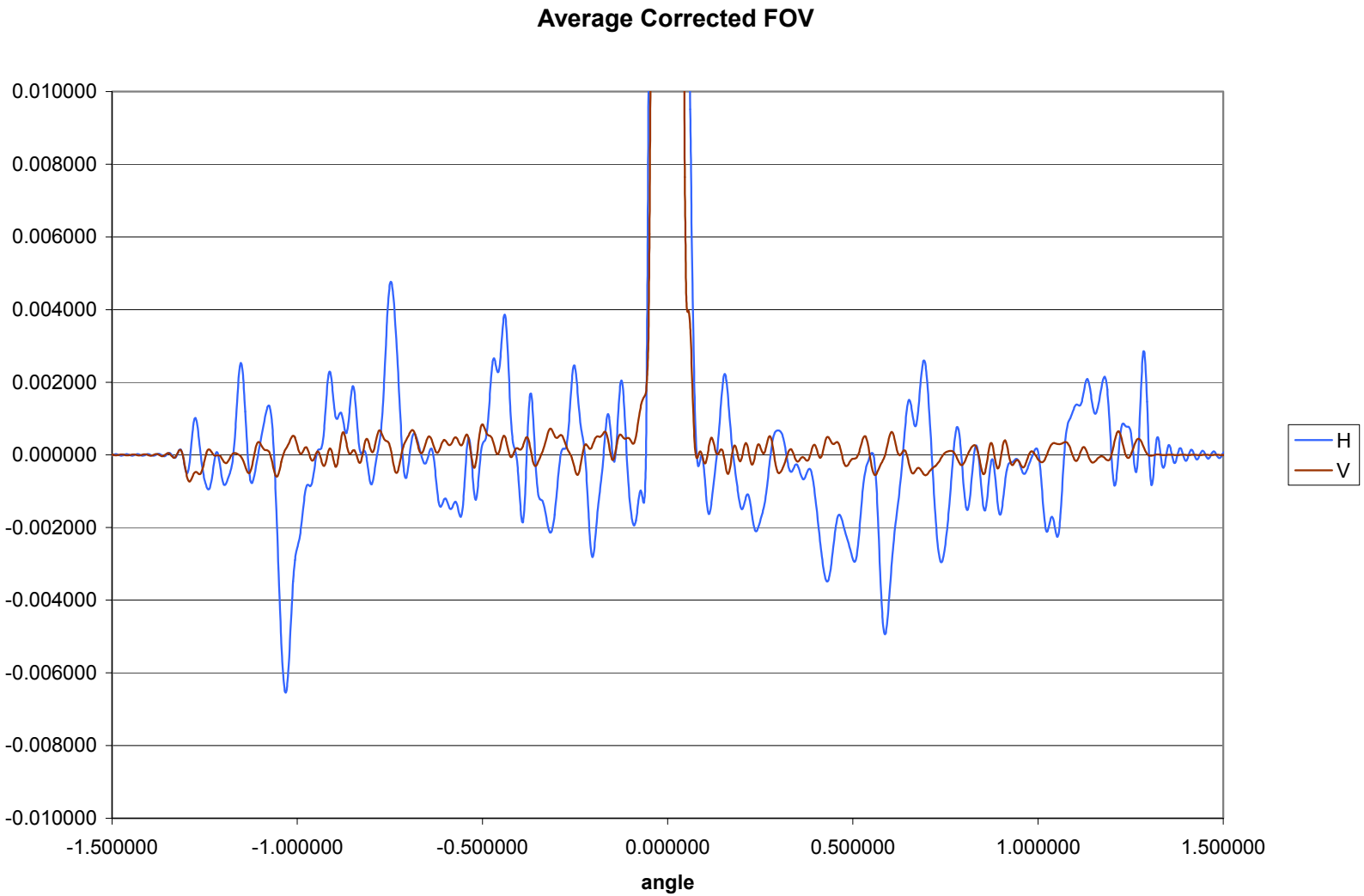

FOV Calibration Summary

- FOV determined to –21 dB noise floor
  - Reality of negative sidelobes in H polarization pattern questionable but to exclude them would require objective criterion for rejecting positive sidelobes
  - Can compare separate retrievals of OH for the two polarizations
- This measurement meets the intent of the Science Requirements and is the best we can do with this type of compact range

Optical vs RF Boresight

- Center visible light in MLS THz focal aperture using TV camera
  - Result is $-1.05^{o} \pm 0.01^{o}$
- Measure center of FOV pattern in air and fit to Gaussian down to –5 dB
  - Result is $-1.0679^{o} \pm 0.0002^{o}$ for H mixer and $-1.0671^{o} \pm 0.0006^{o}$ for V mixer
  - Uncertainty is the band-to-band scatter for each mixer
- Differences are within alignment precision and corresponds to 0.95 km on limb
- Meets Science Requirement of 1.3 km knowledge
  - Measurements include optical survey of boresight in relation to spacecraft mount points that have 10 arc second accuracy

THz Performance and Calibration

FOV-Related Performance Requirements

- Performance determined from FOV calibration
- Optical boresight based on position of primary focal aperture determined with respect to optical cubes to an accuracy of 10 arc sec (0.15 km on limb)
- THz boresight measured with respect to optical boresight in the vertical with an accuracy of 0.5 km on limb (measured difference is 0.95 km)
- Overall budget meets relative vertical boresight knowledge requirement of 1.3 km
- Relative vertical boresight of H polarization to V polarization is 0.037 ±0.01 km (requirement = 1.3 km)
- Vertical width of pattern is < 2.4 km (H pol.) and < 2.1 km (V pol.) ± 0.02 km (requirement = 2.5 km)
- Horizontal FOV requirements met by analysis
- Beam efficiency is 100% ± 2% vs. requirement of 95%

Conclusions

- All required Pre-ship calibrations have been performed to necessary accuracy
- All calibration requirements are met with current instrument configuration
- All performance requirements are met

Bill Read's Summary has been moved to the beginning of this document

Topic 2

Comparisons of results from ‘other’ forward models and MLS production forward model

Comparison of two forward models for EOS MLS

Hugh C. Pumphrey

Institute for Meteorology

School of Geosciences

The University of Edinburgh

What does the Forward model *do*?

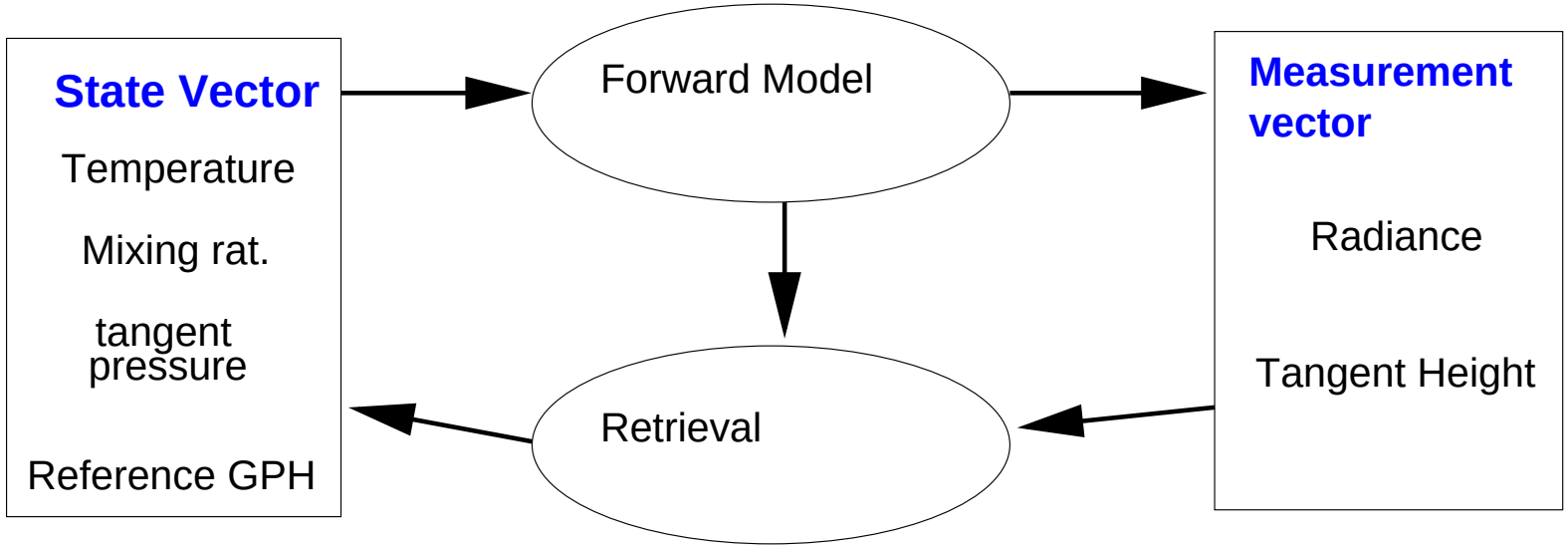

What does the Forward model *do*?

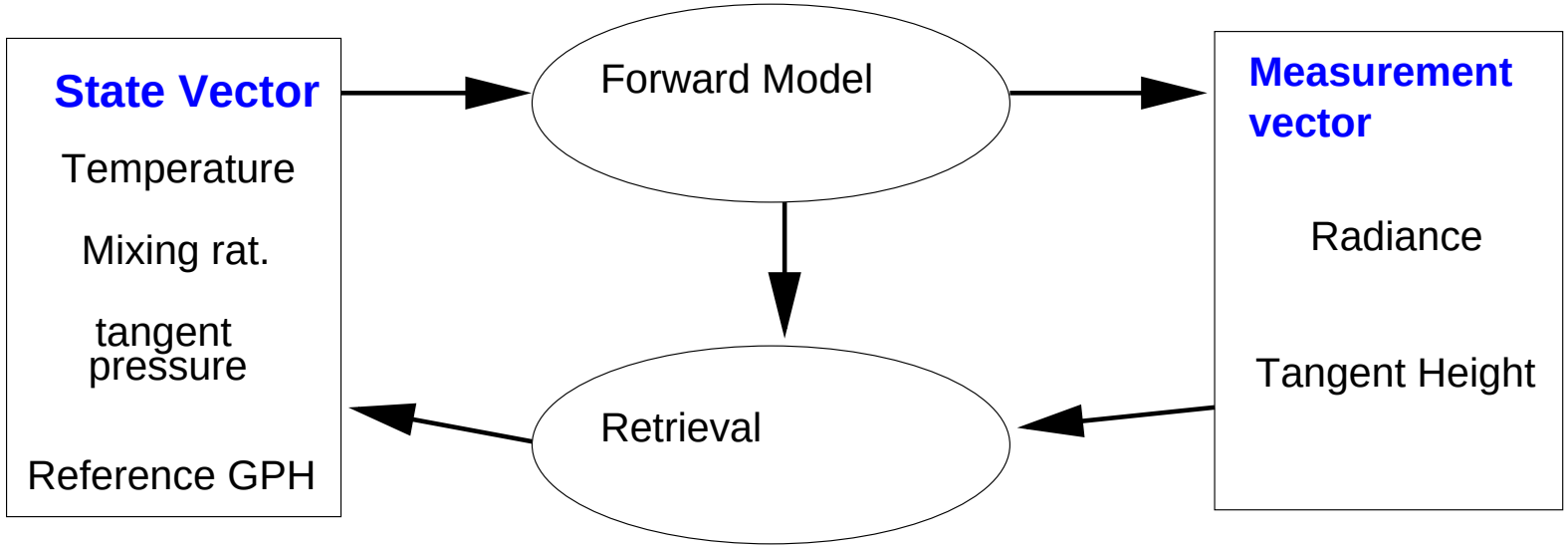

- It calculates what the instrument would measure, for a given atmosphere.

What does the Forward model *do*?

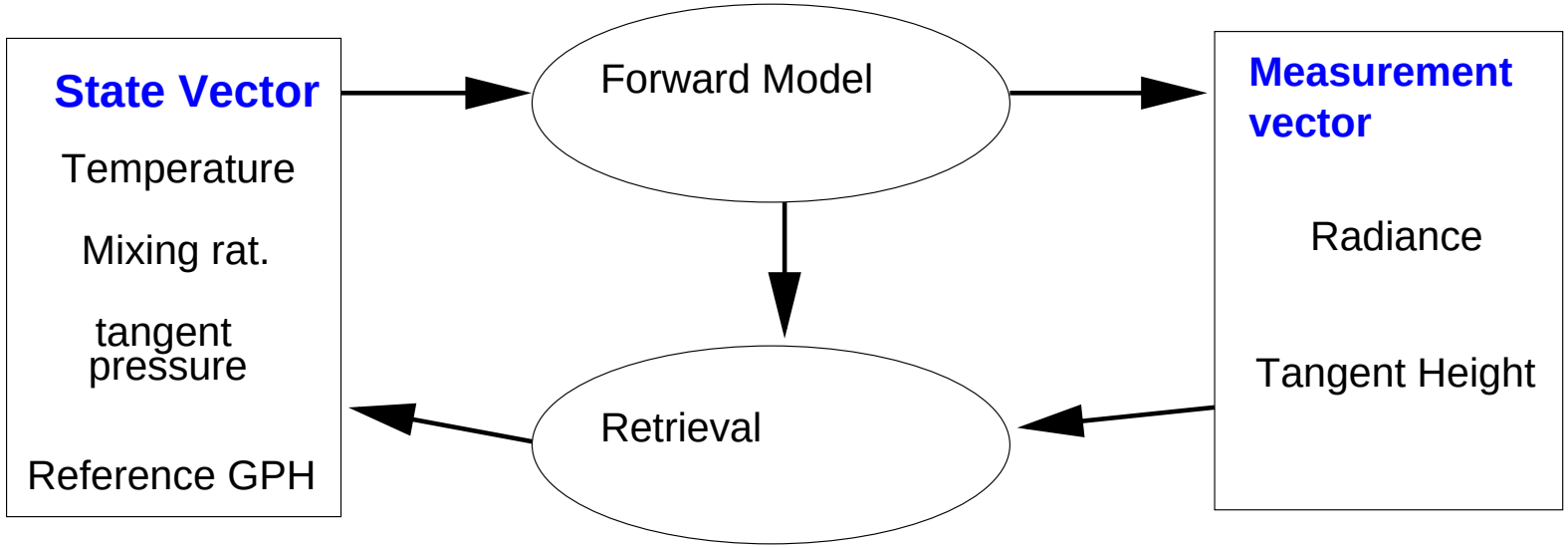

- It calculates what the instrument would measure, for a given atmosphere.
- This is necessary step for us to infer the state of the atmosphere from the measurements

The Two Forward Models

- The JPL forward model
  - Written by Bill Read.
  - Used in the operational retrieval.
  - 2-D (Can model line-of-sight gradients)
- The University of Edinburgh (UoE) forward model
  - Written by me, Hugh Pumphrey
  - Used by UoE for our own retrievals
  - only 1-D (assumes homogeneous atmosphere for any one scan)
  - …so JPL FM is run in 1-D mode for comparisons

Plotting example: Antenna motion

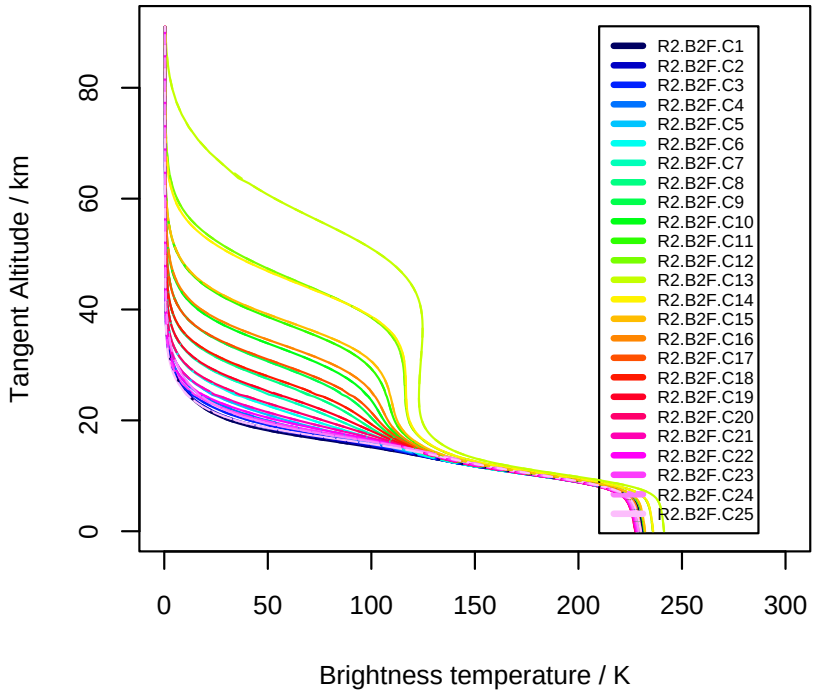

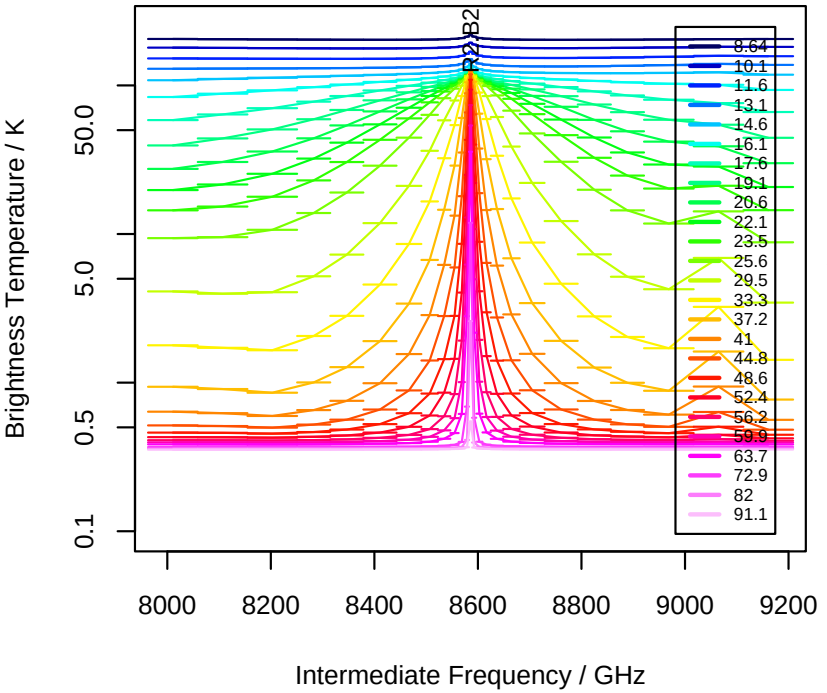

Pretending that the antenna does stop and stare, when it really moves continuously, gives errors of about 0.05 K, just as Bill said. For this band, anyway …

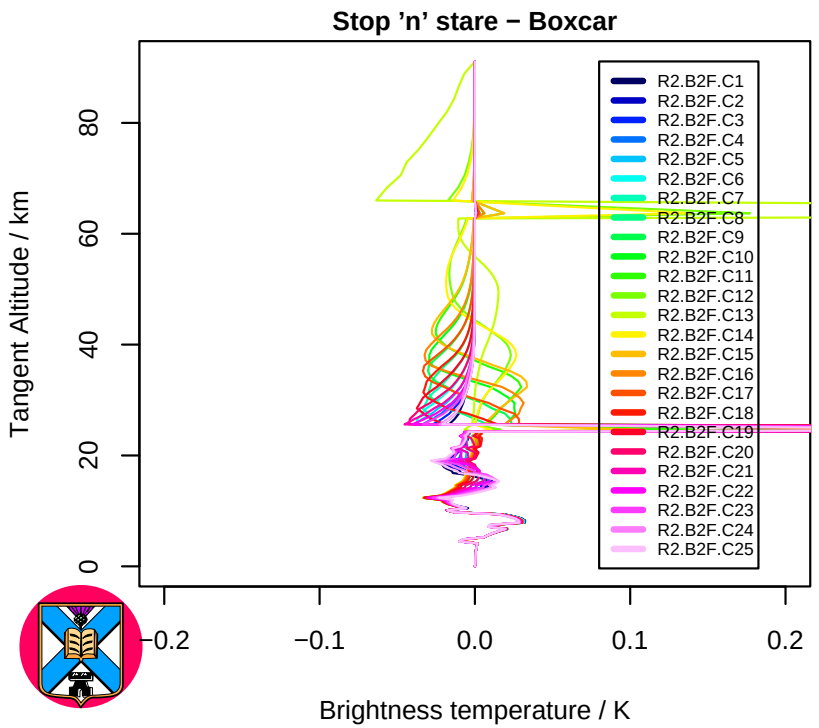

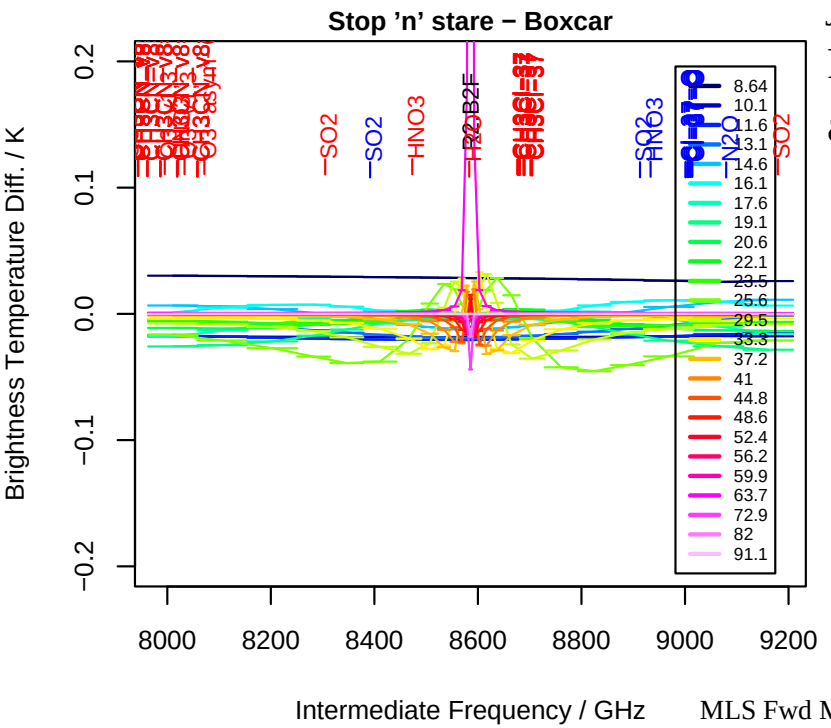

Initial Comparison

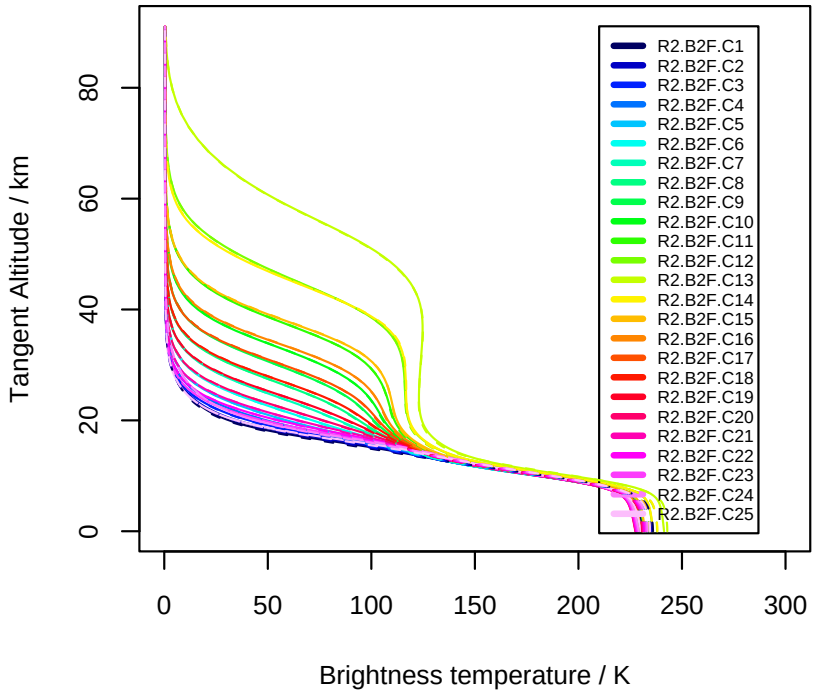

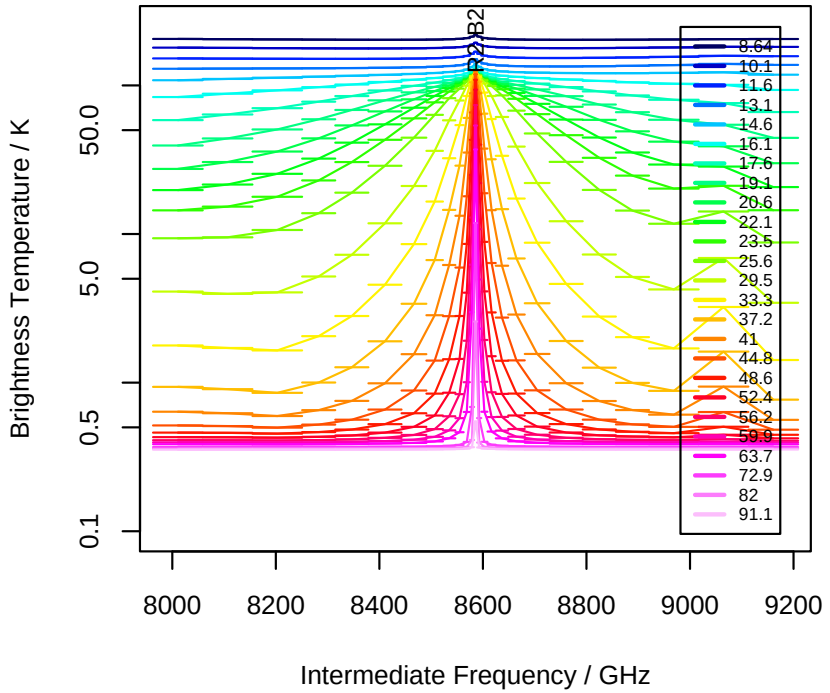

R2:190.B2:H2O
One MAF
Equatorial

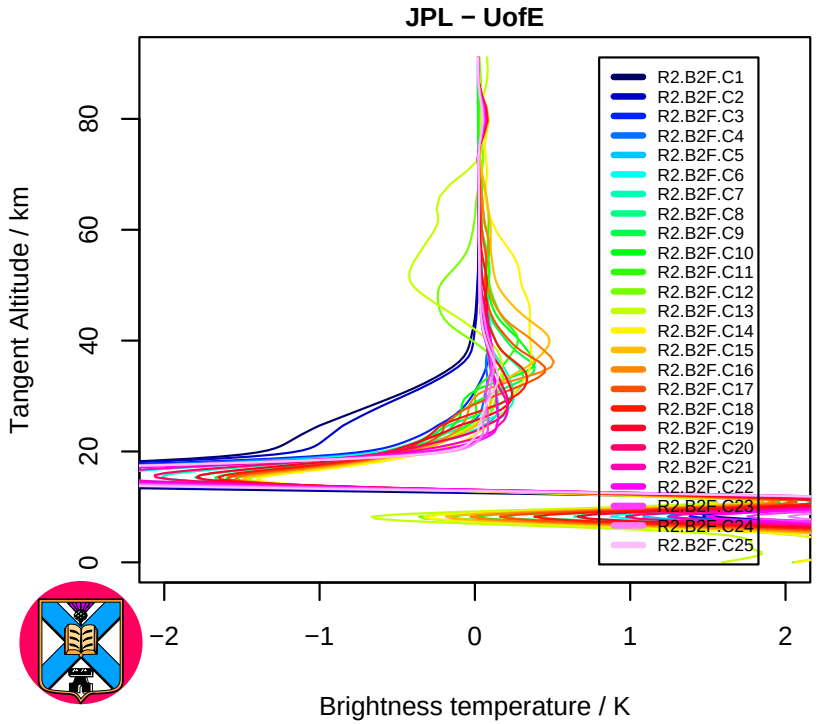

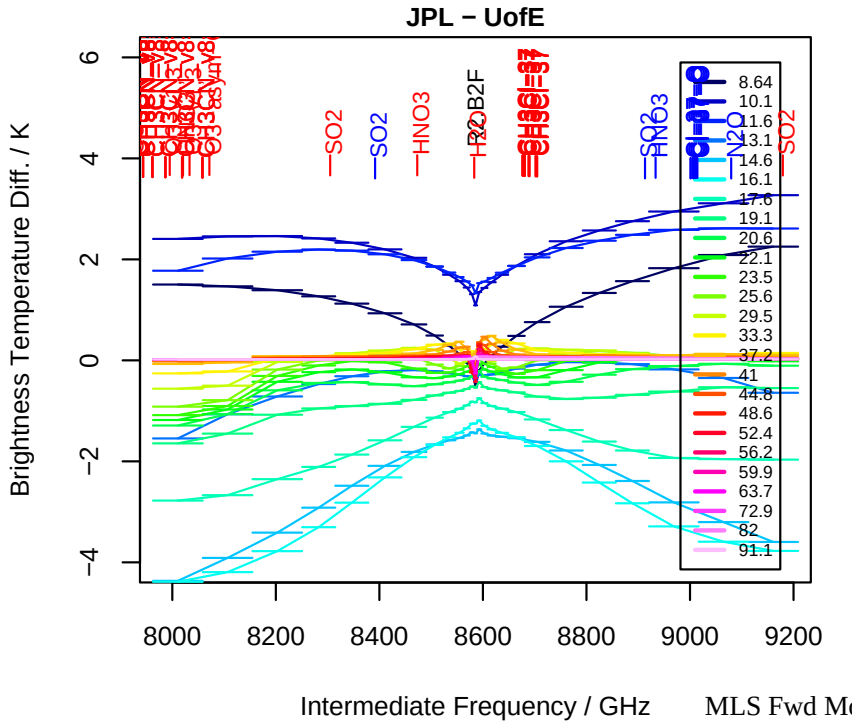

Comparison with a third model

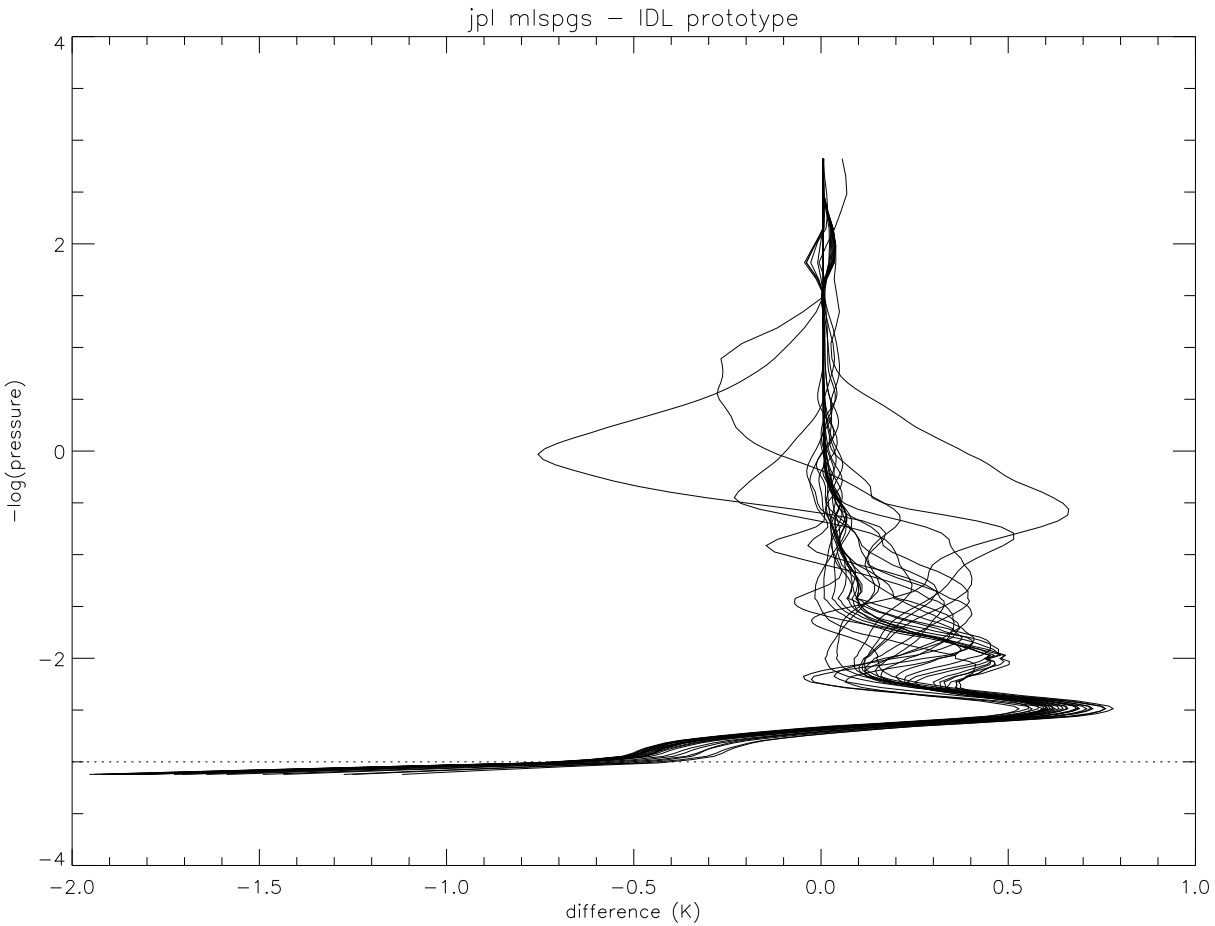

- Differences between JPL and Bill Read's prototyping model
- Differences also in range ± 0.5 K in middle atmosphere
- Agreement much better in troposphere.

Modelling and retrieval: more detail

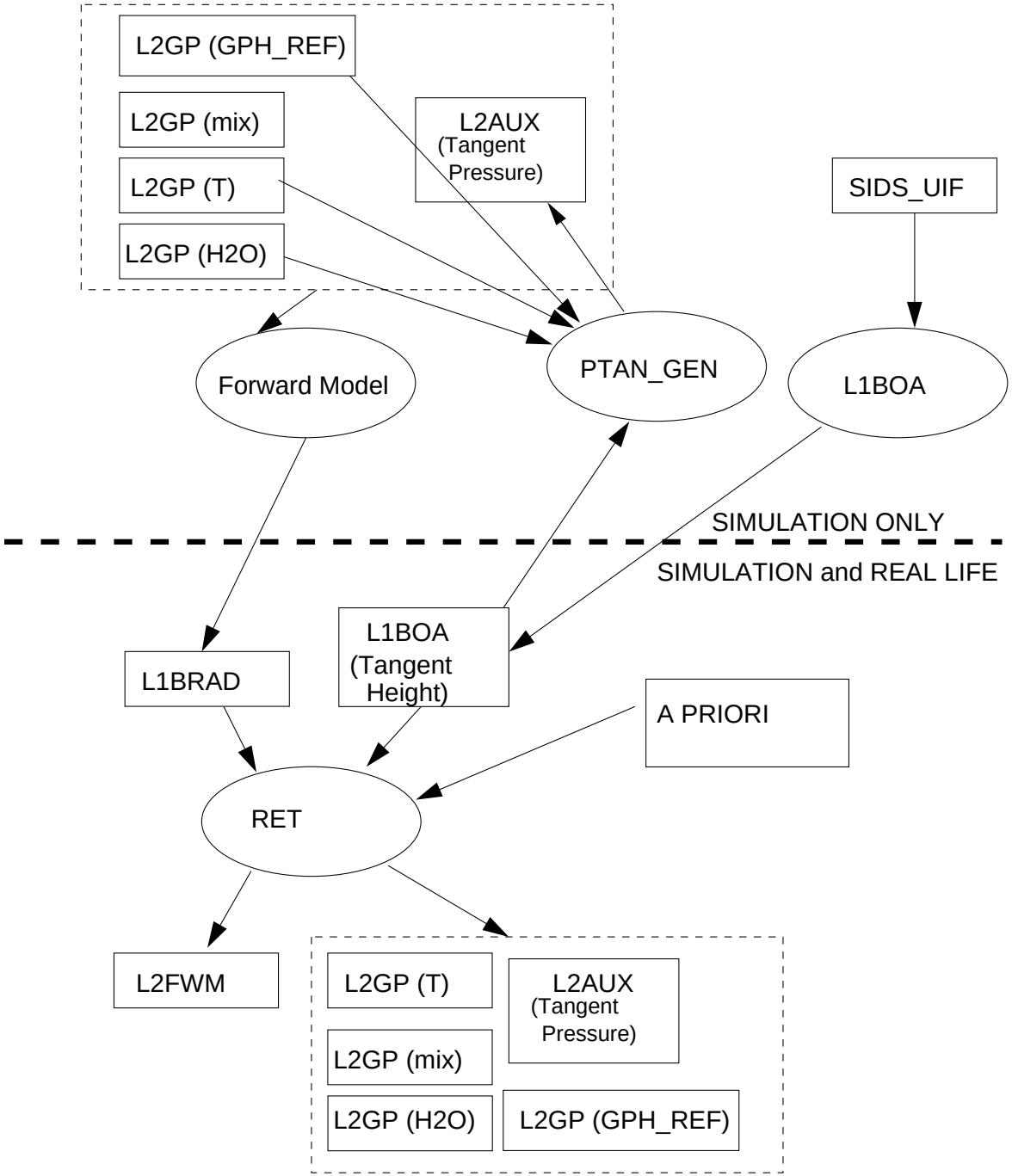

Forward Model phases

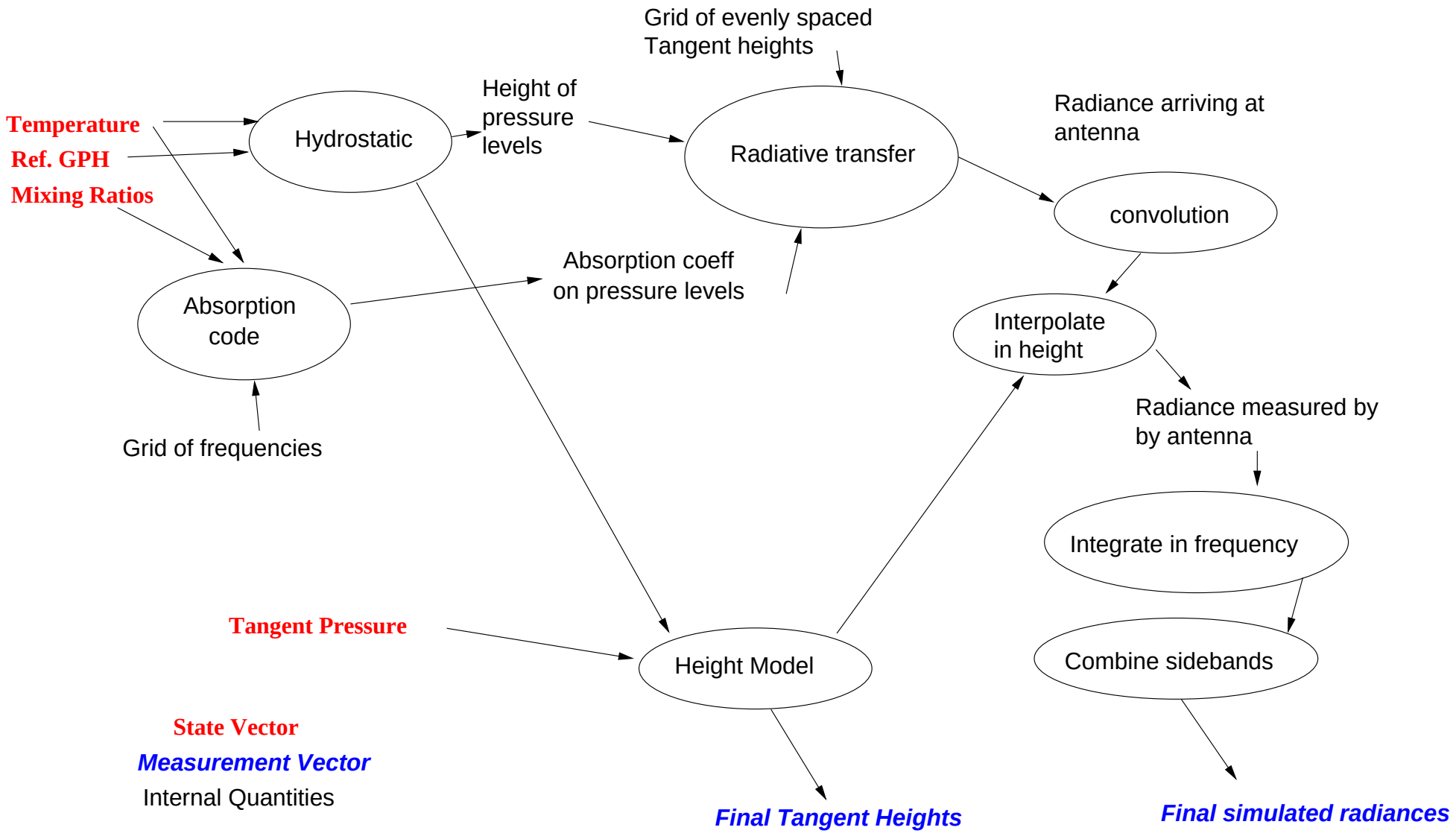

Hydrostatic balance

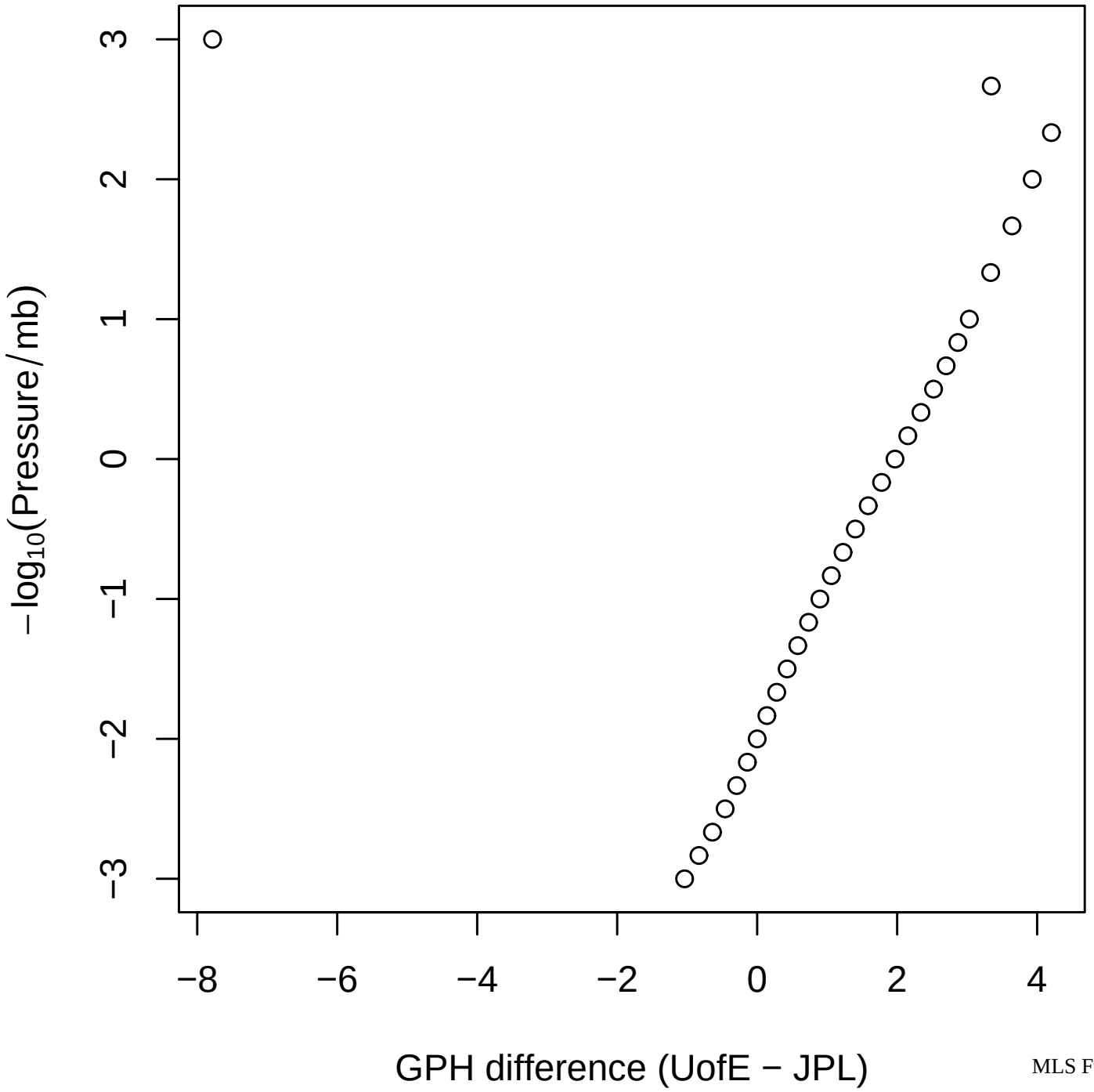

“True” tangent pressures

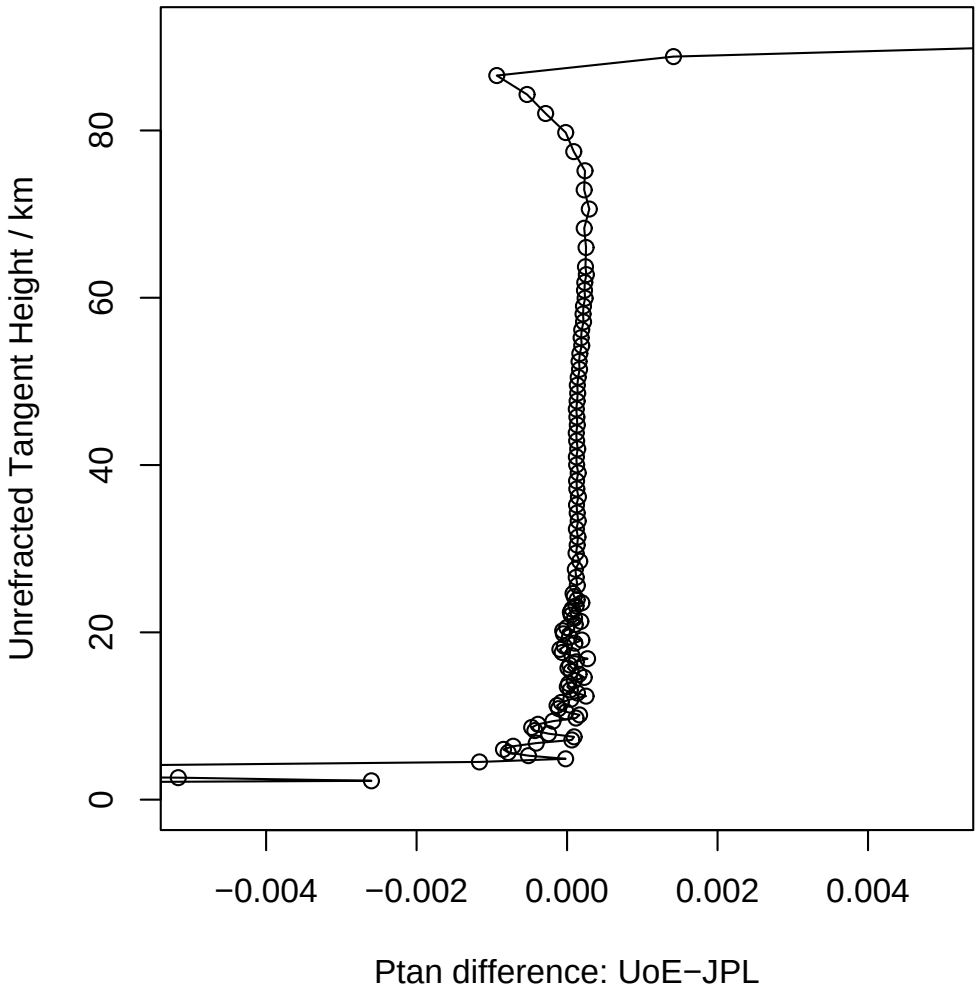

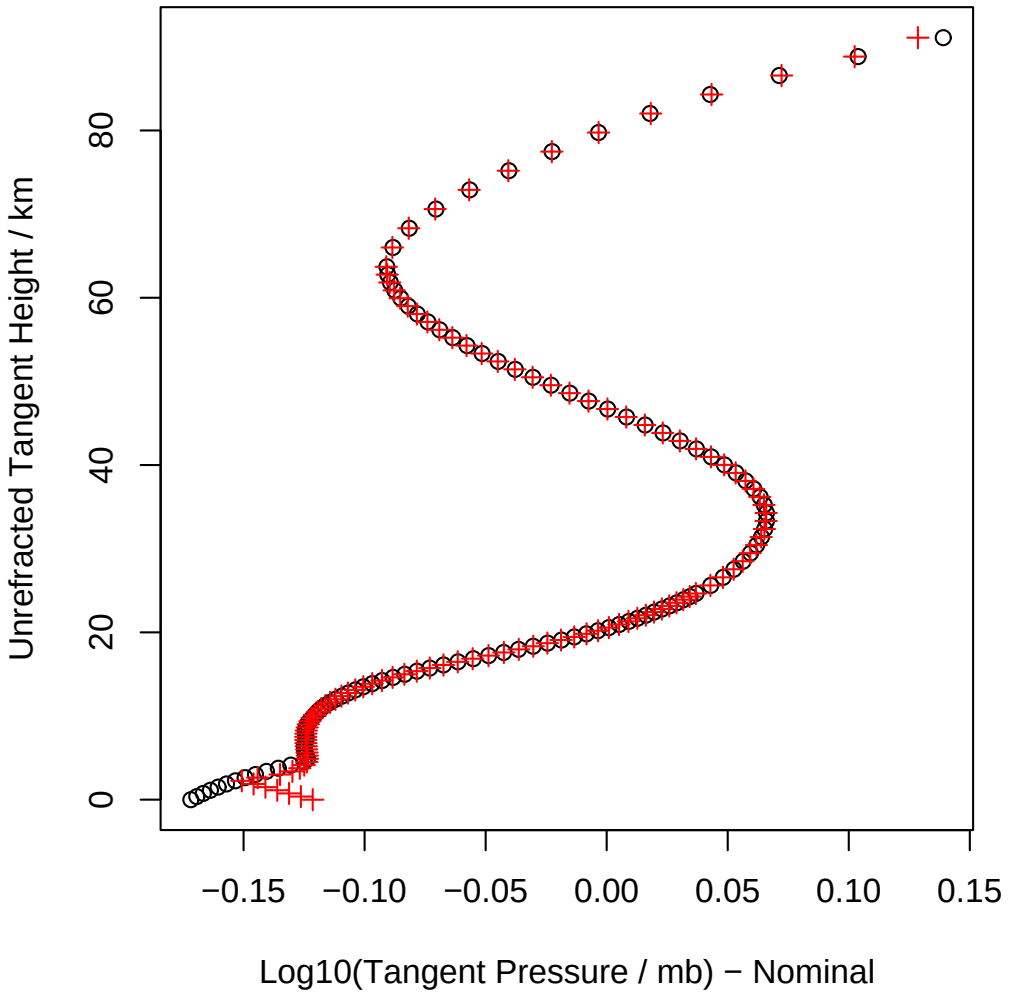

Monochromatic radiances

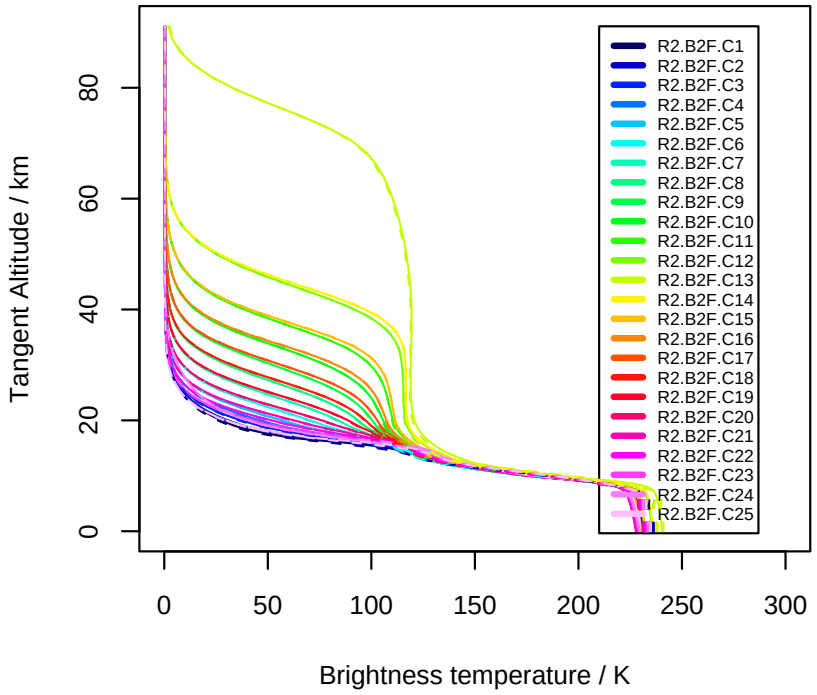

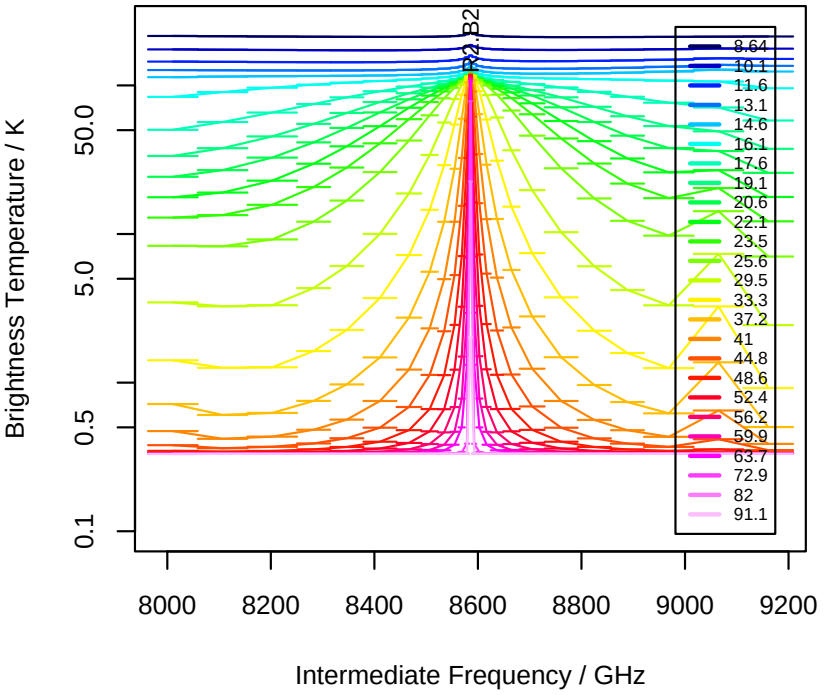

Probs in Channels 1-2 (8000 GHz IF) visible at this stage. Must be an RT thing, not an antenna/filter thing.

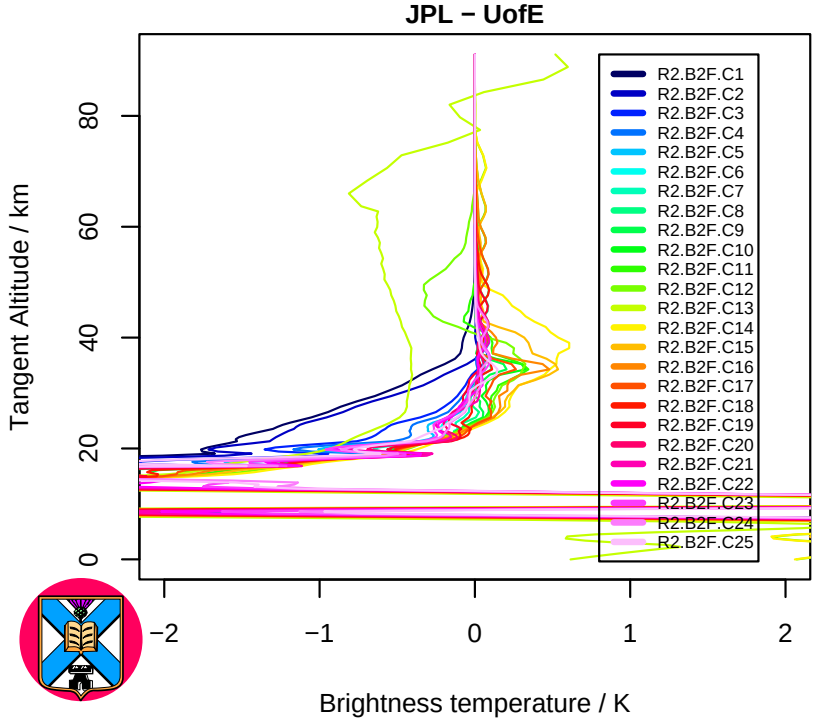

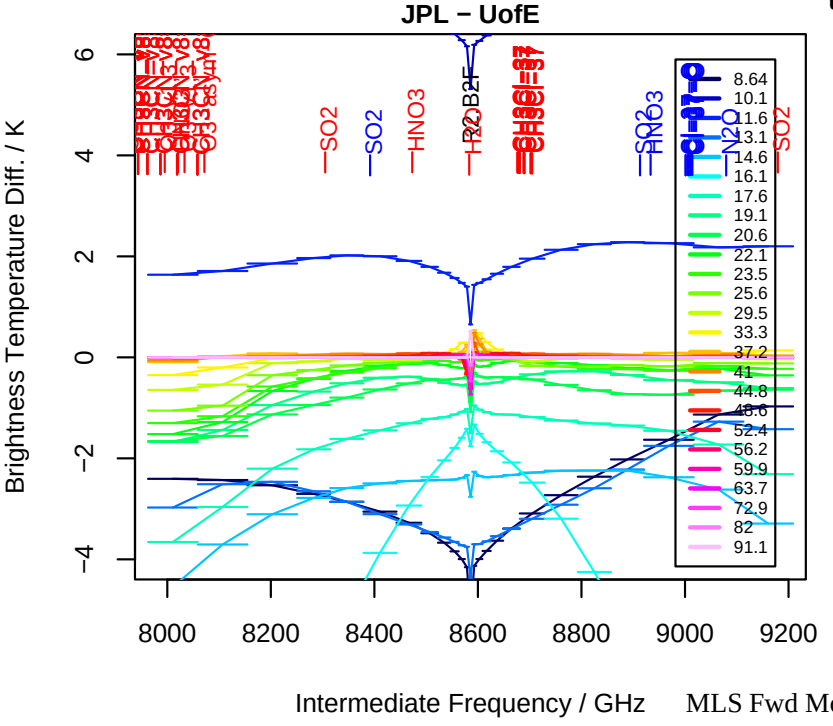

Antenna convolution

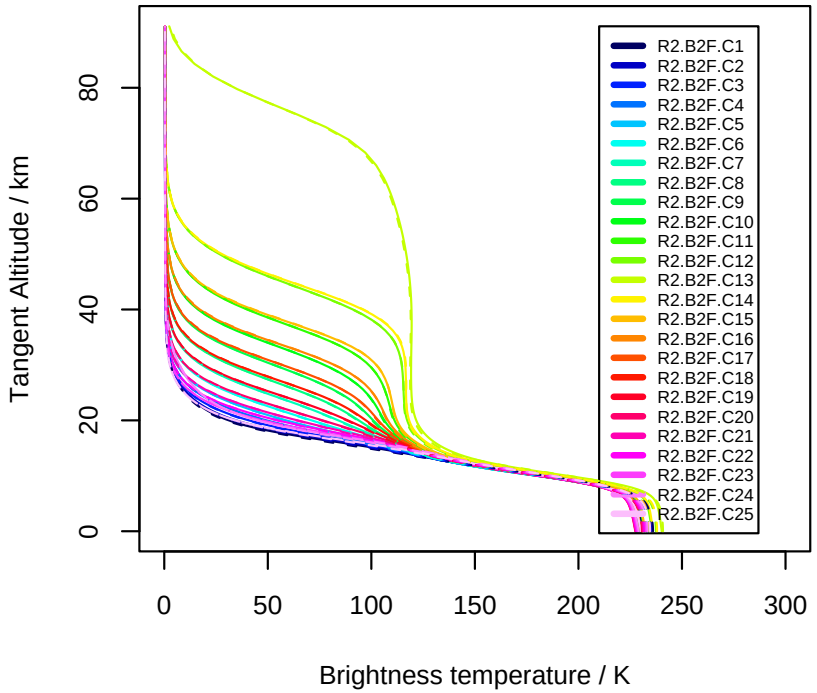

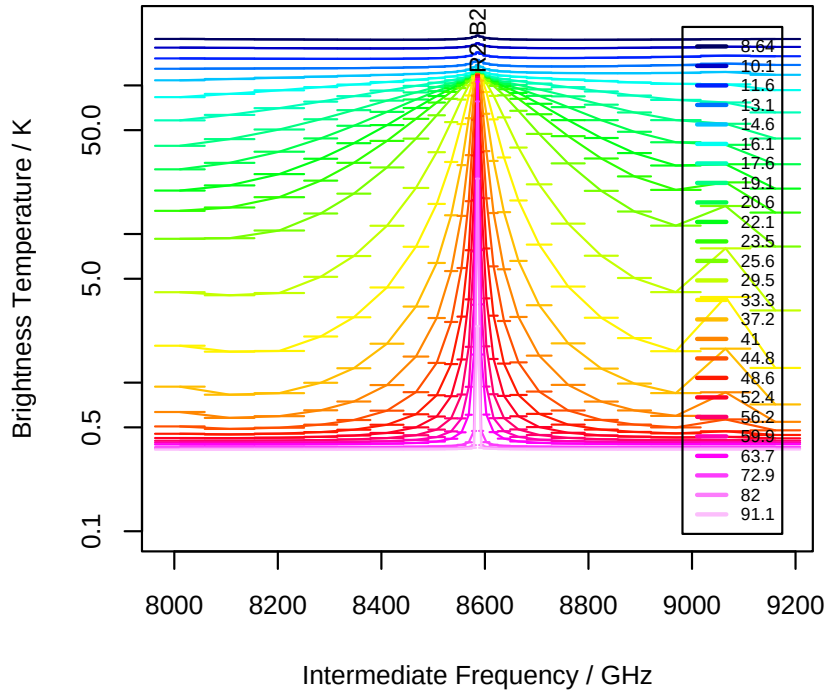

Differences like previous slide. Convolution not a problem.

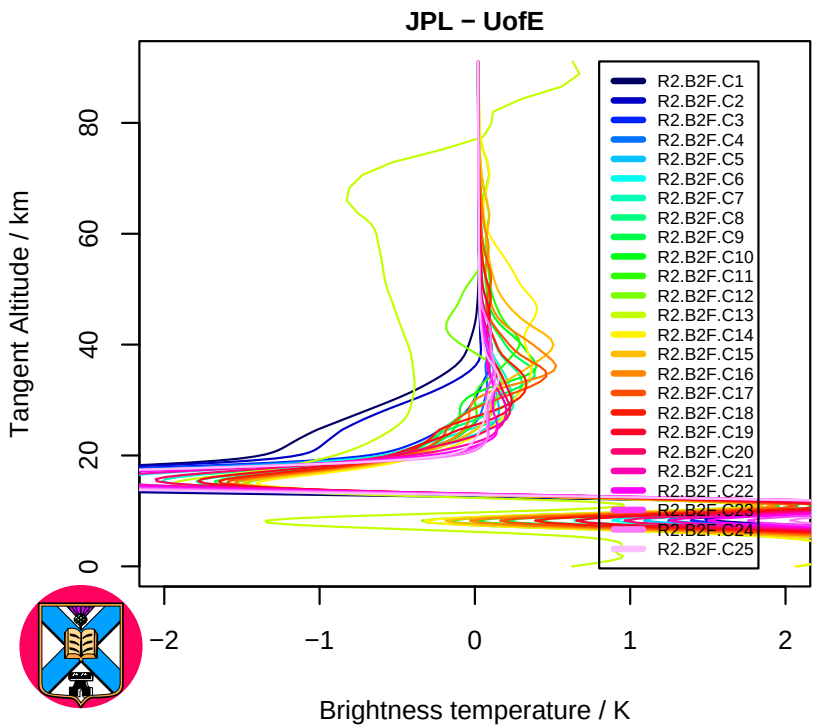

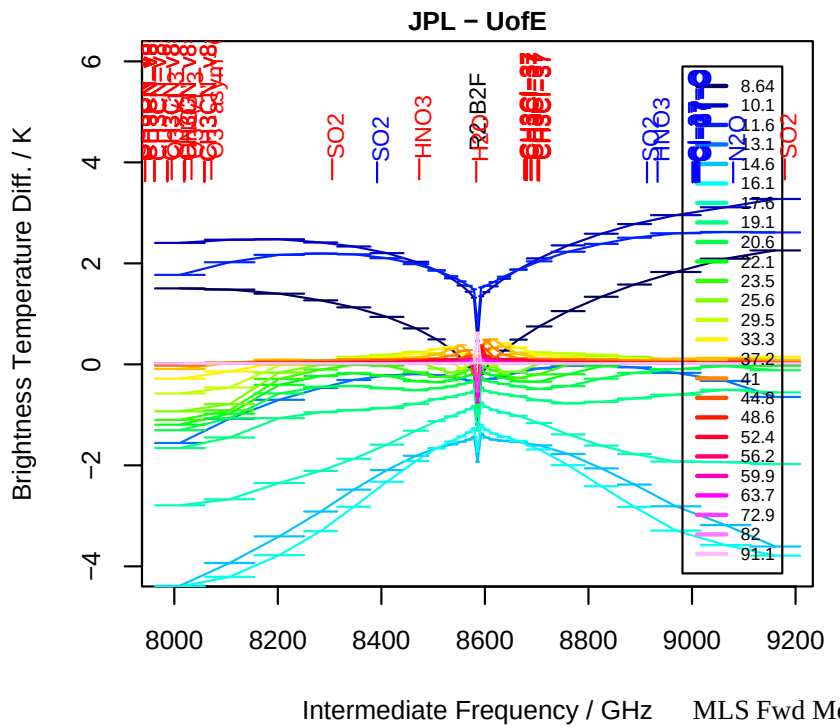

Integration over filters

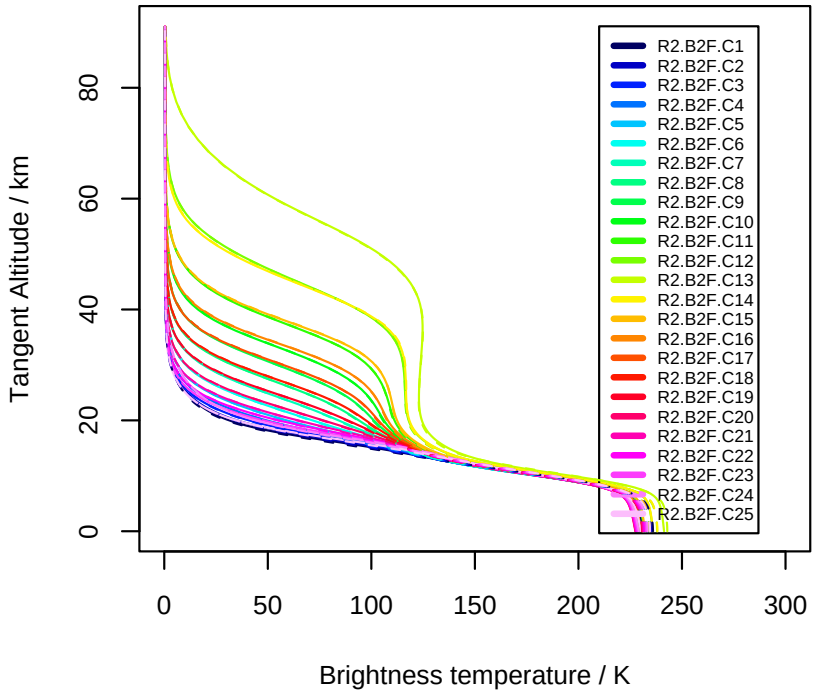

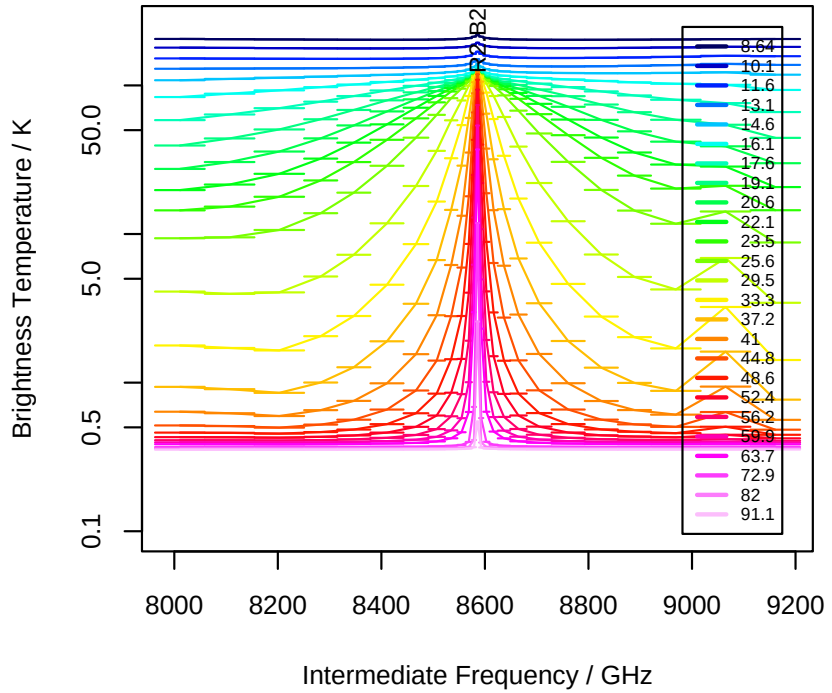

You saw this at the beginning. Note the agreement is similar to the previous slide except in the centre channel.

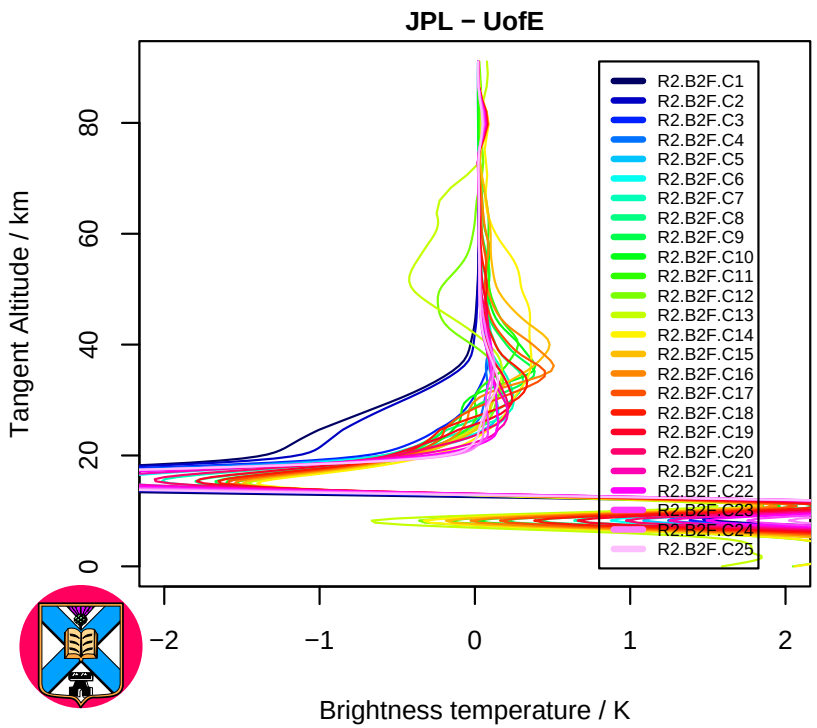

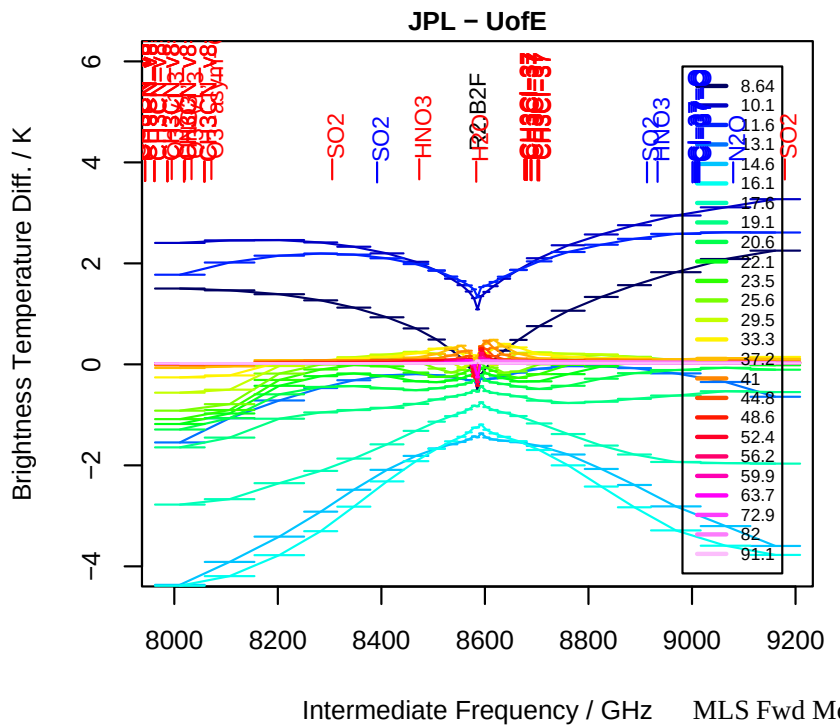

Review

- Agreement is reasonable
- Errors in middle atmosphere $\leq 0.5\,\mathrm{K}$
  - That is true of monochromatic unconvolved radiances
  - Including antenna and filters introduces little extra differences between the models
  - we need to investigate the absorption coefficient and radiative transfer code further.

How lines are chosen

- All spectral data comes from the JPL line catalog(ue)
- JPL lines are hand-picked
- UoE lines are chosen automatically by the program
  - A frequency is picked: the line centre frequency if the line is in the band, the edge of the band otherwise
  - The absorption due to that line is calculated at that frequency, at 46 mb and some nominal temperature and mixing ratio
  - If the value is above a threshhold, the line is included

Spectral lines used: B2LF

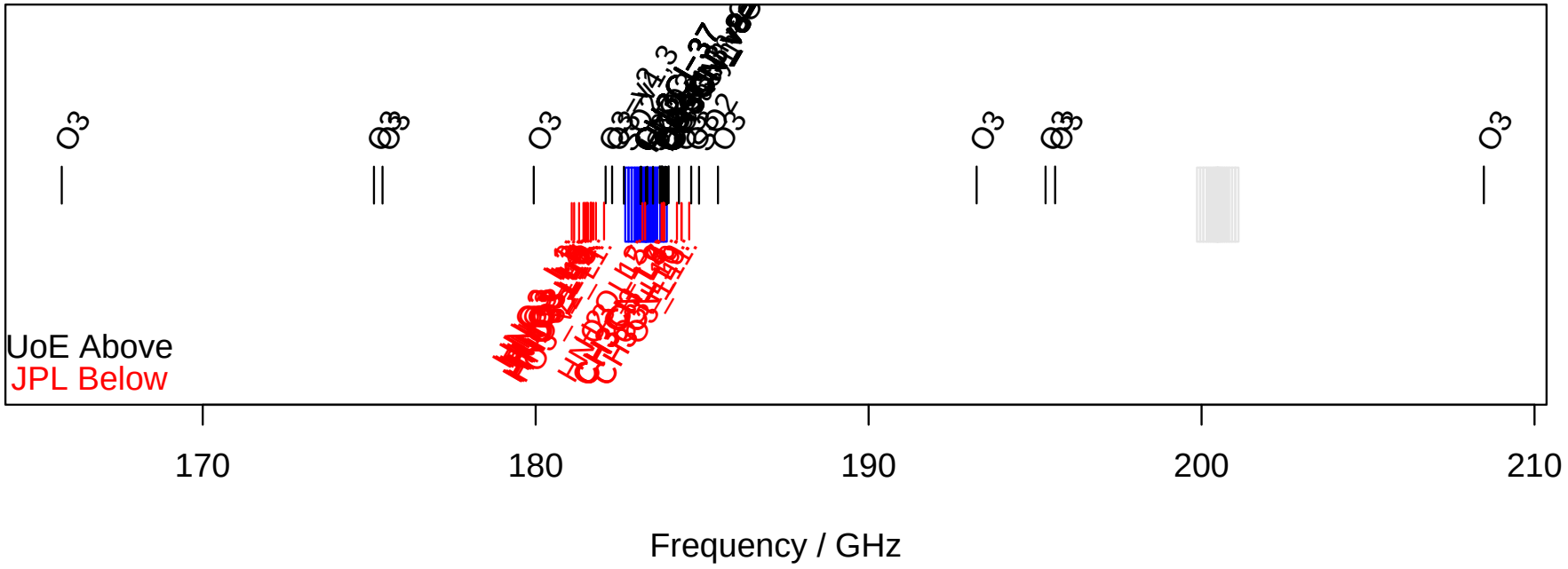

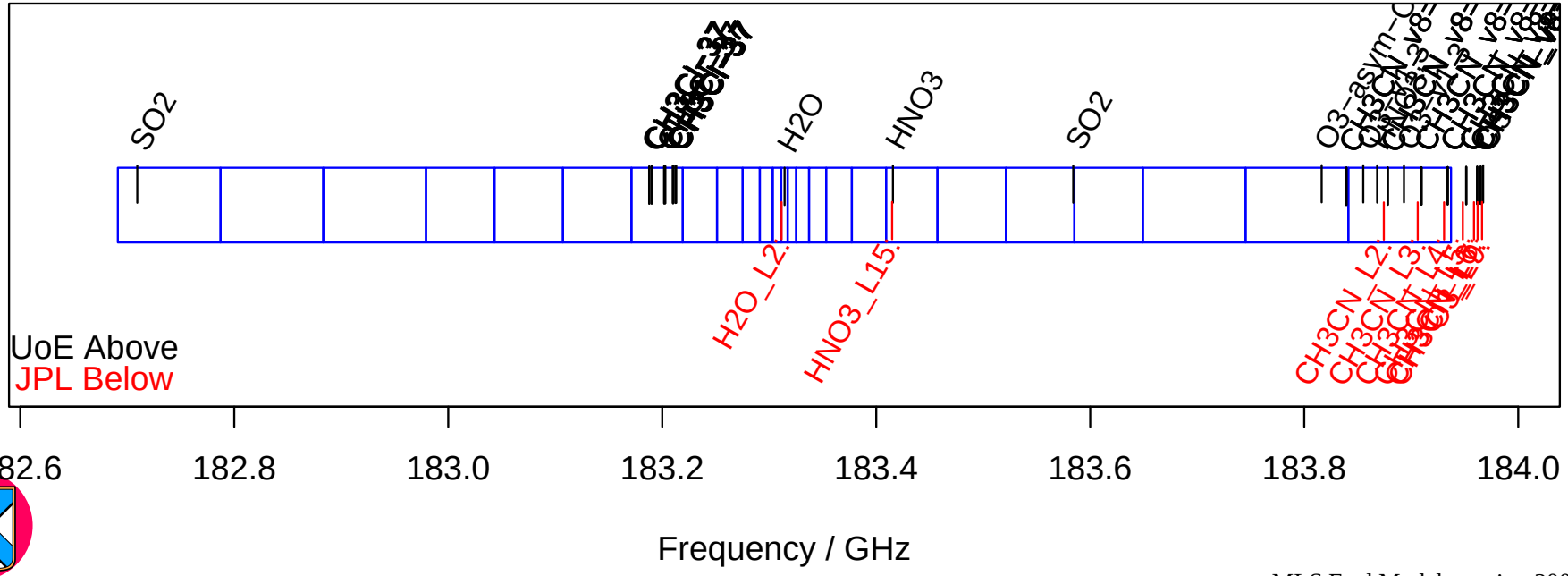

Spectral lines used: B2UF

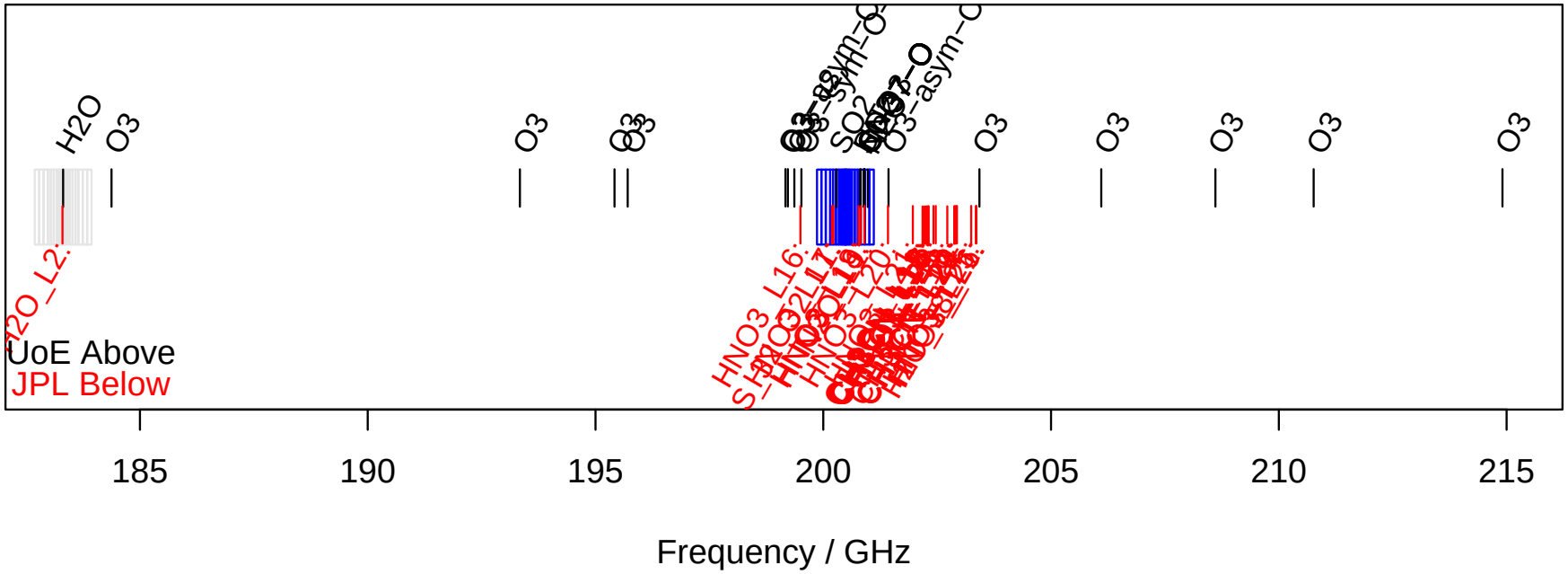

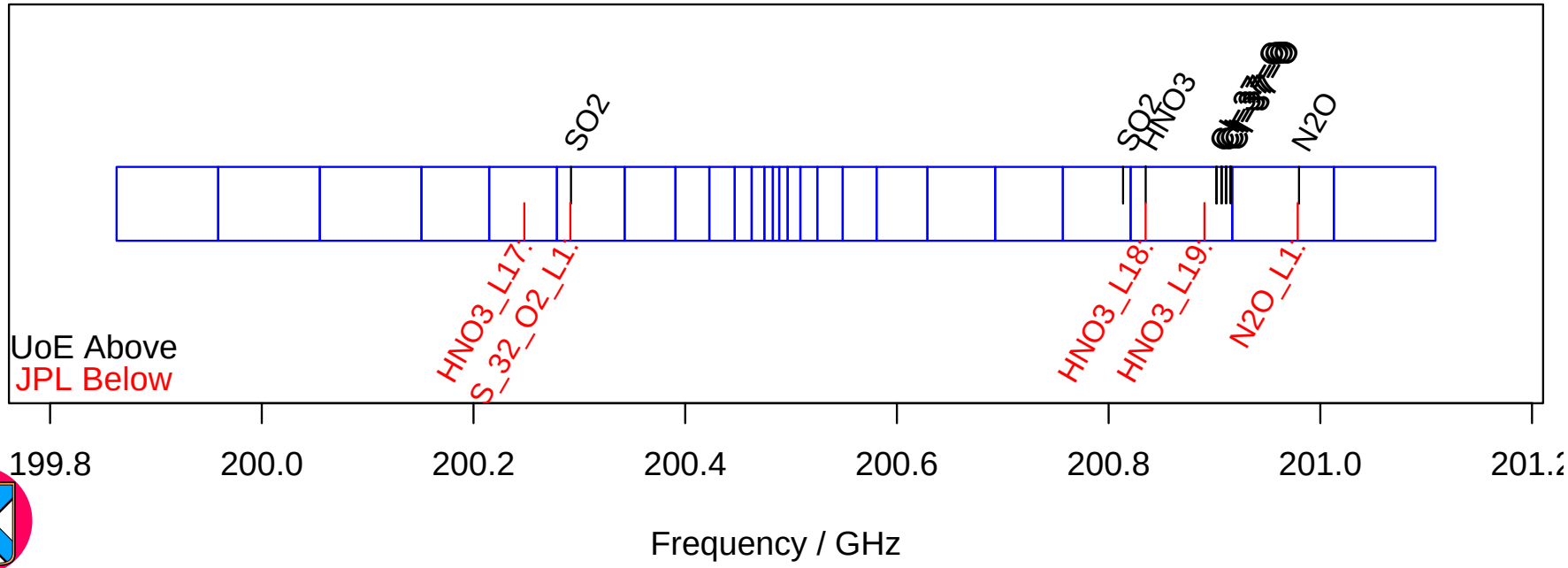

Comparison with H_2O *only*

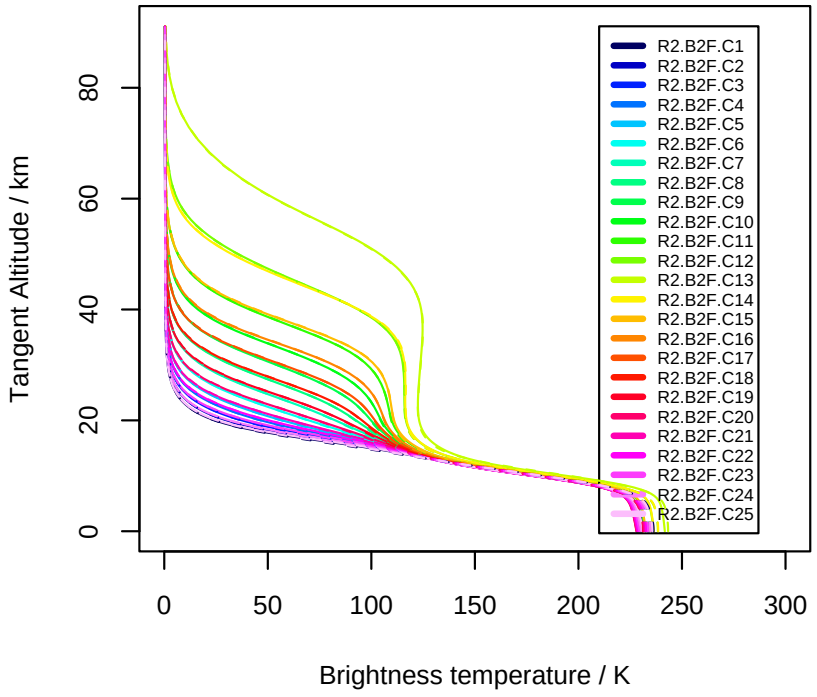

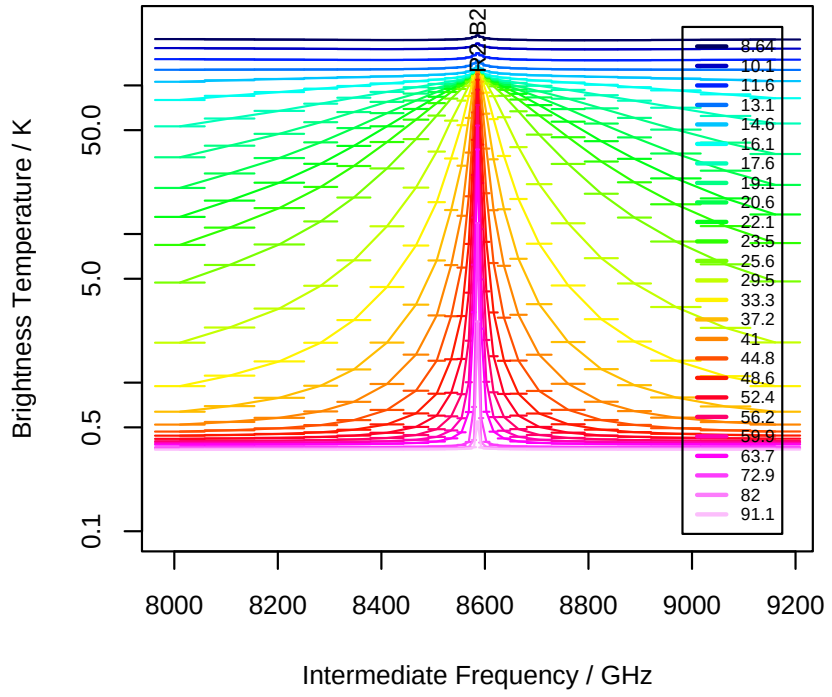

Differences in C1 and C2 have gone. Clearly due to differences in line choice. Differences above 25 km remain. Maybe line shape?

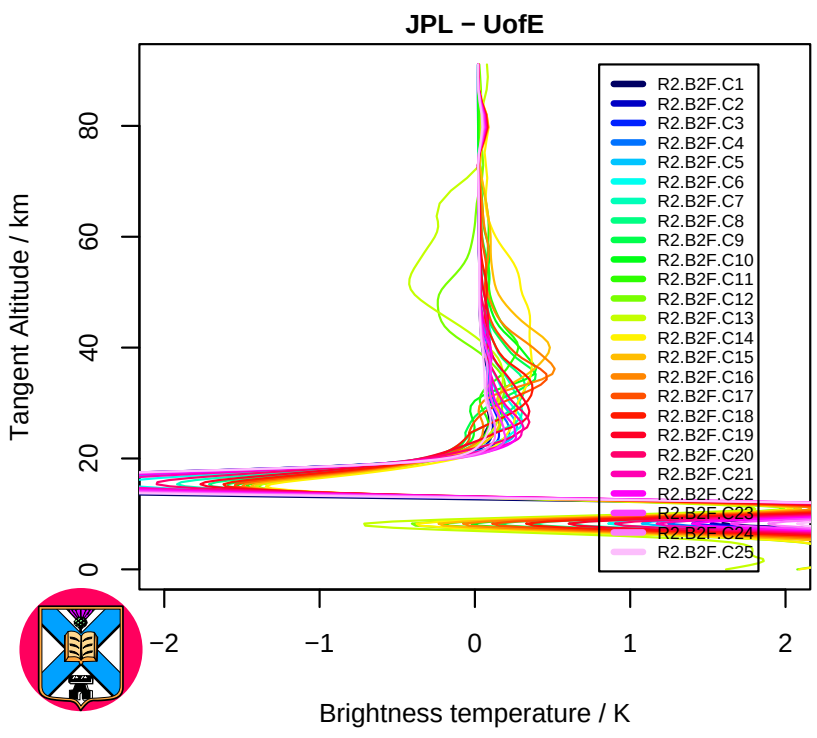

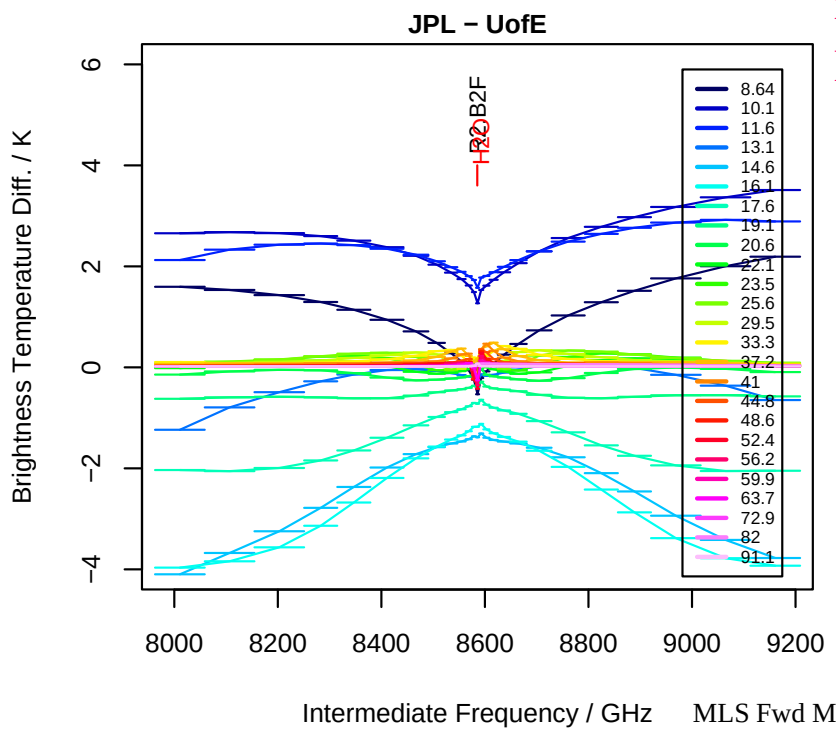

Band 5 (ClO)

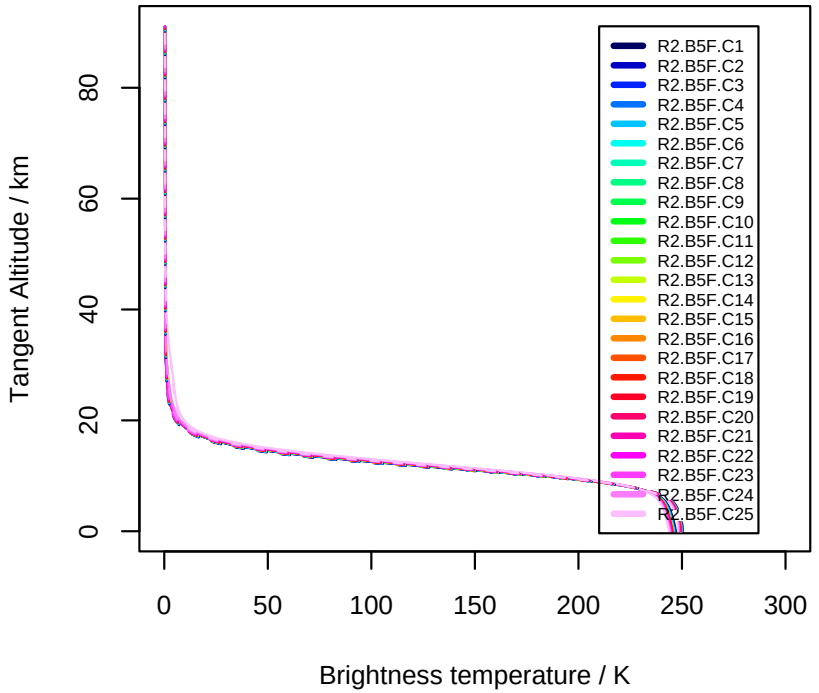

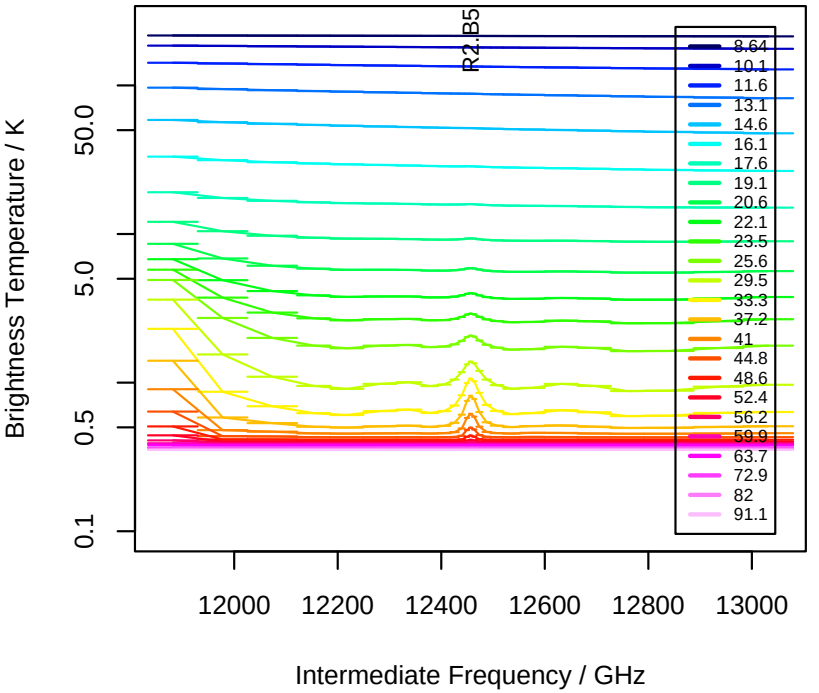

Most differences spectrally flat (or at least smoothly varying)

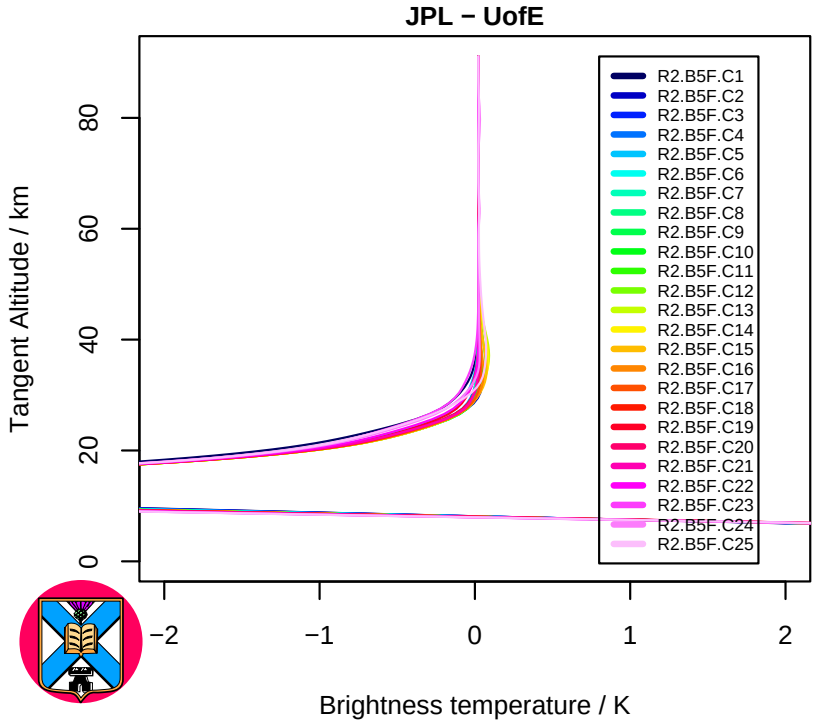

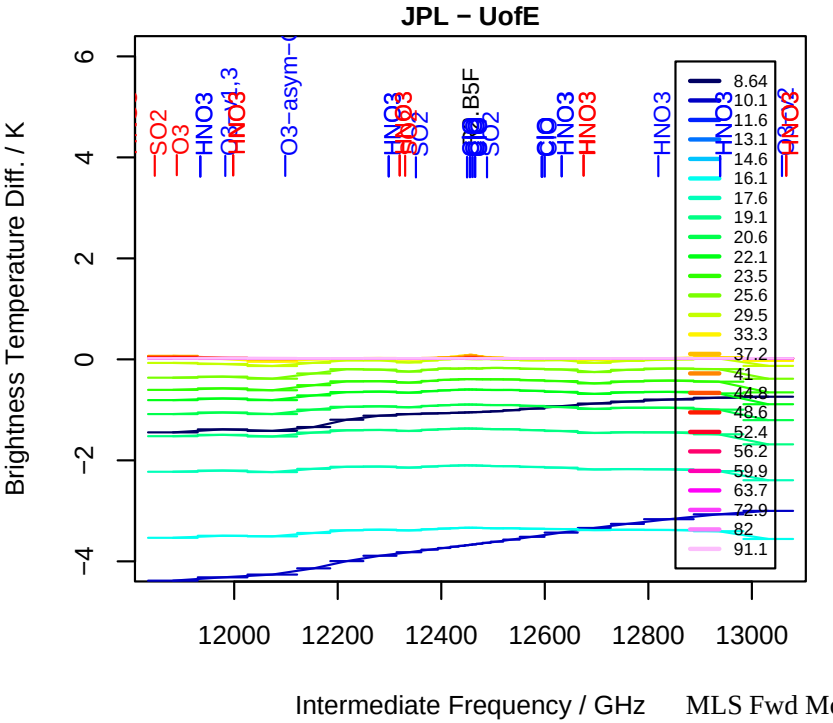

Band 7 (O_3) Monochromatic

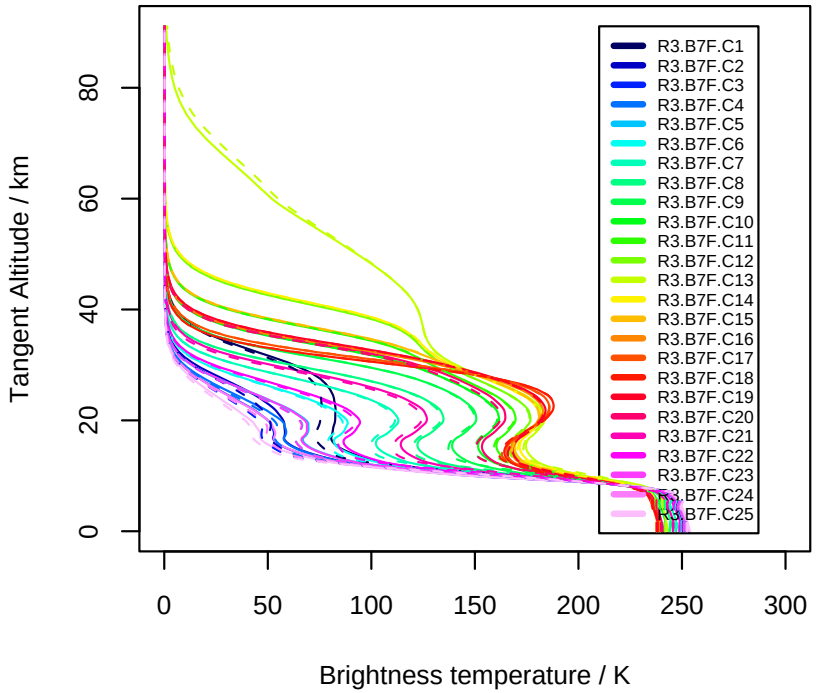

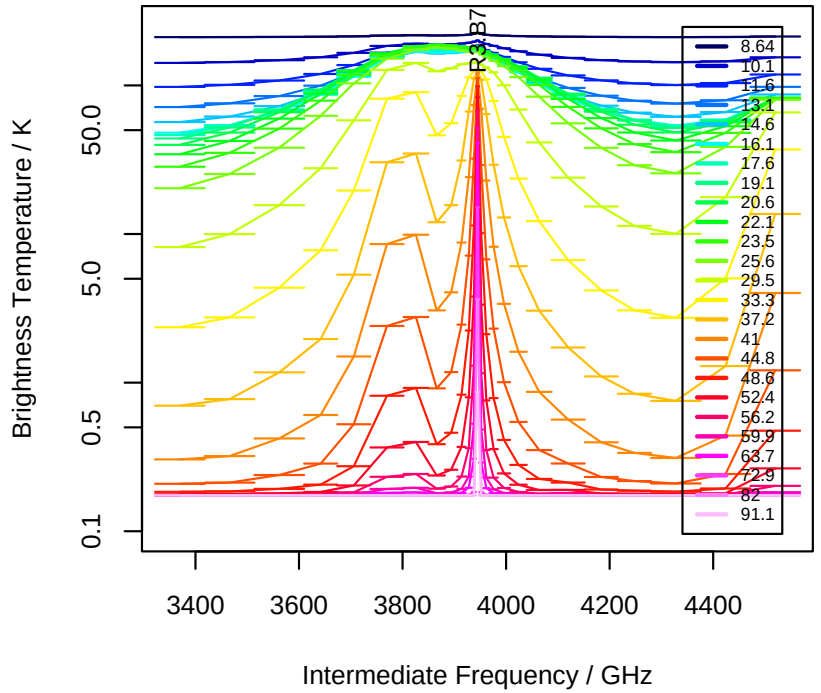

Large differences. We need to compare lines used.

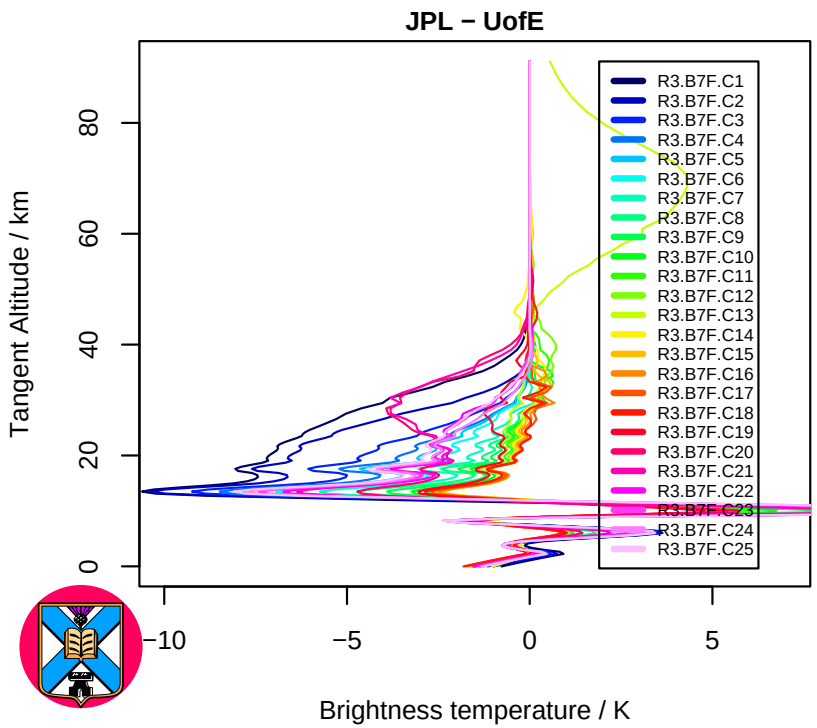

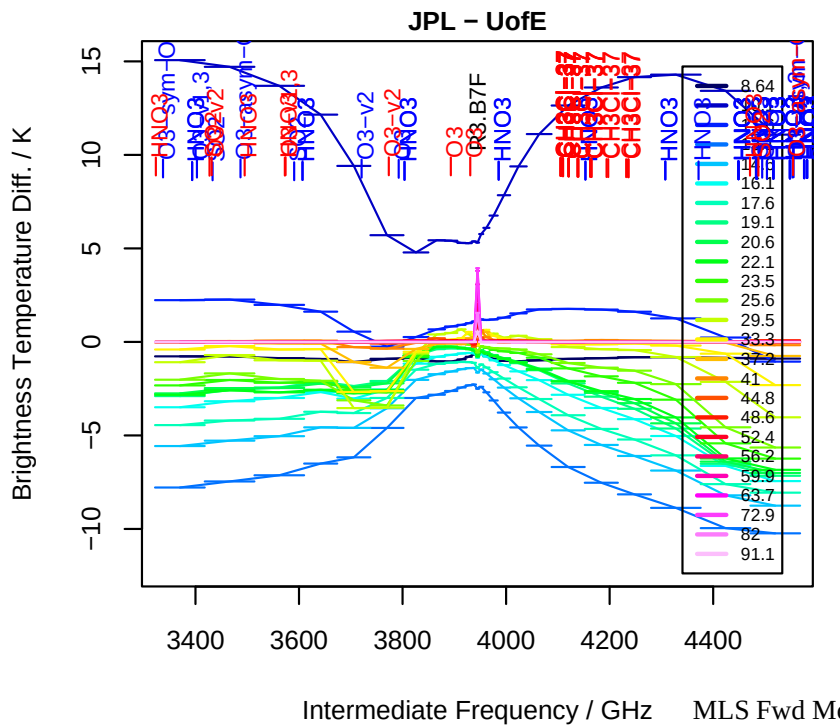

Spectral lines used: B7UF, B7LF

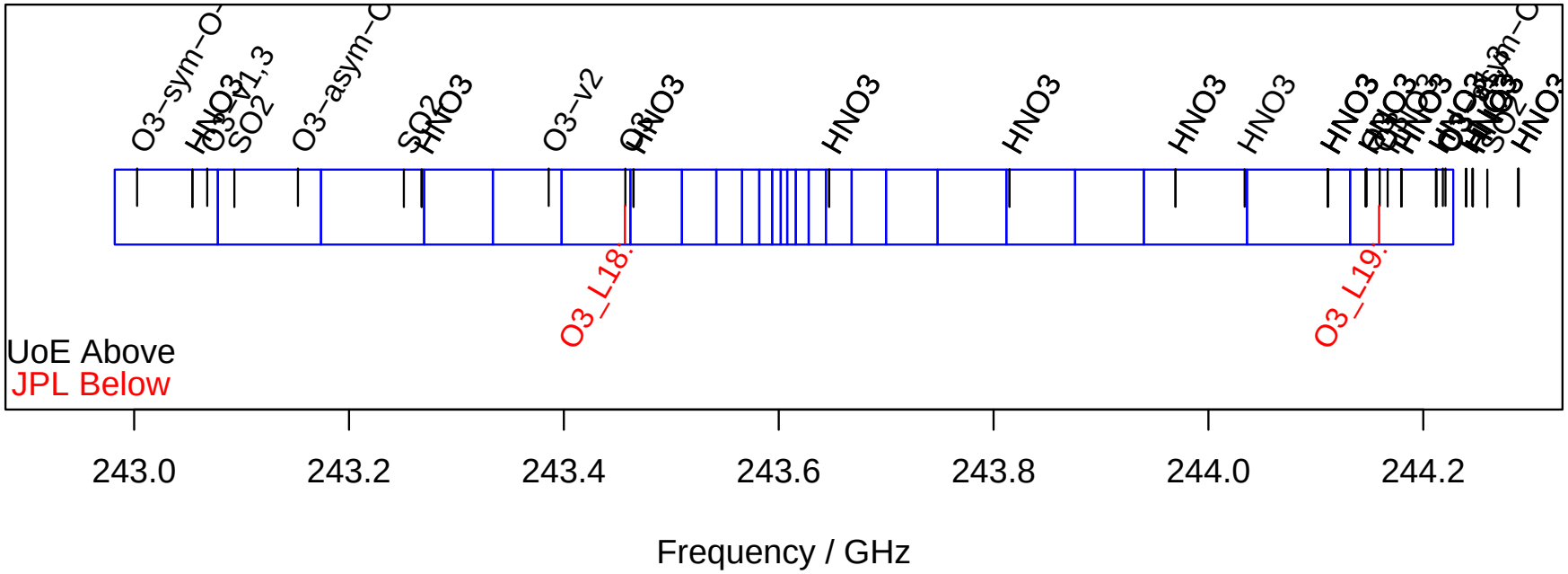

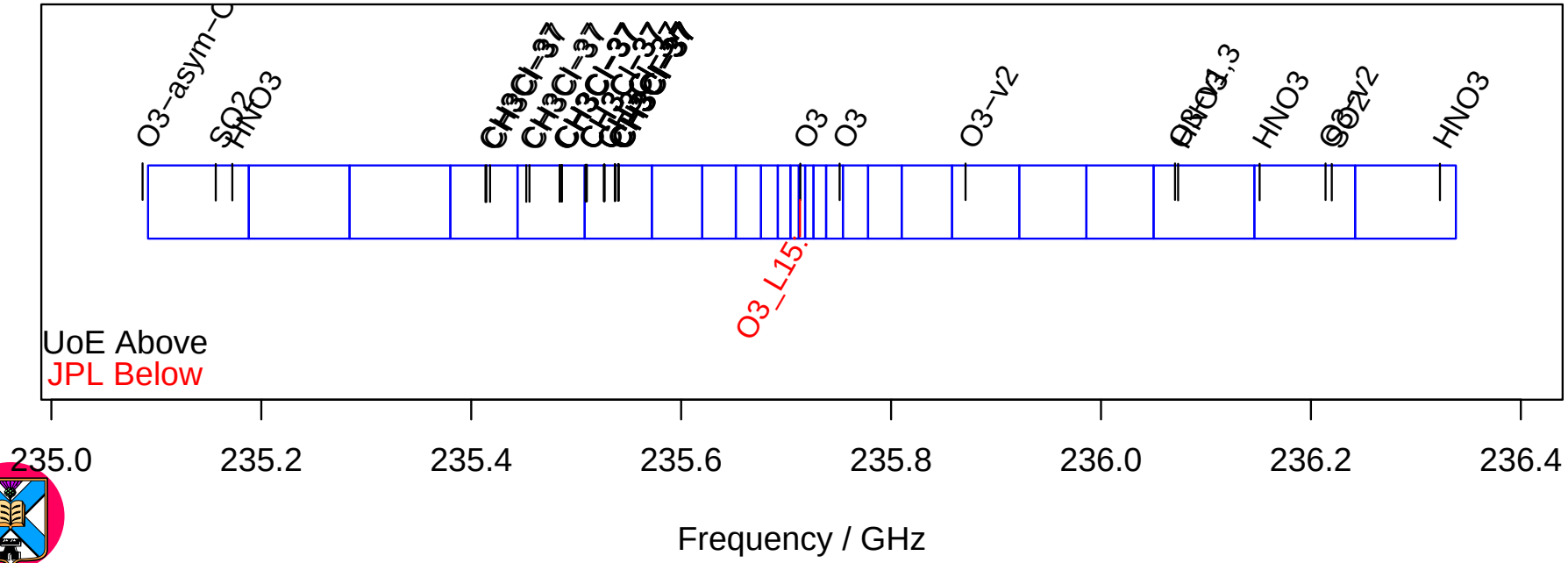

Radiances B7UF, B7LF

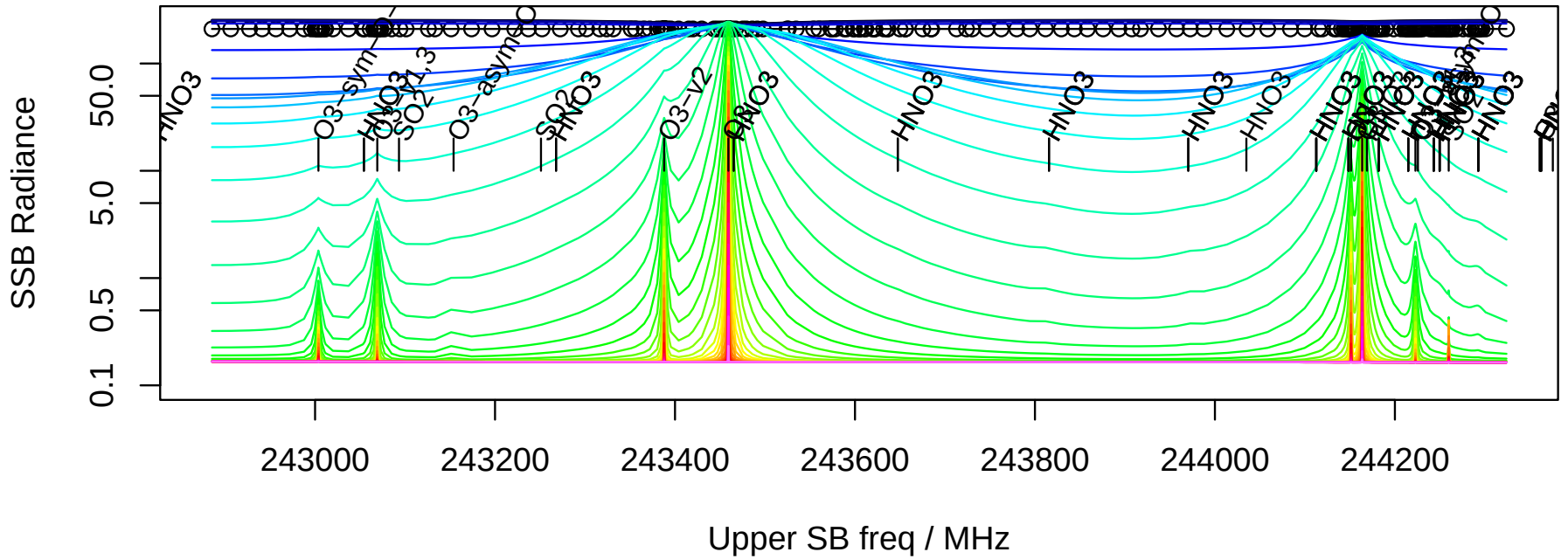

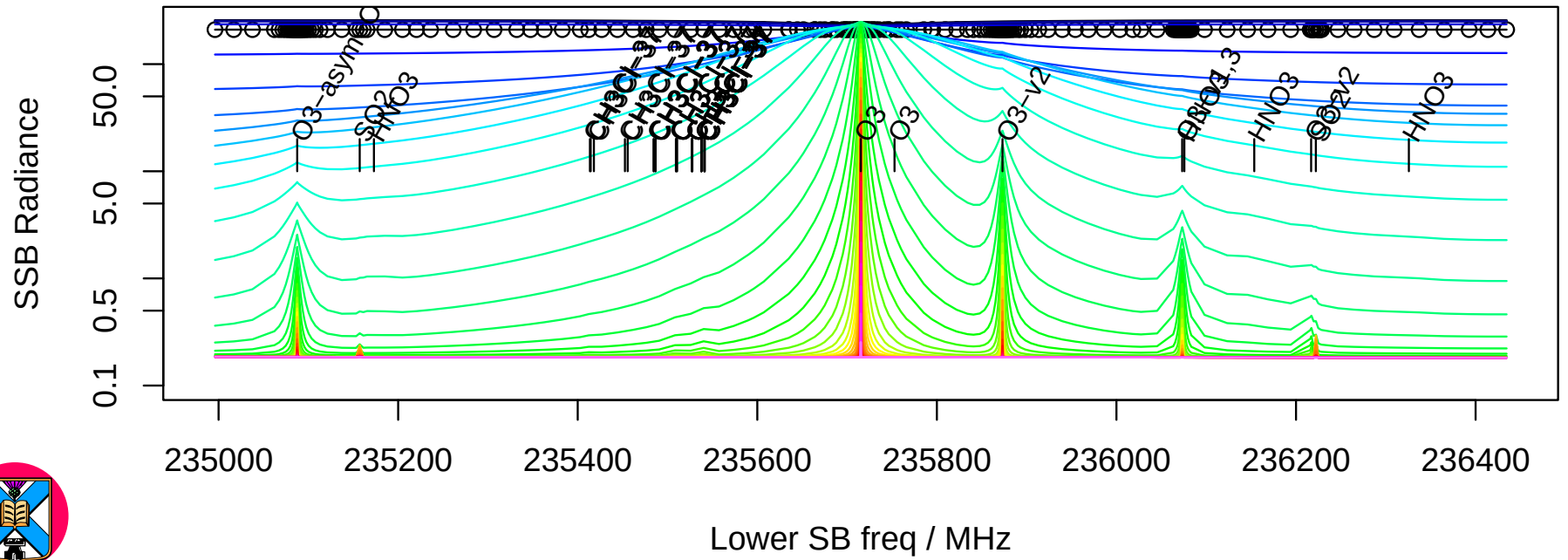

Band 7 (O_3) Monochromatic

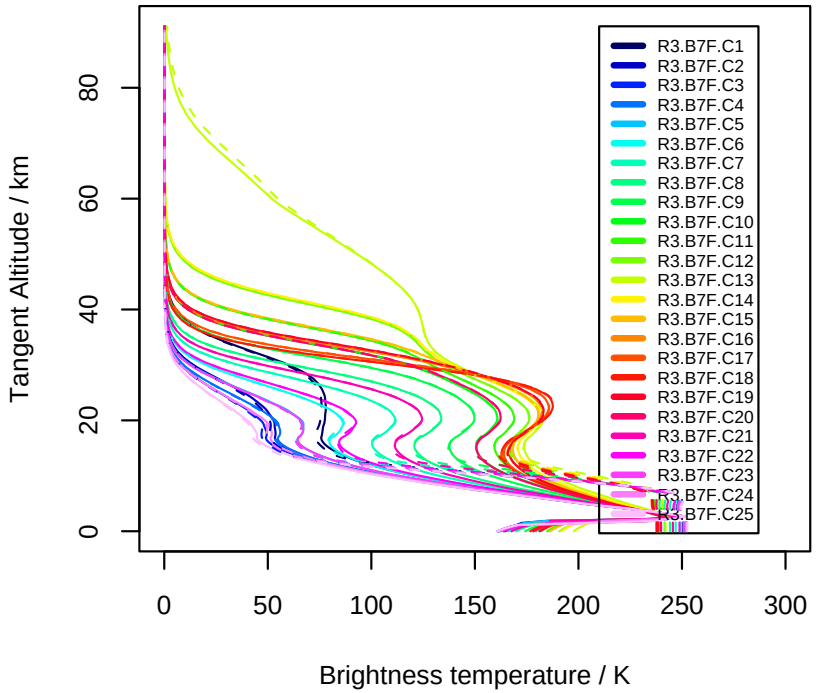

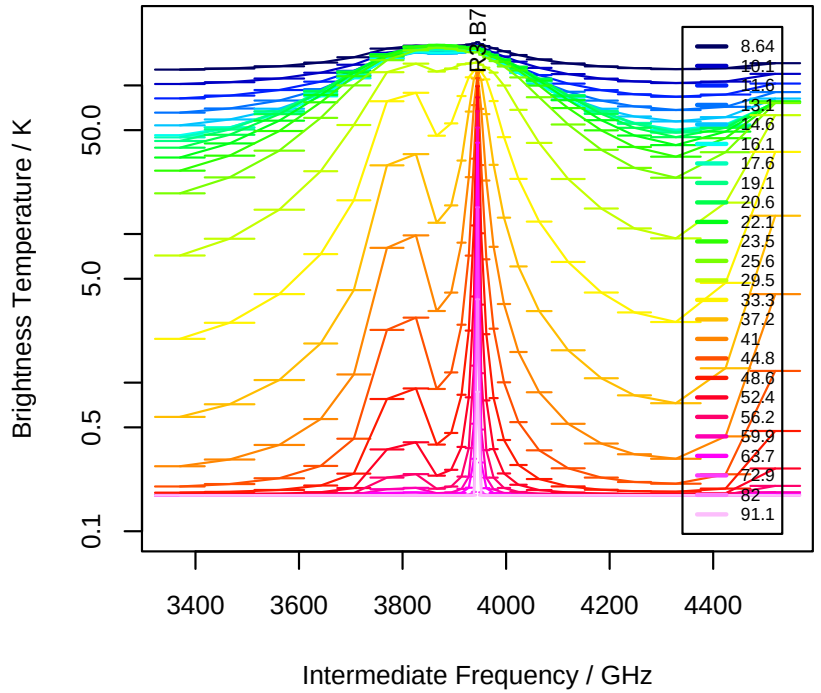

Only ground-state non-isotope O_3 used in UoE model. Differences much smaller.

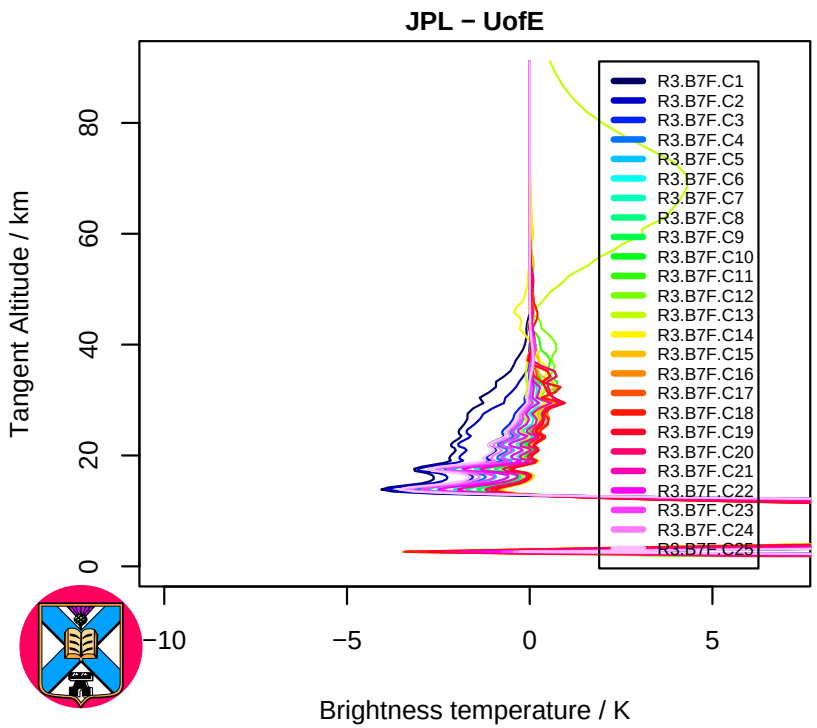

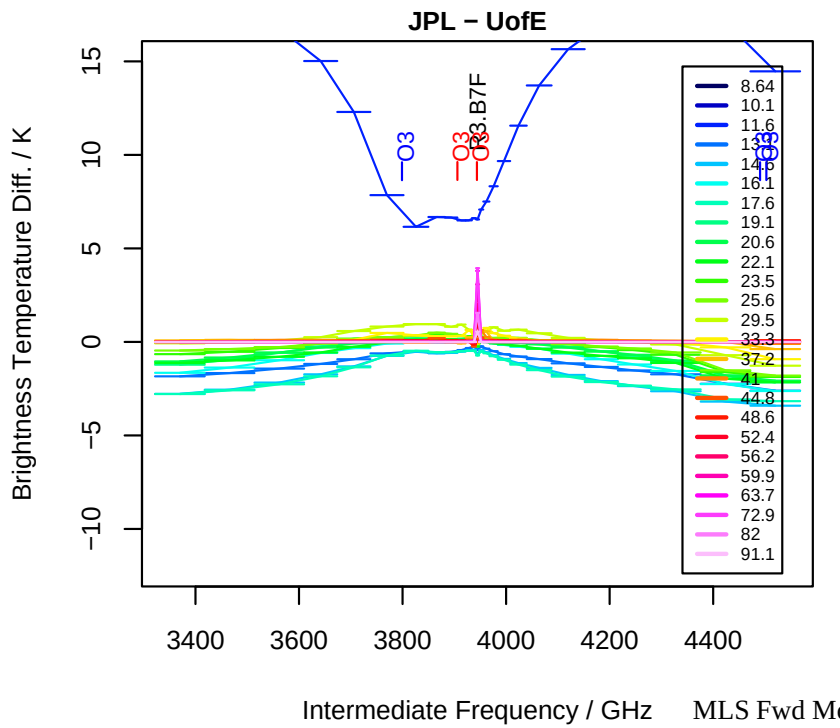

Band 7 (O_3) Monochromatic

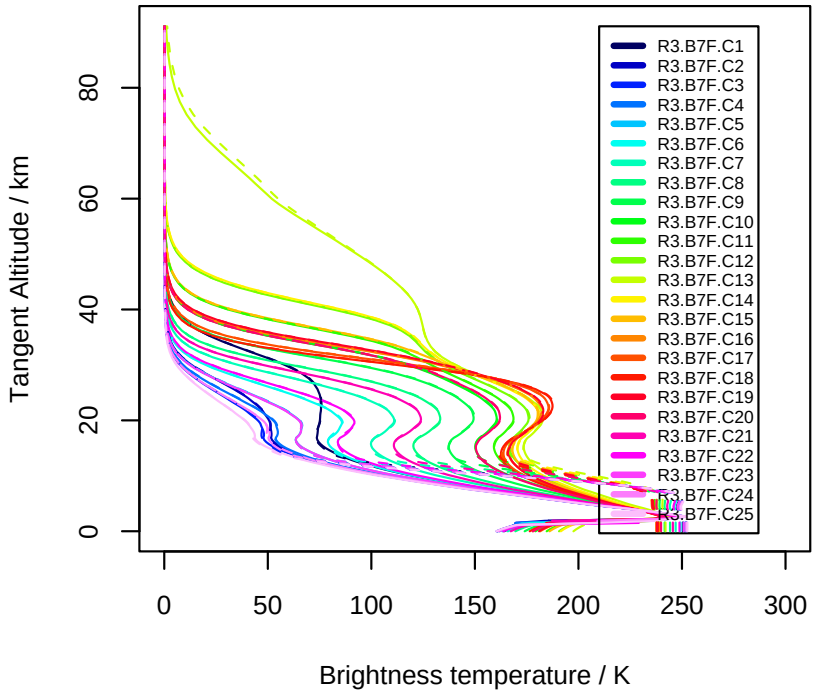

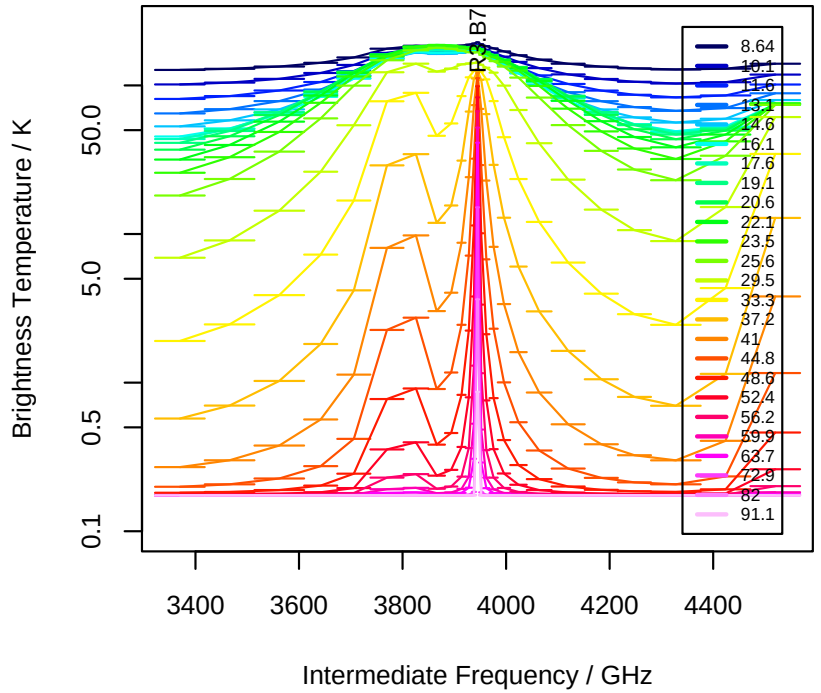

UoE uses exactly the same lines as JPL. Differences now similar to B2F.

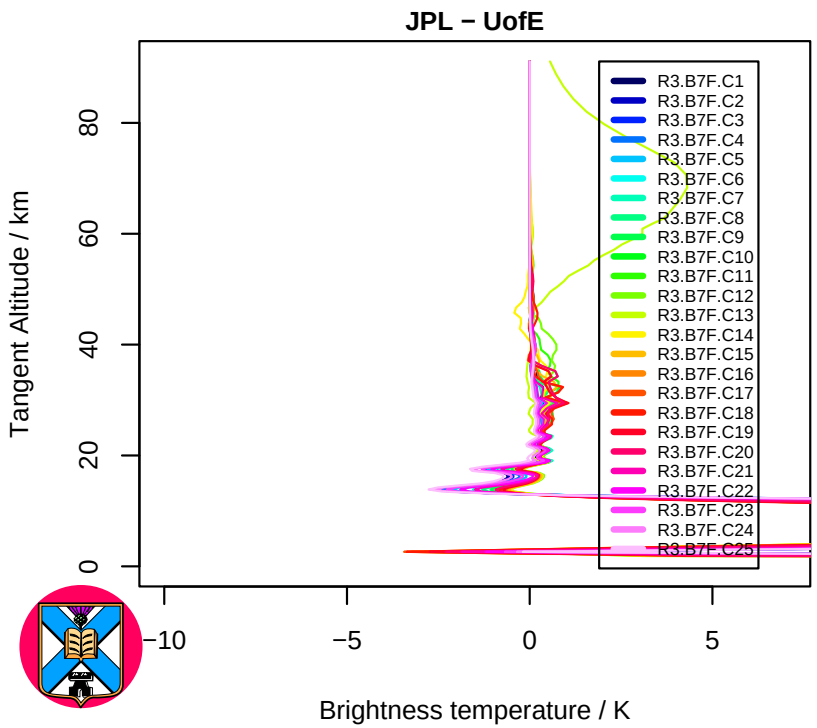

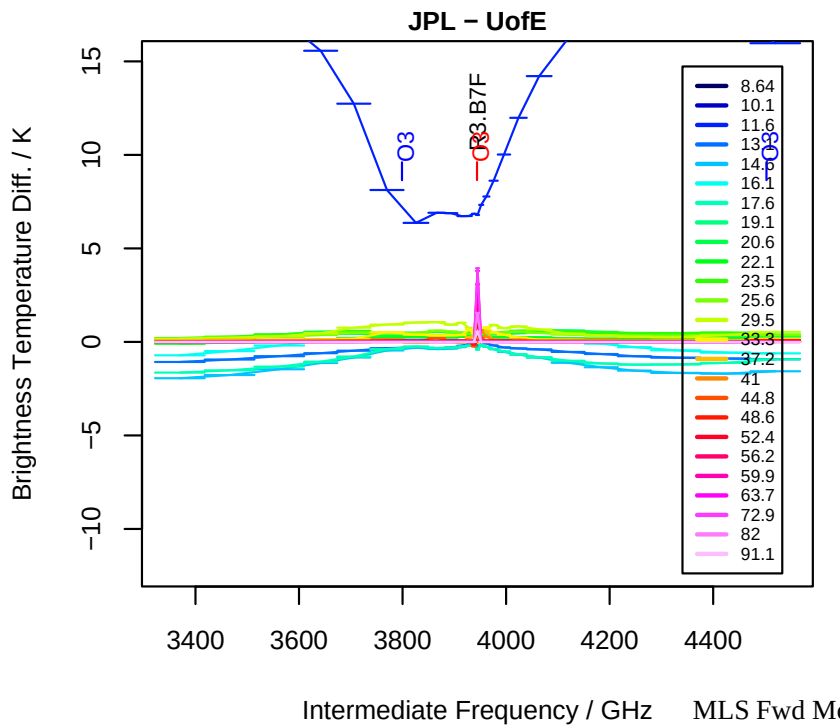

Band 7 (O_3) Mono + antenna

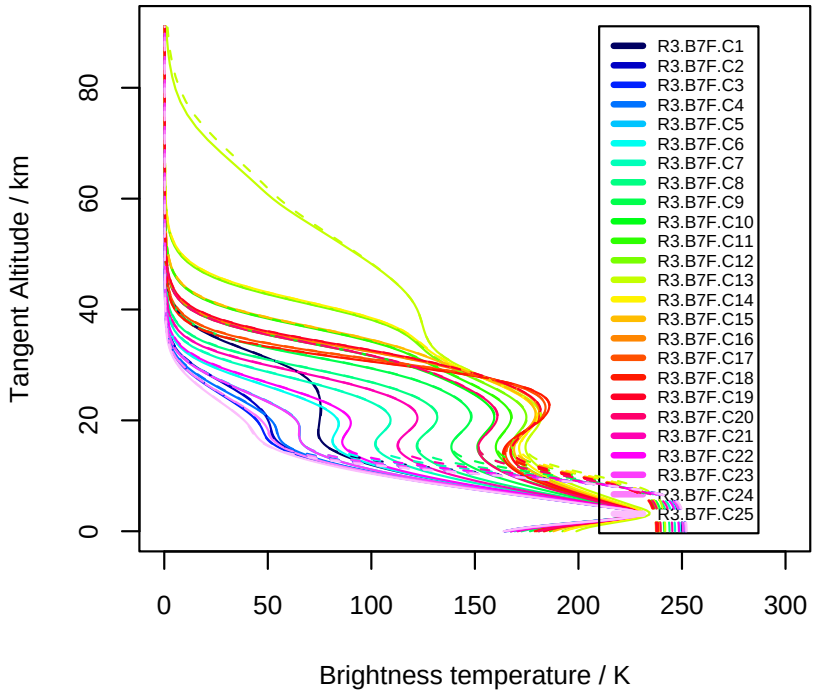

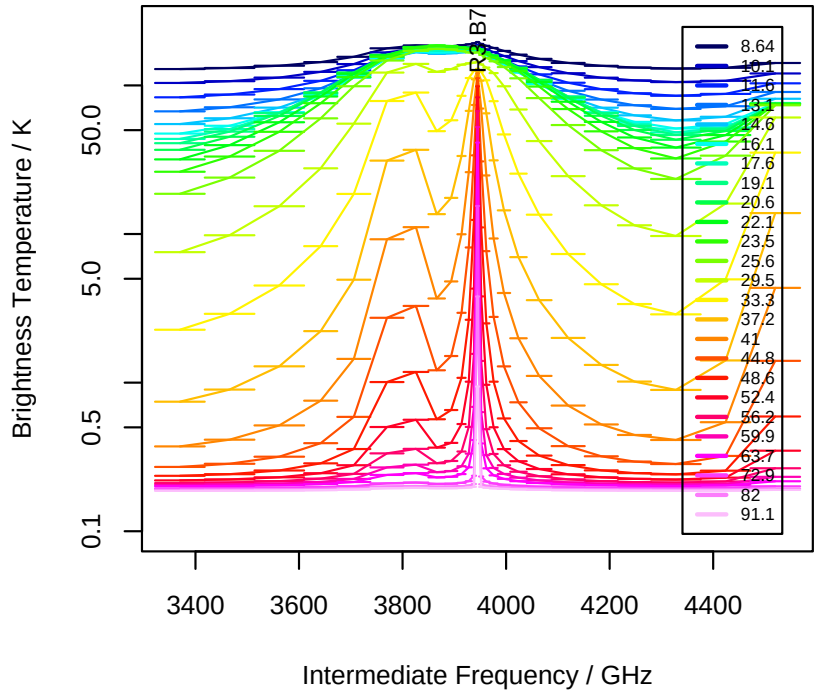

UoE again uses exactly the same lines as JPL. Antenna doesn't change differences much.

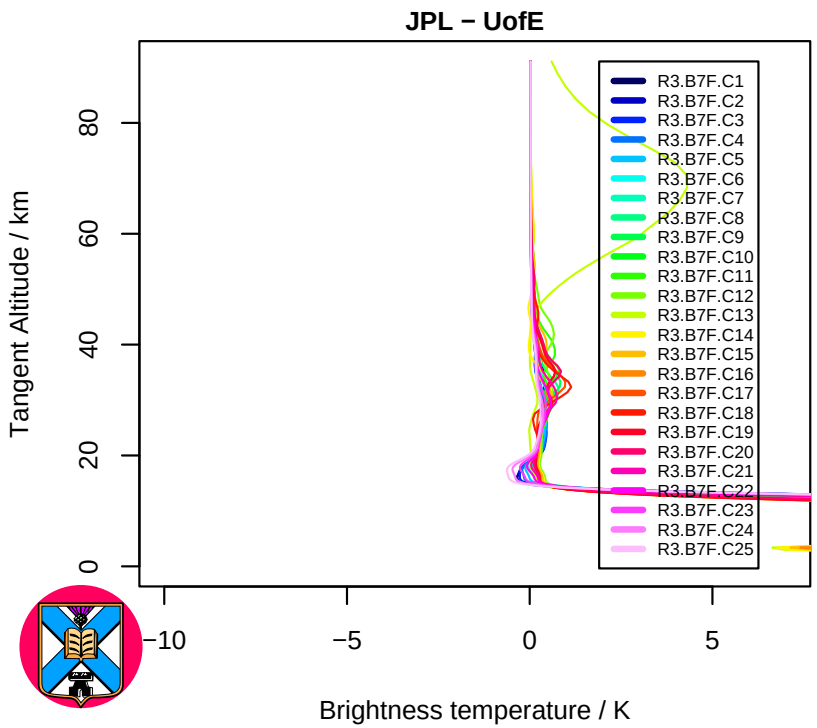

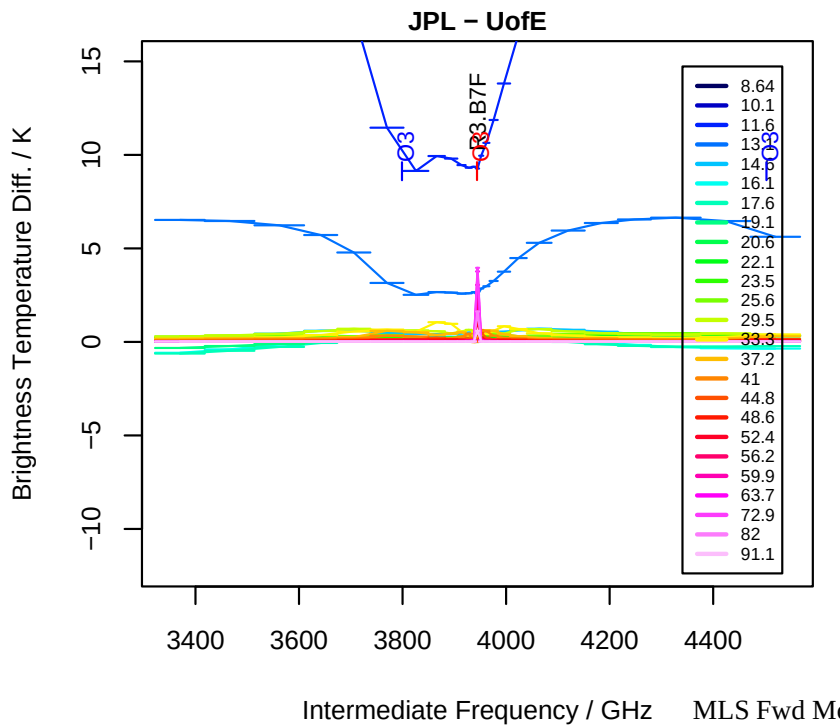

Band 7 (O_3) antenna + filters

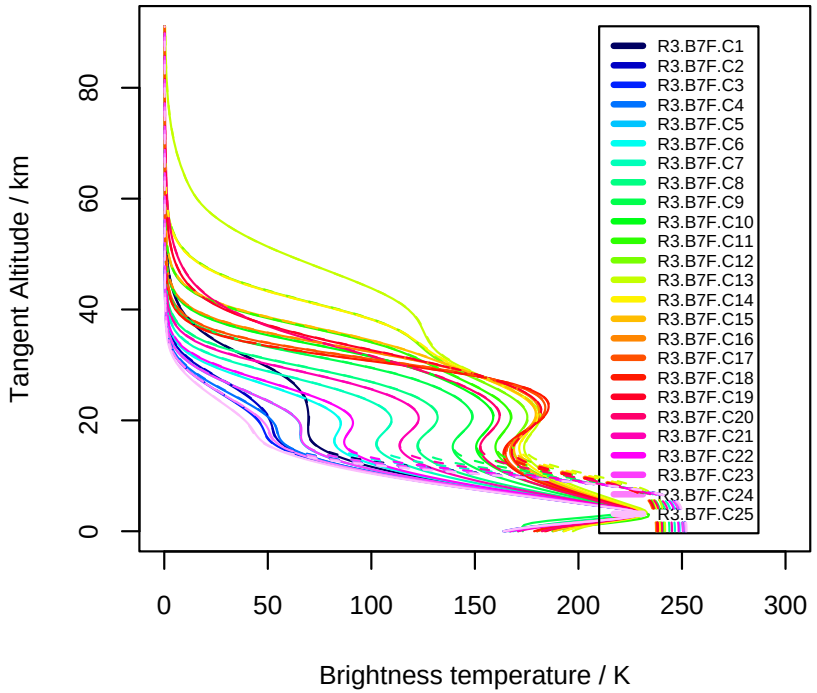

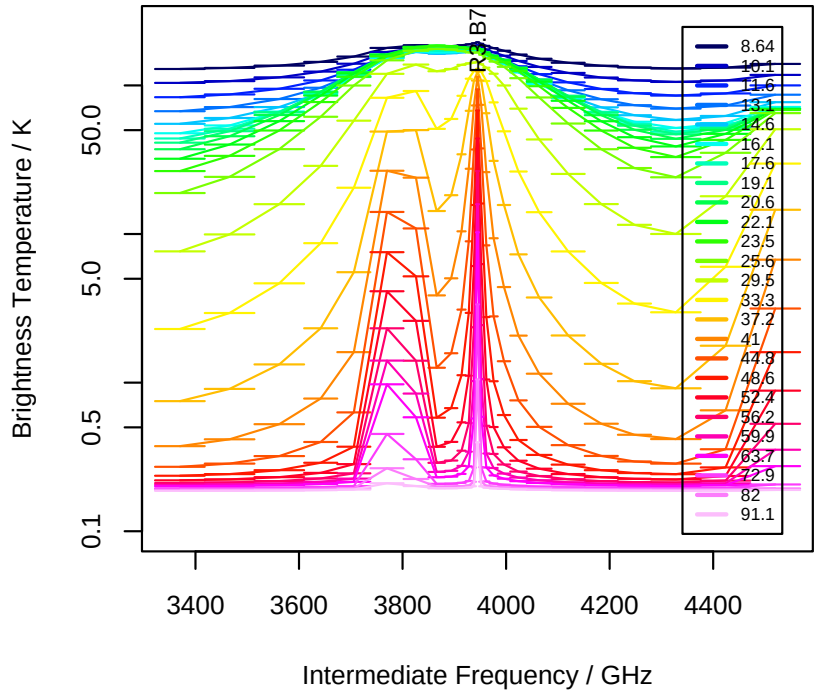

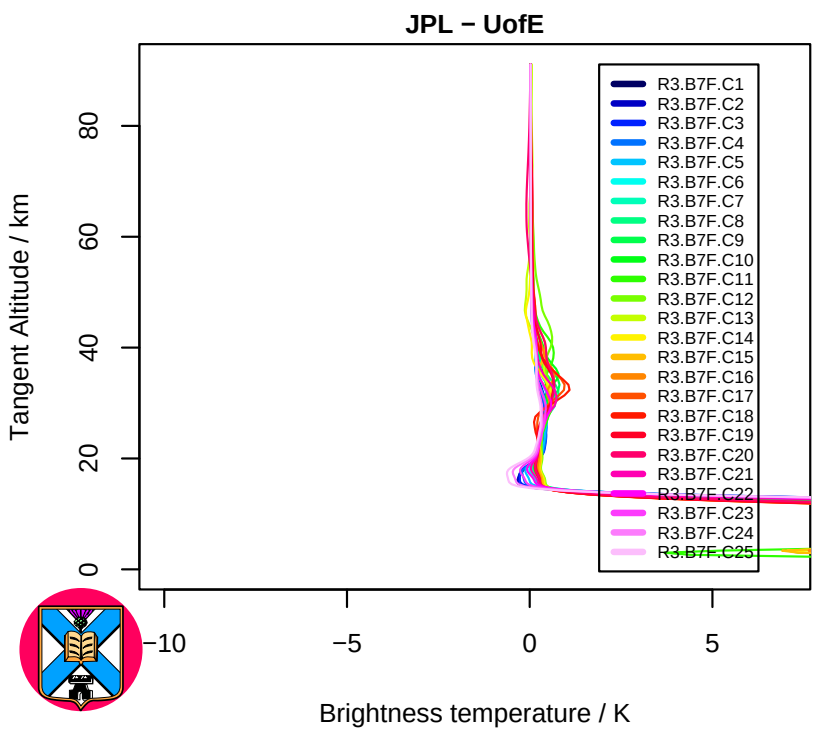

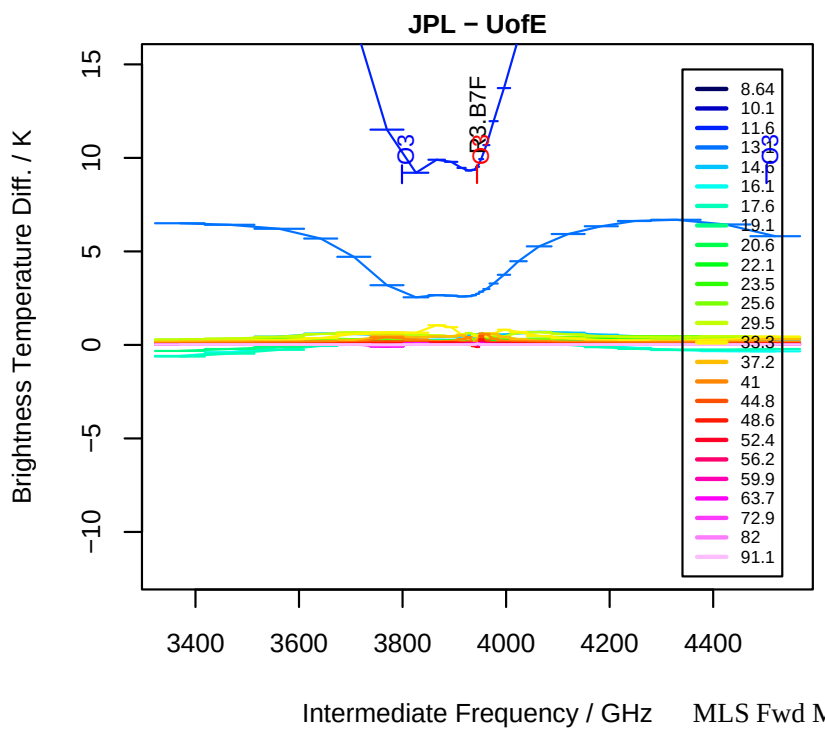

UoE again uses exactly the same lines as JPL. Filters change only line centre channel, which now agrees OK. (Errors in monochromatic case must affect only the very centre of the line.)

Band 13 (HCl) Monochromatic

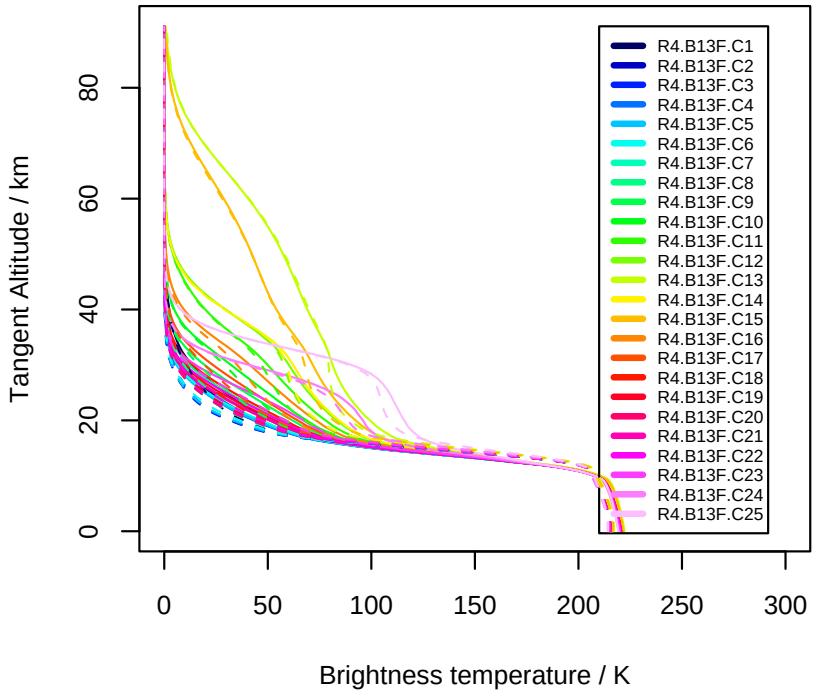

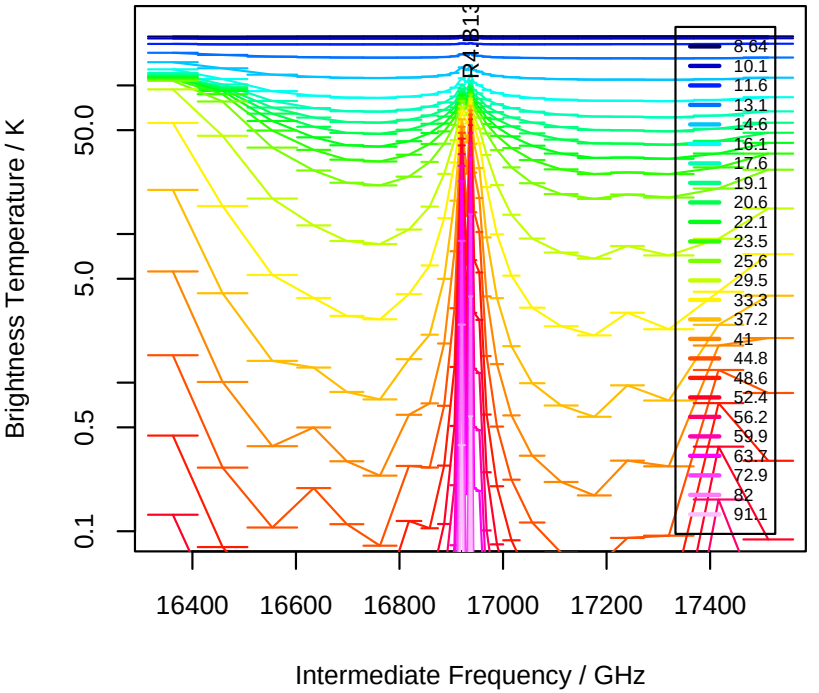

Large differences. Check lines again.

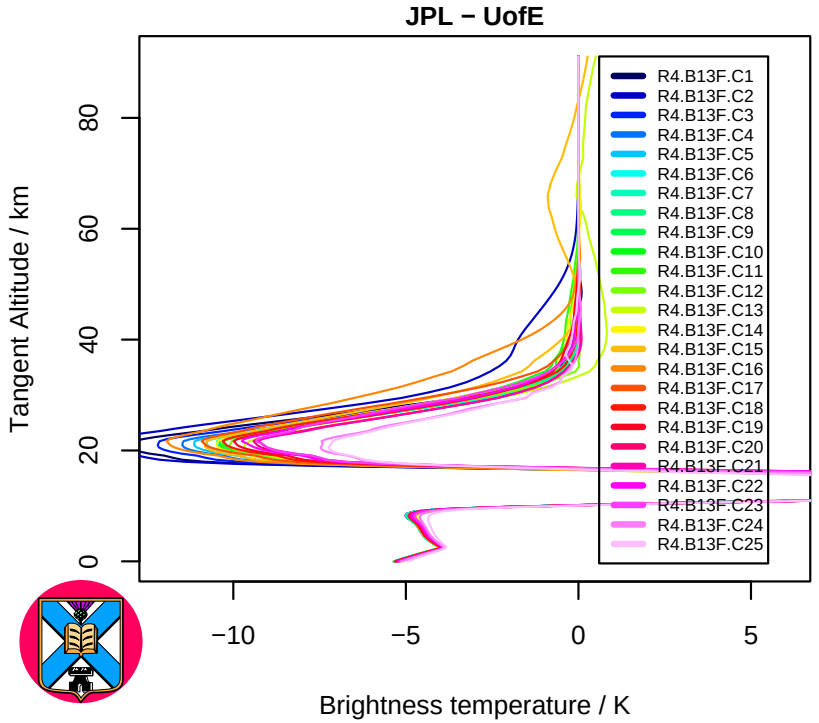

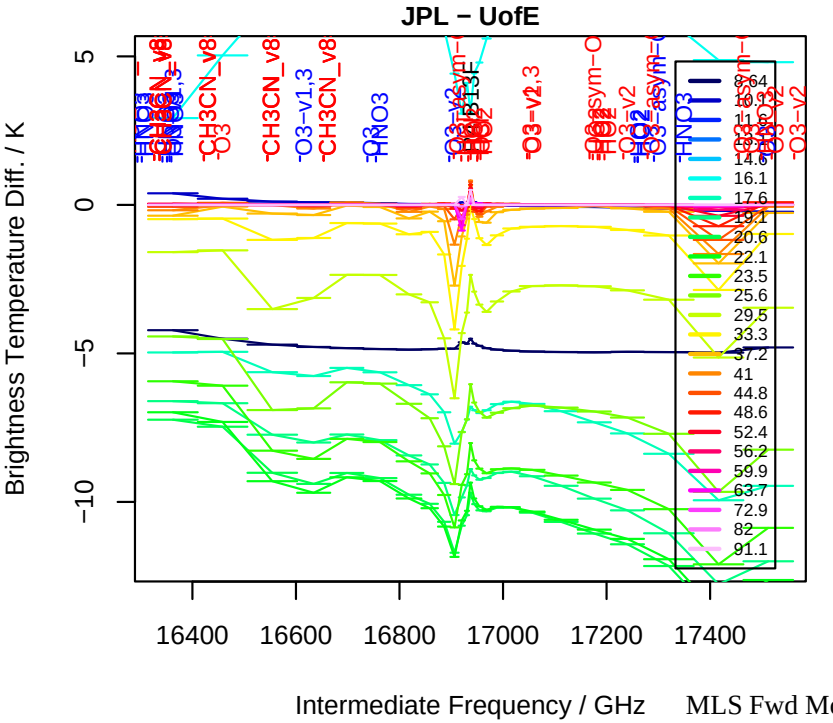

Spectral lines used: B13LF

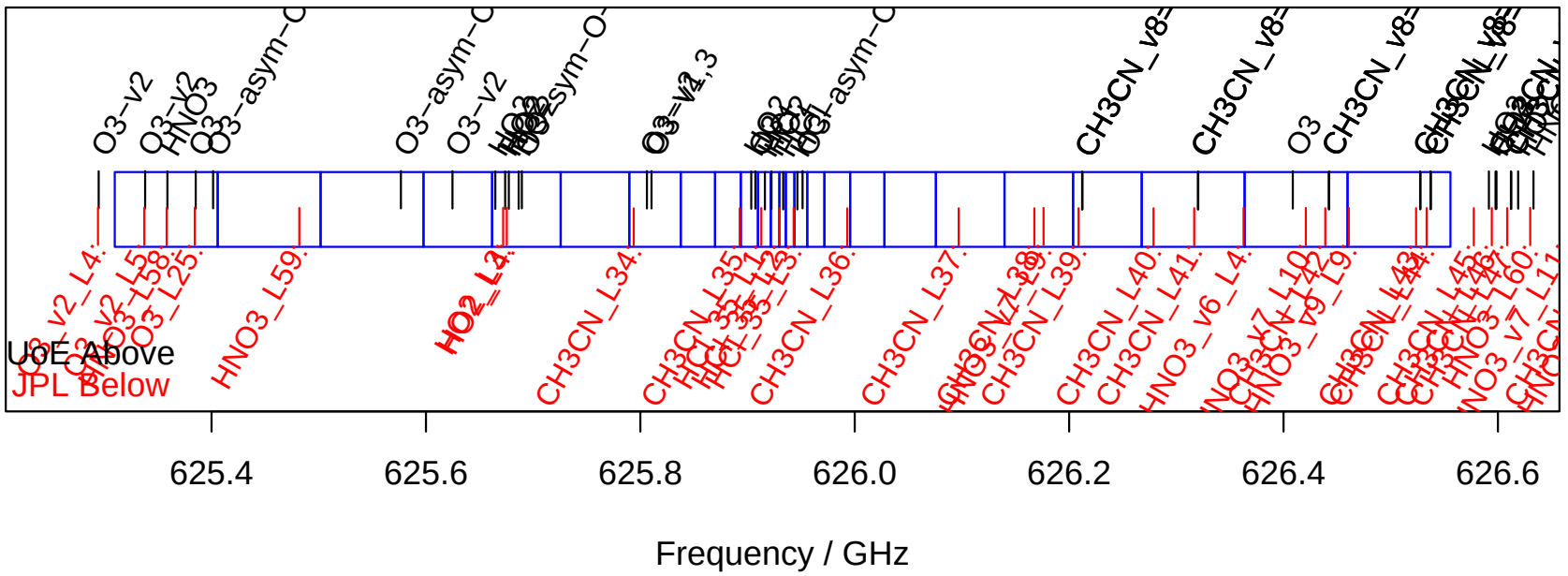

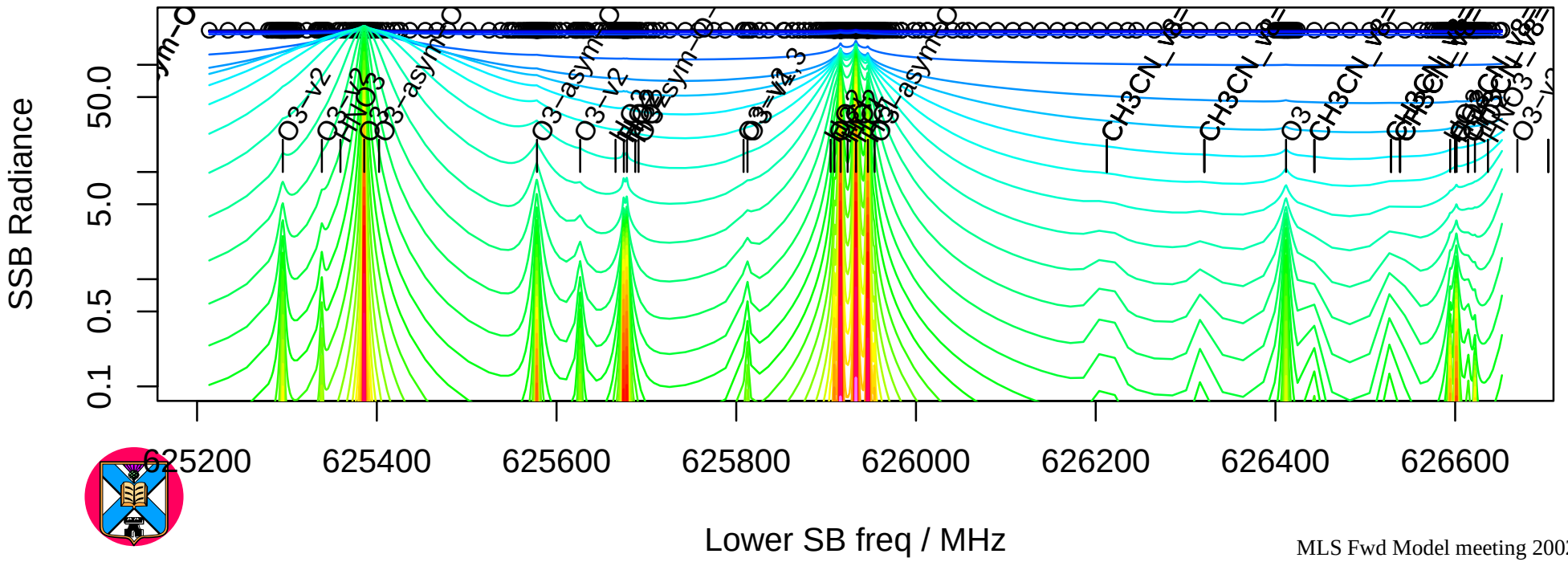

Band 13 (HCl) Monochromatic

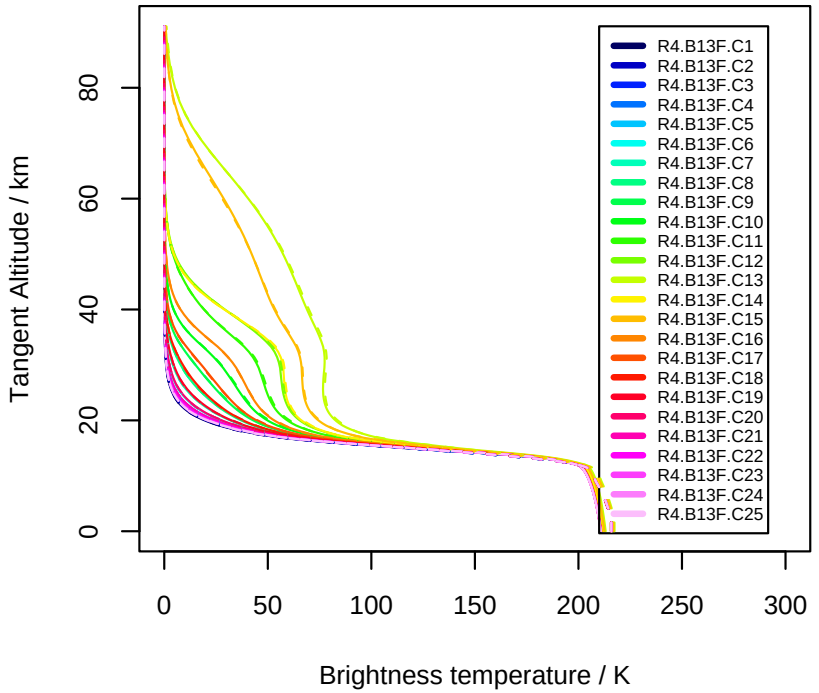

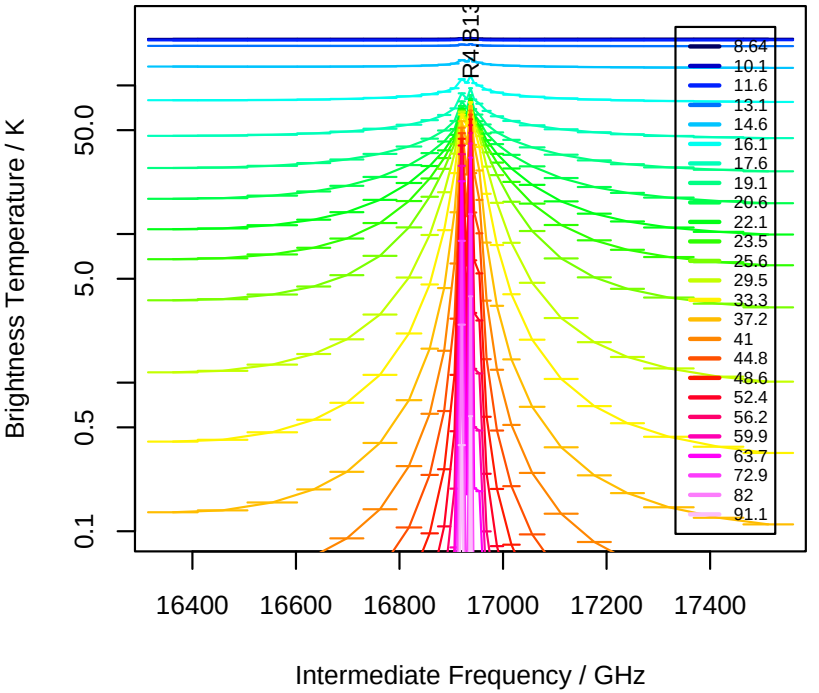

Only H_2O and HCl considered. Again we have differences of 0.5-1 K. Line shape???

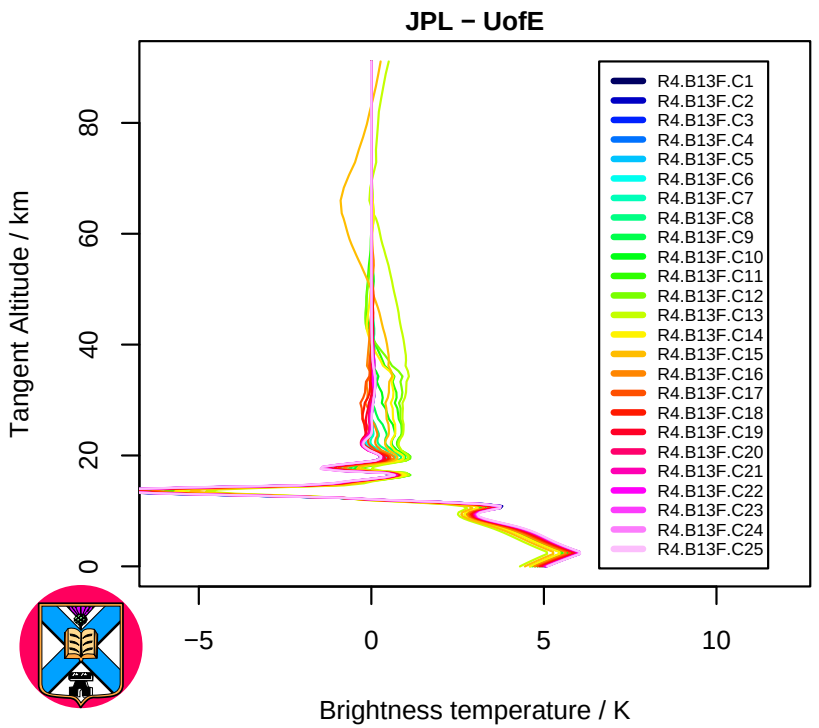

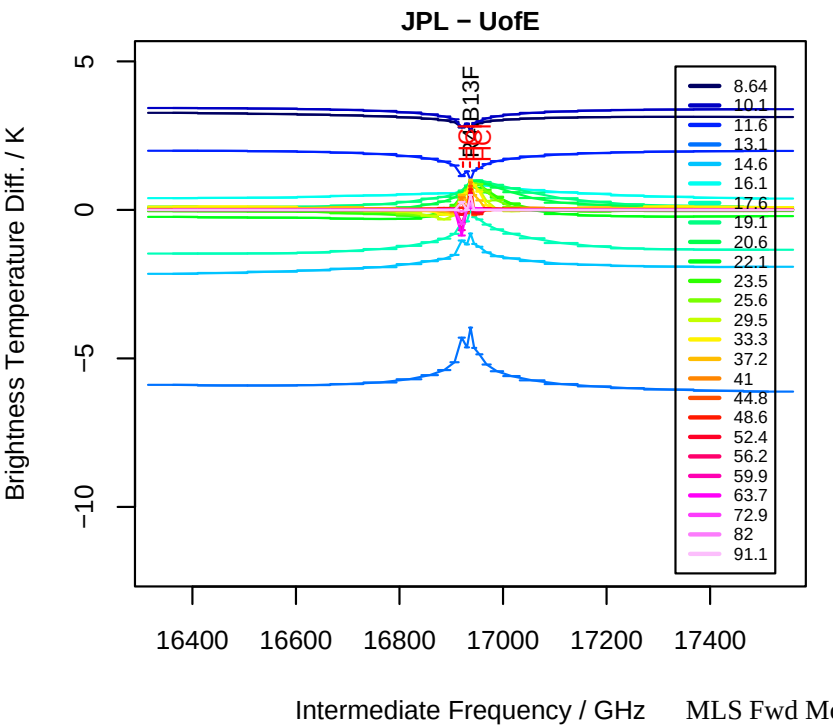

Band 13 (HCl) Monoc. + antenna

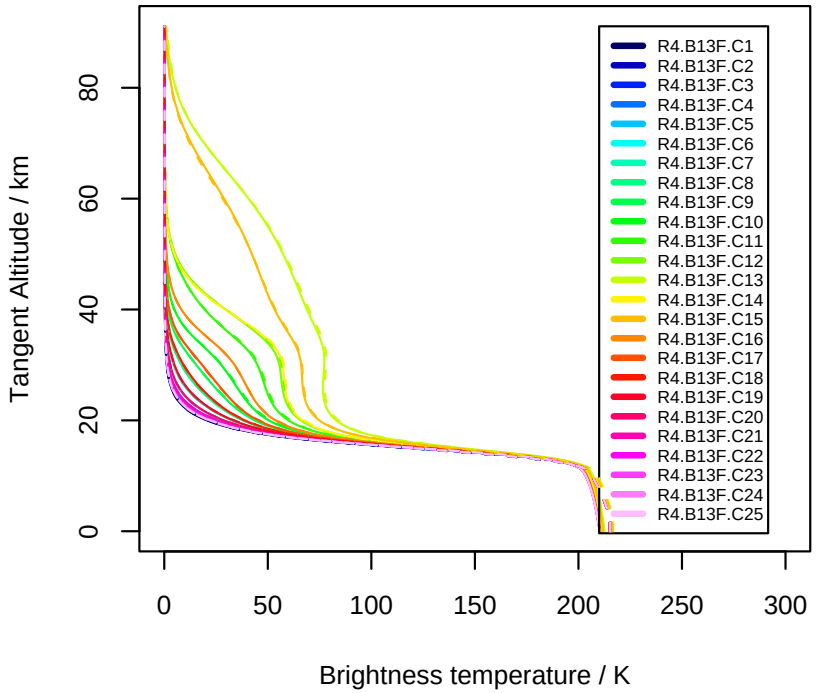

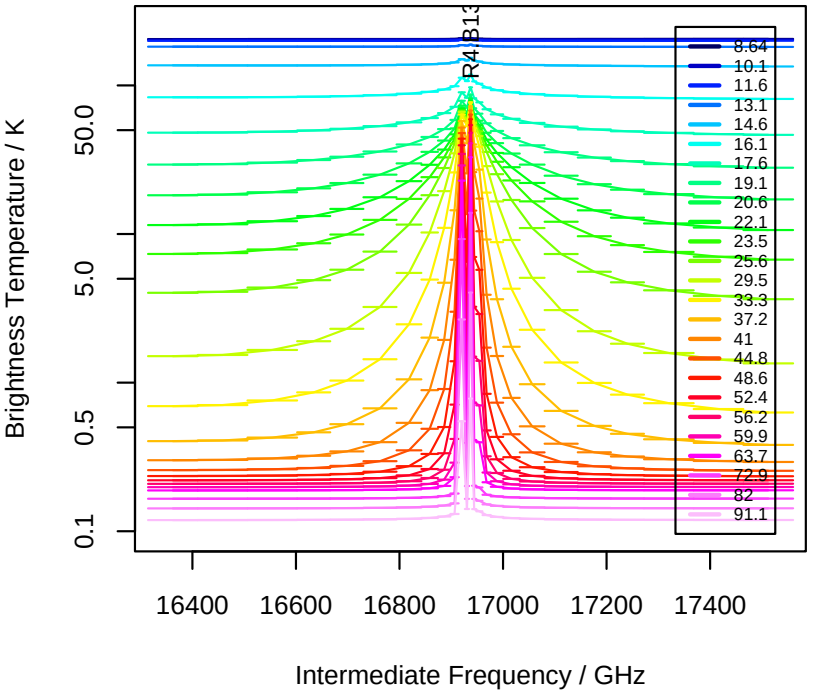

Antenna pattern narrower than R2 and R3. Effect on differences smaller.

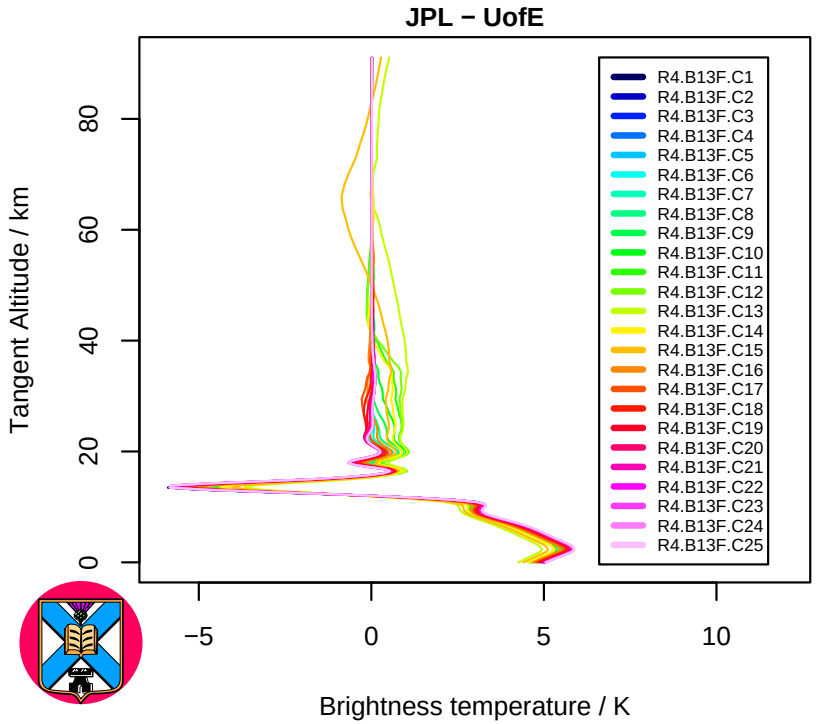

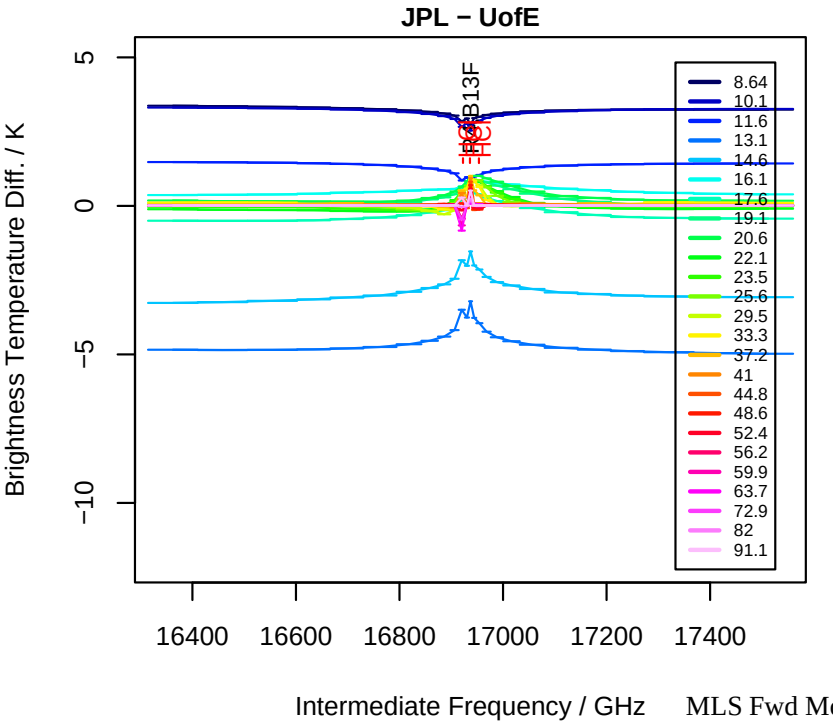

Band 1 (T/p) Monochromatic

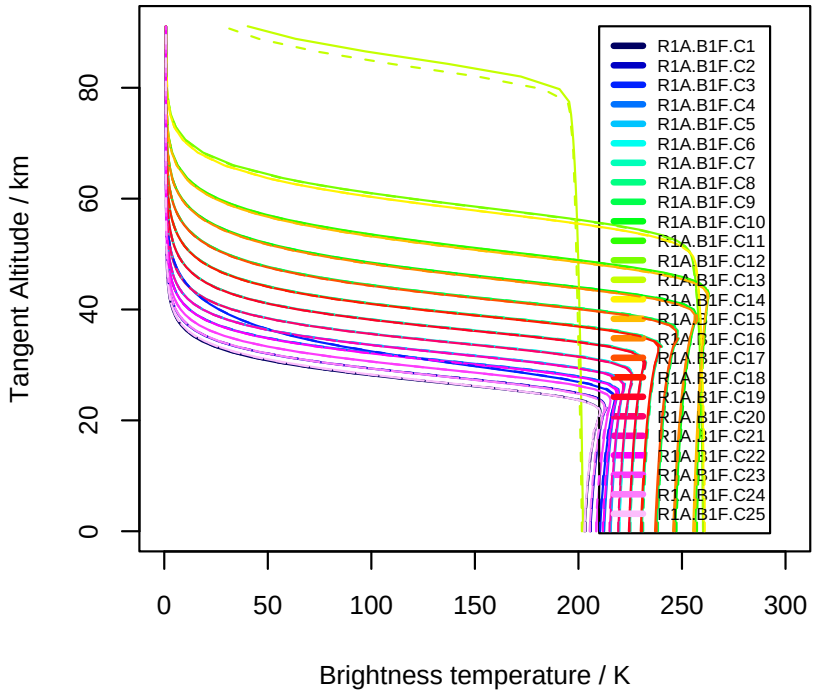

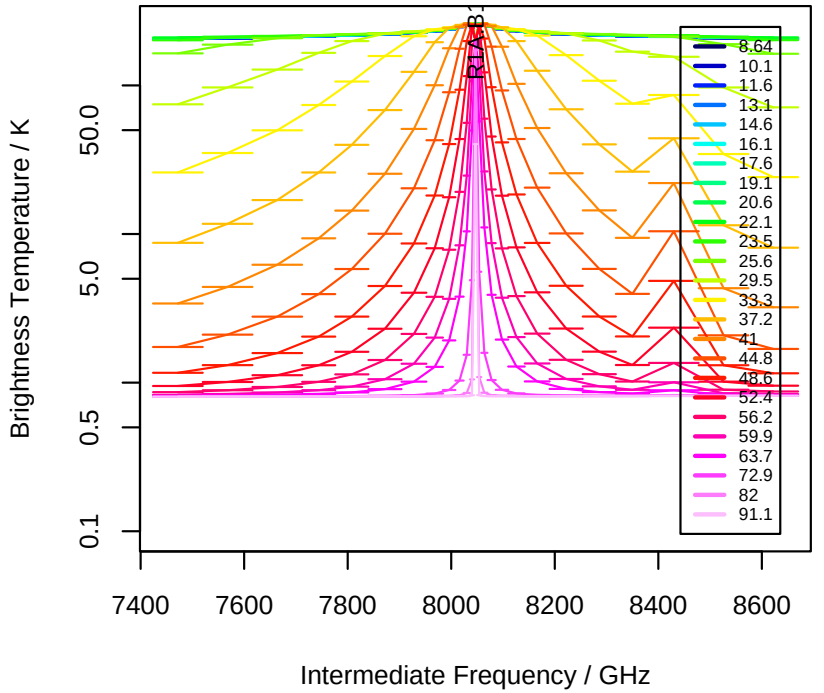

1 K difference probably same thing as the 0.5 K error in B2. (Remember B1 is SSB.)

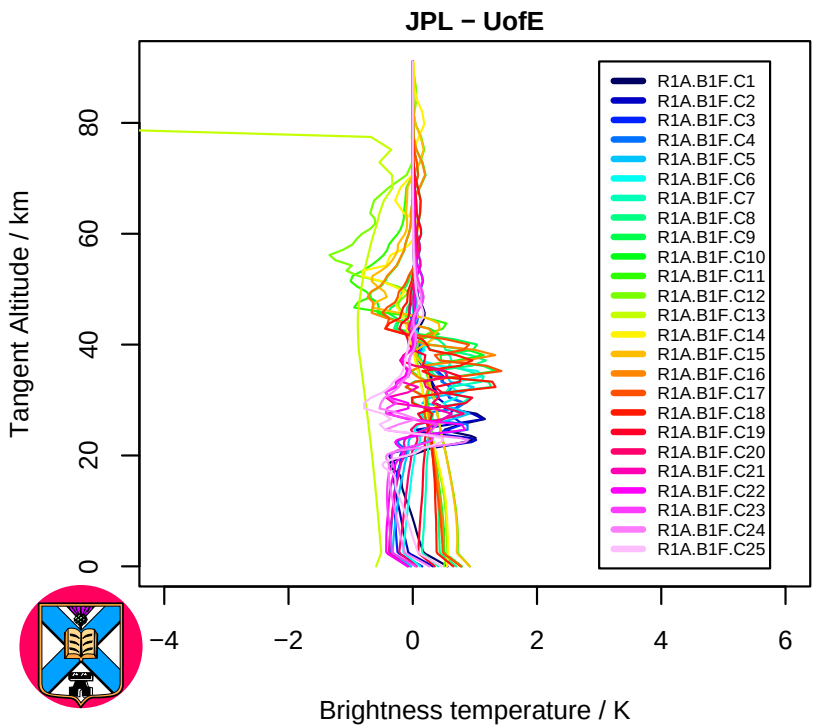

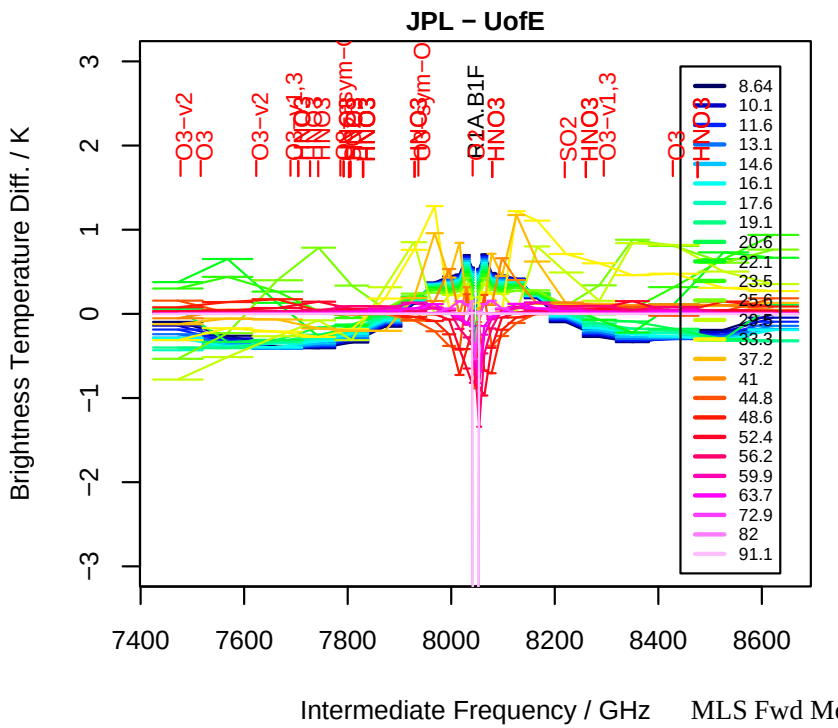

Band 1 (T/p) Mono + antenna

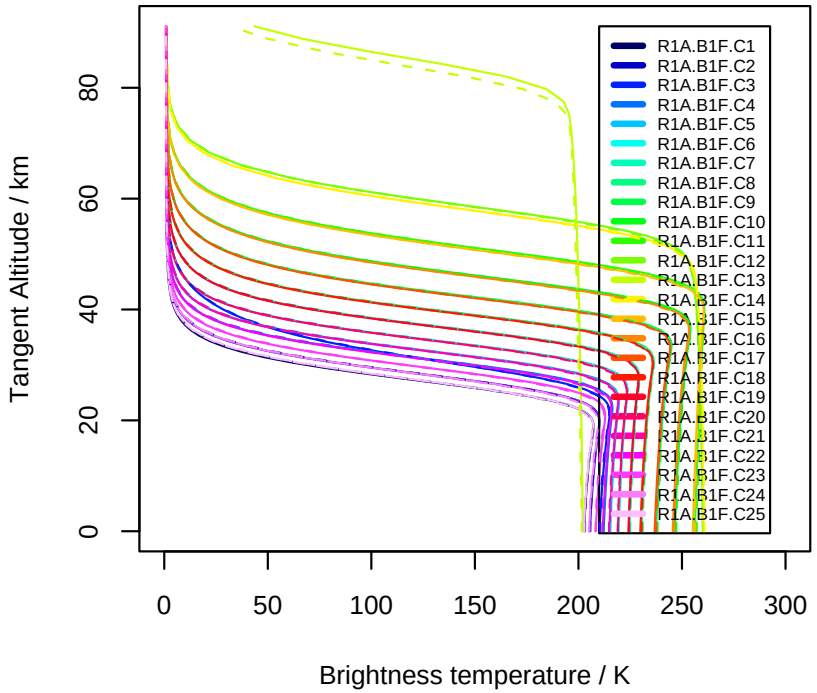

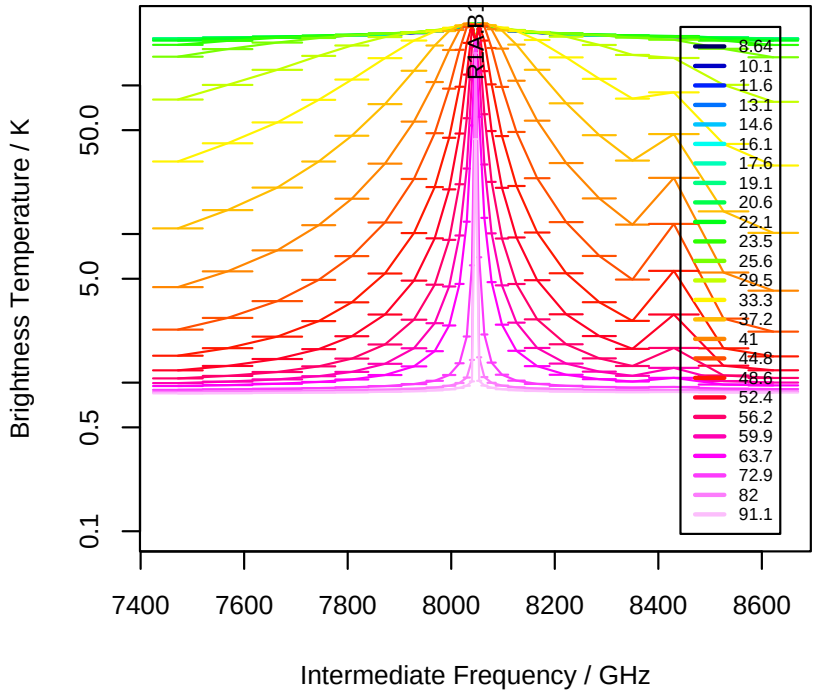

Antenna makes differences jump from 1 K to 2 K. This didn't happen in B2 or B7. Must double-check that we are using the same antenna data for both models.

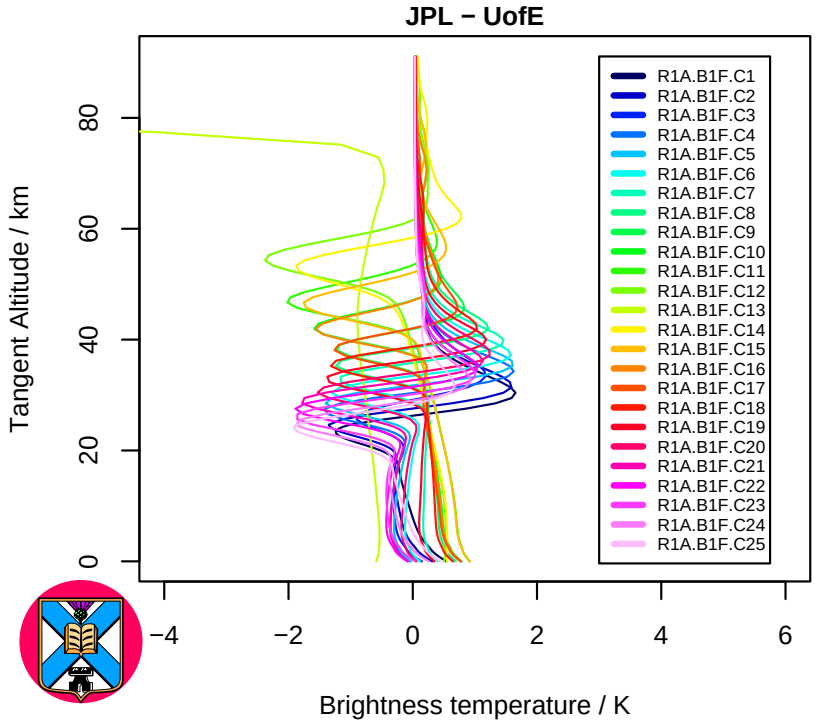

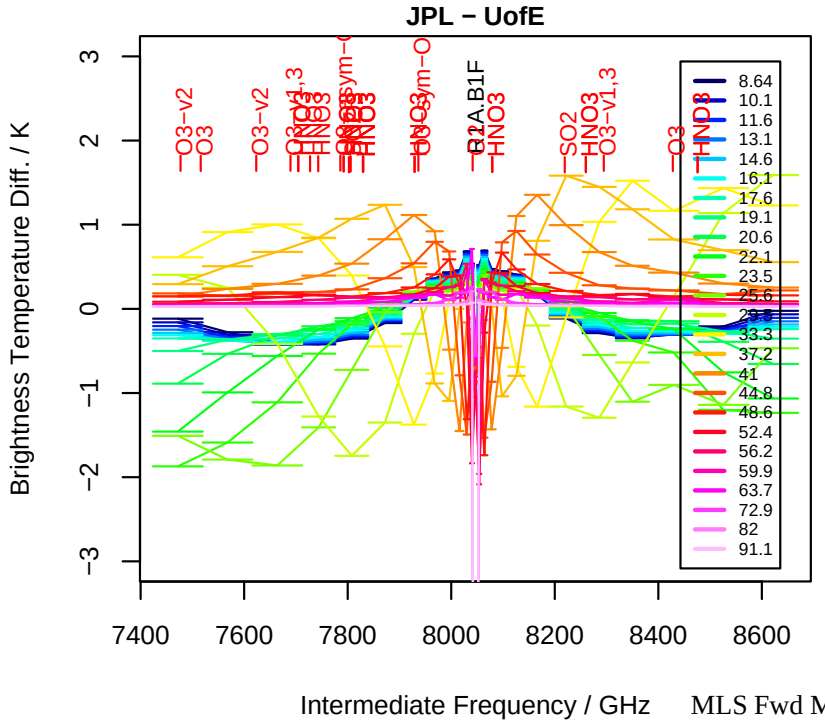

Conclusions

- The two FMs agree passably well
  - …but only if the spectral line data match up.
- It would be good if they agreed better
  - Need to audit the JPL spectroscopy file
  - Need to check H_2O line shape (and presumably others)
  - Need to check R1A.B1F antenna data.
- A problem area is the troposphere and lower stratosphere
  - That's because its much harder to know which lines to use
  - ... because the far wings of many lines affect the passband
  - and there are other spectrally flat emissions and absorptions too.
  - UoE Model needs to add logarithmic interpolation for H_2O

Clear-sky Forward Models Comparison

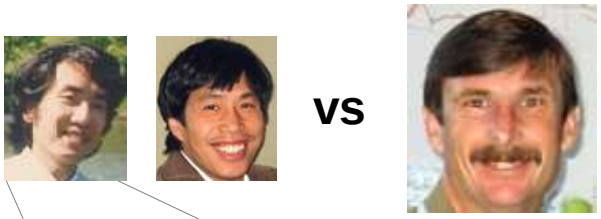

vs

Jonathan H. Jiang

MLS science meeting

December 11-12, 2002

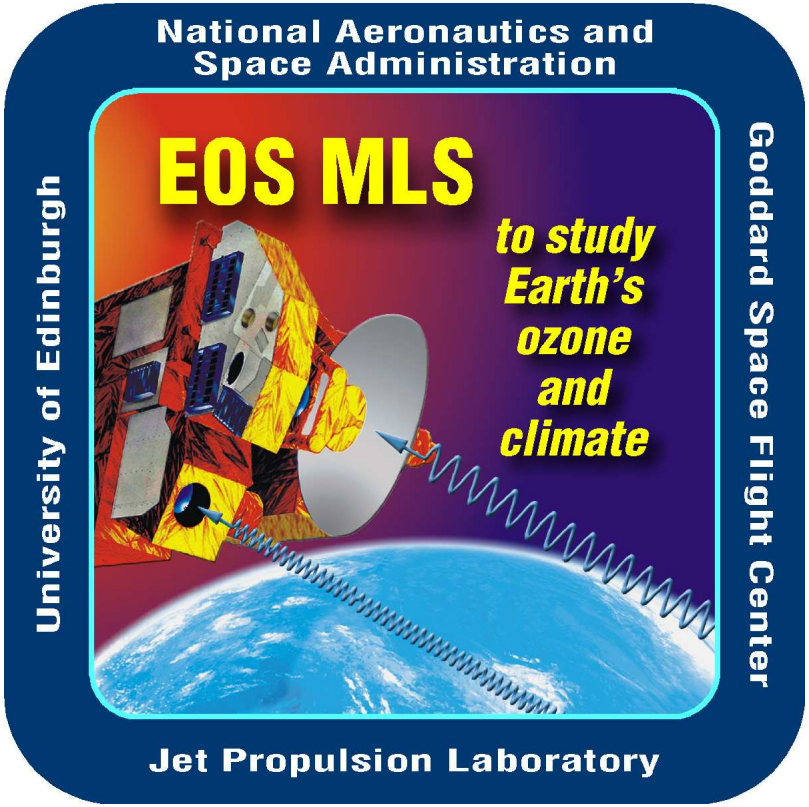

Clear-Sky Radiative Transfer Calculation

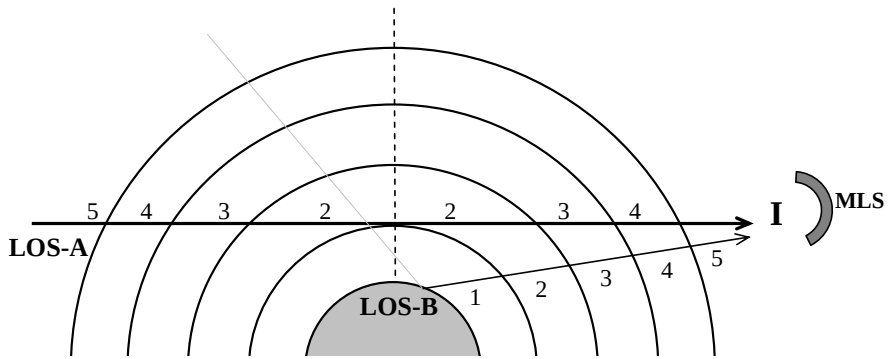

Cloud Forward Model

Model Levels: **N = 5** $\omega_0 = 0$

Model Layers: **L ≡ N–1 = 4** $\Delta s_n = (z_{n+1} - z_n)/\mu_n$

LOS-A

Downward:

$$I_5 = I_c$$
$$I_4 = I_5 e^{-\beta_4 \Delta s_4} + B_4 e^{-\beta_4 \Delta s_4}$$
$$I_3 = I_4 e^{-\beta_3 \Delta s_3} + B_3 e^{-\beta_3 \Delta s_3}$$
$$I_2 = I_3 e^{-\beta_2 \Delta s_2} + B_2 e^{-\beta_2 \Delta s_2}$$

Upward:

$$I_3 = I_2 e^{-\beta_3 \Delta s_3} + B_3 e^{-\beta_3 \Delta s_3}$$
$$I_4 = I_3 e^{-\beta_4 \Delta s_4} + B_4 e^{-\beta_4 \Delta s_4}$$
$$\mathbf{I} = I_4$$

LOS-B

$$I_1 = \varepsilon_s I_s + (1 - \varepsilon_s) I_2 + B_1 e^{-\beta_1 \Delta s_1}$$
$$I_2 = I_1 e^{-\beta_2 \Delta s_2} + B_2 e^{-\beta_2 \Delta s_2}$$
$$I_3 = I_2 e^{-\beta_3 \Delta s_3} + B_3 e^{-\beta_3 \Delta s_3}$$
$$I_4 = I_3 e^{-\beta_4 \Delta s_4} + B_4 e^{-\beta_4 \Delta s_4}$$
$$\mathbf{I} = I_4$$

Bill's Forward Model

(B_n in Cloud FWM is $(B_n+B_{n+1})/2$ in Bill's FWM)

LOS-A

$$\mathbf{I} = \frac{B_4 + B_5}{2} + \frac{B_3 - B_5}{2} e^{-\beta_4 \Delta s_4}$$
$$+ \frac{B_4 - B_2}{2} e^{-\beta_4 \Delta s_4 - \beta_3 \Delta s_3} + \frac{B_2 - B_3}{2} e^{-\beta_4 \Delta s_4 - \beta_3 \Delta s_3 - \beta_2 \Delta s_2}$$
$$+ \frac{B_3 - B_2}{2} \varepsilon_s e^{-\beta_4 \Delta s_4 - \beta_3 \Delta s_3 - \beta_2 \Delta s_2} + \frac{B_4 - B_2}{2} \varepsilon_s e^{-\beta_4 \Delta s_4 - \beta_3 \Delta s_3 - 2\beta_2 \Delta s_2}$$
$$+ \frac{B_5 - B_3}{2} \varepsilon_s e^{-\beta_4 \Delta s_4 - 2\beta_3 \Delta s_3 - 2\beta_2 \Delta s_2} + \left(I_c - \frac{B_4 + B_5}{2} \right) \varepsilon_s e^{-2\beta_4 \Delta s_4 - 2\beta_3 \Delta s_3 - 2\beta_2 \Delta s_2}$$

$$\varepsilon_s = 1.0$$

LOS-B

$$\mathbf{I} = \frac{B_4 + B_5}{2} + \frac{B_3 - B_5}{2} e^{-\beta_4 \Delta s_4} + \frac{B_2 - B_4}{2} e^{-\beta_4 \Delta s_4 - \beta_3 \Delta s_3}$$
$$+ \frac{B_1 - B_3}{2} e^{-\beta_4 \Delta s_4 - \beta_3 \Delta s_3 - \beta_2 \Delta s_2} + \frac{B_1 - B_2}{2} e^{-\beta_4 \Delta s_4 - \beta_3 \Delta s_3 - \beta_2 \Delta s_2 - \beta_1 \Delta s_1}$$
$$+ \frac{B_2 - B_1}{2} \varepsilon_s e^{-\beta_4 \Delta s_4 - \beta_3 \Delta s_3 - 2\beta_2 \Delta s_2 - \beta_1 \Delta s_1} + \frac{B_3 - B_1}{2} \varepsilon_s e^{-\beta_4 \Delta s_4 - \beta_3 \Delta s_3 - \beta_2 \Delta s_2 - 2\beta_1 \Delta s_1}$$
$$+ \frac{B_4 - B_2}{2} \varepsilon_s e^{-\beta_4 \Delta s_4 - \beta_3 \Delta s_3 - 2\beta_2 \Delta s_2 - 2\beta_1 \Delta s_1} + \frac{B_5 - B_3}{2} \varepsilon_s e^{-\beta_4 \Delta s_4 - 2\beta_3 \Delta s_3 - 2\beta_2 \Delta s_2 - 2\beta_1 \Delta s_1}$$
$$+ \left(I_c - \frac{B_4 + B_5}{2} \right) \varepsilon_s e^{-2\beta_4 \Delta s_4 - 2\beta_3 \Delta s_3 - 2\beta_2 \Delta s_2 - 2\beta_1 \Delta s_1}$$

$$\varepsilon_s \le 1.0$$

Gas Absorption Coefficient Calculation

Cloud Forward Model

$$\beta_{gas} = \beta_{dry} + \beta_{wet} + \beta^{line}$$

$$\beta_{dry} = \frac{0.042 S_d \nu^2}{w_d[1+(\nu/w_d)^2]} + A_{dry}(\nu)$$

$S_d = 6.14 \cdot 10^{-4} p(300/T)^2$ **Debye strength**

$w_d = 5.6 \cdot 10^{-3}(p_d + 1.1e)(300/T)$ **Debye width**

$A_{dry}(\nu) = 0.65 \times 10^{2\log_{10}(p/1013)}(300/T)^2 \nu^2 \alpha_{N_2-N_2}(\nu)$ **Collision-induced abs**

$\alpha_{N_2-N_2}(\nu) = [a_1 e^{-c_1(300/T)\nu^2} + a_2 e^{-c_2(300/T)\nu^2}(d^2+\nu^2)](300/T)^b$

$a_1 = 7.7 \text{ x } 10^{-10}$ $a_2 = 1.0 \text{ x } 10^{-13}$
$b = 1.7$ $c_2 = 1.0 \text{ x } 10^{-4}$
$c_1 = 1.5 \text{ x } 10^{-3}$ $d = 60$

$$\beta_{wet} = 7.53 \times 10^{-16}(300/T)^{4.2}\nu^2 pe + 1.40 \times 10^{-14}(300/T)^{6.18}\nu^2 e^2$$

$$\beta^{line} = (10^{-12}) n F(\nu, \nu_{ul}) \Im_{ul} \frac{\nu}{\nu_{ul}} \frac{e^{-E_i/kT}(1-e^{-h\nu_{ul}/kT})}{e^{-E_i/300k}(1-e^{-h\nu_{ul}/300k})} \frac{Q_{rs}(300)}{Q(T)}$$

$$F(\nu,\nu_{ul}) = \frac{1}{\pi}\frac{\nu}{\nu_{ul}}\left[\frac{\Delta\nu - Y_k(\nu_{ul}-\nu)}{(\nu_{ul}-\nu)^2+\Delta\nu^2} + \frac{\Delta\nu - Y_k(\nu_{ul}+\nu)}{(\nu_{ul}+\nu)^2+\Delta\nu^2}\right]$$ **Line-shape**

$Y_k = p[\delta_k(300/T)^{0.8} + \gamma_k(300/T)^{1.8}]$ **Interference-Coeff.**

$\delta_k = a_4 \times 10^{-3} p(300/T)^{a_5}$

$\gamma_k = a_3 \times 10^{-3}[p(300/T)^{0.8-a_6} + 1.1e(300/T)]$

Molecules included: $H_2O, O_3, N_2O, O^{18}O, H_2^{18}O, O_2$

Bill's Forward Model

$$\beta_{gas} = \beta_{dry} + \beta_{wet} + \beta^{line}$$

$$\beta_{dry} = f_{O_2}\frac{6.87 \times 10^{-9}\nu^2 p^2 (300/T)^{2.8}}{\nu^2 + [0.56p(300/T)^{0.8}]^2} + A_{dry}(\nu)$$

$$A_{dry}(\nu) = f_{N_2}^2 \times p^2\nu^2(300/T)^{3.7}[6.918\times10^{-20} e^{[-1.669\times10^{-12}\nu^2(300/T)]} + 9.997\times10^{-33} e^{[-1.113\times10^{-13}\nu^2(300/T)]}(1.798\times10^6+\nu^2)]$$

$f_{O_2} = 0.2095$, $f_{N_2} = 1.29 \times 0.79^2$, units are hPa, km, MHz, K

$$\beta_{wet} = f_{H_2O}[A\nu^2 p^2 (300/T)^B + 5.967\times10^{-16}\nu^2 p^2 (300/T)^3]$$

A, B depend on Radiometer (Page 51 of Bill's ATBD)

$$\beta^{line} = f_{H_2O}\sum_{i=1}^{lines}\sqrt{\frac{\ln 2}{\pi}}\frac{10^{-6}}{k}\frac{p}{Tw_d}10^{S_i}\left(\frac{\nu}{\nu_i}\right)^2\left(\frac{1}{\pi}\int_{-\infty}^{\infty}\frac{y_i - Y_i(x_i-t))e^{-t^2}}{y_i+(x_i-t)^2}dt + \frac{1}{\sqrt{\pi}}\frac{y_i - Y_i z_i}{z_i^2+y_i^2}\right)$$

S_i is Eq 9.1 in Bill's ATBD

$$x_i = \frac{\sqrt{\ln 2}(\nu_i - \nu)}{w_d}, \quad y_i = \frac{\sqrt{\ln 2} w_{ci} p}{w_d}, \quad z_i = \frac{\sqrt{\ln 2}(\nu_i+\nu)}{w_d}$$

$$\nu_i = \nu_{0i} + \Delta\nu_{0i} p(300/T)^{n\Delta\nu_{oi}}; \quad w_d = 3.58117369\times10^{-7}\nu\sqrt{\frac{T}{M}}$$

Model Components and Structure in EOS MLS L2 Software

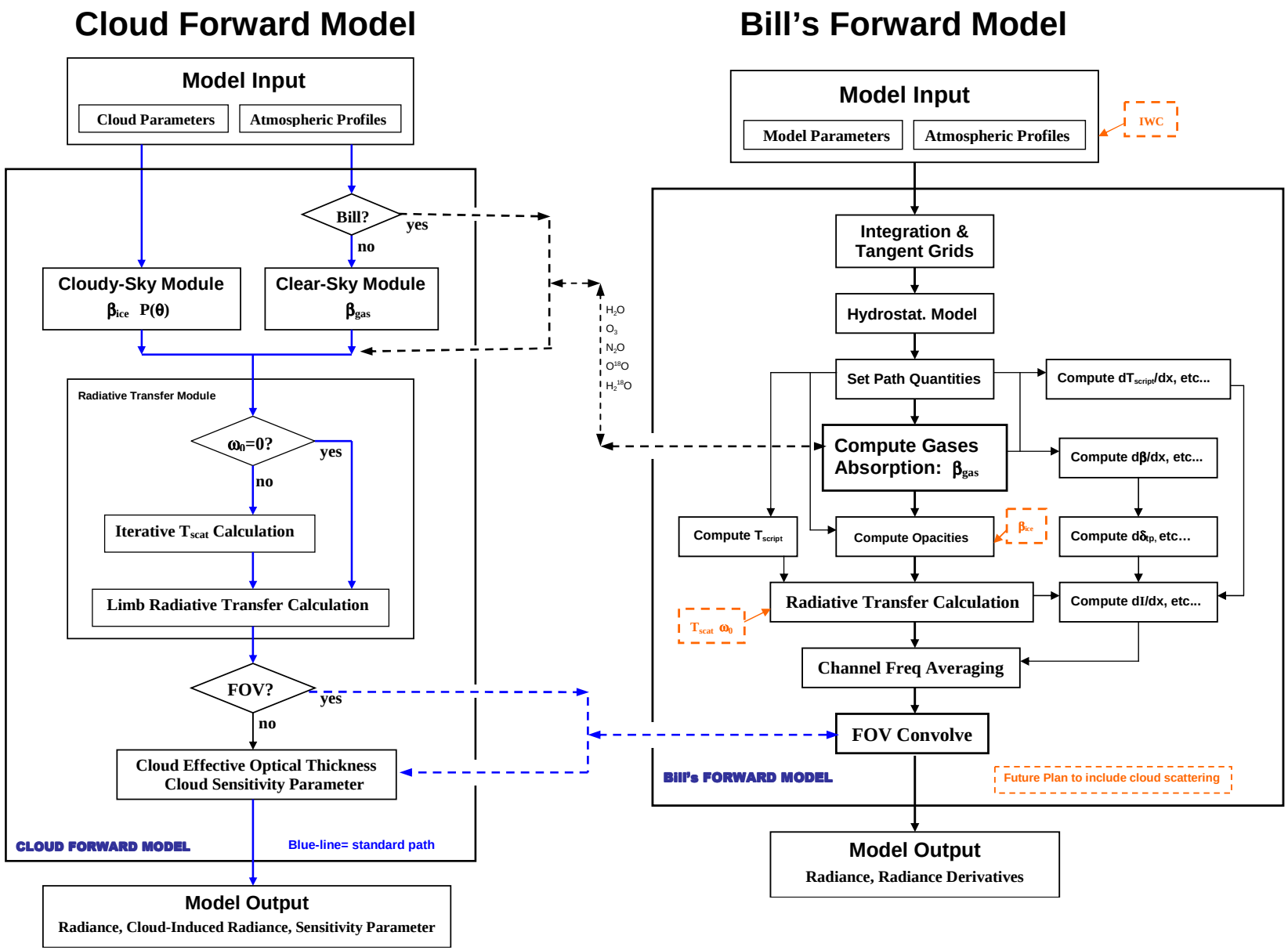

Comparisons Between CFM Clear-Sky T_b to Bill's Clear-Sky T_b

R1A

Clear-Sky Radiances (K)

Differences CFM – Bill

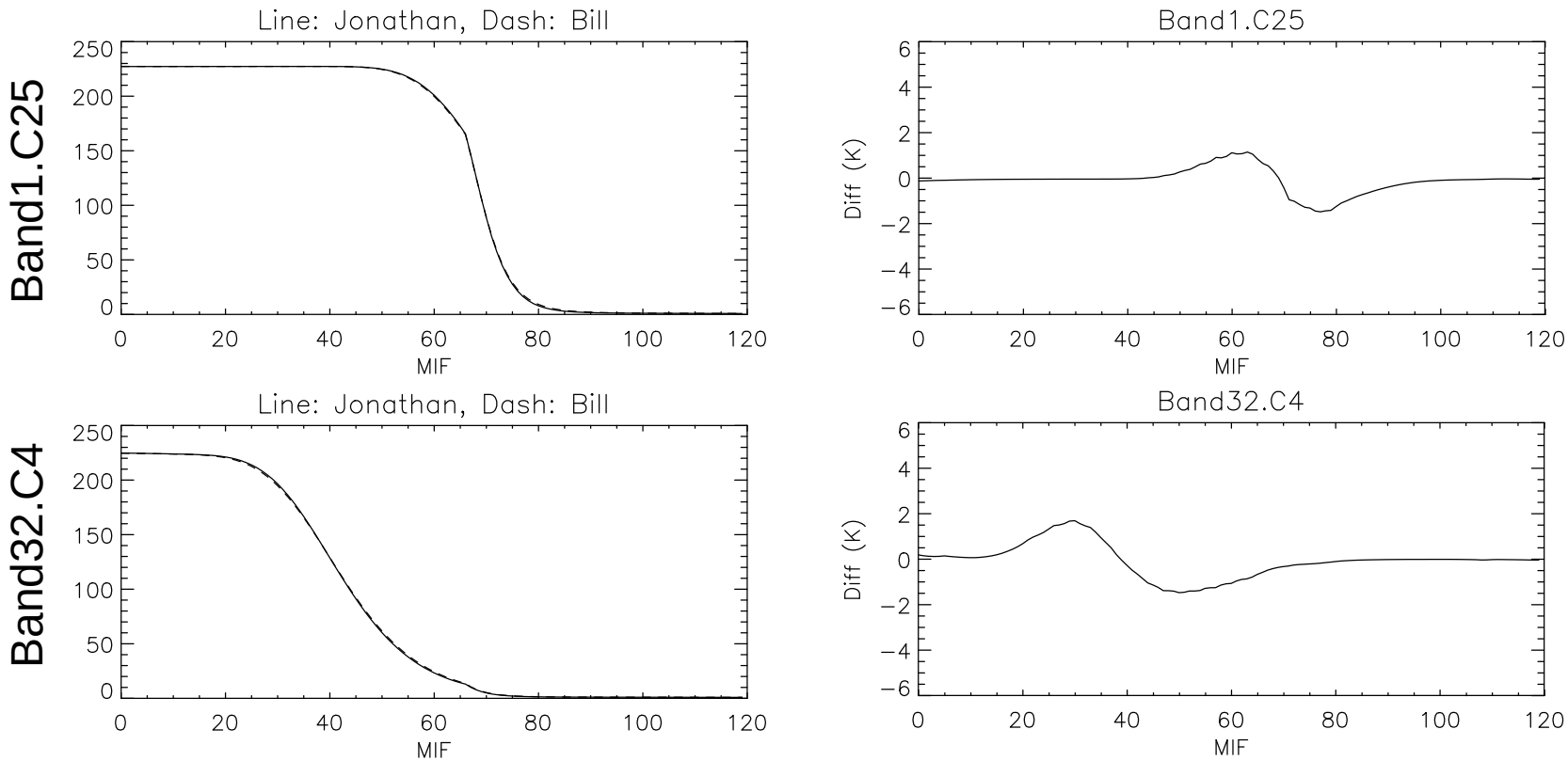

~jonathan/emls/clear/radiances

R2

Clear-Sky Radiances (K)

Differences CFM – Bill

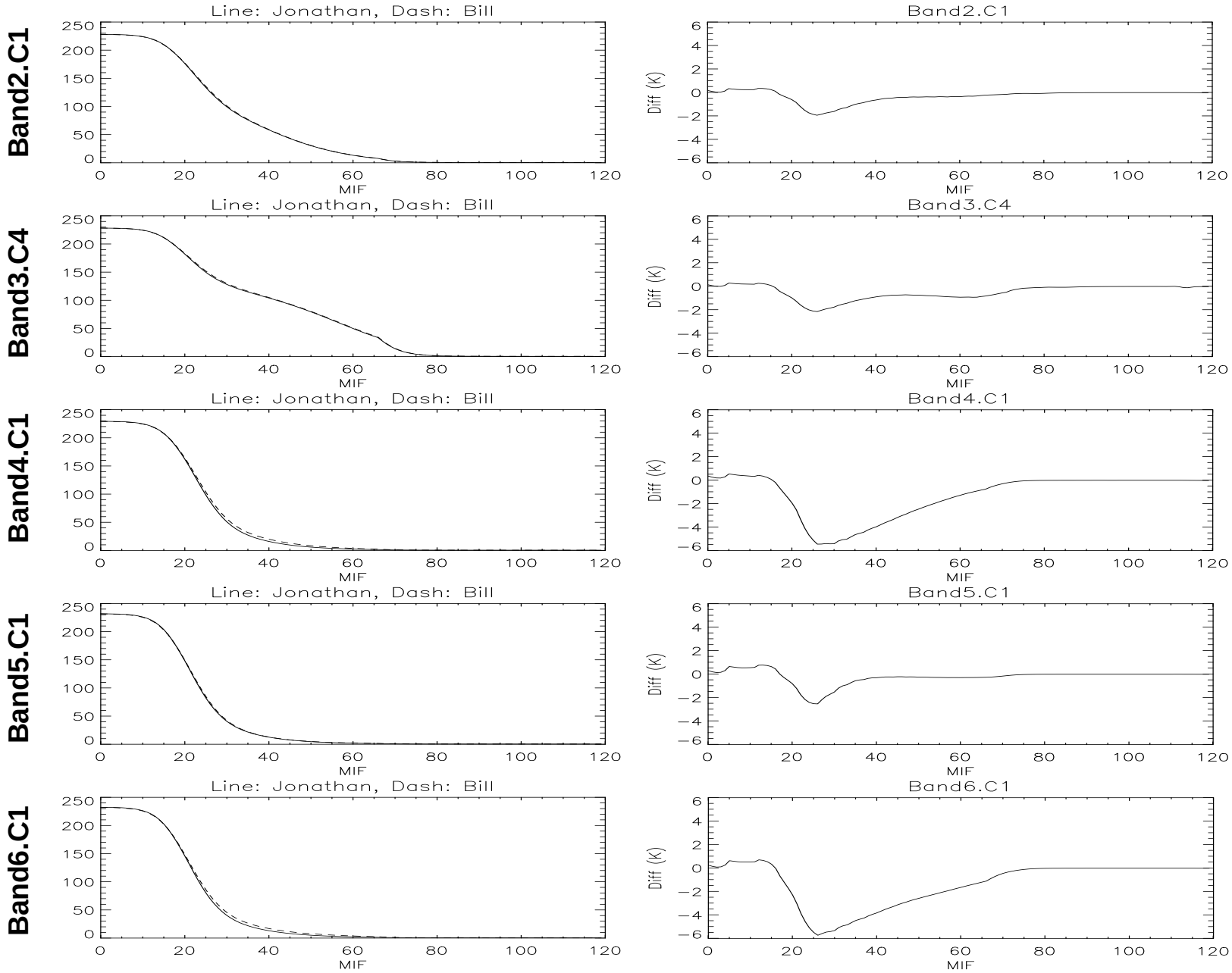

Differences (CFM-Bill) in T_b from SIDS simulation (day51)

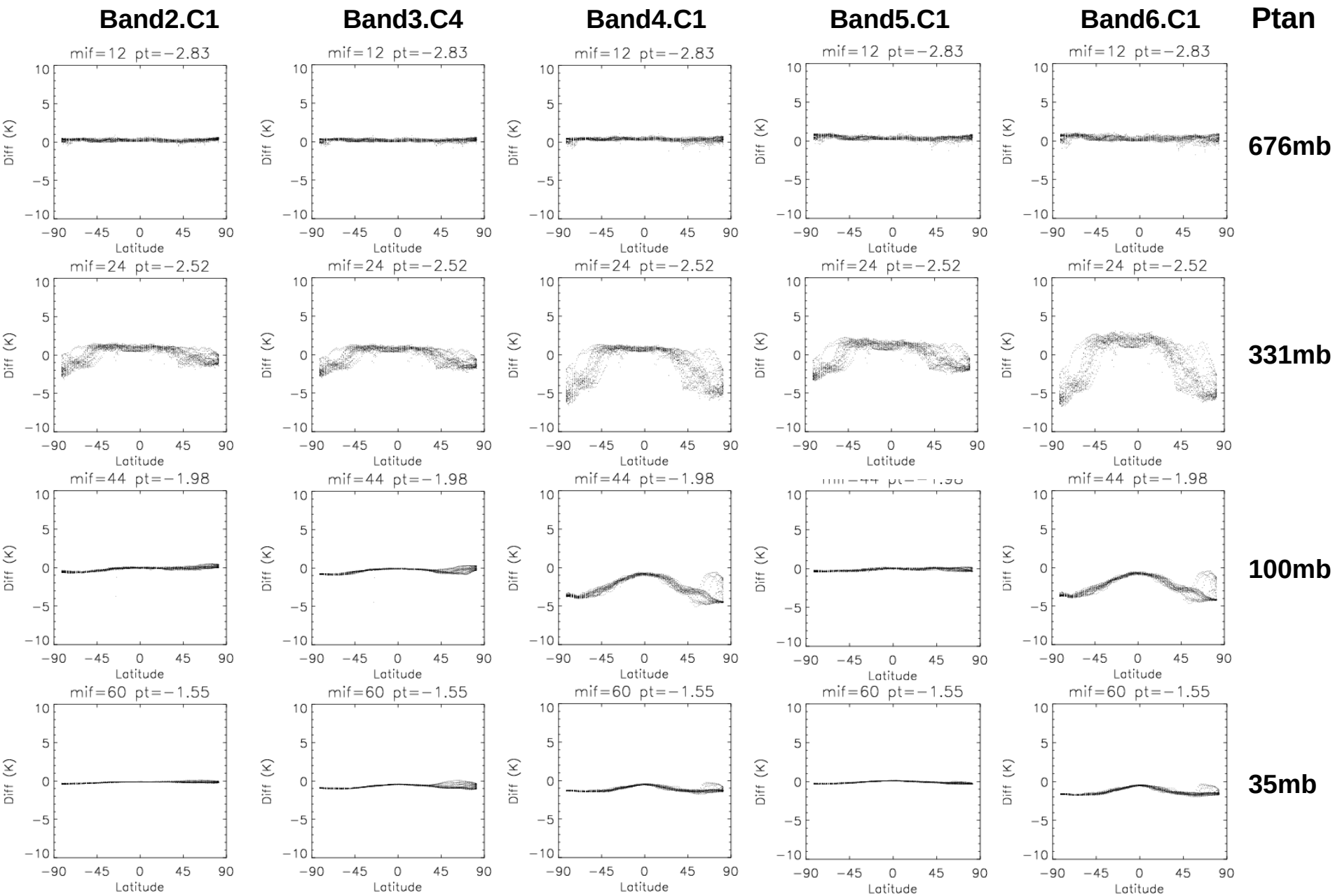

Band1.C25 **Band32.C4** **Ptan**

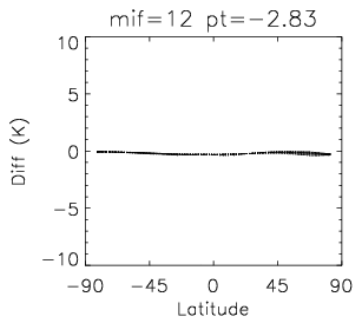

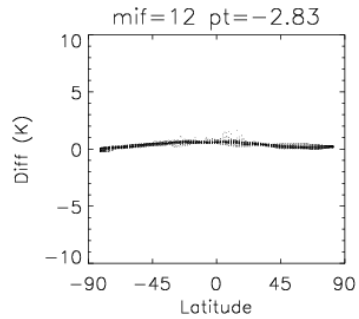

676mb

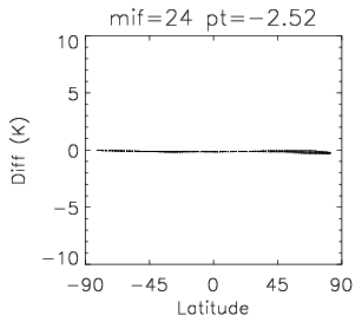

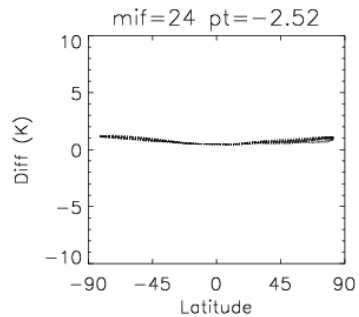

331mb

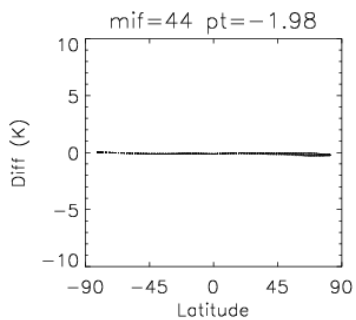

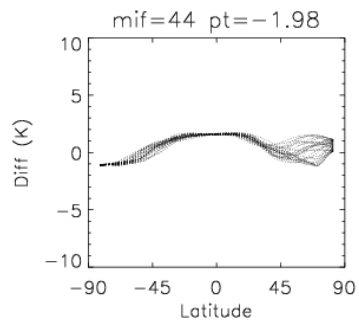

100mb

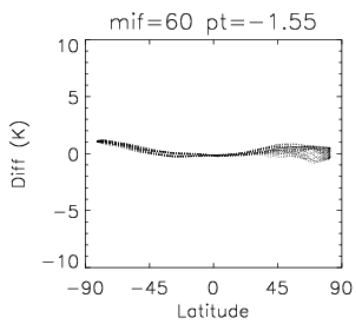

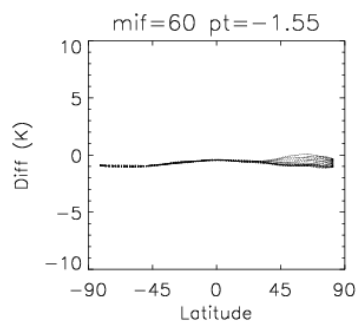

35mb

Differences (CFM-Bill) in T_b^{wet}

From SIDS simulation (day51)

Why need T_b^{wet}?

$$\Delta T_{cir}^{flag} = T_b^{obs} - T_b^{wet}$$

Model method to flag cloud induced radiances

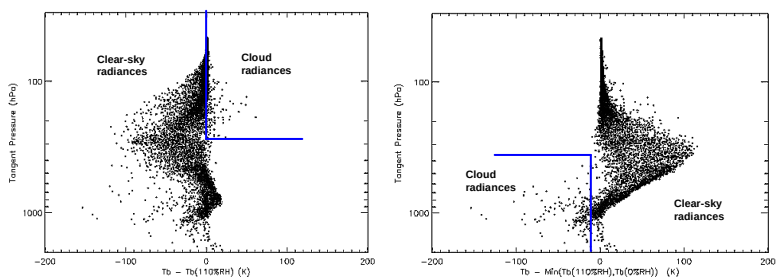

R1A

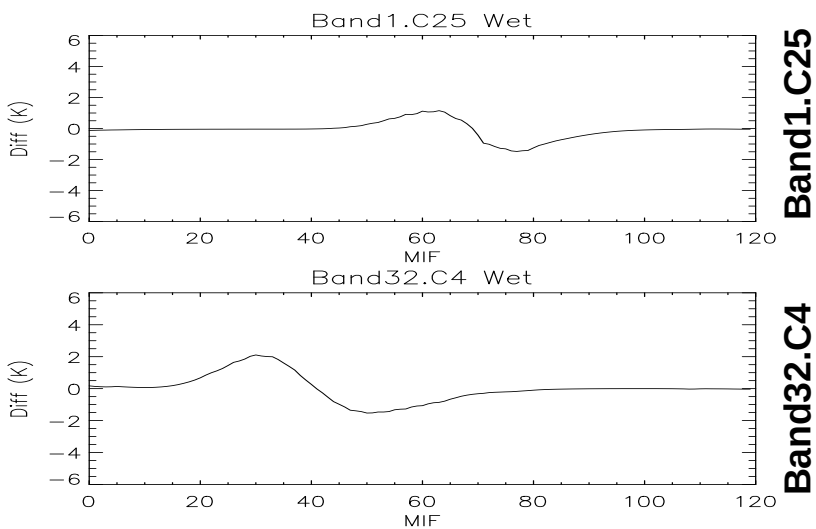

R2

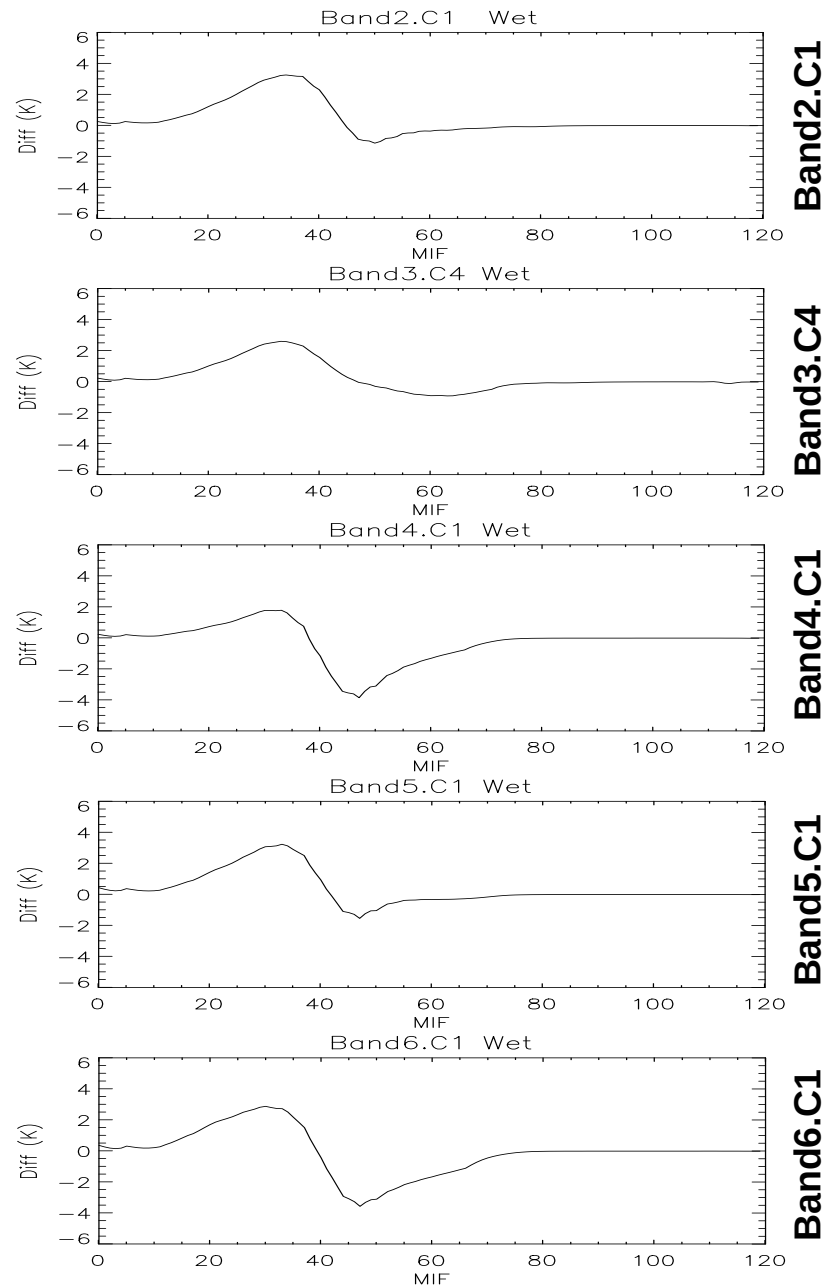

Differences (CFM-Bill) in T_b^{wet} from SIDS simulation (day51)

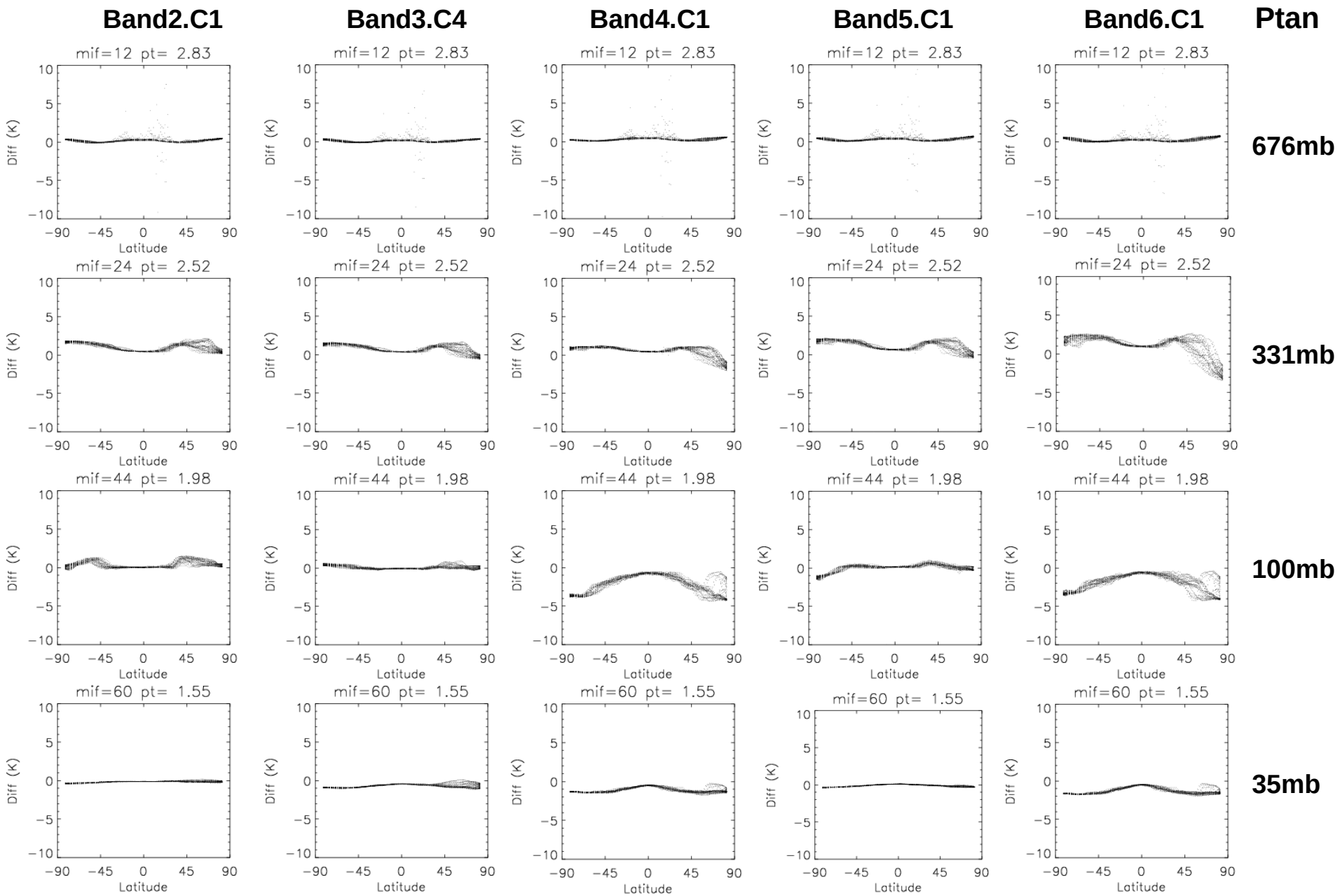

Band1.C25 **Band32.C4** **Ptan**

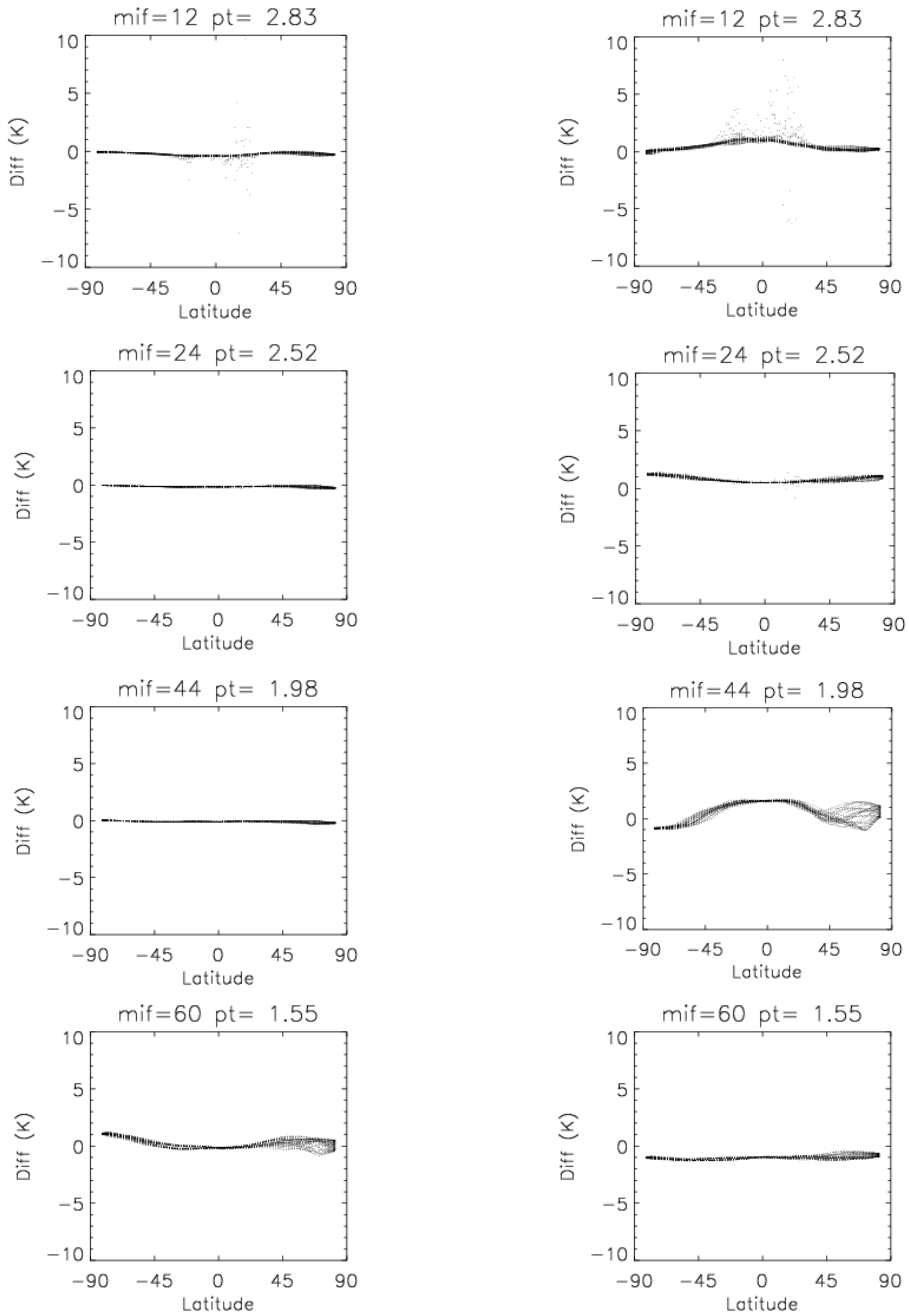

676mb

331mb

100mb

35mb

Conclusion

- For wing channels, and within high and low tangent height ranges important for the cloud retrieval algorithm, the clear-sky radiative transfer calculation in Cloud Forward Model is in good agreement (< ~2K) with Bill's Forward Model.

- Future plan includes:
  - Add a correction term to account for integration in the presence of temperature gradient?
  - Add channel frequency averaging?
  - Add more lines?
  - etc.

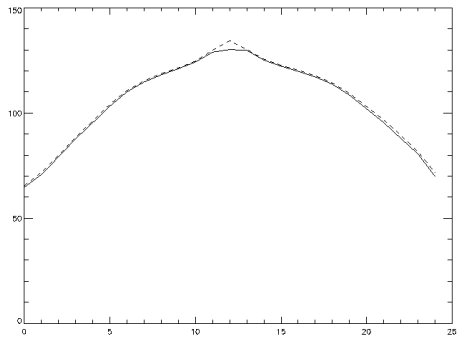

Topic 3

‘Cloud-sky’ and ‘polarized’ (magnetic) forward models

EOS MLS Cloud Forward Model

Overview/Status/Results/Plans

Jonathan H. Jiang

MLS Science Meeting

December 11-12, 2002

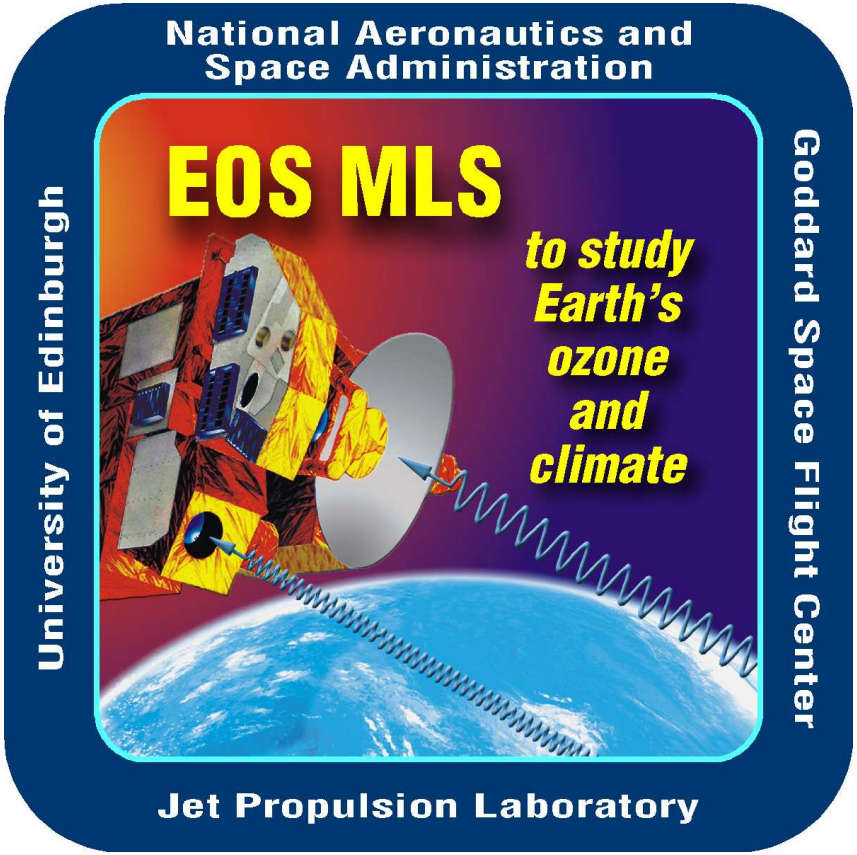

Overview

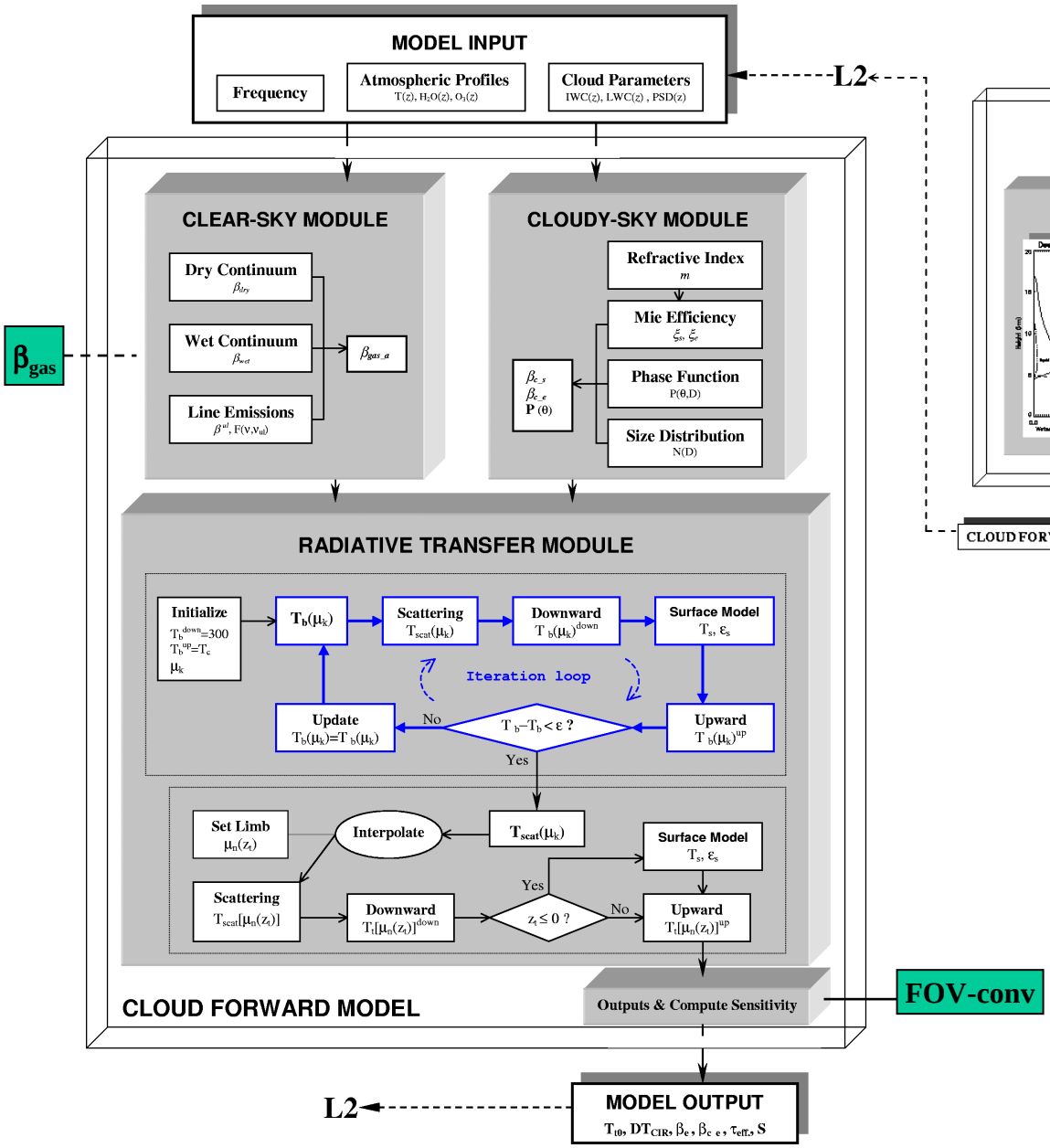

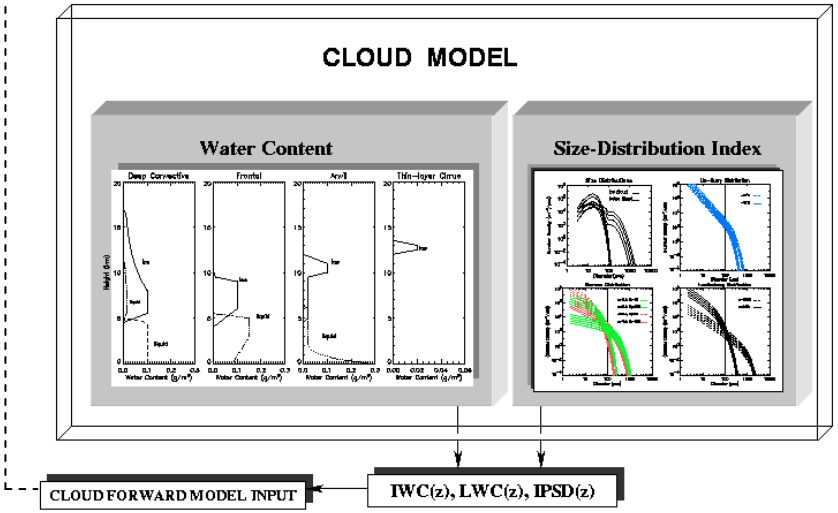

Model Structure

Model Input:
Input atmospheric profiles, cloud parameters, and frequency from Level 2.
Clear-Sky Module:
Computes clear-sky gases absorption coefficients.
Cloudy-Sky Module:
Computes cloud scattering, extinction coefficients, and phase function.
Radiative Transfer Module:
Performs the radiative transfer calculations.
Model Output:
Output cloud radiance related parameters to Level 2.

Cloud Model

A program generates Cloud Forward Model input cloud parameters, which includes vertical profiles of cloud iwc-water-content (IWC), liquid-water-content (LWC) and size-distribution indices.

Examples from Cloudy-Sky Module Calculation for EOS MLS Frequencies

Dielectric Constants

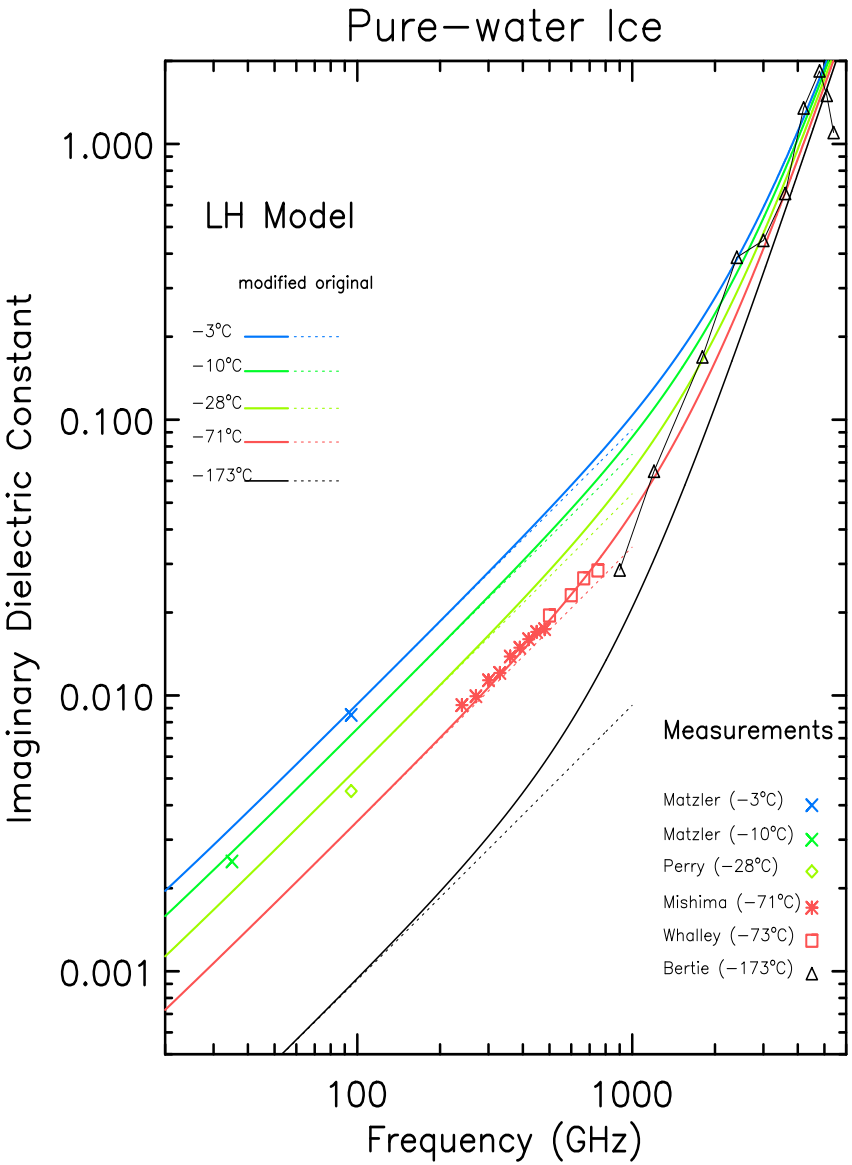

Mie Efficiencies ξ

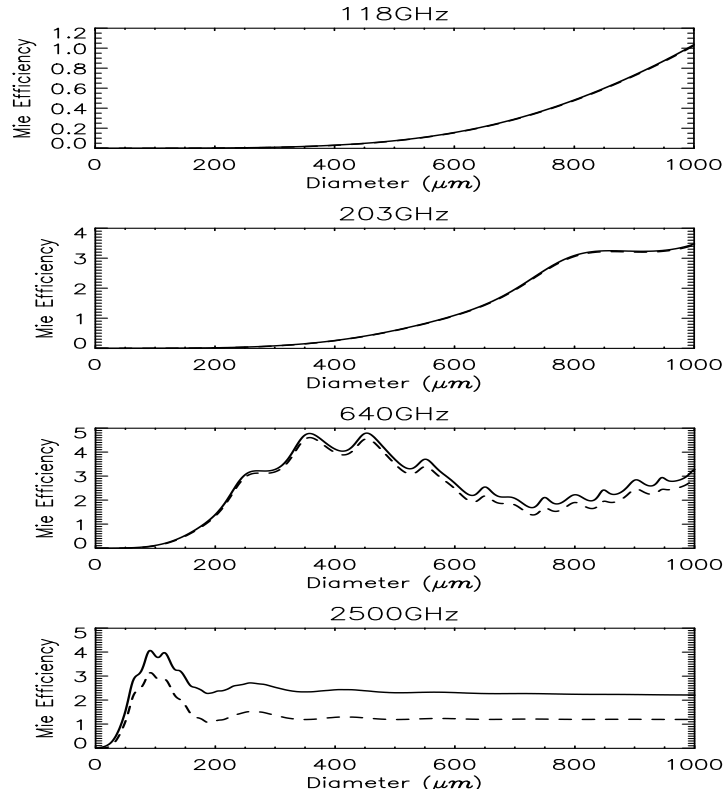

Phase functions P(θ)

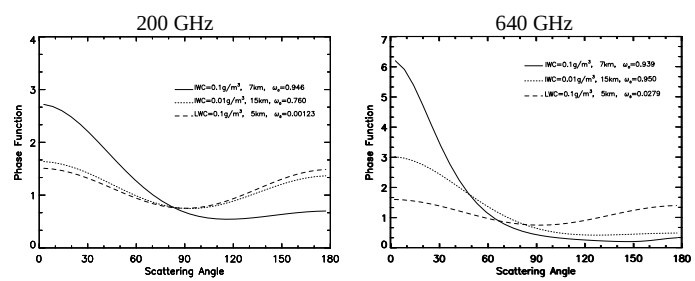

Ice Particle Size Distributions

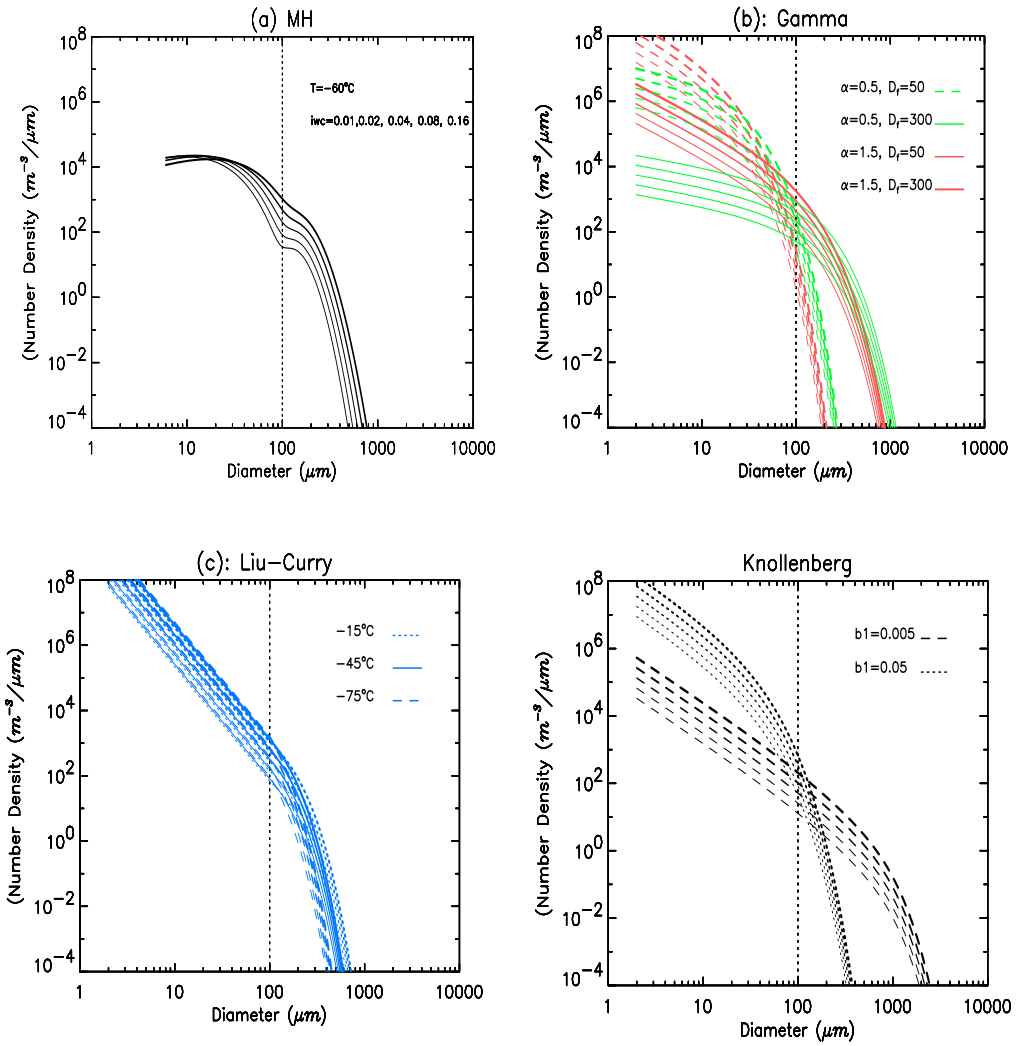

Relationship of cloud extinction to ice water content (IWC)

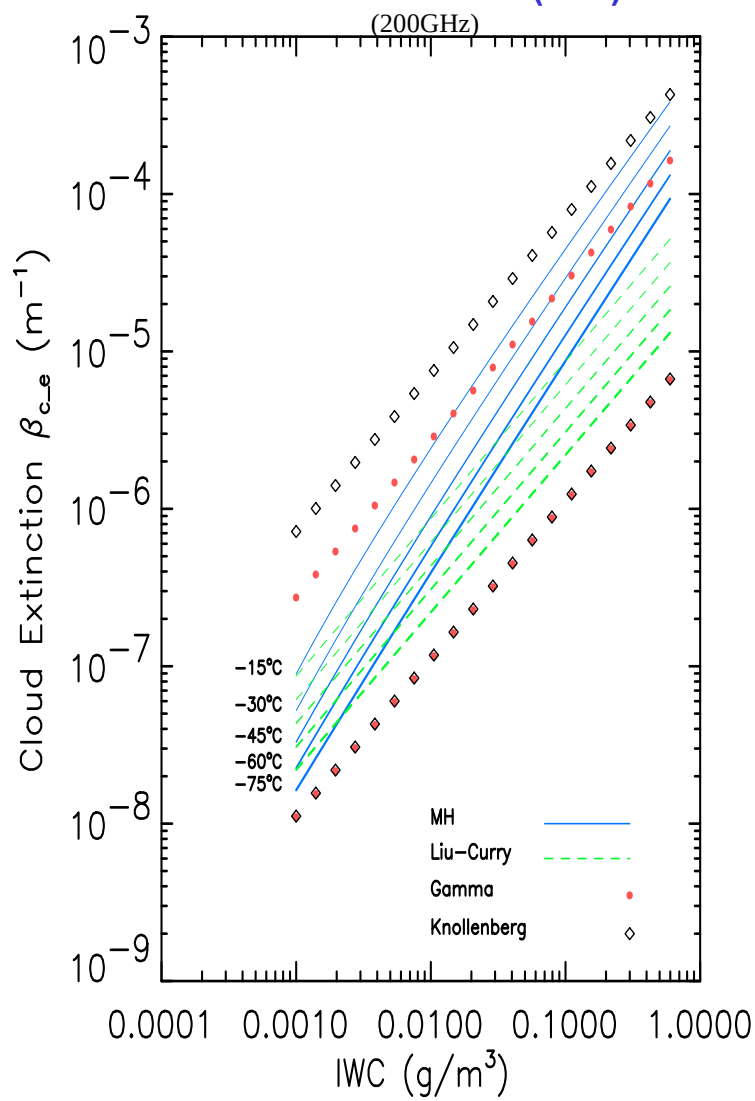

Status

- **Algorithm**
  - Completed ATBD.
  - Completed implementation into L2 software.
  - Completed interfacing cloud forward model with cloud retrieval module.
  - Generated Cloud L2gp files based on RHI >100%.
- **Simulations**
  - Generated cloud parameters and radiances for convective and frontal types (5-10% of total profiles).
  - Generated cloud SIDS radiances for all bands and radiometers.
  - Clear-sky radiative transfer calculation in good agreement (< ~2K) with Bill's forward model.

Clouds Ice L2gp Files

(1) Compute Relative Humidity (RHI) using *Goff-Gratch formulation*, with the water vapor mixing ratio (H_2O) and Temperature (T) provided by Bob Harwood, as

$$RHI = 100.0 \frac{H_2O \times P}{E_s}$$

$$E_s = 10^{S_{ice}}$$

$$S_{ice} = -9.09718(273.16/T - 1) - 3.56654\log_{10}(273.16/T) + 0.876793(1 - T/273.16) + 0.78583503$$

where P is pressure, and E_s is saturated vapor pressure of ice phase.

(2) Set the critical value for ice cloud formation as RHI ≥ *100%*, that is:

Cloud Ice Water Content = IWC, if RHI ≥ 100
Cloud Ice Water Content = 0, if RHI < 100

(3) Replacing H_2O with $H_2O_{\text{-cld}}$ after formation of ice clouds

$$H_2O_{\text{-cld}} = E_s/P, \quad \text{if RHI} \geq 100$$
$$H_2O_{\text{-cld}} = H_2O, \quad \text{if RHI} < 100$$

(4) The cloud ice water content is determined as a ratio of the water vapor profile that condensed out to form ice clouds, as the following:

$$IWC = A \times (H_2O - H_2O_{\text{-cld}}) \qquad g/m^3$$

The scale factor A is chosen so that range of computed IWC (~0.0001-0.3) is comparable with the observations.

(5) Finally the IWC is also scaled by a random number (0< S_{random}<1), considering that the clouds are randomly variable in nature, that is, clouds are different even under the same condition. Thus,

$$IWC = S_{random} \cdot IWC \qquad g/m^3$$

We currently assume ice clouds do not exist in 500mb < P < 40mb levels.

Simulated Cloud Ice

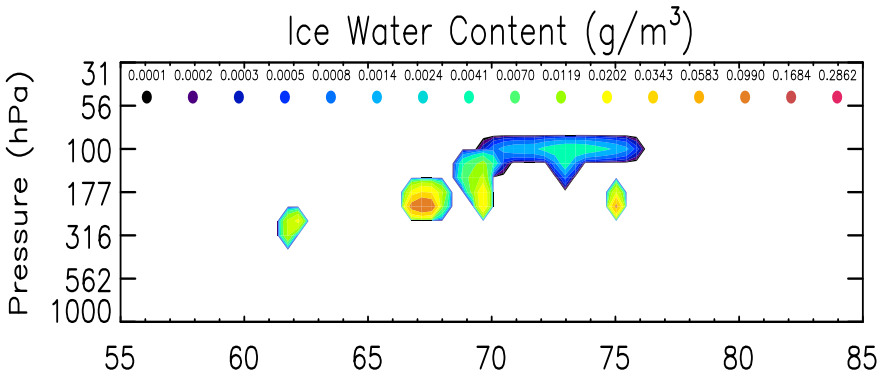

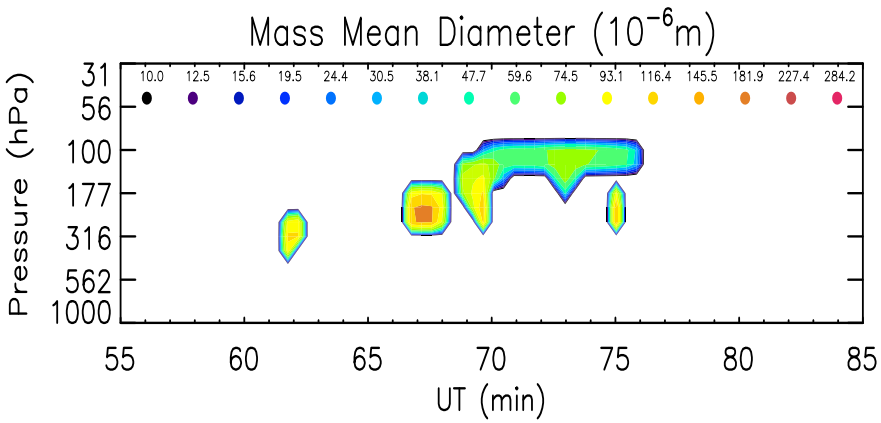

Simulated Cloud Extinction

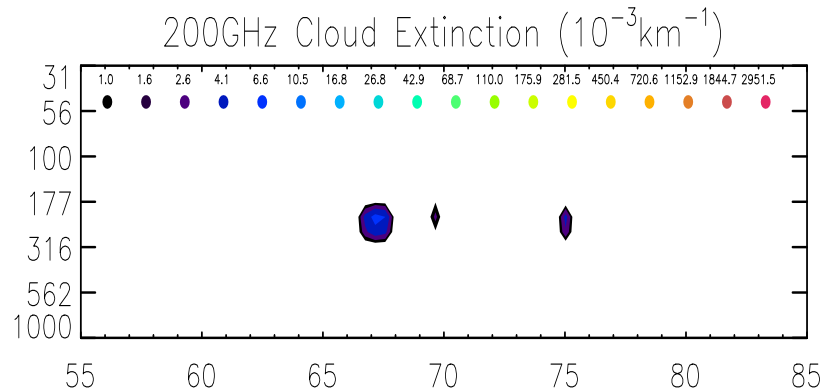

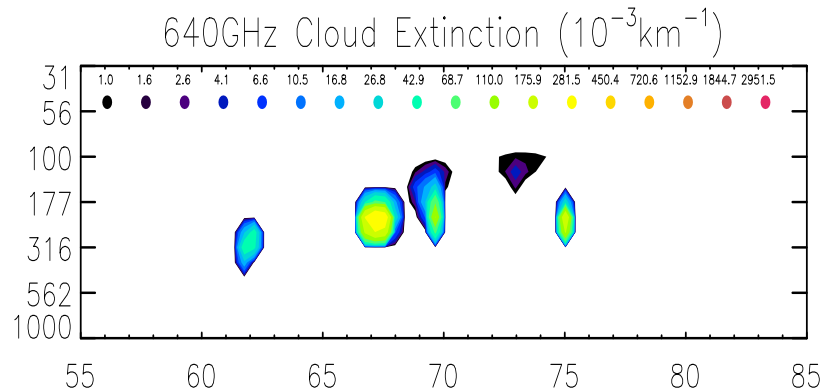

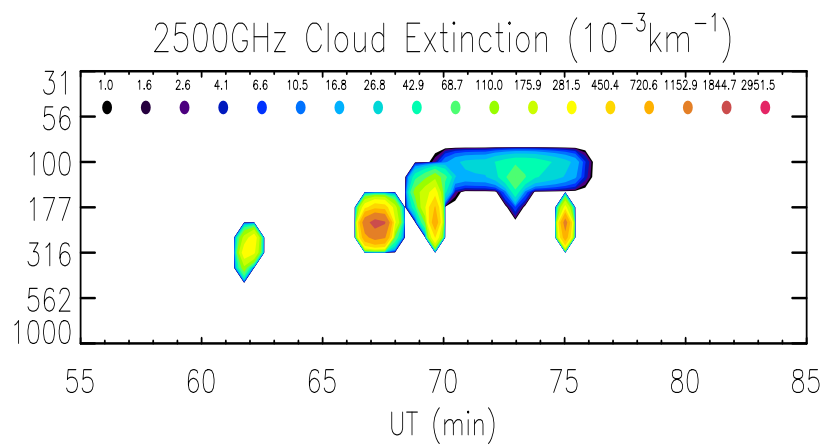

Simulated Cloudy-Sky Radiances

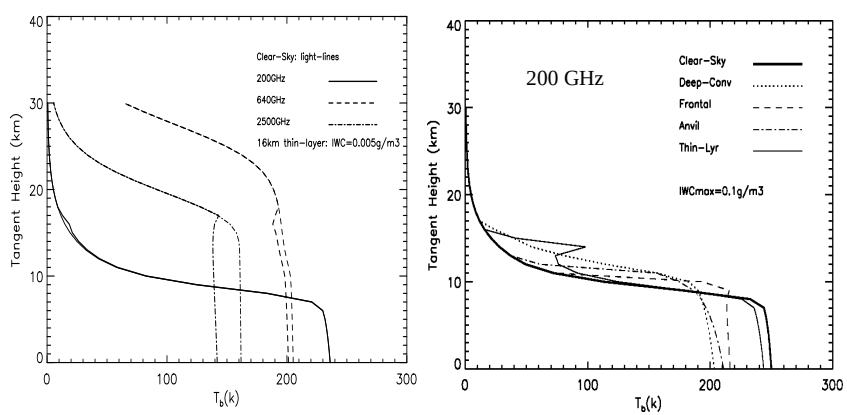

Simulated Cloud Induced Radiances along a portion of orbit

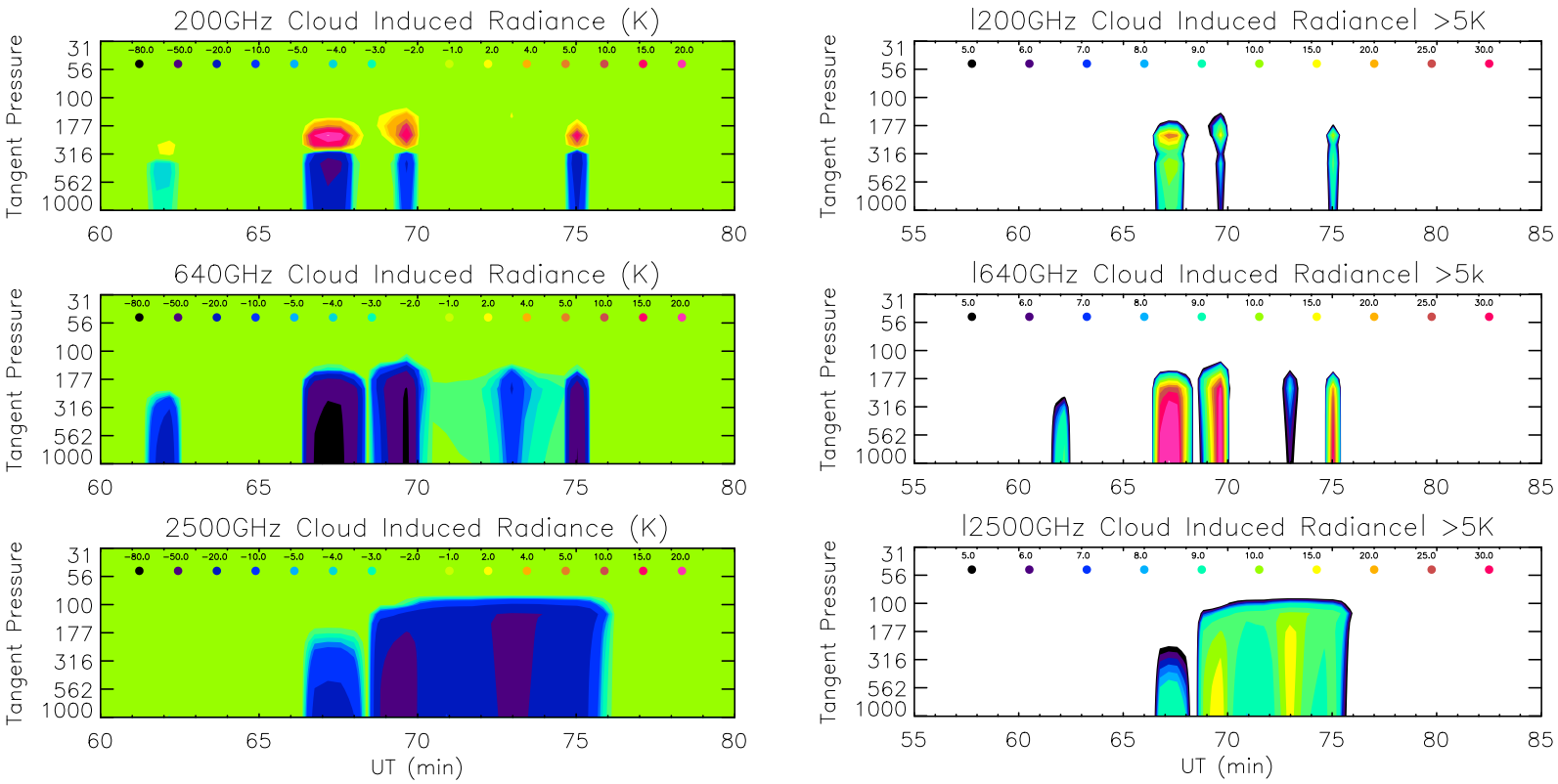

Simulated Ice Water Content **IWC** (g/m^3)

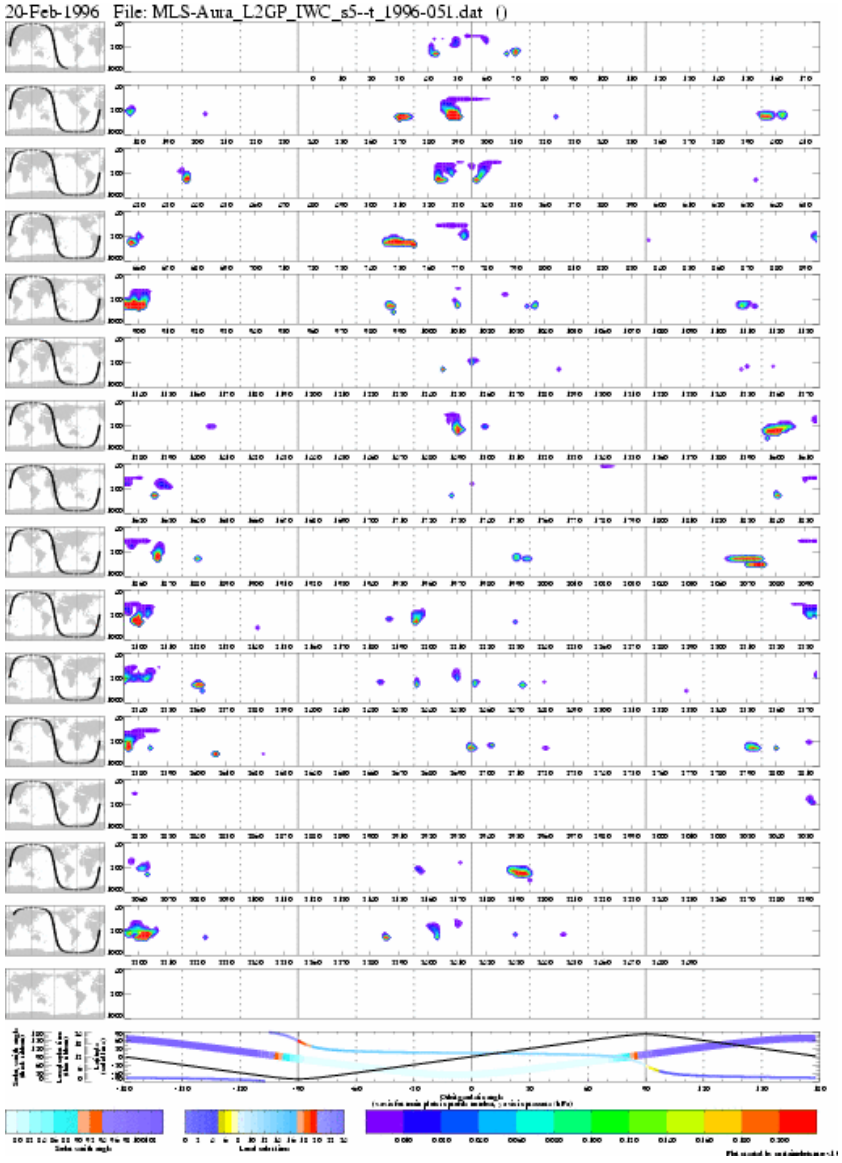

Simulated Cloud Induced Radiance **DT$_{cir}$**(k)

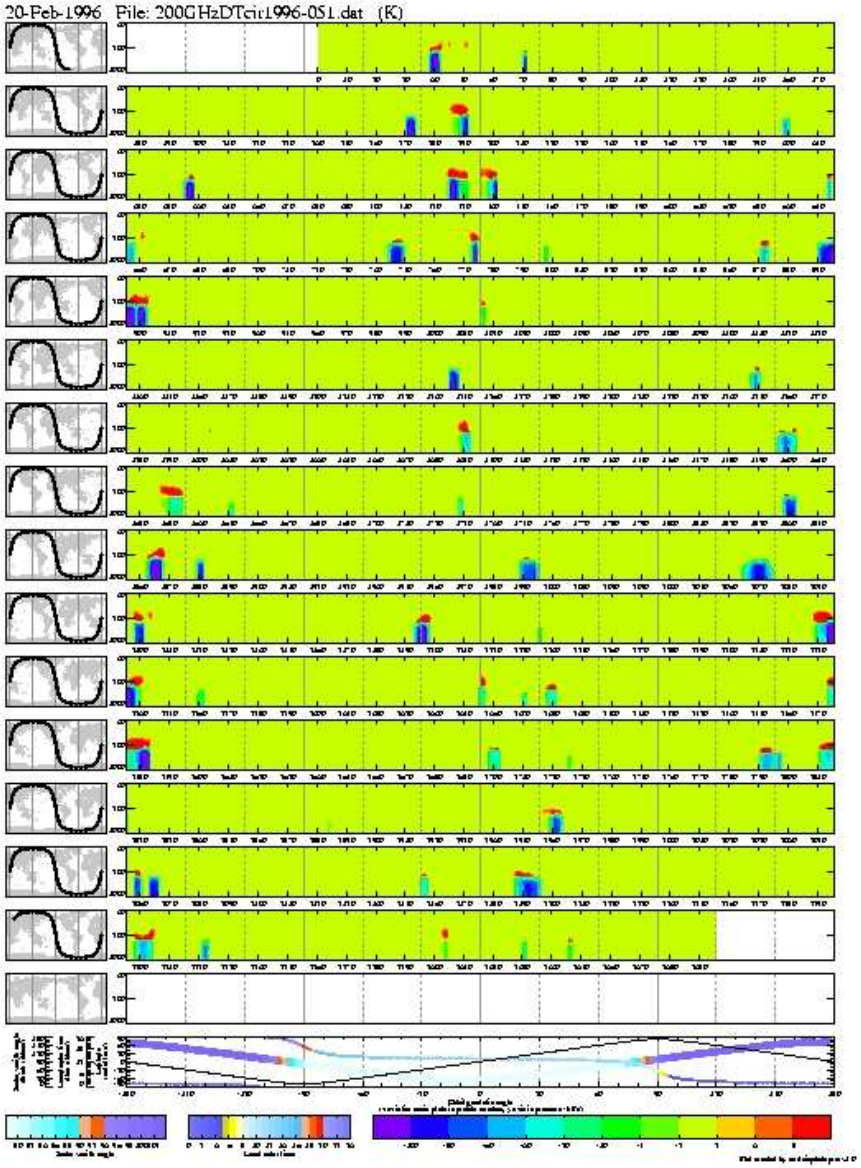

Examples of simulated cloud induced radiances at different bands

~jonathan/emls/cloud/DTcir

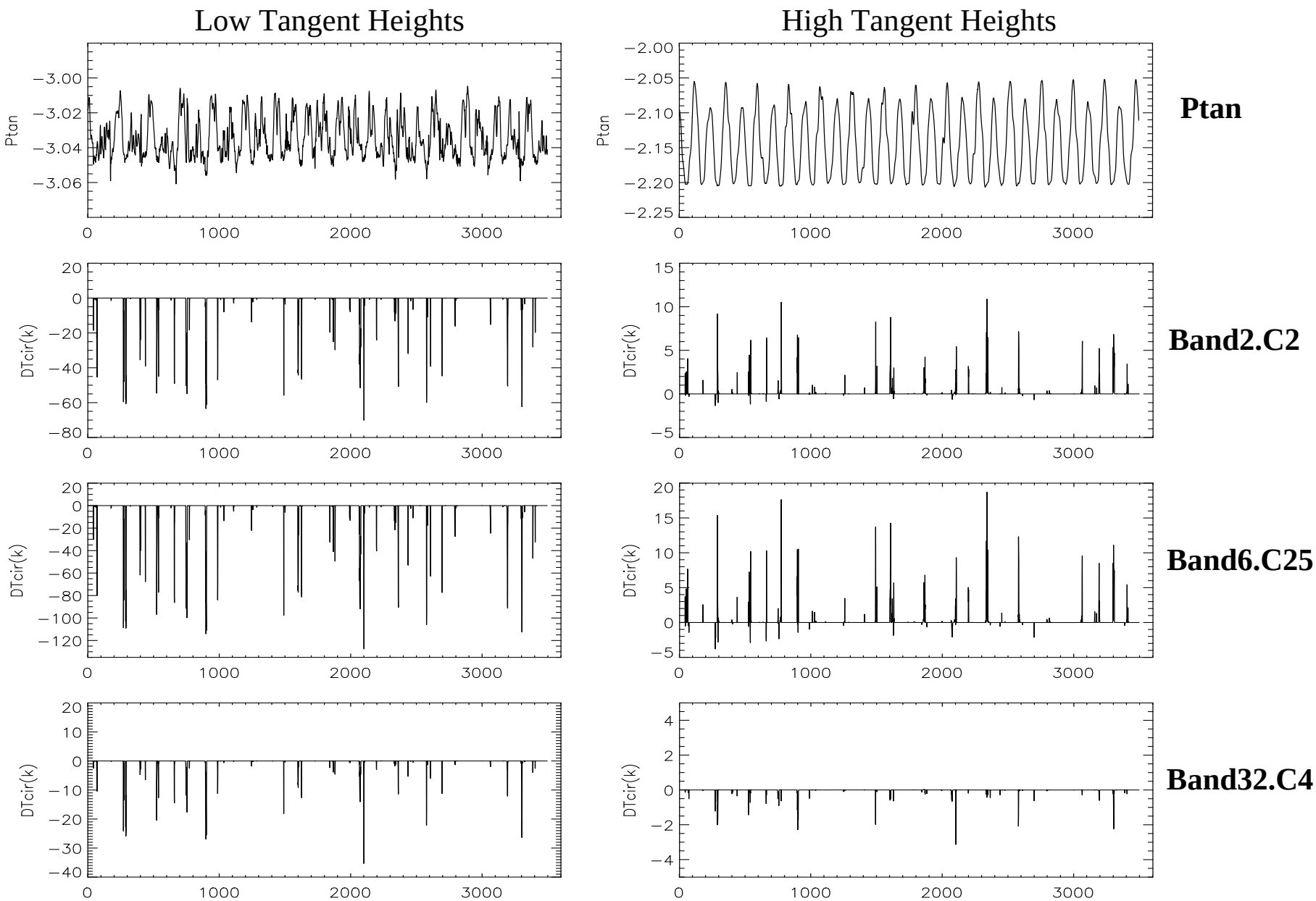

Near-term plan

(Dec-Jan-Feb)

- Improve overall Cloud Forward Model codes and L2cf to meet production standard (help from Paul)
- Test L2AUX (HDF4/HDF5) reader and writer (help from Paul)
- Visualization tools for cloud telecom (help from Ryan)
- Test cloud flag and cloud retrieval
  - core+R2 on cloudy radiances
  - cloud flag algorithm
  - core+R2+flag
  - cloud ice retrieval
- Future upgrade Bill's code to include treatment of clouds (help from Bill, Van)

University of Edinburgh Cloudy Sky Model: Plans and Status

Cory Davis

December 12, 2002

Overview

- Goals
- Forward model
  - method
  - single scattering properties of non-spherical particles
- Plans

Goals

This study follows on from work done by Bond and Wu but will extend the research in the following areas:

- the influence of large particles with consideration of their likely prevalence and non-sphericity
- mixed phase clouds
- inhomogeneity of the cloud field in the field of view.

The primary components of the study:

1. build a radiative transfer model with scattering and emission/absorption of cirrus and mixed-phase cloud.

2. run the model with realistic cloud data obtained from existing or planned measurement campaigns.

3. study the retrieval problem. Establish the circumstances under which

   (a) sensitivity can be retained for gaseous species

   (b) optically thick clouds can be detected and flagged

   (c) cloud properties can be determined

   ,and to establish the effect on the retrieved target species

4. Study of use of other available information in the retrieval. (TES, OMI, HIRDLS...)

Forward model: Monte Carlo?

Attractive when moving beyond plane parallel geometry

- reducing grid size is not as big a problem as for DOM and requires less memory.
- considerably easier to implement

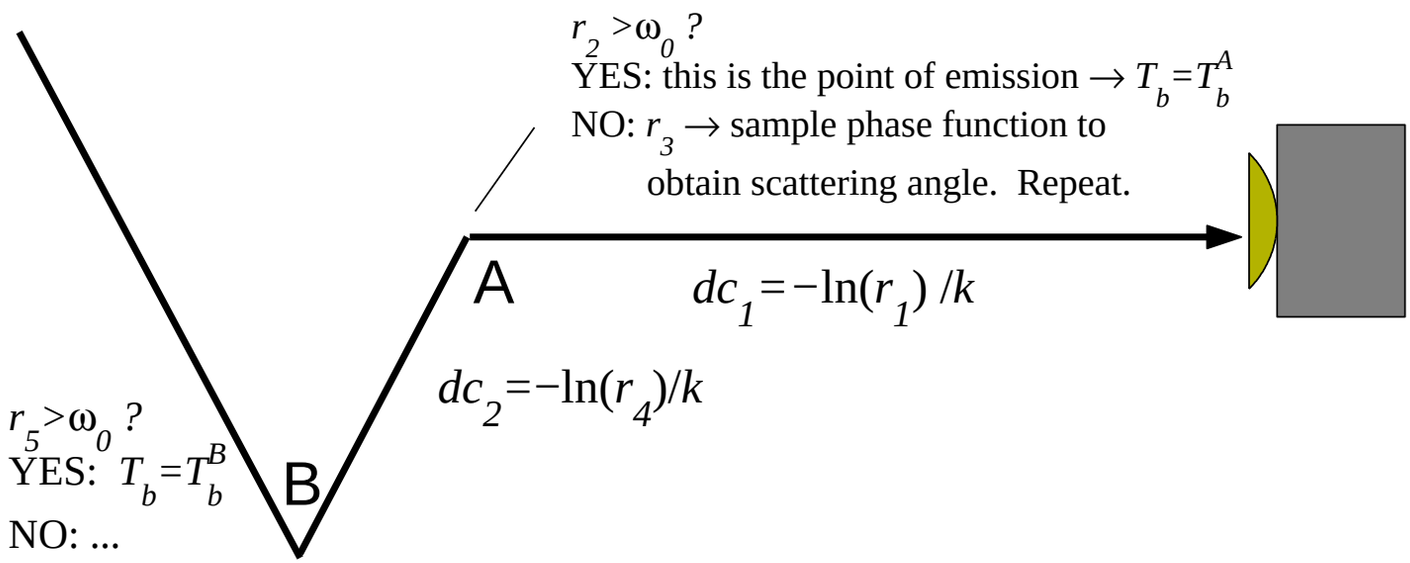

- repeat this 1,000,000 times and calculate $\bar{T}_b$–Liu et al. [1996],Roberti et al. [1994]

The VRTE

The vector radiative transfer equation:

$$\frac{d\mathbf{I}(\mathbf{n})}{ds} = -n_0\langle\mathbf{K}(\mathbf{n})\rangle\mathbf{I}(\mathbf{n}) + \mathbf{K_a}(\mathbf{n})I_b(T) + n_0\int_{4\pi}\langle\mathbf{Z}(\mathbf{n},\mathbf{n}')\rangle\mathbf{I}(\mathbf{n}')d\mathbf{n}' \quad (1)$$

$$\mathbf{I} = \begin{bmatrix} I \\ Q \\ U \\ V \end{bmatrix} \quad (2)$$

How do we now define the path length in a Monte Carlo simulation?

If $\mathbf{K}$ is diagonal (which is the case for randomly oriented nonspherical particles) we are still OK. I'd like to find out what $\mathbf{K}$ might look like for a realistic cirrus cloud before deciding on the radiative transfer modelling method.

ARTS?

- open source forward modelling tool for remote sensing developed by a group at the University of Bremen led by Stefan Beuhler
- equally applicable to nadir, slant and limb viewing
- a choice of 1D, 2D or 3D atmospheres
- currently polarized scattering capability is being added, with only the 1-D case operational.
- scattering is treated separately and confined to a ’cloud-box’. The radiation field in the cloud box is calculated using a DOM type method.
- I am going to spend some time evaluating ARTS as a means of expediting the forward model development component of my project.

The extinction matrix via the T-matrix method

- The extinction matrix generally has 7 independent elements: $K_{jj}, K_{12} = K_{21}, K_{13} = K_{31}, K_{14} = K_{41}, K_{23} = -K_{32}, K_{24} = -K_{42}$, and $K_{34} = -K_{43}$
- T-matrix method: the incident, internal, and scattered fields are solved for using the extended boundary condition method (null field method). ”T-matrix” transforms the incident field spherical vector function coefficients to those for the scattered wave.
- from the T-matrix for a given particle you can get the scattering amplitude matrix $\mathbf{S}$

$$\begin{bmatrix} E_\theta^{sca} \\ E_\phi^{sca} \end{bmatrix} = \frac{exp(ikR)}{R}\mathbf{S}(n', n) \begin{bmatrix} E_\theta^{inc} \\ E_\phi^{inc} \end{bmatrix} \tag{3}$$

- from $\mathbf{S}(\mathbf{n}, \mathbf{n}')$ it is straightforward to get $\mathbf{K}(\mathbf{n})$, $\mathbf{K_a}(\mathbf{n})$, and $\mathbf{Z}(\mathbf{n}, \mathbf{n}')$

T-matrix cont.

- T-matrix particularly practical when dealing with rotationally symmetric particles
- freely available T-matrix code developed by Michael Mishchenko (GISS) gives $\mathbf{S}(\mathbf{n}, \mathbf{n}')$ for oblate or prolate spheroids, oblate or prolate cylinders, or chebyshev particles
- At this stage it seems a sensible idea to **approximate hexagonal column and plate cirrus crystals by cylinders**
- convenient speculation: the more complicated shapes are less likely to be preferentially oriented and less likely to contribute to a polarization signal–treat as equivalent spheres.

Results and limitations

- large hexagonal column – L = 600 μm, f=240 GHz.
- First we consider the column to be lying horizontally in a fixed orientation. In this case extinction matrix elements are functions of both θ and ϕ.

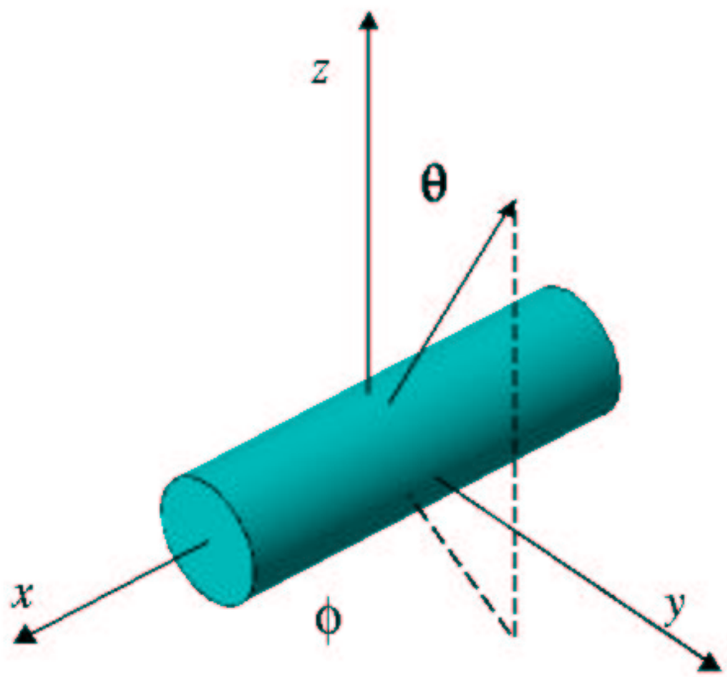

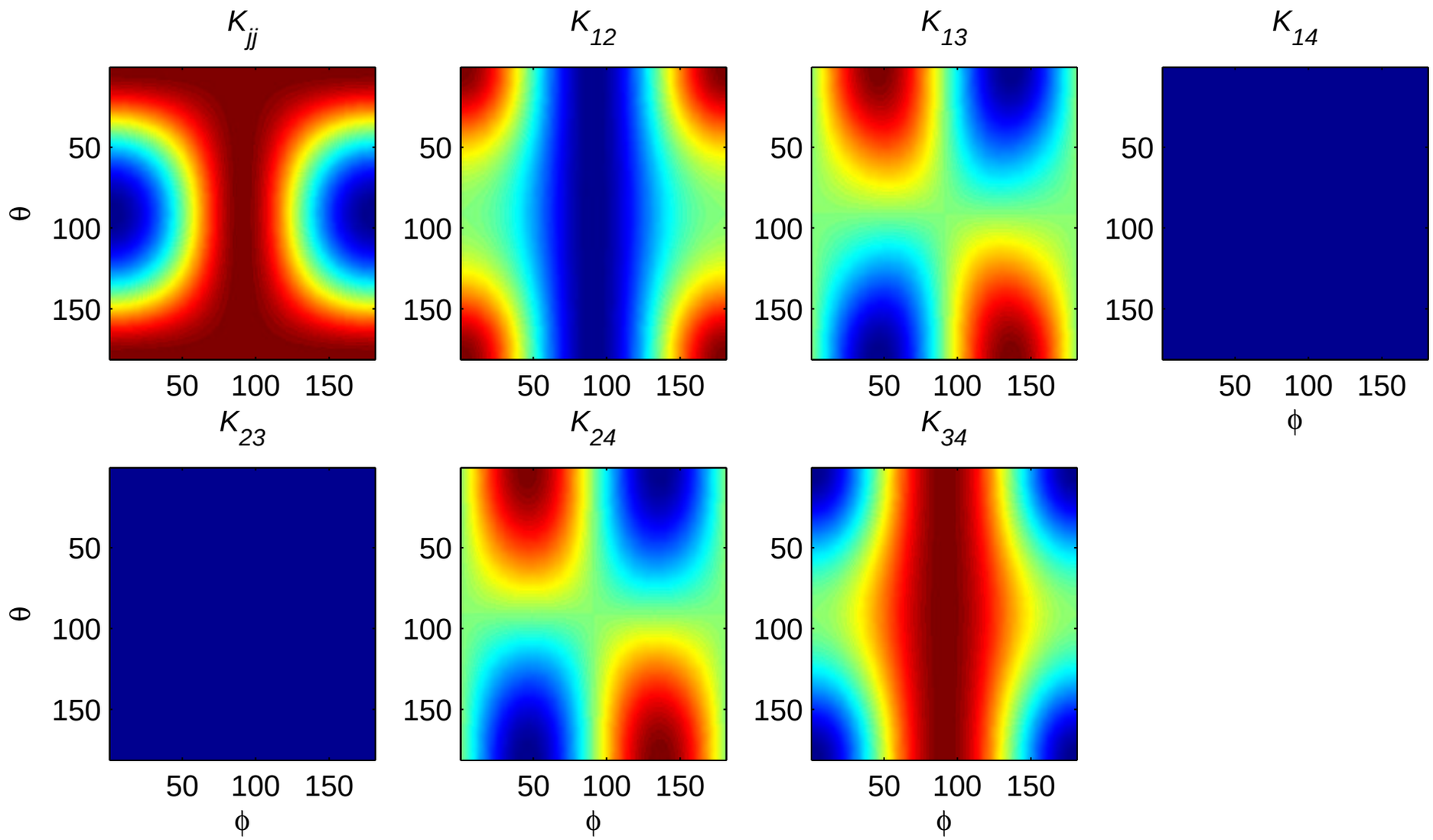

Figure 1: Extinction matrix elements for a horizontally aligned cylinder

- Averaging $\mathbf{K}$ over ϕ leaves only K_{jj}, K_{12} (=K_{21}), and K_{34}(=-K_{43})
- Compare with the Mie calculations for an equivalent sphere to check the T-matrix calculations and demonstrate the magnitude of ‘non-spherical’ features missed by Mie theory.
- To make this comparison we calculate the extinction cross-section, which describes the effect on the total radiance I, the first component of the Stokes vector.

$$C_{ext} = \frac{1}{I_{inc}} \left[K_{11} I_{inc} + K_{12} Q_{inc} + K_{13} U_{inc} + K_{14} V_{inc} \right] \tag{4}$$

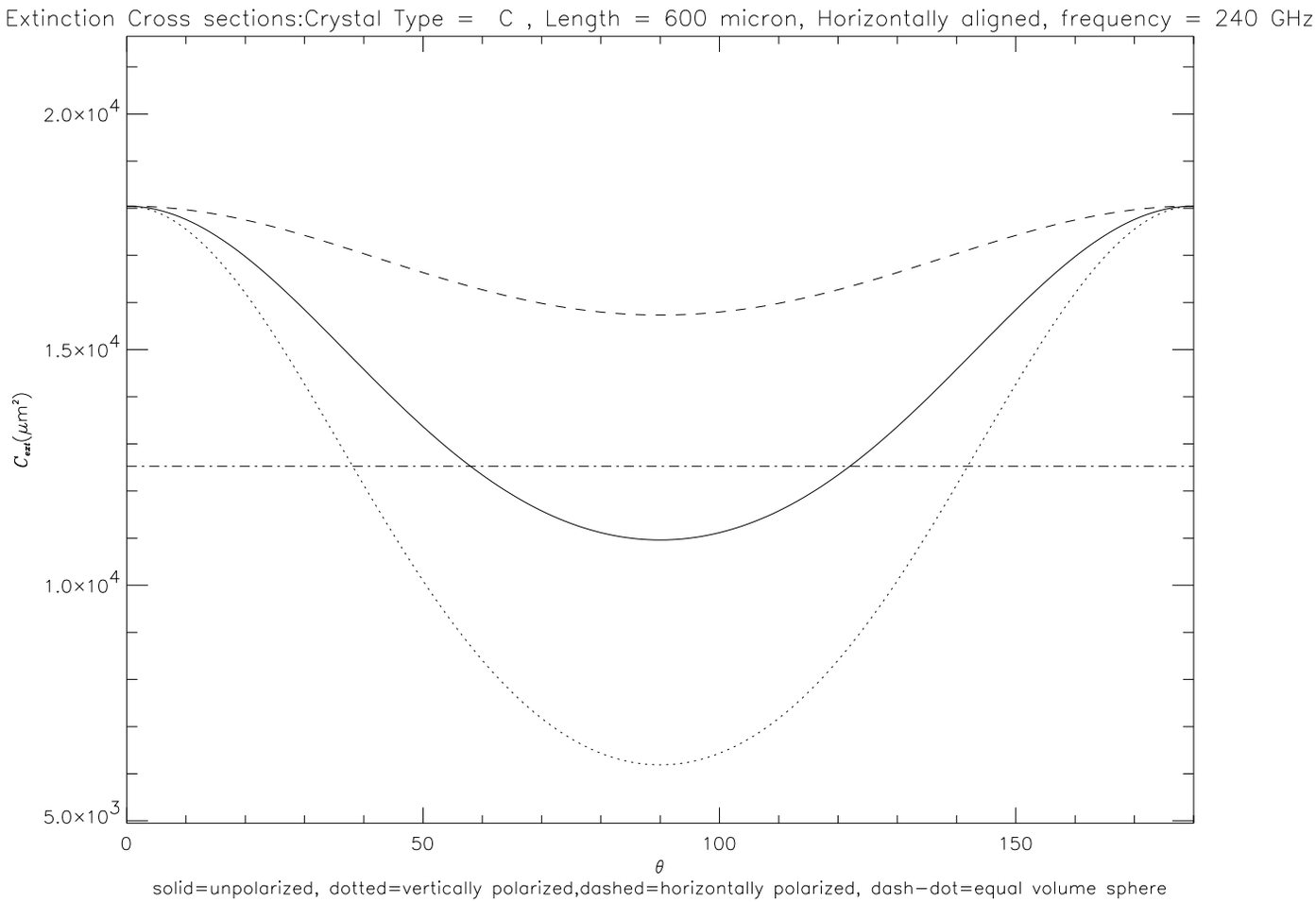

Figure 2: Non spherical extinction cross section for unpolarized, vertically, and horizontally polarized light, and extinction cross section for an equal volume sphere

- the polarizing effect of the extinction matrix might be counteracted to some extent by the scattering integral in the VRTE
- also need to average over all particle shapes and sizes
- these results at least show a potential for non-spherical particles to influence MLS radiances that is worth further consideration
- Czekala [1998] : RT calculations at 200 Hz for limb sounding – non-spherical particles with a preferred orientation have a significant effect on brightness temperature (up to 15K) and polarization difference (up to 30 K).
- the results for plate crystals are very similar. For 240GHz plate T-matrix calculations are only convergent up to 225 μm

What next?

- complete a survey of available cirrus size and habit distribution data
- consider tropical and midlatitude cases separately
  - Midlatitude: FIRE-I, FIRE-II, ARM,...
  - Tropical: CEPEX $\Rightarrow$ MH97, EMERALD?
- use these distributions to calculate the extinction matrix for realistic cirrus clouds
- Begin with a 1-D scattering atmosphere: sensitivity tests on the influence of size/habit/orientation distributions, hopefully provide a useful comparison with the JPL model as soon as possible
- Move on to a 3-D atmosphere to look at the influence of cloud inhomogeneity in the line of sight.
- Study the retrieval problem...

References

H. Czekala. Effects of ice particle shape and orientation on polarized microwave radiation for off nadir problems. *Geophys. Res. Lett.*, 25(10):1669–1672, 1998.

Q. Liu, C. Simmer, and E. Ruprecht. Three-dimensional radiative transfer effects of clouds in the microwave spectral range. *Journal of Geophysical Research*, 101 (D2):4289–4298, 1996.

Hans R. Pruppacher and James D. Klett. *Microphysics of Clouds and Precipitation*. Kluwer Academic Publishers, 1997.

L. Roberti, J. Haferman, and C. Kummerow. Microwave radiative transfer through horizontally inhomogeneous precipitating clouds. *J. Geophys. Res.*, 99(D8): 16707–16718, 1994.

Polarized Forward Model: Overview of Plans and Status

EOS-MLS Forward Model Meeting

Michael Schwartz
[*michael@mls.jpl.nasa.gov*]

11-12 December, 2002

Magnetic Forward Model

- The Magnetic Forward model will provide radiances and derivatives w.r.t. Temperature, Tangent Pressure, Geomagnetic Field, O_2 mixing ratio and winds near the Zeeman-split 118-GHz O_2 line.
- Above ~ 60 km, three Zeeman components are resolved and absorption is polarization-dependent.
- Different polarizations are coupled, so relative phases are important and the two polarizations cannot generally be modeled by two scalar equations.
- Full magnetic forward model will share much of the code of scalar forward model.

Outline

- O_2 microwave spectrum
- Tensor Radiative Transfer
- Magnetic augmentation of existing scalar forward model
- Plans for next four months

O_2 118.75-GHz line

- O_2 electronic groundstate has spin $s = 1$.
- Band of lines near 60 GHz and isolated line at 118.75 GHz are transitions between states of coupled spin ($s = 1$) and molecular rotation N (N is odd).
- The 118.75 line is a transition from N=1, J=1 to N=1, J=0
- Zeeman splitting: Electronic spin has an associated magnetic moment ($\vec{\mu}$=2.00229 $\mu_B \vec{s}$) which couples to the geomagnetic field $\vec{B}_{earth}$.
- $\vec{s}$ precesses rapidly around $\vec{J}$ so Zeeman splitting is proportional to m, the QN for J_z, where $\hat{z}$ is the geomagnetic field direction.

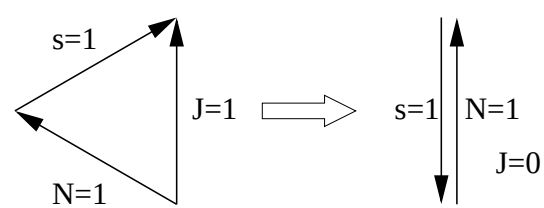

Zeeman Splitting in Geomagnetic Field

- For $\{N = 1, J = 1\}$ state, energy shifts are: $\mathcal{H}_z = \frac{1}{2}\kappa m|B_{earth}|$ with $\kappa = 2.8024$ MHz/gauss
- Typical $|B_{earth}|$ are between 0.6 gauss at high latitudes and 0.25 gauss near the equator.
- σ_+ and σ_- lines typically split down/up by less than 1 MHz.
- cartoon is very much not to scale.

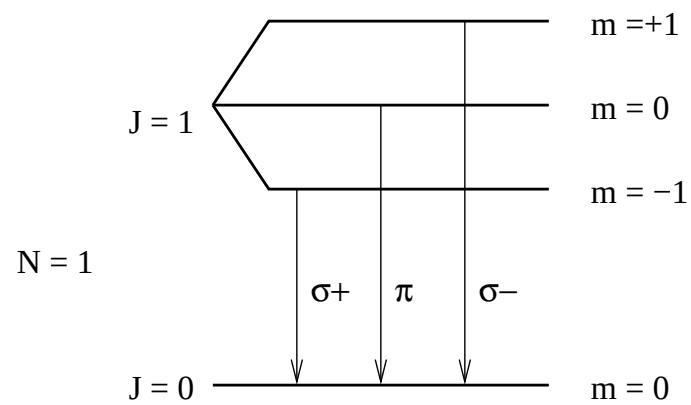

Tensor Susceptibility χ_{ij}

χ is the coupling of the magnetic dipole moment to the field

$$\chi_{ij} \sim \sum_{\alpha,\beta} \langle\alpha|\, \mu_i \,|\beta\rangle \langle\beta|\, \mu_j^\dagger \,|\alpha\rangle$$

where i, j are Cartesian components of the dipole operator and $\hat{z}$ is in the direction of the geomagnetic field.

In circular polarization basis χ is diagonal

$$\chi^{(3)} = \begin{bmatrix} \chi_+ & 0 & 0 \\ 0 & \chi_- & 0 \\ 0 & 0 & \chi_0 \end{bmatrix}$$

Spatial components depend upon Δm of the transition.

$\Delta m = +1$: couples to χ_+, right circular polarization
$\Delta m = -1$: couples to χ_-, left circular polarization
$\Delta m = 0$: couples to χ_0, linear polarization in $\hat{z}$ direction

Susceptibility in IFOVPP frame

Rotate to Instrument Field of View Plane Polarized frame in which $\vec{E}$ in $\hat{x}$, $\vec{H}$ in $\hat{y}$,propagation in $\hat{z}$.

$$R_\theta = \begin{bmatrix} \cos\theta & 0 & \sin\theta \\ 0 & 1 & 0 \\ -\sin\theta & 0 & \cos\theta \end{bmatrix}$$

$$R_\phi = \begin{bmatrix} \sin\phi & -\cos\phi & 0 \\ \cos\phi & \sin\phi & 0 \\ 0 & 0 & 1 \end{bmatrix}$$

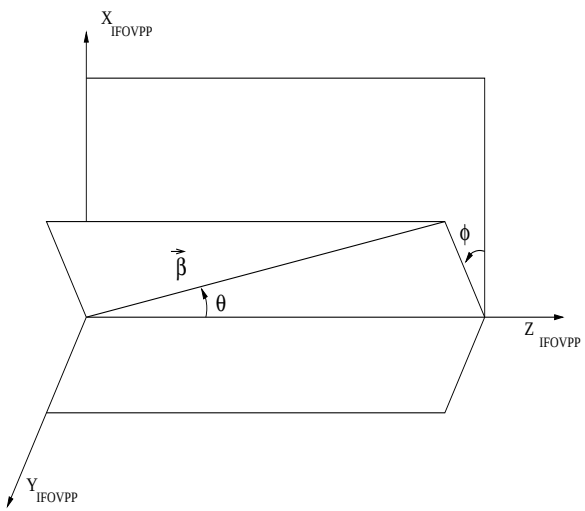

In the Instrument Field of View Plane Polarized frame,

$$\chi^{(3)} = R_\phi R_\theta \chi^{(3)\prime} R_\theta^\dagger R_\phi^\dagger$$

The $\rho_{\Delta m}$ Matrices

The matrices $\boldsymbol{\rho}_{\Delta m}$ are the components of $\boldsymbol{\chi}$ proportional to $\chi_{\Delta m}$ in the IFOVPP reference frame with the z row and column removed.

$$\boldsymbol{\rho}_{\pm 1} = \begin{bmatrix} \cos^2\phi + \sin^2\phi\cos^2\theta & -\sin\phi\cos\phi\sin^2\theta \mp \imath\cos\theta \\ -\sin\phi\cos\phi\sin^2\theta \pm \imath\cos\theta & \sin^2\phi + \cos^2\phi\cos^2\theta \end{bmatrix},$$

$$\boldsymbol{\rho}_{0} = \begin{bmatrix} \sin^2\phi\sin^2\theta & \sin\phi\cos\phi\sin^2\theta \\ \sin\phi\cos\phi\sin^2\theta & \cos^2\phi\sin^2\theta \end{bmatrix}.$$

Propagation Matrix

$$\mathbf{G} = ik_0 \sum_{\Delta m=-1}^{1} \boldsymbol{\rho}_{\Delta m}(\theta, \phi)\beta_{\Delta m}.$$

$$\beta_{\Delta m} = S\xi_{m,\Delta m}F(\nu, \nu')$$

- S is unsplit line strength,
- F is complex error function of which the Voigt shape is the real part.
- ξ is $\{\frac{1}{2}, 1, \frac{1}{2}\}$ for $\Delta m = \{+1, 0, -1\}$ for the 118-GHz line

Given Maxwell Equations and assuming plane waves in $\hat{z}$ direction, the wave equation for $\vec{H}$ may be written in terms of a propagation matrix $\mathbf{G}$.

Field Propagation

Magnetic field, $\vec{H}$, through a uniform layer of thickness z:

$$\vec{H}(z,\omega) = \exp[-\mathbf{G}(\omega)z]\vec{H}(0,\omega).$$

Electric field $\mathbf{E}$ may be written in terms of Magnetic Field $\mathbf{H}$:

$$\mathbf{E}(z_n,\omega) = \frac{\mathbf{G}(\omega)}{i\omega\epsilon_0}\exp[-\mathbf{G}(z_n,\omega)dz_n]\begin{pmatrix} H_y(0,\omega) \\ -H_x(0,\omega)\end{pmatrix}$$

$$\mathbf{E_p} \equiv \begin{pmatrix} -E_y \\ E_x \end{pmatrix}, \quad \mathbf{H} \equiv \begin{pmatrix} H_x \\ H_y \end{pmatrix}$$

The first element from each of the two vectors define the first linear polarization basis vector and the second elements define the second.

Tensor Radiative Transfer

The propagation matrix, $\mathbf{G}$, governs propagation of the intensity coherence matrix, $\mathbf{I} = \langle \mathbf{E_p}(\omega)\mathbf{H}^\dagger(\omega)\rangle$:

$$\frac{d\mathbf{I}}{ds} + \mathbf{G}\,\mathbf{I} + \mathbf{I}\,\mathbf{G}^\dagger = (\mathbf{G} + \mathbf{G}^\dagger)B$$

where B is the scalar source function

$$B = \frac{h\nu}{k(\exp\{\frac{h\nu}{kT}\} - 1)}$$

In a linear polarization basis,

$$\mathbf{I} = \begin{bmatrix} I_{||} & I_{|} + \imath I_{\circ} \\ I_{|} - \imath I_{\circ} & I_{\perp} \end{bmatrix}.$$

where $I_{||}$, $I_{\perp}$, $I_{|}$, and $I_{\circ}$ are co-polarized intensity, cross-polarized intensity and linear and circular coherence respectively.

Differential Temperature Tensor Radiative Transfer

The tensor equation of radiative transfer may be cast in the same form as the scalar equation, but with tensor $\mathcal{T}$.

$$\mathbf{I}(x) = \sum_{i=1}^{2n} \mathcal{T}_i \, \Delta B_i$$

where layer 1 is closest to the observer and ΔB is defined in terms of layer boundary temperatures:

$$\begin{aligned}
\Delta B_i &= \frac{B_{i+1} - B_{i-1}}{2}, \\
\Delta B_1 &= \frac{B_1 + B_2}{2}, \\
\Delta B_{2N} &= I_{2N+1} - \frac{B_{2N-1} + B_{2N}}{2},
\end{aligned}$$

Transmission Matrix $\mathcal{T}$

The tensor $\mathcal{T}$ is a sandwich of layer field transmission matrices with the earliest times on the inside.

$$
\begin{aligned}
\mathbf{E}_i &= \exp\left(-\int_{s_i}^{s_{i-1}} \mathbf{G}(s')\,ds'\right) \\
\mathcal{T}_i &= \mathbf{E}_1\mathbf{E}_2\ldots\mathbf{E}_{n-1}\mathbf{E}_{n-1}^{\dagger}\ldots\mathbf{E}_2^{\dagger}\mathbf{E}_1^{\dagger}
\end{aligned}
$$

$$
\begin{aligned}
\mathbf{P}_1 &= \mathbf{1} \\
\mathbf{P}_2 &= \mathbf{E}_1 \\
\mathbf{P}_3 &= \mathbf{E}_1\mathbf{E}_2 \\
\mathbf{P}_n &= \mathbf{E}_1\mathbf{E}_2\cdots\mathbf{E}_{n-1}
\end{aligned}
$$

$$
\mathcal{T}_i = \mathbf{P}_i\mathbf{P}_i^{\dagger}
$$

Incremental Opacity

The form of the incremental opacity is very similar to that in the scalar model, with $\sum_k \Delta\delta^k_{i\to i-1} \to \int_{s_i}^{s_{i-1}} \mathbf{G}(\mathbf{s'})\,ds'$. The incremental opacity integral is

$$\Delta\delta^k_{i\to i-1} = \frac{\Delta s^{refr}_{i\to i-1}}{\Delta s_{i\to i-1}} \sum_{\Delta M=-1}^{+1} \rho_{\Delta M}(\theta,\phi) \times \int_{\zeta_i}^{\zeta_{i-1}} f^k(\zeta,\phi(\zeta),\nu)\,\beta_{\Delta M}(P(\zeta),\mathcal{B}(\zeta),T(\zeta),\nu)\,\frac{ds}{dh}\frac{dh}{d\zeta}d\zeta$$

Derivatives

$$
\begin{aligned}
\frac{\partial \mathbf{I}}{\partial x_j} &= \sum_{k=1}^{i-1} \left\{ \frac{\partial \mathcal{T}_i}{\partial x_j} \Delta B_i + \mathcal{T}_i \frac{\partial \Delta B_i}{\partial x_j} \right\} \\
\frac{\partial \mathcal{T}_i}{\partial x_j} &= \frac{\partial \mathbf{P}_i \mathbf{P}_i{}^\dagger}{\partial x_j} \\
&= \sum_{k=1}^{i-1} \left\{ \mathbf{E}_1 \ldots \mathbf{E}_{k-1} \frac{\partial \mathbf{E}_k}{\partial x_j} \mathbf{E}_{k+1} \ldots \mathbf{E}_{i-1} \mathbf{P}_i{}^\dagger + \mathbf{P}_i \mathbf{E}_{i-1}{}^\dagger \ldots \mathbf{E}_{k+1}{}^\dagger \frac{\partial \mathbf{E}_k^\dagger}{\partial x_j} \mathbf{E}_{k-1}{}^\dagger \ldots \mathbf{E}_1{}^\dagger \right\} \\
&= \sum_{k=1}^{i-1} \left\{ \mathbf{P}_k \frac{\partial \mathbf{E}_k}{\partial x_j} \mathbf{P}_{k+1}^{-1} \mathcal{T}_i + \mathcal{T}_i{}^\dagger \mathbf{P}_{k+1}^{\dagger\,-1} \frac{\partial \mathbf{E}_k{}^\dagger}{\partial x_j} \mathbf{P}_k{}^\dagger \right\}
\end{aligned}
$$

(Note, $\mathcal{T} = \mathcal{T}^\dagger$ is manifestly hermitian.)

$$
\begin{aligned}
\frac{\partial \mathbf{I}}{\partial x_j} &= \sum_{i=1}^{2N} \mathcal{Q}_{j,i} \mathcal{T}_i + \mathcal{T}_i^\dagger \mathcal{Q}_{j,i}^\dagger, \\
\mathcal{Q}_{j,i} &= \frac{1}{2} \frac{\partial \Delta B_i}{\partial x_j} \mathbf{1} - \Delta B_i \mathcal{W}_{j,i}, \\
\mathcal{W}_{j,i} &= \sum_{k=1}^{i-1} \mathbf{P}_k \frac{\partial \mathbf{E}_k}{\partial x_j} \mathbf{P}_{k+1}^{-1}
\end{aligned}
$$

Derivatives (continued)

- Need derivatives for T, B,θ, ϕ, O_2 mixing ratio, wind, pointing.
- Derivatives of matrix exponentials are evaluated using Sylvester's identity.
- resulting expressions involve $\frac{\partial \Delta\delta_i}{\partial x}$ which will be ported from UARS code.

EOS-MLS L2 context

Goal is working magnetic FM (radiances and derivatives) in the context of the scalar FM in the context of L2 Software by April

Much of the scalar model can be used directly.

- Viewing geometry, gridding
- "Metrics" $s \rightarrow h$, $h \rightarrow \zeta$, refraction
- Zvi's Voigt lineshape (provides real and imaginary parts)
- Frequency "filter shape" convolution like other DACS

Notes on Geomagnetic Field Model

- Core field is typically between 0.6 gauss and 0.25 gauss.
- Lines move in and out. This will make L2's job difficult.
- Variation along path will look like broadening
- International Geomagnetic Reference Field (IGRF) supplies supplies main (core) field without external sources.
  - ⇨ 12th order spherical harmonic representation extrapolated from 5 year epochs
  - ⇨ we have Fortran code
  - ⇨ rotate to Instrument Field of View Plane Polarized (IFOVPP) frame.
- Models are available for 1st order diurnal (order percent?)
- Magnetic storms and Auroral contributions may be larger than core
- Current goal is to get SW working with IGRF for April.
- Research topic: operational models, ISTP Spacecraft (?)

New Fortran Modules for Polarized FM

x is $\{\sigma_+, \pi, \sigma_-\} \rightarrow$ {sp, pi, sm}

get_B_path	This function returns geomagnetic field magnitude and angles $\mathcal{B}$, θ and ϕ in IFOVPP	mjs
get_beta_path	3X complex: Same as scalar with Zeeman shifts but return both real and imaginary	UARS port
get_alpha_path	3X complex: sum over species (really only need O_2.) Adding scalars $\{\frac{1}{4}, \frac{1}{2}, \frac{1}{4}\}$ will put them on diagonal.	UARS port
get_rho_path	3X Tensor: requires angles $\{\theta, \phi\}$ in IFOVPP	UARS port
inc_opt_depth	Tensor: $\sum_x$[rho_path_x alpha_path_x]*del_s	UARS port
matrix_exp	Tensor: Sylvester's Identity	UARS port
build_tau_path	Tensor: Make product matrices $\mathbf{P}_i$ and build $\mathcal{T}_i$	UARS port
tensor_radtran	Tensor: same form as scalar, but four complex components	UARS port
mag_derivative	Tensor: magnetic derivative module	UARS port
get_path_d_opacity_dy	Tensor: modules for y={$\mathcal{B}$, θ, ϕ, T, mixing-ratio, pointing, molecular velocity}	UARS port
matrix_exp_derivative	Tensor: from Sylvester's identity	UARS port
get_path_W_y	Tensor: W_i for y derivative	UARS port
get_path_Q_y	Tensor: Q_i for y derivative	UARS port
ant_polar_proj	Project tensor $\mathbf{I}$ onto antenna. If cross pol is down -40dB, we may just take co-pol.	MJS/UARS

Planned Milestones and Tentative Dates

- All magnetic-specific software modules complete (late January)
- Full Mag. FM Operational in MLS Level 2 environment (mid Feb)
- Test Mag. FM for reasonableness
  - Radiances: Do lines have expected field dependance?
  - Radiances: Does $B_{earth} = 0$ agree with scalar calculation?
  - Radiances: Do $\theta = 0$ and $\theta = 90°$, $\phi = 0°$ or $\phi = 90°$ agree with appropriate scalar calculations?
  - Derivatives: Compare to Finite Differences for some test cases.
- Determine whether CPU limitations require linearization
  - Profile code and take any easy speedups
  - If linearization is required:
    - develop L2PC (bins in B_{earth}, $\cos^2(\theta)$)
    - test L2PC model- desire 0.2K agreement
- Test with L2 operational software (April)
  - Core
  - Core + R2
  - Core + R3